

# A data-driven reconstruction of global land use change - dynamics, drivers and impacts



Karina Winkler



## Propositions

1. Only a timely, comprehensive and synergistic combination of diverse data enables global land use changes to be appropriately represented in Earth system models.  
(this thesis)
2. Divergent paths of land use change between the Global North and Global South are linked through globalised trade.  
(this thesis)
3. Decentralised agricultural systems are more sustainable than centralised ones.
4. Scientific findings solely remaining in the academic bubble have no societal benefit.
5. Short-term contracts in science prevent long-term success.
6. Innovative thinking needs unconstrained disorder.
7. Rules deserve to be broken decently.

Propositions belonging to the thesis, entitled

”A data-driven reconstruction of global land use change – dynamics, drivers and impacts”

Karina Winkler

Wageningen, 2 May 2023



A data-driven reconstruction of global  
land use change –  
dynamics, drivers and impacts

Karina Winkler

## **Thesis committee**

### **Promotor**

Prof. Dr M. Herold

Professor at the Laboratory of Geo-information Science and Remote Sensing  
Wageningen University & Research

### **Co-promotors**

Prof. Dr M. Rounsevell

Institute of Meteorology and Climate Research  
Atmospheric Environmental Research (IMK-IFU)  
Karlsruhe Institute of Technology (KIT)

Dr R. Fuchs

Institute of Meteorology and Climate Research  
Atmospheric Environmental Research (IMK-IFU)  
Karlsruhe Institute of Technology (KIT)

### **Other members**

Prof. Dr Lars Hein, Wageningen University & Research

Dr Kathleen Hermans, IAMO, Halle (Saale), Germany

Dr Jasper van Vliet, VU University Amsterdam

Dr Kees Klein Goldewijk, Utrecht University

This research was conducted under the auspices of the C.T. de Wit Graduate School of  
Production Ecology & Resource Conservation (PE&RC)

# A data-driven reconstruction of global land use change – dynamics, drivers and impacts

Karina Winkler

## **Thesis**

submitted in fulfilment of the requirements for the degree of doctor  
at Wageningen University

by the authority of the Rector Magnificus

Prof. Dr A.P.J. Mol,

in the presence of the

Thesis Committee appointed by the Academic Board

to be defended in public

on Tuesday 2 May 2023

at 1:30 p.m. in the Omnia Auditorium.

Karina Winkler

A data-driven reconstruction of global land use change – dynamics, drivers and impacts,  
252 pages.

PhD thesis, Wageningen University, Wageningen, the Netherlands (2023)

With references, with summary in English and German

ISBN 978-94-6447-589-0

DOI <https://doi.org/10.18174/587224>





# Summary

People have shaped the surface of our planet for many centuries. However, the global expansion of land use is fuelling climate change and threatening biodiversity. At the same time, there is an ever-increasing need to supply our growing world population with food, energy and materials. This makes land use the linchpin for solving our biggest global sustainability challenges concerning food security, climate change and biodiversity loss. Despite this crucial role of land use, existing data on long-term land use change lacks the spatial, temporal and thematic depth to comprehensively represent land use dynamics and their impact on the ecosystem and climate in models. Therefore, and in order to better understand land use change processes and feed Earth system and climate models, there is an urgent need for global land use reconstructions with high spatial, temporal and thematic resolution.

This PhD thesis synergistically combines multiple open data streams (remote sensing-based land cover maps, land use reconstructions and statistics) to examine the multiple dimensions of global land use change, specifically: (1) its spatiotemporal dynamics, (2) its underlying drivers, and (3) its impacts on carbon emissions. For this, the HHistoric Land Dynamics Assessment+ (HILDA+) is developed and analysed in the course of this thesis.

Chapter 2 studies global land use dynamics by presenting the first version of HILDA+ at a spatial resolution of 1 km, a temporal resolution of yearly time steps, and a temporal coverage of six decades (1960-2019). As a result, we estimate that land use changes have affected almost a third (32%) of the global land surface within this period. Compared to previous land use reconstructions, land use change is around four times greater in extent. Furthermore, we identify globally diverging land use change processes, with afforestation and cropland abandonment in the Global North versus deforestation and agricultural expansion in the South. By analysing the temporal rate of global land use change, we observe a transition from accelerating to decelerating land use change after 2005, mainly caused by a decrease of agricultural expansion in the Global South. The findings indicate that geographically diverging patterns of global land use change are linked by globalised trade of commodities and land.

Chapter 3 illuminates the spatiotemporal patterns of global changes in agriculture - par-

ticularly expansion, abandonment, intensification and extensification of cropland and pasture/rangeland - during six decades (1960-2020). For this, an updated version of HILDA+ (including more, higher-resolution input data and finer cropland classes) is presented and analysed. We find that high-income countries pursued an intensification-abandonment trajectory in croplands and pasture/rangelands, whereas low-income countries intensified less but substantially increased their agricultural area over time. The results sustain the hypothesis that agricultural intensification is induced when land prices rise due to a scarcity of land for further expansion. Strikingly, middle-income countries show both large cropland expansion and high rates of intensification. The findings indicate that intensification of high-profit crops (e.g. soy bean and oil palm) stimulated further agricultural expansion in emerging middle-income countries. This involves the large-scale expansion of tree crops, such as oil palm, cocoa and rubber, which is found to be the underlying cause of more than half of the global deforestation.

Chapter 4 analyses the global land use transitions of the last six decades (1960-2019) based on the first version of the HILDA+ land change data. As the main finding, it reveals that agricultural expansion accounted for the largest share of global land use change ( $\sim 7.6$  million km<sup>2</sup>), which is an area as large as Greece every year. Notably, the global expansion of agriculture into non-forested areas was over three times larger than expansion into forests in that period. Chapter 4 also offers an explorative analysis of the causal relations between land use transitions and their drivers at the global scale. Our findings underline the dominating role of humans, particularly, the importance of economic drivers and the (as yet) small influence of environmental factors on global land use transitions in comparison to that. Agricultural expansion is the major land use transition in the Global South with strong links to globalised markets. Conversely, agricultural abandonment, forest expansion and intensive forestry dominates in the Global North, driven by economic growth, intensified production and policy regulations. This supports the hypothesis, that forest expansion in the Global North goes along with the displacement of land use, especially deforestation and agricultural expansion, to the Global South.

Chapter 5 analyses the climate impacts, in particular the carbon emissions, caused by land use change. It particularly focuses on the effect of using high resolution land use data as an input variable to carbon modelling. For this, the HILDA+ land use data is fed into in the Bookkeeping of Land Use Emissions (BLUE) model. In a next step, the model output based on HILDA+ is compared with that based on the standard land use dataset LUH2. HILDA+ has an around 25 times higher resolution than LUH2. The findings show, that using HILDA+ data leads to  $\sim 65\%$  lower carbon emissions than LUH2-based estimates. The agreement of carbon fluxes is higher in the mid-latitudes compared to tropical regions. Interestingly, the carbon emissions from agricultural land use change show opposite trends for the last decades between LUH2- and HILDA+-based estimates. Reasons for the deviations in carbon fluxes lie in different implementations of shifting cultivation (LUH2: prescribed assumptions vs. HILDA+: data-derived gross

changes) and the different capabilities of capturing successive transitions (LUH2: lower vs. HILDA+: higher detection). Our findings suggest that the current implementation of land use change processes (e.g. shifting cultivation and other successive transitions) and, above all, the spatial resolution in land use datasets used for carbon models needs to be reconsidered.

Chapter 6 studies carbon fluxes from above-ground biomass in Europe, with a particular focus on Eastern Europe during the last decade (2010-2019). It further illuminates the influence of possible underlying drivers from land use, management and environmental change. This is done by comparing multiple data sources - satellite-based biomass estimates, CO<sub>2</sub> inversions, land use emission models, and inventories. Land use-related and environmental indicators are used for a driver analysis. We show that the land-based carbon sink in Eastern Europe accounted for ~75% of the entire European carbon uptake. Strikingly, we found a declining trend in the Eastern European land-based carbon sink, which was likely driven by changes in land use and land management, along with increasing natural disturbances. Despite the high overall importance of environmental factors such as soil moisture, nitrogen and CO<sub>2</sub> for enhancing the land sink, we find indicators of a saturation effect of the regrowth in abandoned former agricultural areas, combined with an increase in wood harvest, particularly in European Russia. Our findings contribute to a better understanding of the role of land use and management for climate mitigation in Eastern Europe.

Summarising the main findings, this PhD thesis shows (1) how the synergistic combination of multiple open data reveals unprecedented spatiotemporal dynamics and geographically diverging patterns of global land use change, (2) the significance of the indirect socioeconomic drivers of land use change, and why acting on them is critical when implementing sustainable, climate-adapted land use pathways, (3) how higher-detailed land use data translates into new findings about global carbon emissions and, finally, as shown for the example of Eastern Europe, how land use, land management and environmental factors interact and affect carbon fluxes as climate mitigation options.



# Zusammenfassung

Die Menschheit hat die Oberfläche des Planeten über viele Jahrhunderte hinweg gestaltet. Die weltweite Ausdehnung der Landnutzung treibt jedoch den Klimawandel voran und bedroht die biologische Vielfalt. Gleichzeitig steigt die Nachfrage nach Nahrungsmitteln, Energie und Rohstoffen für die wachsende Weltbevölkerung ständig an. Dies macht die Landnutzung zum Dreh- und Angelpunkt für die Lösung unserer größten globalen Nachhaltigkeitsprobleme: Ernährungssicherheit, Klimawandel und Verlust der biologischen Vielfalt. Trotz dieser entscheidenden Rolle der Landnutzung fehlt es den vorhandenen Daten über langfristige Landnutzungsänderungen an räumlicher, zeitlicher und thematischer Tiefe, um die Landnutzungsdynamik und ihre Auswirkungen auf das Ökosystem und das Klima in Modellen umfassend darzustellen. Um Prozesse des Landnutzungswandels besser zu verstehen sowie Erdsystem- und Klimamodelle zu speisen, besteht daher ein dringender Bedarf an globalen Landnutzungsrekonstruktionen mit hoher räumlicher, zeitlicher und thematischer Auflösung.

In dieser Dissertation werden mehrere offene Daten (fernerkundungsbasierte Landbedeckungskarten, Landnutzungsrekonstruktionen und Statistiken) synergetisch kombiniert, um die verschiedenen Dimensionen des globalen Landnutzungswandels zu untersuchen: (1) seine räumlich-zeitliche Dynamik, (2) die ihm zugrunde liegenden Treiber und (3) seine Auswirkungen auf das Klima bzw. auf die Kohlenstoffemissionen. Zu diesem Zweck wird im Rahmen dieser Arbeit das HIstoric Land Dynamics Assessment+ (HILDA+) entwickelt und analysiert.

In Kapitel 2 wird die globale Landnutzungsdynamik untersucht, indem die erste Version von HILDA+ mit einer räumlichen Auflösung von 1 km, einer zeitlichen Auflösung von jährlichen Zeitschritten und einer zeitlichen Abdeckung von sechs Jahrzehnten (1960-2019) vorgestellt wird. Im Ergebnis schätzen wir, dass Landnutzungsänderungen innerhalb dieses Zeitraums fast ein Drittel (32%) der globalen Landfläche betroffen haben. Im Vergleich zu früheren Landnutzungsrekonstruktionen ist das Ausmaß der Landnutzungsänderung damit etwa viermal so groß. Darüber hinaus stellen wir fest, dass die Prozesse der Landnutzungsänderung weltweit voneinander abweichen: Aufforstung und Aufgabe von landwirtschaftlicher Flächen im globalen Norden gegenüber Entwaldung und landwirtschaftlicher Expansion im Süden. Bei der Analyse der zeitlichen Entwicklung des

globalen Landnutzungswandels stellen wir einen Übergang von einem beschleunigten zu einem verlangsamten Landnutzungswandel nach 2005 fest, der vor allem durch einen Rückgang der landwirtschaftlichen Expansion im globalen Süden verursacht wird. Die Ergebnisse deuten darauf hin, dass geografisch divergierende Muster des globalen Landnutzungswandels durch den globalisierten Handel mit Rohstoffen und Land miteinander verbunden sind.

Kapitel 3 beleuchtet die raum-zeitlichen Muster der globalen Veränderungen in der Landwirtschaft - insbesondere die Ausdehnung, Kontraktion, Intensivierung und Extensivierung von Acker- und Weideflächen - während sechs Jahrzehnten (1960-2020). Zu diesem Zweck wird eine aktualisierte Version von HILDA+ (mit mehr, höher aufgelösten Eingangsdaten und feineren Ackerlandklassen) vorgestellt und ausgewertet. Wir stellen fest, dass die Länder mit hohem Einkommen bei Ackerland und Weide-/Rangeland einen Intensivierungs-/Abbaukurs verfolgten, während die Länder mit niedrigem Einkommen ihre landwirtschaftliche Fläche im Laufe der Zeit zwar weniger intensivierten, aber erheblich vergrößerten. Die Ergebnisse stützen die Hypothese, dass die Intensivierung der Landwirtschaft durch steigende Bodenpreise ausgelöst wird, die auf eine Verknappung der für eine weitere Expansion verfügbaren Flächen zurückzuführen sind. Auffallend ist, dass Länder mit mittlerem Einkommen sowohl eine starke Ausweitung der Anbaufläche als auch hohe Intensivierungsraten aufweisen. Die Ergebnisse deuten darauf hin, dass die Intensivierung von gewinnbringenden Kulturen (z.B. Sojabohnen und Ölpalmen) eine weitere Ausdehnung der Landwirtschaft in den Schwellenländern mit mittlerem Einkommen anregt. Dazu gehört auch die großflächige Ausdehnung von Baumkulturen wie Ölpalmen, Kakao und Kautschuk, die für mehr als die Hälfte der weltweiten Entwaldung verantwortlich ist.

In Kapitel 4 werden die globalen Landnutzungsänderungen der letzten sechs Jahrzehnte (1960-2019) auf der Grundlage der ersten Version der HILDA+-Landänderungsdaten analysiert. Die wichtigste Erkenntnis ist, dass der größte Teil der globalen Landnutzungsänderungen auf die Ausweitung der Landwirtschaft zurückzuführen ist ( $\sim 7,6$  Mio. km<sup>2</sup>), was einer Fläche entspricht, die jedes Jahr so groß ist wie Griechenland. Bemerkenswert ist, dass die globale Ausdehnung der Landwirtschaft in nicht bewaldete Gebiete mehr als dreimal so groß war wie die Ausdehnung in Wälder in diesem Zeitraum. Kapitel 4 bietet auch eine explorative Analyse der kausalen Beziehungen zwischen Landnutzungsänderungen und ihren Triebkräften auf globaler Ebene. Unsere Ergebnisse unterstreichen die dominierende Rolle des Menschen, insbesondere die Bedeutung wirtschaftlicher Faktoren und den im Vergleich dazu (noch) geringen Einfluss von Umweltfaktoren auf globale Landnutzungsänderungen. Die Ausweitung der Landwirtschaft ist der wichtigste Landnutzungswandel im globalen Süden, der eng mit den globalisierten Märkten verbunden ist. Im Gegensatz dazu dominieren im Globalen Norden die Aufgabe der Landwirtschaft, die Ausdehnung der Wälder und die intensive Forstwirtschaft, angetrieben durch Wirtschaftswachstum, Intensivierung der Produktion und politische

---

Regulierungen. Dies stützt die Hypothese, dass die Ausdehnung der Wälder im globalen Norden mit der Verlagerung der Landnutzung, insbesondere der Entwaldung und der landwirtschaftlichen Expansion, in den globalen Süden einhergeht.

Kapitel 5 analysiert die Klimaauswirkungen, insbesondere die Kohlenstoffemissionen, die durch Landnutzungsänderungen verursacht werden. Der Fokus liegt hier insbesondere auf den Auswirkungen der Verwendung von hochauflösenden Landnutzungsdaten als Eingangsvariable für die Kohlenstoffmodellierung. Zu diesem Zweck werden die HILDA+ Landnutzungsdaten in das Bookkeeping of Land Use Emissions (BLUE)-Modell eingespeist. In einem nächsten Schritt wird die Modellausgabe auf der Grundlage von HILDA+ mit derjenigen auf der Grundlage des Standard-Landnutzungsdatensatzes LUH2 verglichen. HILDA+ hat eine etwa 25-mal höhere Auflösung als LUH2. Die Ergebnisse zeigen, dass die Verwendung von HILDA+-Daten zu ~65% niedrigeren Kohlenstoffemissionen führt als LUH2-basierte Schätzungen. Die Übereinstimmung der Kohlenstoffflüsse ist in den mittleren Breiten höher als in den Tropen. Interessanterweise zeigen die Kohlenstoffemissionen aus landwirtschaftlichen Landnutzungsänderungen in den letzten Jahrzehnten entgegengesetzte Trends zwischen LUH2- und HILDA+-basierten Schätzungen. Die Abweichungen bei den Kohlenstoffflüssen lassen sich auf eine unterschiedliche Umsetzung des Wanderfeldbaus (LUH2: vorgeschriebene Annahmen vs. HILDA+: aus Daten abgeleitete Bruttoveränderungen) und unterschiedliche Erfassung von aufeinanderfolgenden Übergängen (LUH2: geringere vs. HILDA+: höhere Erkennung) zurückführen. Unsere Ergebnisse legen nahe, dass die derzeitige Umsetzung von Landnutzungsänderungen (z.B. Wanderfeldbau und andere sukzessive Übergänge) und vor allem die räumliche Auflösung der für Kohlenstoffmodelle verwendeten Landnutzungsdatensätze überdacht werden muss.

In Kapitel 6 werden die Kohlenstoffflüsse aus oberirdischer Biomasse in Europa untersucht, wobei der Schwerpunkt auf Osteuropa im letzten Jahrzehnt (2010-2019) liegt. Außerdem wird der Einfluss möglicher zugrunde liegender Faktoren wie Landnutzung, Bewirtschaftung und Umweltveränderungen beleuchtet. Dies geschieht durch den Vergleich mehrerer Datenquellen - satellitengestützte Biomasseschätzungen, CO<sub>2</sub>-Inversionen, Landnutzungsemissionsmodelle und -Verzeichnisse. Landnutzungs- und Umweltindikatoren werden für eine Treiberanalyse verwendet. Wir zeigen, dass die landbasierte Kohlenstoffsенke in Osteuropa etwa 75% der gesamten europäischen Kohlenstoffaufnahme ausmacht. Auffallend ist der rückläufige Trend in der osteuropäischen landbasierten Kohlenstoffsенke, der wahrscheinlich durch Veränderungen in der Landnutzung und Landbewirtschaftung sowie durch zunehmende natürliche Störungen verursacht wurde. Trotz der insgesamt großen Bedeutung von Umweltfaktoren wie Bodenfeuchtigkeit, Stickstoff und CO<sub>2</sub> für die Erhöhung der Landsenke finden wir Anzeichen für einen Sättigungseffekt des Waldaufwuchses in verlassenen landwirtschaftlichen Gebieten in Verbindung mit einer Zunahme der Holzernte, insbesondere im europäischen Russland. Unsere Ergebnisse tragen zu einem besseren Verständnis der Rolle von Landnutzung und -management für

den Klimaschutz in Osteuropa bei.

Zusammenfassend zeigt diese Dissertation, (1) wie die synergetische Kombination verschiedener offener Daten noch nie dagewesene räumlich-zeitliche Dynamiken und geografisch divergierende Muster des globalen Landnutzungswandels aufzeigt, (2) die Bedeutung der indirekten sozioökonomischen Triebkräfte der Landnutzungsänderung und warum es bei der Umsetzung nachhaltiger, klimaangepasster Landnutzungspfade entscheidend ist, auf sie einzuwirken, (3) wie detailliertere Landnutzungsdaten zu neuen Erkenntnissen über globale Kohlenstoffemissionen führen und schließlich, wie Landnutzung, Landmanagement und Umweltfaktoren am Beispiel Osteuropa zusammenwirken und dortige Kohlenstoffflüsse als Klimaschutzoptionen beeinflussen.





# Contents

	Page
Summary	vii
Zusammenfassung	xi
Contents	xvii
Chapter 1 Introduction	1
Chapter 2 Spatio-temporal dynamics of global land use/cover change	13
Chapter 3 Expansion versus intensification of global agriculture	41
Chapter 4 Global land use transitions and their drivers	77
Chapter 5 CO <sub>2</sub> emissions based on high-resolution land use data	107
Chapter 6 Impacts of land use and environmental change on the Eastern European land carbon sink	127
Chapter 7 Synthesis	155
References	181
Acknowledgements	223
About the author	227
PE&RC Training and Education Statement	231



# Chapter 1

## Introduction

*Science cannot solve the ultimate mystery of nature. And that is because, in the last analysis, we ourselves are a part of the mystery that we are trying to solve.*

Max Planck

## 1.1 Land use change: Links, concepts and dynamics

### 1.1.1 Land use change at the interface between humans and the environment

Human activity has formed the Earth's surface for many centuries. The rapidly growing world population with changing consumption has increasingly placed demands on land to supply food, animal feed, fibre and fuel. Consequently, land use has expanded around the globe (Alexander et al., 2016). It is estimated that global agricultural areas have increased by around 4.7 million km<sup>2</sup> since 1960 (Klein Goldewijk et al., 2017; Ritchie & Roser, 2013). Simultaneously, about 1.8 million km<sup>2</sup> of the global forest area have been lost since 1990, which is around three times the size of Ukraine (Keenan et al., 2015; Ritchie & Roser, 2021).

Land use change lies at the interface between humans and the environment and is itself closely intertwined with both. Remarkably, anthropogenic land use change is both source and consequence of global environmental change. It significantly alters climate and ecosystem processes by influencing e.g. albedo, surface roughness and material cycling as well as habitats on local to global scales. In this context, deforestation is listed as the second largest human-induced contributor to global greenhouse gas emissions after fossil-fuel combustion (Friedlingstein et al., 2022; Le Quéré et al., 2013). However, land use change that leads to long-term forest gain, as it can be observed in higher latitudes, may act as a regional net carbon sink (Fuchs et al., 2016; Song et al., 2018). Furthermore,

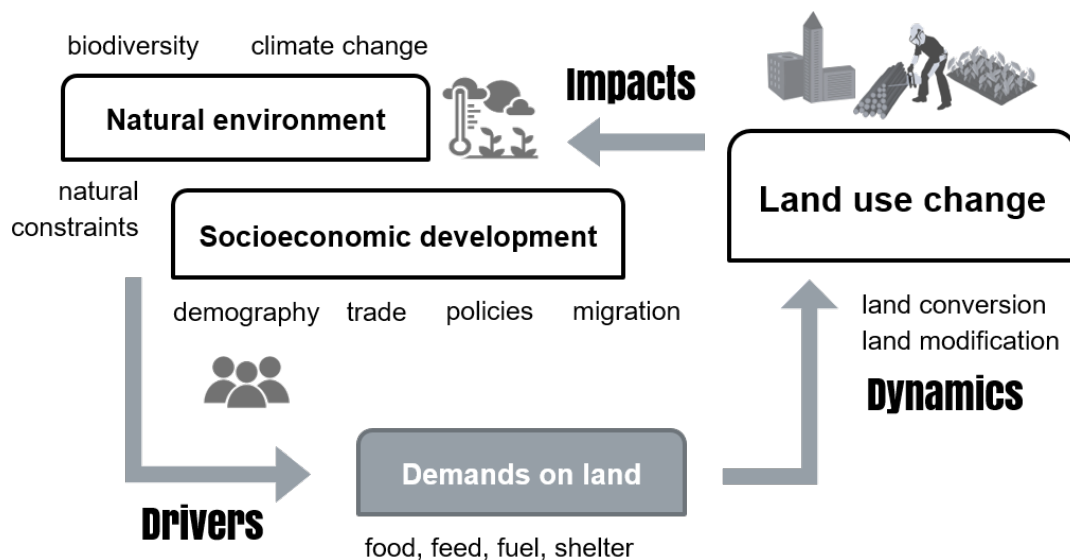


**Figure 1.1:** Schematic overview of the interlinkages of land use change with its drivers and impacts on environment and society.

land use-related pressures such as habitat fragmentation, harvesting and pollution have led to a worldwide reduction of terrestrial biodiversity (Newbold et al., 2015). The natural environment – altered by human land use – in turn determines the suitability of the land for certain uses and, thus, places constraints on land use change. Figure 1.1 gives an overview of the interlinkages of land use change with the natural environment and its socio-economic drivers. It also displays the main themes and research questions of this thesis – the dynamics, the drivers and the impacts of global land use change.

### 1.1.2 Land use, land cover and land management change

Land use change means a change of the land surface. Although the term land use change is used here as an umbrella term for both, strictly speaking, we distinguish between land use and land cover change. Land use change refers to a change in the way humans use the land surface, e.g. a transition from forest (no management) to cropland (agricultural management) (Zvoleff et al., 2014). It describes how humans transform the (natural) land and typically emphasizes the functional role of land for economic activities (Paul & Rashid, 2017). In contrast, land cover change refers to changes in the biophysical properties of the land surface, e.g. a transition from forest to grassland. Hence, land use change can but does not necessarily have to involve land cover change, and vice versa. Here, we refer to land use change that includes both land cover and land use changes as transitions between six major land use/cover categories covering the entire land surface: urban areas, cropland, pasture/rangelands, unmanaged grass/shrubland, forest, and no/sparse vegetation.

Whereas land use change is the conversion of land belonging to one land use/cover category to another, land management change describes a modification of the way land is cultivated and is not necessarily accompanied by a land use conversion. Management options vary by land use category. On croplands, for example, management can involve inputs such as crop varieties, cropping frequency, fertiliser or pesticide application, irrigation schemes and also the use of machinery for soil cultivation. A change in land management can affect the land productivity and, thus, cause either intensification (increasing productivity) or disintensification (or extensification; decreasing productivity) (Meyfroidt et al., 2018).

Figure 1.2 shows schematic examples of land use, land cover and management change on a gridded land surface. Even if presented individually, they are strongly interlinked in practice. The relationship between land use and land management change is addressed by several existing concepts, particularly focussing on the interlinkage of agricultural land use expansion and intensification. These concepts are as follows: First, theories of induced intensification postulate that intensification is the result of a growing demand along with an increasing scarcity of land, which leads to increasing land prices. In short, countries tend to expand before they intensify. Second, the land sparing hypothesis suggests that intensification releases pressure on land by serving a given demand and, hence, causes

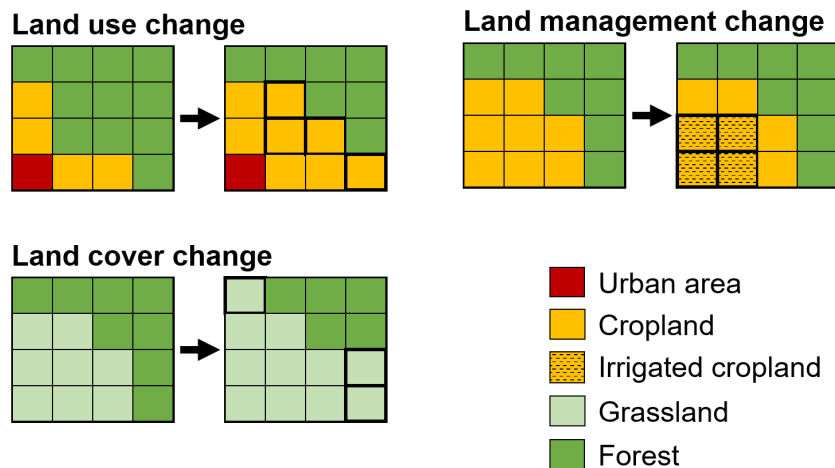


**Figure 1.2:** Example land transitions for land use, land cover and land management change on a spatial grid. Grid cells that changed are framed.

less agricultural expansion. Finally, the hypothesis of the rebound effect (also Jevon’s paradox) contrasts with the land sparing concept. It states that the increasing profitability of agriculture through (market-driven) intensification stimulates further agricultural expansion (García et al., 2020; Meyfroidt et al., 2018).

Eventually, land change can also be displaced to distant world regions. Agricultural intensification, for example, may not only cause a change in nearby agricultural area, but also place new socio-economic demands, indirectly affecting other regions via migration and trade (Matson & Vitousek, 2006; Stürck et al., 2018).

### 1.1.3 Net versus gross land use change

An important consideration when studying land use change is the difference between net and gross change (Fuchs, 2015; Fuchs et al., 2016; Li et al., 2018; Prestele et al., 2017). The analysis of land use change is generally based on a comparison of land use/cover (typically with focus on a specific land use/cover category) in a particular region at different time steps. Thereby, net land use change is obtained by taking the difference in area of a certain land use/cover category, aggregated over a region of interest, between two time steps. Such net changes can be derived from land use inventories, e.g. from the Food and Agriculture Organization of the United Nations (FAO) which comprises land use areas for each country at annual time steps. In contrast, gross land use change refers to the sum of all area gains and losses within a particular region. A comparison reveals higher gross change than net change values (see sample calculation for forest in Figure 1.3). The larger the aggregated areas (e.g. at country- or regional scales), the higher is the difference between net and gross land use change.

However, the issue of net and gross changes is not only spatial in nature. Land use change

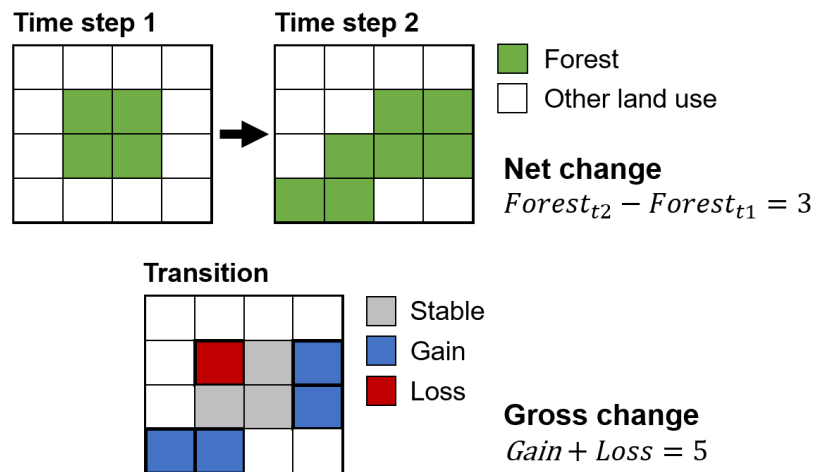


**Figure 1.3:** : Sample calculation for net and gross land use changes.

studies are often aggregated not only over space but also over time. Therefore, taking the difference in land use areas from two time steps disregards changes that have taken place on one and the same grid cell in the meantime. This can lead to an underestimation of the full extent of land use change. As with the spatial dimension, the higher the temporal aggregation (the larger the time steps), the higher is the difference in gross and net land use changes.

## 1.2 Drivers of land use change

The underlying processes of land use change have been analysed from different thematic, spatial and temporal viewpoints. Studies of land use and ecosystem change frequently distinguish between indirect and direct drivers. Accordingly, indirect drivers are the underlying anthropogenic (socio-economic) causes of land use change, e.g. demography, politics, economy/trade and consumption, and are often channelled through direct drivers at different scales. In contrast, direct drivers have obvious and local impacts on the land surface, e.g. production factors, management as well as environmental and climatic influences (Díaz et al., 2015; Kleemann et al., 2017; Lambin et al., 2003).

Many studies address wide-ranging drivers of land use change at regional scales. For example, agricultural production of high-profit crops or livestock, political incentives, regulations or regime shifts, market opportunities, technologies and mechanisation, changing consumption, increasing wealth, the transition from a rural to an urban society as well as climate and environmental change are found to be major drivers of land use change at the regional level (Arima et al., 2011; Hong et al., 2021; Junquera et al., 2020; Piquer-Rodríguez et al., 2018; Reenberg & Fenger, 2011; Sy et al., 2015; Tahmasebi et al., 2020; van Vliet et al., 2015, 2012; Wigley et al., 2010). Overall, socio-economic, political, technological, natural and cultural drivers are listed as major driver groups of land use change

(Munteanu et al., 2014; Plieninger et al., 2016; van Vliet et al., 2015). At the global scale, commodity production, forestry, shifting cultivation, and wildfires have been identified as drivers of forest loss (Curtis et al., 2018). Population growth and changing consumption are considered to be the strongest indirect drivers of agricultural expansion for food and bioenergy production (Alexander et al., 2015).

What is more, distant drivers of land change as well as its indirect impacts are becoming increasingly important, since globalised trade geographically interlinks socio-ecological systems. Thus, regional policies and consumption patterns may have unintended, distant impacts such as unsustainable land management or greenhouse gas emissions due to land conversion being exported to other world regions (Meyfroidt et al., 2013). Such cases of land use displacements have been demonstrated in the Amazon, where deforestation for pasture is followed by commercial cropland expansion (Arima et al., 2011; Piquer-Rodríguez et al., 2018; Sy et al., 2015).

Hence, land use change is driven by the complex interplay of economic, technological, institutional, demographic, sociocultural, location, and environmental factors that operate at different spatial and temporal scales (Bürgi et al., 2022).

## 1.3 Environmental impacts of land use change

### 1.3.1 Land use change and carbon

Estimates show that land use change has contributed around one third to all cumulated anthropogenic CO<sub>2</sub> emissions from 1850 to 2019 (Friedlingstein et al., 2022). Land use change, particularly deforestation, is the second largest contributor to greenhouse gas emissions, after fossil fuel combustion (Arneeth et al., 2019; Friedlingstein et al., 2022; IPCC, 2022). Generally, land use change affects CO<sub>2</sub> fluxes between the land and the atmosphere through different processes: deforestation, afforestation, logging and forest degradation (including harvest activity), shifting cultivation, and regrowth of forests following wood harvest or abandonment of agriculture (Friedlingstein et al., 2022).

Emissions from land use change emerge from the carbon transfer from soil and biomass to the atmosphere through e.g. deforestation, harvest, or the conversion of grass- to croplands. Thus, these land use change processes act as carbon sources. In contrast, land use change can also sequester carbon from the atmosphere in biomass and soil and thus act as a carbon sink. Land use changes that lead to such carbon uptake are e.g. afforestation and vegetation regrowth after abandonment of agricultural land or harvest (Pongratz et al., 2014). These activities can be targeted as means to reduce emissions or to re-sequester carbon from the atmosphere and will be essential for reaching net zero emissions in the future (Crippa et al., 2021; Goldstein et al., 2020; Griscom et al., 2017; Harper et al., 2018). Here, forest-related land use activities are at the forefront of the

debates. Halting deforestation and forest degradation on the one hand and supporting afforestation and forest regeneration on the other hand are widely discussed measures of climate mitigation (Gatti et al., 2021; Hoegh-Guldberg et al., 2019; Lewis et al., 2019; Maxwell et al., 2019; Roe et al., 2019).

Nevertheless, carbon sources and sinks from land use change are not equally distributed around the world. Whereas carbon sources are mostly found in tropical regions of the Global South (deforestation in Latin America, South-East Asia and Africa), regional carbon sinks have evolved more recently in the Global North (afforestation and forest regrowth in North America and Europe) (IPCC, 2022). Overall, the global net CO<sub>2</sub> flux from land use change adds up to a carbon source, consisting of carbon emissions of around 1.1 GtC per year during the last decade (Friedlingstein et al., 2022).

### 1.3.2 Land use change and biodiversity

Apart from the climate, land use and land management change also has an impact on biodiversity – through e.g. habitat loss, modification and fragmentation, soil and water degradation as well as overexploitation of native species (Davison et al., 2021; Marques et al., 2019; Newbold et al., 2016). This may result in a reduction of species richness – a change in species composition or decrease in species abundance at different spatial scales (Davison et al., 2021).

From all land use types, agricultural expansion for cattle farming has been identified as major driver of biodiversity loss, followed by the cultivation of cereals and oil seeds as well as forest management. However, the production of oil seeds recently showed the largest increase in biodiversity impacts. Again, a North-South divide is found in the impact of land use on biodiversity, which is larger overall in the South than in the North (Marques et al., 2019).

## 1.4 The need for land use reconstructions

When assessing the biogeochemical and biophysical effects of land use change, long-term land change reconstructions become inevitable, since former land use strongly controls the dynamics of greenhouse gas emissions (Fuchs et al., 2016; Hurtt et al., 2011). Overall, understanding land change dynamics is crucial for overcoming today’s pressing global sustainability challenges such as climate change, biodiversity loss, and food security (Heistermann et al., 2006; Liu & Yang, 2015). Therefore, a spatially explicit reconstruction of global land use change is an essential data input to Earth system and climate models to support climate change adaptation and mitigation as well as to biodiversity models for assessing impacts on species richness and ecosystem services (Bayer et al., 2017).

In spite of its societal relevance, understanding how global land use/cover has changed across space and through time is limited by a lack of comprehensive data and large

uncertainties within existing land use/cover reconstructions (Bayer et al., 2017; Prestele et al., 2017). As a precondition for fully analysing direct and indirect impacts of land use change on climate and biodiversity, an enhanced level of detail and a stronger embedding of observational data in global land use reconstructions become inevitable. Furthermore, for promoting and investigating global pathways of sustainable agricultural production, land use change has to be interlinked with indicators of management intensity.

Even in the age of satellites, “big data” and a growing trend of open access to information, land use/cover data are still constrained by fragmented content, varying scales, a lack of spatial or temporal detail and inconsistent time series (Fuchs et al., 2013; Pongratz et al., 2017). Satellite remote sensing refers to land cover (the biophysical properties of a land surface, e.g. grassland) and provides high spatial resolution, but short temporal coverage. In contrast, inventories and statistics mostly concern land use (the purpose for, and activities by which humans utilise land, e.g. grazing, cropping), encompass long time spans, but are bound to administrative units and, thus, lack spatial detail. Each data source on its own lacks one critical component – space, time or theme – and, thus, is unable to capture the full scale of land use dynamics.

## 1.5 Data availability and research needs

Since land systems are complex, a large amount of land use models have emerged from multiple disciplinary fields, mostly focussing on local to national scales (Fuchs, 2015; Klein Goldewijk & Ramankutty, 2004). However, a global assessment is critical, since the main drivers of land use change such as climate or socio-economic factors (e.g. global trade) and its impacts are not limited to regional boundaries and are in fact substantially interlinked (Meiyappan et al., 2014). The comparison of global-scale models revealed that data input still causes the largest uncertainty in land change projections (Ballantyne et al., 2015; Prestele et al., 2016). Likewise, greenhouse gas emissions caused by land use and its changes represent the main source of uncertainty in assessing the global carbon budget (Friedlingstein et al., 2022). Datasets on land use/cover hold considerable limitations for land change reconstruction at large scales, such as fragmented content, varying formats and scales, or lacking spatial explicitness (Fuchs et al., 2015b, 2013; Pongratz et al., 2017; Yang et al., 2014). Therefore, long-term, large-scale, detailed and spatially explicit reconstructions of land change are still scarce, although the availability of observational data is growing (e.g. remote sensing products). Still, notable effort has been made during the last decades.

Ramankutty & Foley (1999) from the Center for Sustainability and the Global Environment (SAGE) calibrated land cover classifications against historic cropland inventories for extrapolating global agricultural areas (annual; 1700-1992;  $\sim 0.083^\circ$  grid size). Furthermore, the HYDE database (Klein Goldewijk, 2001; Klein Goldewijk et al., 2010, 2011, 2017) provides a reconstruction model of land use patterns based from FAO inventories

and historical population estimates (HYDE3.2: 10,000 BC to up to 2015 AD;  $\sim 0.083^\circ$  grid size). Building on a combination of SAGE and HYDE datasets with additional population data, Pongratz et al. (2008) reconstructed global agricultural areas and accompanying land cover changes (annual; 800 to 1992;  $0.5^\circ$  grid size). Kaplan et al. (2010, 2012) developed a land change inventory based on population size and suitability maps for agriculture (annual; 1000 BC to 1850 AD;  $\sim 0.083^\circ$  grid size). However, most reconstructions only include net change, the areal difference of a land cover type between two time steps, instead of considering gross change as the sum of all class-to-class land transitions. This can lead to serious underestimations of land change dynamics (Bayer et al., 2017; Fuchs et al., 2016). Building on the HYDE data, Hurtt et al. (2011) generated a harmonised set of global land-use change scenarios, which was recently updated (Chini et al., 2021; Hurtt et al., 2020) to LUH2 (annual; 850 2100;  $0.25^\circ$  grid size). The authors included gross changes, but did not empirically derive them for all LULC types (partly extracted from HYDE and based on assumption on shifting cultivation). Finally, Fuchs et al. (2013) presented a first, empirically derived, high-resolution and consistent reconstruction of land use change over Europe: the HIstoric Land Dynamics Assessment (HILDA), which is based on multiple data sources such as statistical inventories (FAO), remote sensing products, and historic maps (decadal; 1900-2010; 1 km grid size). Here, empirically derived gross changes were incorporated in the allocation procedure and compared to the net change reconstruction in a follow-up study, displaying their added value to the assessment of land change dynamics (Fuchs, 2015; Fuchs et al., 2015a).

In summary, existing long-term land use reconstructions at the global scale often rely on only a few observational data streams and are built on assumptions concerning, for example, the allocation of cropland (HYDE3.2, LUH2) or wood harvests (LUH2). They also have rather coarse spatial resolutions of up to  $0.25^\circ$  (LUH2) and/or limited land use categories (SAGE cropland, HYDE3.2). Although recent progress was made by GLASS-GLC (Liu et al., 2020) in assessing long-term, land cover change at an unprecedented spatial resolution (5 km) and temporal coverage (1982 2015), GLASS-GLC only refers to land cover (not land use) and relies on a single satellite sensor (AVHRR) as a data source. More importantly, none of the existing data on land use change fully account for gross changes. However, identifying gross changes in land use dynamics is essential when quantifying the climatic and environmental impact of land use/cover change (Bayer et al., 2017). Moreover, information on land management such as fertilisation, irrigation, pesticide use or harvest rates are often neglected but of crucial importance for a detailed analysis of land use dynamics. Such within-class changes affect twice as much of the global land surface (42-58%) than generic, class-to-class land conversions (18-29%), having climate impacts of about the same magnitude (Luyssaert et al., 2014).

We live in a data-rich age where a variety of information is publicly available – Earth observation data with very high spatial resolution as well as statistics with long-term coverage. This leads to the hypothesis that land use changes could be reconstructed

with unprecedented detail, namely with high spatial resolution, global scale, temporal coverage and thematic completeness. This increased level of detail in contrast to existing models would allow to reveal and analyse completely different and previously unseen patterns of human influence (e.g. management activities) on the land surface. First of all, high-frequency transitions, e.g. between cropland and pastures, could shed light on land management intensities. Second, the temporal evolution of land use changes could be analysed in relation with far-reaching socio-economic events such as political disruptions or economic crises. Eventually, new insights into more complex processes of land use change such as shifting cultivation or forest regrowth after agricultural abandonment could be gained. In a nutshell, a higher spatial, temporal and thematic detail in land use maps would help to uncover the full dynamics of land use change.

## 1.6 Objective and research questions

As a consequence of the above-mentioned shortcomings, this thesis aims to consistently reconstruct global land use change through the synergistic use of different open data types at unprecedented level of spatial, temporal and thematic detail. It is hypothesised that all major global land change processes can be captured by building on both long-term land use inventories from statistics and high-resolution land use/cover datasets from remote sensing. Based on a newly developed, open and global dataset on land use change, this thesis investigates the following research questions:

- A. What can synergistically and consistently combined open data reveal about the **spatio-temporal dynamics of global land use change** over the past six decades?
- B. What were the main **drivers** of global land use transitions in the past six decades?
- C. What are the **climate impacts** of land use change and what role do high-resolution land use dynamics play in the carbon cycle?

Figure 1.1 shows how the research questions are embedded in the human-environment linkages of global land use change.

## 1.7 Outline of the thesis

This thesis consists of five main chapters, each addressing one or more of the research questions presented above.

**Chapter 2 and 3** study the spatio-temporal dynamics of global land use change and, thus, address research question A and touch on aspects of research question B in the discussion. **Chapter 2** presents the Historic Land Dynamic Assessment+ (HILDA+), a data-driven reconstruction of global land use change from 1960 to 2019 at 1 km spatial

and annual temporal resolution. It investigates how heterogeneous open data streams can be used to consistently capture and analyse the spatio-temporal dynamics of global land use change. **Chapter 3** focusses on agricultural land use change by linking changes in global cropland and pasture/rangeland from HILDA+ to management intensities. Here, the spatio-temporal dynamics and the relationship of agricultural expansion and intensification during the past six decades are analysed globally and at the country-level. Both Chapter 2 and 3 discuss potential drivers underlying the observed spatio-temporal patterns of land use change in general (Chapter 2) and agricultural land use change in particular (Chapter 3).

**Chapter 4** addresses research question A and B by analysing major global land use transitions and exploring their direct and indirect drivers. For this purpose, the most important land use transitions are derived from the annual land use changes of HILDA+. Causal relationships between land use transitions and multiple driver indicators from land management and production, environment, demography, politics and economy are identified and examined.

**Chapter 5 and 6** refer to research question C by studying the impacts of land use change in terms of carbon emissions at global and regional scales. **Chapter 5** addresses the climate impacts of global land use change, particularly the effect of using high-resolution maps on global land use change from HILDA+ for modelling land use emissions. For this, HILDA+ data is fed into a global book-keeping model of land use emissions. Modelling results are then evaluated against emission estimates based on land use change data with coarser spatial resolution. **Chapter 6** illuminates the climate impacts of land use change in a regional, Eastern European context. Therein, the role of land use, management and environmental factors on the Eastern European carbon fluxes from above-ground biomass during the last decade (2010-2019) is analysed.



## Chapter 2

# Spatio-temporal dynamics of global land use/cover change

This chapter is based on:

Winkler, K., Fuchs, R., Rounsevell, M., & Herold, M. (2021). Global land use changes are four times greater than previously estimated. *Nature Communications*, *12*, 2501. DOI: <https://doi.org/10.1038/s41467-021-22702-2>.

Supplementary material can be found in the online publication.

*History is a backward-looking prophet: for what it was, and against what it was, it announces what it will be.*

Eduardo Galeano

## Abstract

Quantifying the dynamics of land use change is critical in tackling global societal challenges such as food security, climate change and biodiversity loss. Here we analyse the dynamics of global land use change at an unprecedented spatial resolution by combining multiple open data streams (remote sensing, reconstructions and statistics) to create the HIstoric Land Dynamics Assessment+ (HILDA+). We estimate that land use change has affected almost a third (32%) of the global land area in just six decades (1960-2019) and, thus, is around four times greater in extent than previously estimated from long-term land change assessments. We also identify geographically diverging land use change processes, with afforestation and cropland abandonment in the Global North and deforestation and agricultural expansion in the South. Here, we show that observed phases of accelerating ( $\sim$ 1960-2005) and decelerating ( $\sim$ 2006-2019) land use change can be explained by the effects of global trade on agricultural production.

## 2.1 Introduction

About three-quarters of the Earth’s land surface has been altered by humans within the last millennium (Arneth et al., 2019; Luyssaert et al., 2014). Successfully tackling global sustainability challenges such as climate change, biodiversity loss, and food security depends on land use change, since it strongly affects carbon sources (Le Quéré et al., 2013) and sinks (Arneth et al., 2014; Popp et al., 2014), causes habitat loss (Powers & Jetz, 2019) and underpins food production (Lambin & Meyfroidt, 2011). In particular, the mitigation potential of land use activities, including those related to forests and agriculture, has been recognised as essential in meeting climate targets under the Paris Agreement, making land use a central component of many international policy debates (Arneth et al., 2019; Grassi et al., 2017). Therefore, quantifying and understanding global land use change and its spatio-temporal dynamics is critical in supporting these debates. Yet, in spite of its societal relevance, understanding how global land use/cover has changed across space and through time is limited by a lack of comprehensive data and the large uncertainties within existing land use/cover reconstructions (Bayer et al., 2017; Prestele et al., 2017).

Even in the age of satellites, “big data” and a growing trend of opening access to information, land use/cover data are still constrained by fragmented content, varying scales, a lack of spatial or temporal detail and inconsistent time series (Fuchs et al., 2013; Pongratz et al., 2017). Satellite remote sensing refers to land cover (the biophysical properties of a land surface, e.g. grassland) and provides high spatial resolution, but short temporal coverage. In contrast, inventories and statistics mostly concern land use (the purpose for, and activities by which humans utilise land, e.g. grazing, cropping), encompass long time spans, but are bound to administrative units and, thus, lack spatial detail. Each data source on its own lacks one critical component – space, time or theme - and, thus, is unable to capture the full scale of land use dynamics.

Existing global, long-term land use reconstructions often rely on only a few observational data streams and are built on assumptions concerning, for example, the allocation of cropland as in HYDE3.2 (Klein Goldewijk et al., 2017) or wood harvests as in LUH2 (Hurtt et al., 2020). They also have rather coarse spatial resolutions of up to 0.25°, as in LUH2 (Hurtt et al., 2020) and limited land use categories, as in SAGE cropland (Ramankutty & Foley, 1999), HYDE3.2 (Klein Goldewijk et al., 2017). Although recent progress was made by GLASS-GLC (Liu et al., 2020) in assessing long-term, land cover change at an unprecedented spatial resolution (5 km) and temporal coverage (1982-2015), GLASS-GLC only refers to land cover (not land use) and relies on a single satellite sensor (AVHRR) as a data source. More importantly, none of the existing data on land use change fully account for gross change, in other words, all of the land transitions between land use/cover categories that occur during a given time period.

**Table 2.1:** Land use/cover (LUC) datasets used for HiLDA+ LUC reconstruction and their specifications (thematic, spatial and temporal coverage)

Dataset and reference	Used thematic coverage	Spatial coverage	Used temporal coverage	Spatial resolution	Data type
Copernicus LC100	LCCS 22 classes	global	2015-2019	100 m	raster
ESA CCI Land Cover	LCCS 22 classes	global	1992-2015	300 m	raster
GLAD UMD VCF	tree canopy, bare ground, short vegetation	global	1982-2015	0.05 deg	raster
GLC2000	FAO LCCS 22 classes	global	2000	1 km	raster
GLCNMO	LCCS 22 classes	global	2003 2008, 2013	30 arc sec 15 arc sec	raster
Global Human Settlement Layer (GHSL)	built-up area (fractional)	global	1975, 1990, 2000, 2014	1 km	raster
Global Urban Footprint (GUF)	built-up area (fractional)	global	2011/12	2.8 arc sec	raster
GlobCover	LCCS 22 classes	global	2005/2006, 2009	300 m	raster
Globeland30	10 LUC classes	global	2000, 2010	30 m	raster
Gridded Livestock World v3 (GLW)	density of ruminants	global	2010	5 arc min	raster
Hansen GFC	tree cover (fractional) loss and gain year	global	2000-2015	30 m	raster
MODIS MCD12Q1	IGBP 17 classes	global	2001-2013 (yearly)	500 m	raster
Ramankutty cropland	cropland	global	2000	5 arc min	raster
AAFC Land Use Canada	15 LUC classes	Canada	1990, 2000, 2010	30 m	raster
Australia DLCD V2.1	LCCS 22 classes	Australia	2002-2014	500 m	raster
CORINE	44 LUC classes with change layers	Europe (changing extent)	1990, 2000, 2006, 2012, 2018	100 m	raster
LUC classification of India	11 LUC classes (IGBP scheme)	India	1985, 1995, 2005	100 m	raster
MoEF Indonesia	22 LUC classes	Indonesia	2000, 2003, 2006, 2009	300 m	raster
NLCD Land Cover (CONUS)	16 LUC classes	U.S.	2001, 2006, 2011	30 m	raster

Dataset and reference	Used thematic coverage	Spatial coverage	Used temporal coverage	Spatial resolution	Data type
RCMRD Land Cover	6 LUC classes with country-specific sub-classes	Botswana, Ethiopia, Lesotho, Malawi, Namibia, Rwanda, Tanzania, Uganda, Zambia	different years between 2000 and 2014	30 m	raster
South Africa Land Cover	35/72 LUC classes	South Africa	1990, 2013-14	30 m	raster

\* LUC = land use/land cover, LCCS = Land Cover Classification System, IGBP = International Geosphere-Biosphere Programme

However, identifying gross changes in land use dynamics is essential when quantifying the climatic and environmental impact of land use/cover change (Bayer et al., 2021).

To analyse and better understand the spatio-temporal dynamics of global land use change, we combined multiple, high-resolution remote sensing data (see Table 2.1) with long-term statistical data streams such as FAO land use (FAO, 2019a) and population (FAO, 2019b) to assess annual changes in land use/cover from 1960 to 2019 at a spatial resolution of 1 km.

Based on open datasets, we developed a model called HILDA+ (Historic Land Dynamics Assessment+, <https://landchangestories.org/hildaplus-mapviewer/>), which harmonises spatially explicit land use/cover information with land use inventories at the national scale and allocates these changes to the global land surface. The approach fully incorporates data-derived, annual gross changes between six land use/cover categories: urban, cropland, pasture/rangeland, forest, unmanaged grass/shrubland, sparse/no vegetation (see Table 2.2). This enables the quantification of the spatial extent of land use change in unprecedented detail and provides tracking of the annual dynamics through time. In this paper, we present the gains and losses in major land use/cover categories, identify different land use change patterns and compare these across the globe.

## 2.2 Material and methods

We reconstructed land use/cover change dynamics for six land use/cover categories (urban, cropland, pasture/rangeland, forest, unmanaged grass/shrubland, sparse/no vegeta-

**Table 2.2:** Defined target land use/cover categories of HILDA+

Final land use/cover category	Definition and description
1. Urban	Artificial surfaces, urban and built-up areas, including urban parks and sports areas, green spaces, industrial, deposits, extractions sites (mining etc.)
2. Cropland	Herbaceous and woody crops (also for hay production) including tree/shrub crops, orchards, plantations, multiple/layered crops, incl. mosaics (with cropland area fraction $\geq 40\%$ )
3. Pasture/rangeland	Managed herbaceous plants (cover $\geq 10\%$ ) including managed grasslands (e.g. prairies, steppes, savannah, mosaics with tree/shrubs): grasslands or meadows used for e.g. livestock grazing or hay production with different intensities
4. Forest	Trees with $> 5\text{m}$ height (cover $\geq 10\%$ ) including forest plantation, trees on seasonally or permanently flooded areas, including mangroves
5. Unmanaged grass-/shrubland	Natural herbaceous plants (cover $\geq 10\%$ ) including grasslands (e.g. prairies, steppes, savannah, mosaics with tree/shrubs) or natural shrub cover ( $\geq 10\%$ ), including permanently or regularly flooded areas (wetlands), (herbaceous) wetlands
6. Sparse/no vegetation	Bare areas, sparse vegetation (2-10%), snow and ice, rocks, sand, mudflats

tion) based on multiple sources of observational data, from which country-scale change extents and mean fractional area were derived per 1x1 km grid cell from 1960 to 2019. We calculated the country- and year-specific areas of change for each land transition between these categories. A base map for the year 2015 served as a starting point for the change allocation procedure, which, at first, runs backward in time (2015-1960) and, subsequently, forward in time (2015-2019). For each time step and country, land use/cover change was allocated to selected candidate pixels by using ranked gridded class fractions and the data-derived change extents. Each of these iterative procedures yielded a global land use/cover map, which served as the new base map for the next time step. A visualisation of the HILDA+ reconstruction framework, which evolved from the approach of the HILDA over Europe (Fuchs et al., 2013), is given in Figure 2.1. Methodological steps of the involved change allocation procedure are shown in Figure 2.2.

### 2.2.1 Preprocessing of remote sensing-based land use/cover data

The HILDA+ reconstruction was derived from multiple, openly available global, continental, regional, and national land use/cover datasets (see Table 2.1).

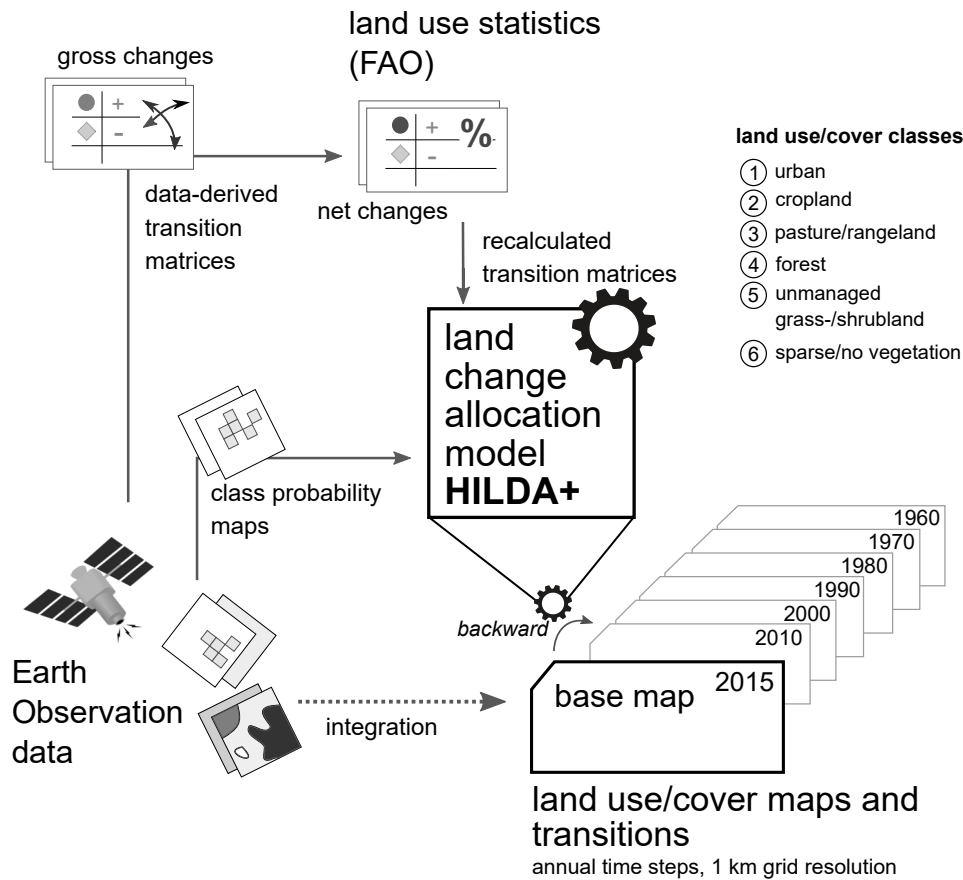


**Figure 2.1:** Graphical overview of the HILDA+ (Historic Land Dynamics Assessment+) framework, a data-driven global land use/cover change allocation model

### 2.2.2 Harmonisation of land use/cover maps

We defined a common generalised classification scheme for harmonising the remote sensing-based land use/cover products. The classification scheme was based on six land use/cover classes that aim to encompass the major land use changes caused by people and, at the same time, to find a common ground for the input datasets that differ in thematic detail. This classification relates to the FAO land use definitions (Food and Agriculture Organization of the United Nations (FAO), 2019a) and the LCCS land cover classification scheme (Di Gregorio and Jansen, 2000) and, thus, combines land cover with land use information. Accordingly, the available land use/cover maps were reclassified based on their inherent classification schemes (see Table 2.3). The reclassified maps were converted into binary masks for each of the generalised land cover categories. Subsequently, these were reprojected and resampled into the target projection (Eckert IV), the final spatial extent and grid resolution (1 km) by proportional averaging of the pixel values. Maps of area fractions under each land cover category from Table 2.3 are the result of this processing step.

For those years when no observational datasets were available, remote sensing products

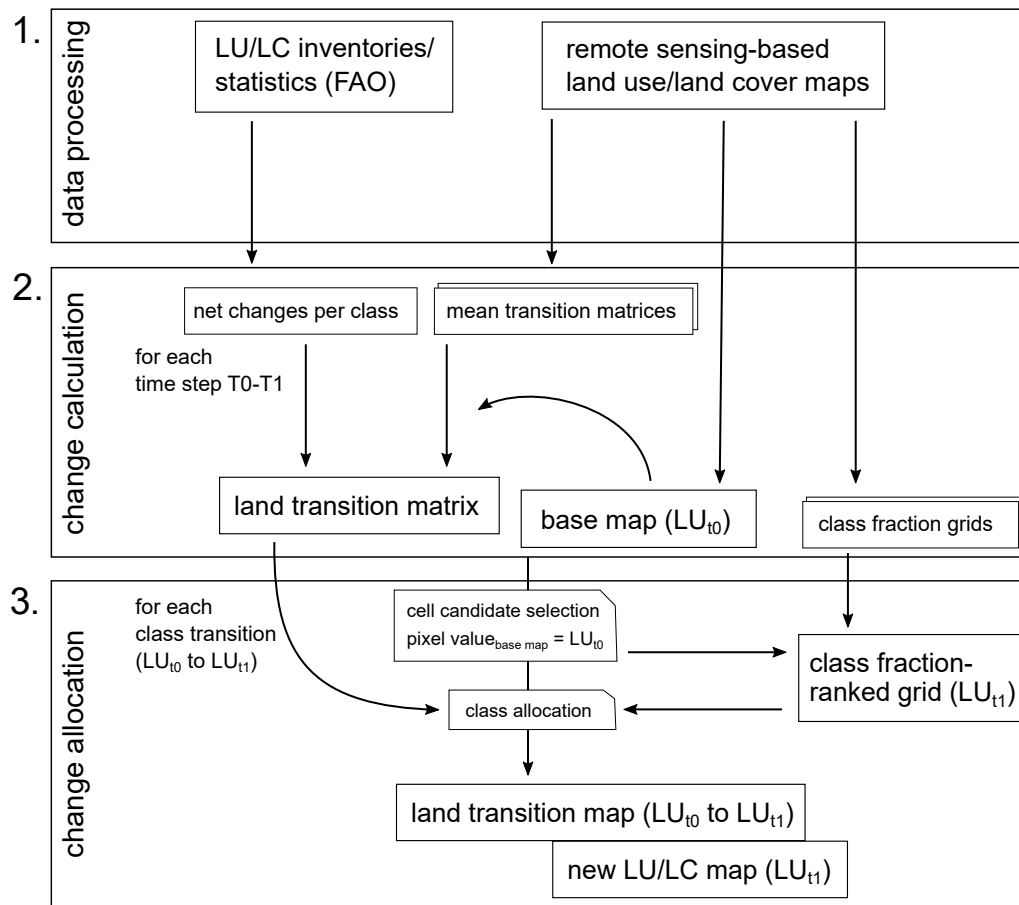


**Figure 2.2:** Methodological steps of the land use/cover change allocation procedure. (1) Input datasets are preprocessed and harmonised. (2) land use/cover change matrices are calculated for each time step (annually) and each country. In the backward mode (2015-1960),  $LU_{t_0}$  refers to land use/cover classes in a specific year (time step 0),  $LU_{t_1}$  refers to a land use/cover classes in the previous year (time step 1). In the forward mode (2015-2019),  $LU_{t_1}$  refers to a land use/cover classes in the subsequent year (time step 1). (3) All combinations of land transitions between land use/cover classes are iteratively allocated on the map.

with a sufficiently long time series (ESA CCI, MODIS MCD12Q1, GLAD UMD VCF) were back-casted in a stepwise manner, based on a linear extrapolation of the mean trend of the first five observed values in time.

Table 2.3: Generalised land cover classes used for dataset harmonisation

Land cover category	Copernicus LC100	ESA CCI LC	GLC2000	GLCNMO Cover	GlobeLand30	MODIS MCD12Q1	Definition and description
1. Urban	50	190	22	190	80	13	Artificial surfaces, urban and built-up areas, including urban parks and sports areas, green spaces, industrial, deposits, extractions sites (mining etc.)
2. Cropland	40	10-12, 20, 30, 40	16-18	11, 14, 20, 30	10	12, 14	Herbaceous and woody crops (also for hay production) including tree/shrub crops, orchards, plantations, multiple/layered crops, incl. mosaics (with cropland area fraction $\geq 40\%$ )
3. Grassland	30	110, 130	13	120, 140	30	9, 10	(Natural) herbaceous plants (cover $\geq 10\%$ ) including grasslands: prairies, steppes, savannah, mosaics with tree/shrubs
4. Forest	111-116, 121-126	50, 60-62, 70-72, 80-82, 90, 100, 160, 170	10	40, 50, 60, 70, 90, 100	20, 27	1-5, 8	Trees with $> 5m$ height (cover $\geq 10\%$ ) including forest plantation, trees on seasonally or permanently flooded areas, including mangroves
5. Shrubland	20, 90, 100	120-122, 140, 180	11, 12	110, 130, 150, 170, 180	40, 50, 70	6, 7, 11	Shrub cover ( $\geq 10\%$ ), including permanently or regularly flooded areas (wetlands), (herbaceous) wetlands
6. Sparse/no vegetation	70	150-153, 200-202, 220	14, 19, 21	200, 220	90, 100	15, 16	Bare areas, sparse vegetation (2-10%), snow and ice, rocks, sand, mudflats

### 2.2.3 Probability maps for land use/cover categories

For each of the harmonised land cover categories (see Table 2.33) and year of the study period, we derived maps of the average area fractions per grid cell if more than one data source was available. All available datasets were treated as equal. Note that data-inherent uncertainties such as misclassification, over- and under-representation of certain land use/cover categories in individual datasets are propagated to some degree. However, such inconsistencies are attenuated by relying on multiple datasets instead of a single data source.

Based on the resulting maps of area fractions, we derived probability maps for our final land use/cover categories (see Table 2.2), which were the basis of the change allocation procedure. The rules for assembling these class probability maps and, on this, converting the generalised land cover maps (see Table 2.3) to our target land use/cover categories (see Table 2.2) are displayed in Table 2.4.

**Table 2.4:** Rules for assembling class probability maps for the target land use/cover categories

Land use/cover category	Rule for probability maps
1. Urban	Mean (all available year-specific urban area fractions)
2. Cropland	Mean (all available year-specific cropland area fractions)
3. Pasture/rangeland	Mean (Mean [all available year-specific grassland area fractions], GLW ruminant density)
4. Forest	Mean (all available year-specific forest/tree cover area fractions)
5. Unmanaged grass-/shrubland	Mean (Mean [all available year-specific shrubland area fractions], Mean [all available year-specific grassland area fractions])
6. Sparse/no vegetation	Mean (all available year-specific other land area fractions)

For separating managed from unmanaged grasslands, we first combined the maps for grassland and shrubland by calculating the mean of their area fractions. We used the resulting maps as probability layers for land use/cover category 5: Unmanaged grass/shrubland. For generating the probability layers of land use/cover category 3: Pasture/rangelands, we used the Gridded Livestock World v3 (GLW, see Table 2.1), which indicates the density of ruminants for the reference year 2010, as an additional indicator of pasture usage. We calculated the mean of the GLW ruminant densities and the area fraction of combined grassland and shrubland categories and used the resulting maps as probability layers for land use/cover category 3: Pasture/rangelands. Note that, in contrast to grass- and shrubland area fractions, ruminant density information is static (year 2010). Changes in ruminant numbers over time were not considered.

### 2.2.4 Base map calibration

We used the recently released Copernicus LC100 Global Land Cover map for the reference year 2015 to generate a base map for the subsequent reconstruction of land use/cover change. After reclassifying the map into the generalised land cover categories (see Table 2.3), we reprojected and resampled it into the targeted projection (Eckert IV), spatial extent and grid resolution (1 km) using majority cell values (mode), resulting in a preliminary land cover map. We calibrated this preliminary base map to FAO national land use statistics for forest, cropland and pasture area (Food and Agriculture Organization of the United Nations (FAO), 2019a) using the derived area fractions for each category. The rules applied for the base map calibration procedure are given in Table 2.5.

**Table 2.5:** Rule-set for calibrating the base map to FAO land use statistics

Land use category	if base map class area > FAO land use area	if base map class area < FAO land use area
<b>Forest</b> (FAO: Forest)	Forest cells with lowest forest area fractions (ranked) were converted to the non-forest category with highest area fraction.	Non-forest cells with highest woody area fractions (ranked mean of forest and shrubland area fractions) were converted to forest area (excluding woody area fraction below 5%).
<b>Cropland</b> (FAO: Arable land and Permanent cropland)	Cropland cells with lowest cropland area fractions (ranked) were converted to the non-cropland category with highest area fraction (excluding forest).	Non-cropland cells (forest excluded) with highest cropland area fractions were converted to cropland area (excluding cropland area fraction below 5%).
<b>Pasture/rangeland</b> (FAO: Permanent meadows and pastures)	Pasture cells with lowest pasture probability (ranked sum of grassland area fraction and pasture/rangeland probability mask 2015, see Table 2.4) were converted to the non-pasture category with highest area fraction (excluding forest and cropland).	Non-pasture cells (cropland and forest excluded) with highest pasture probability (ranked sum of grassland area fraction and pasture/rangeland probability mask 2015, see Table 2.4) were converted to pasture area (excluding pasture probability below 5%).

### 2.2.5 Preparing datasets for national land use/cover change matrices

The absolute matrices of land use/cover change, and the land area in each land use/cover category that changes into another category in a specific country and year, were generated from two different data streams: FAO statistics and remote sensing products. First, we prepared tables of FAO land use area (Food and Agriculture Organization of the United Nations (FAO), 2019a) and population statistics (Food and Agriculture Organization of the United Nations (FAO), 2019b) per country and year of the study period. The country extents in the year 2015 were used to ensure a consistent country-specific reconstruction.

Thus, land use and population values were completed for countries that have changed in area over the period of 1960-2015 based on trends in the FAO recorded values for the former country before the respective year of change (see Table 2.6). For Europe, land use/cover values derived from the predecessor HILDA dataset (Fuchs et al., 2013) were used to complete the table for periods without FAO data records (e.g. forest before 1990, agricultural areas before 1961). We filled data gaps in the land use table by linear temporal intra- and extrapolation for each country. Secondly, we derived country-specific gross change ratios from transition matrices based on temporally-consistent, long-term, remote sensing-based land cover maps: ESA CCI Land Cover, and regional high-resolution datasets for specific regions (CORINE, MoEF Indonesia, AAFC Land Use Canada, NLCD Land Cover, and Australia DLCD). For each country, a mean transition matrix was calculated across all available time steps in the original spatial resolution of the datasets.

**Table 2.6:** Countries with changes in area in 1960-2015: Former/subsequent names and years of change (start of records from succeeding country according to FAO)

Former countries	Countries in 2015	Year of change
Sudan (former)	Sudan, South Sudan	2011
Serbia and Montenegro	Serbia, Montenegro	2006
Belgium-Luxembourg	Belgium, Luxembourg	2000
Czechoslovakia	Slovakia, Czechia	1993
Ethiopia PDR	Ethiopia, Eritrea	1993
USSR	Russian Federation, Ukraine, Belarus, Armenia, Azerbaijan, Estonia, Georgia, Kazakhstan, Kyrgyzstan, Latvia, Lithuania, Republic of Moldova, Tajikistan, Turkmenistan, Uzbekistan	1992
Yugoslav SFR	Croatia, The former Yugoslav Republic of Macedonia, Slovenia, Bosnia and Herzegovina, Serbia and Montenegro	1992
Pacific Islands Trust Territory	Marshall Islands, Micronesia (Federated States of), Northern Mariana Islands, Palau	1991
Saint Christopher-Nevis-Anguilla	Anguilla, Saint Kitts and Nevis	1980
Leeward Islands	Antigua and Barbuda, Saint Christopher-Nevis-Anguilla, Montserrat, British Virgin Islands, Dominica	1961

### 2.2.6 Change calculation

We derived net changes in the categories 2: Cropland, 3: Pasture/rangelands, and 4: Forest from the FAO land use inventories (Arable land and Permanent cropland, Permanent meadows and pastures, Forest), applying the relative changes to the areas from the base map, respectively. We used the base map and the relative population development from FAO (Total population) as a proxy for net urban area change (land use/cover 1: Urban areas). The remaining land portion (FAO land area minus Urban, Cropland, Pasture/rangelands, and Forest area) was divided proportionally into land use/cover category 5: Unmanaged grass/shrubland and 6: Sparse/no vegetation according to the area ratio of these categories in the base map.

During the change allocation procedure, a new transition matrix including all gross changes between the land use/cover categories was iteratively built for each time step, each country and each land transition based on the minimum ratio of gross change to class area from the data-derived country-specific mean transition matrix. This ratio represents the average share of land under a specific land use/cover category that is converted to another category, either a gain or a loss in land use/cover category.

### 2.2.7 Change allocation

Based on the recalculated country- and year-specific transition matrices, the magnitude of land use/cover change was distributed over the grid by means of corresponding probability maps for each land use/cover category. This was carried out in three consecutive steps: First (round 1), change was assigned if the respective land use/cover categories held the highest area fraction and were greater than 0.1. Second (round 2), if no candidate pixels were found in round 1, change was allocated to grid cells where the area fraction of the respective land use/cover category was greater than 0.4. Round 3 applied if no candidate pixels were existent after rounds 1 and 2. In the end, no changes were allocated in this step. This procedure was undertaken iteratively for each year (in a back- and forward mode starting from the base year 2015, respectively), for each individual country and for each land transition between two land use/cover categories. The output of each change allocation step of the annual loop was a new global map of land use/cover, which served as the base map for the next processing step.

### 2.2.8 Change analysis

The output of the HILDA+ change allocation procedure are annual maps of global land use/cover states (the distribution of land use/cover categories) and transitions. The transition layers served as the basis for analysing spatial extent, patterns, rates and dynamics of global land use change. Looping through all transition layers, we classified the coded transitions into change and non-change events and counted their occurrence per pixel. The sum of all change occurrences represents the total amount of gross land use/cover

change for the study period. Similarly, land use/cover category-specific changes were derived by classifying the coded land transitions into gain, loss, or stable/non-change events within the respective land use/cover category. Again, we summed up the occurrences of different events iteratively through time. Based on the resulting frequencies, we assigned land use/cover category-specific change on the global grid: gain (single change event), loss (single change event), both gain and loss (multiple change events).

### 2.2.9 Uncertainty assessment

In order to analyse the uncertainty and assess the reliability of the resulting HILDA+ dataset, we derived annual layers of uncertainty information based on the available input land use/cover datasets. The number of available datasets, the maximum deviation in class area fraction and the mean class area fraction from all available datasets per year were used to generate per-pixel quality information. Based on the multi-year mean of dataset agreement (maximum deviation) and class coverage (mean class area fraction), global quality flags were derived and mapped across the globe (see Table 2.7, Figures 2.3 and 2.4).

**Table 2.7:** Quality flags for HILDA+ Global land use/cover change 1960-2019: Rules are based on the global multi-year mean deviation and class area fraction of the respective land use/cover category from available datasets (see Table 2.3).

Quality flag	Category name	Definition/rules
11	good agreement/ high class coverage	deviation $\leq 0.4$ / class area fraction $\geq 0.6$
12	good agreement/ moderate class coverage	deviation $\leq 0.4$ / $0.4 >$ class area fraction $< 0.6$
13	good agreement/ low class coverage	deviation $\leq 0.4$ / class area fraction $\leq 0.4$
21	low agreement/ good class coverage	deviation $> 0.4$ / class area fraction $\geq 0.6$
22	low agreement/ moderate class coverage	deviation $> 0.4$ / $0.4 >$ class area fraction $< 0.6$
23	low agreement/ low class coverage	deviation $> 0.4$ / class area fraction $\leq 0.4$

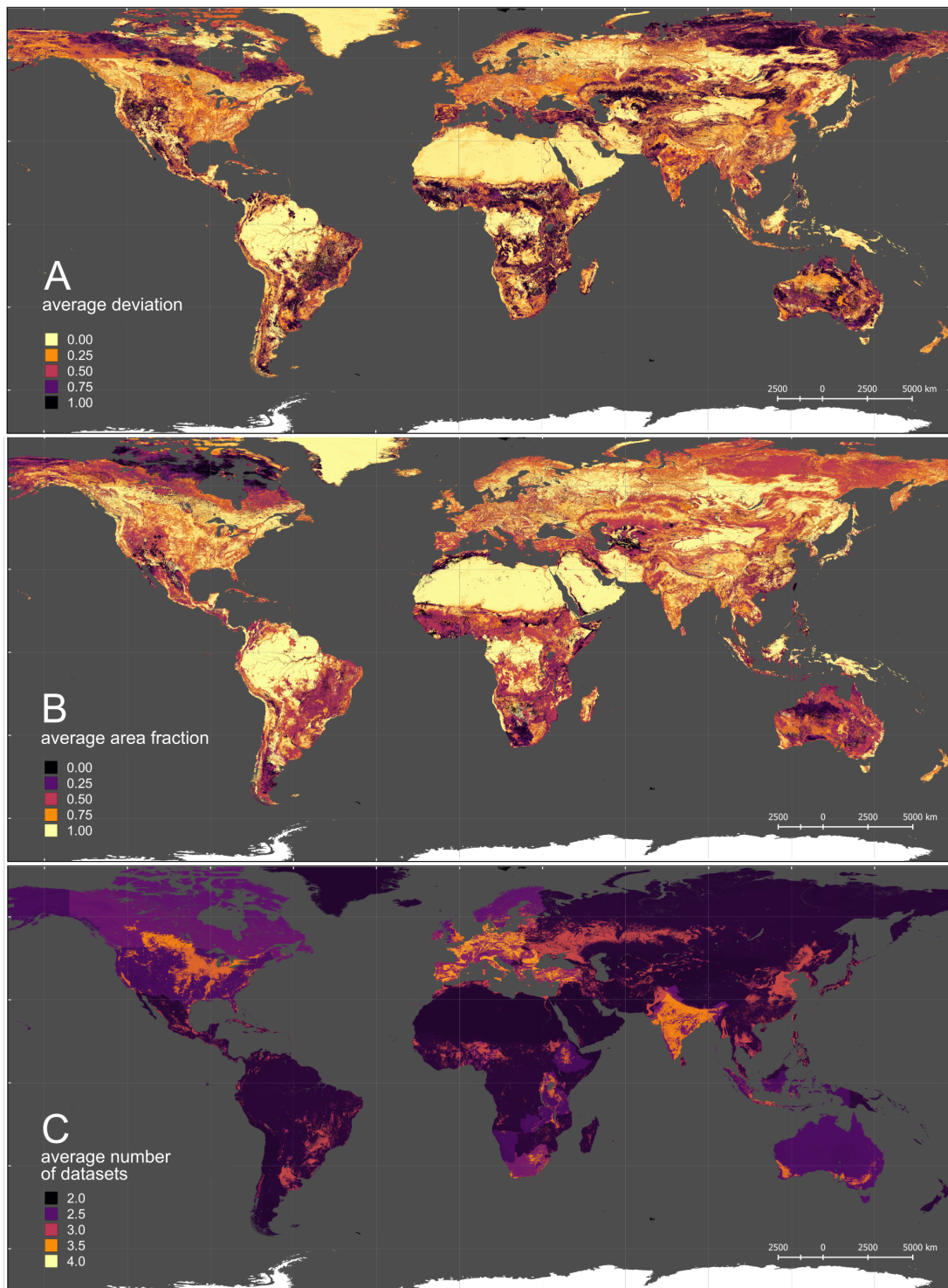


**Figure 2.3:** Spatial distribution of global mean uncertainty information for HILDA+. Global land use/cover change 1960-2019: Multi-year mean of A) maximum deviation of class area fraction, B) land use/cover class area fraction, C) number of available datasets. Layers were derived on an annual basis for each indicated land use/cover category by HILDA+ and averaged for the entire period (1960-2019). Note that, for land use/cover category 3: Pasture/rangeland, class area fractions refer to grassland and, for land use/cover category 5: Unmanaged grass/shrubland, class area fractions comprise grassland and shrubland.

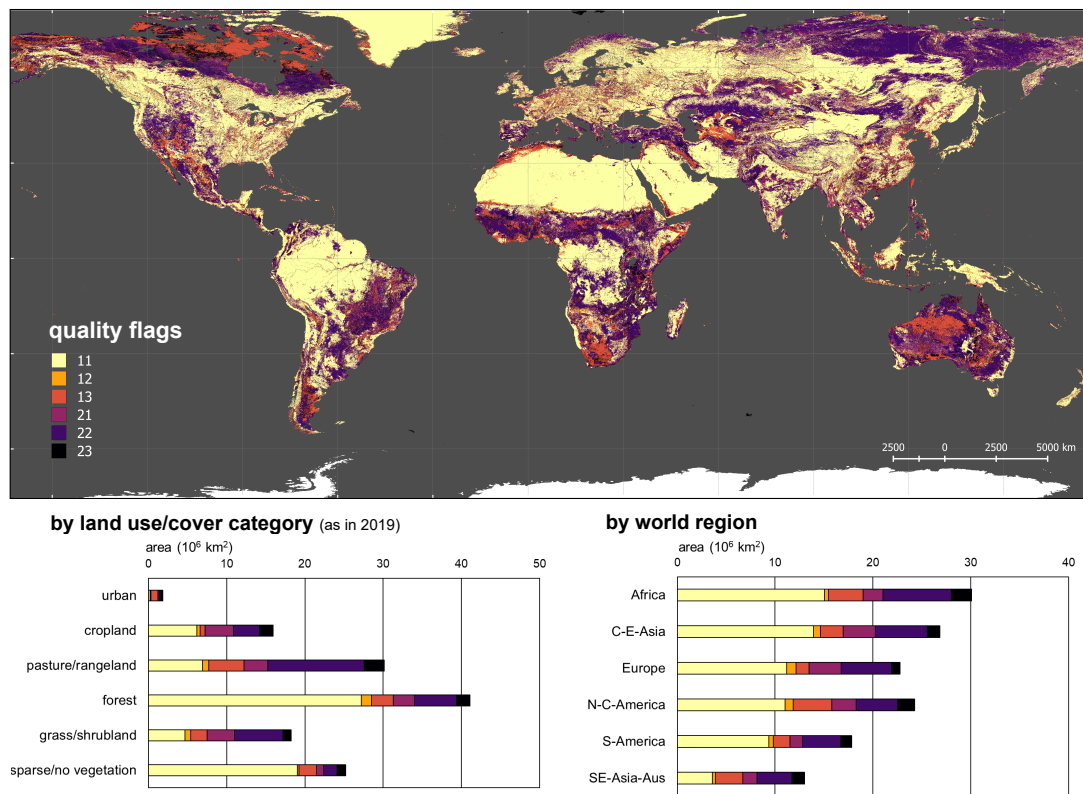


**Figure 2.4:** Spatial distribution of multi-year mean quality flags for HILDA+ global land use/cover change 1960-2019. Quality flags: Good agreement with high (11), moderate (12) and low (13) class coverage; Low agreement with high (21), moderate (22) and low (23) class coverage.

## 2.3 Results and discussion

### 2.3.1 Spatial extent and diverging patterns of global land use change

We estimate that 17% of the Earth's land surface has changed at least once between the six land categories from 1960 to 2019 (see Figure 2.5). When summing all of the individual change events (including areas of multiple change), the total land change extent is 43 million  $\text{km}^2$ , which is almost a third of the global land surface. This means that, on average, a land area of about twice the size of Germany (720,000  $\text{km}^2$ ) has changed every year since 1960.

We identify a global net loss of forest area of 0.8 million  $\text{km}^2$ , but an expansion in global agriculture (i.e. cropland and pasture/rangeland) of 1.0 and 0.9 million  $\text{km}^2$ , respectively.

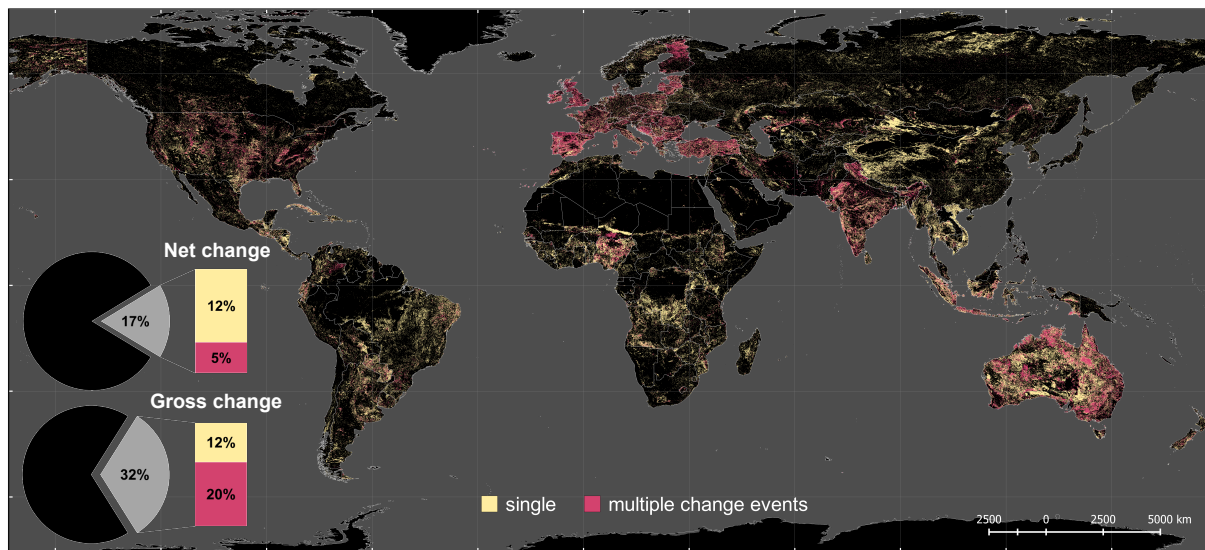


**Figure 2.5:** Spatial extent of global land use/cover change: Share of the total land surface without (net change) and with consideration of multiple changes (gross change) between six major land use/cover categories (urban area, cropland, pasture/rangeland, forest, unmanaged grass/shrubland, non-/sparsely vegetated land) in 1960-2019. The spatial extent of land use/cover change is displayed in yellow (areas with single change events) and red (areas with multiple change events).

However, the global trends in land use change conceal many regionally different trajectories. Whereas forest areas in the Global North (including China) have increased, forest areas in developing countries of the Global South have strongly decreased. The North-South difference in gains and losses of forests, is the opposite for global cropland areas, which have decreased in the Global North and increased in the Global South. The difference between North and South is less pronounced for pasture/rangeland change, since pasture expansion both in China and Brazil accounts for a major part of the global land area (see Figure 2.6).

These globally diverging land use change processes are supported by numerous studies, e.g. forest gain caused by political reforestation incentives in China (Bryan et al., 2018; Chen et al., 2019; Feng et al., 2016), agricultural land abandonment in Europe (Kaplan et al., 2012) and the U.S. (Kauppi et al., 2006; Oswalt et al., 2019; Ramankutty et al., 2010), climate-induced vegetation shifts in Siberia (Esper & Schweingruber, 2004; Kharuk et al., 2013; Tchebakova et al., 2009), and woody encroachment of rangelands in the U.S. (Van Auken, 2000) and Australia (Holmes, 2002). Conversely, tropical deforestation has occurred for the production of beef, sugar cane and soybean (Barona et al., 2010; Macedo et al., 2012) in the Brazilian Amazon, oil palm in Southeast Asia (Austin et al., 2019; Gaveau et al., 2016; Nomura et al., 2019; Wicke et al., 2011), and cocoa in Nigeria and Cameroon (Chatham House, 2018; Kroeger et al., 2017; Ordway et al., 2017).

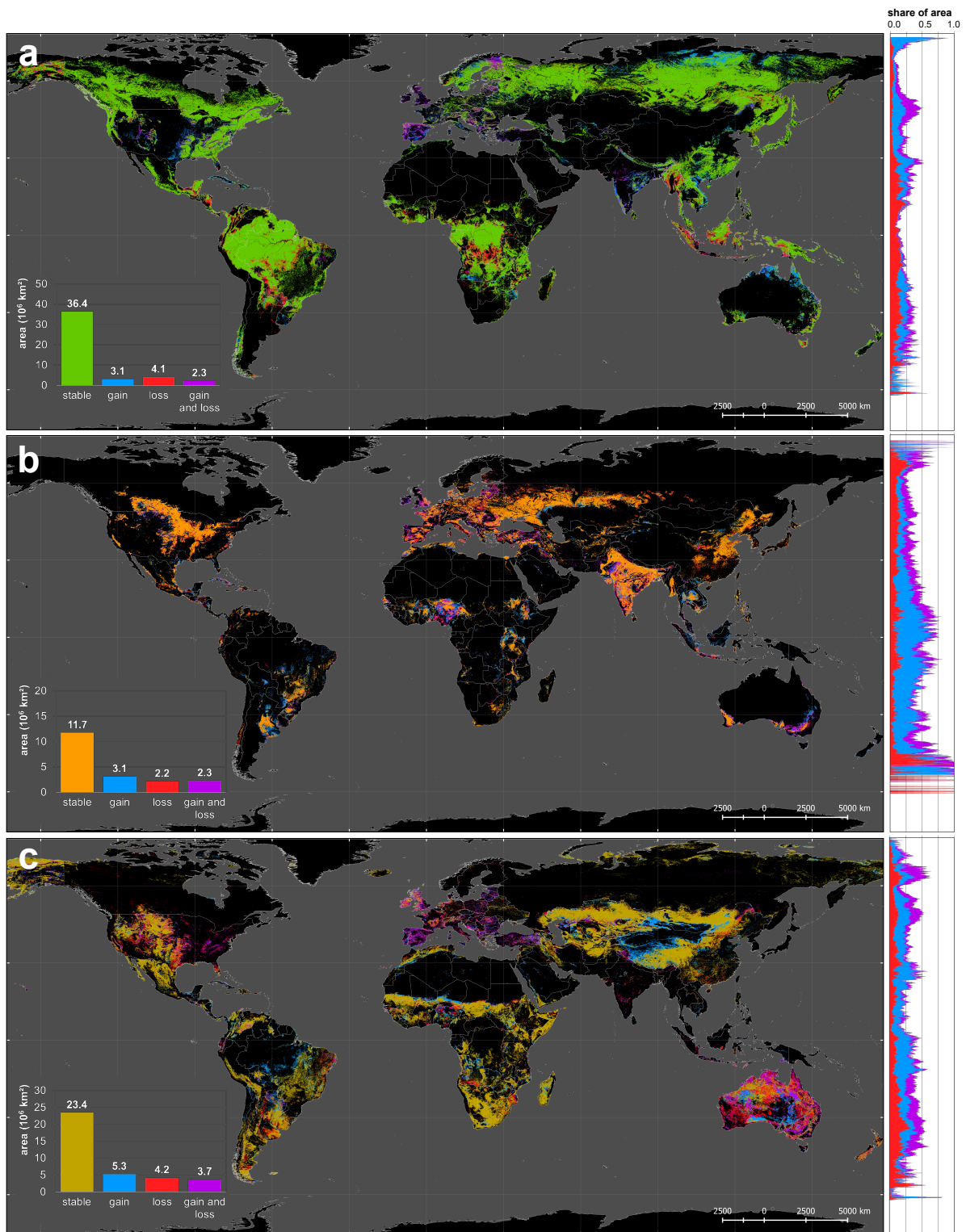


**Figure 2.6:** Global forest, cropland and pasture/rangeland change: Spatial distribution of a) forest, b) cropland, and c) pasture/rangeland extent (stable area) and change (gain and loss) between 1960 and 2019. Area charts on the right show the stacked share of gains, losses and multiple change area (on which both gains and losses have occurred) related to the total area under the respective land use/cover category along each geographic latitude.

Furthermore, rangelands have expanded widely into marginal lands in China (Bryan et al., 2018; Hua & Squires, 2015).

By separating land use change into areas with a single change (e.g. deforestation) or multiple change events (e.g. crop-grass rotation), we see clear patterns across the globe (see Figure 2.5). 38% of all land transitions are single change events, which are most evident in developing countries of the Global South. Around half of the areas with single change events (48%) comprise agricultural expansion, which can be seen, for example, in the expanding pastureland of China or in tropical deforestation in the Amazon. Multiple change events make up 62% of all land transitions. In contrast to single changes, multiple changes dominate in the developed countries of the Global North (e.g. in Europe, the U.S., Australia) and rapidly growing economies (e.g. Nigeria, India). Here, agricultural intensification, as in the EU and the U.S. and/or major transitions in the agricultural sector, for example, the switch from subsistence to commodity crops in Nigeria (FAO, 2020d), have taken place over the last decades. 86% of all multiple change events are agricultural land use changes (land transitions related to cropland or pasture/rangeland). Some of these changes are directly or indirectly linked to land management and agricultural intensification. Cropland-pasture/rangeland transitions (11% of all multiple change events) can indicate areas of crop rotation or mixed crop-livestock systems as in the U.S., Australia and in Europe (Bell & Moore, 2012; Rosenzweig et al., 2018). Most multiple changes (75%) take place between managed and unmanaged land such as the abandonment of cropland, e.g. due to agricultural intensification on more suitable land as in Post-Soviet Eastern Europe (Prishchepov et al., 2013), rangeland-shrub encroachments as in rotational grazing systems in Australia (Eldridge & Soliveres, 2015) or the Mediterranean as well as transitions between agricultural land and forest as in agroforestry systems in western Europe (Rolo & Moreno, 2019).

### 2.3.2 Temporal dynamics of global land use change and its relation to globalised markets

The rate of global land use change was not constant over time. In analysing the temporal dynamics, we identify two different phases: (1) an acceleration phase with an increasing rate of change from 1960 to 2004; and, (2) a decreasing rate of change from 2005 to 2019 (see Figure 2.7). The transition from constant to rising rates of land use change has been discussed in the context of shifting global food regimes and coincides with a period when global food production changed from agro-technological intensification (driven by the Green Revolution in the 1960s) to the production for globalised markets and increasing trade, especially during the 1990s (Anderson, 2010; Krausmann & Langthaler, 2019). We find this acceleration phase to be more distinct in regions of the Global South, as observed in South America, Africa, and Southeast Asia (see Figure 2.7), where production and export of commodity crops have increased, most strikingly since the 2000s (see Supplementary Figure 1 and 2). The growing influence of tele-connected markets is

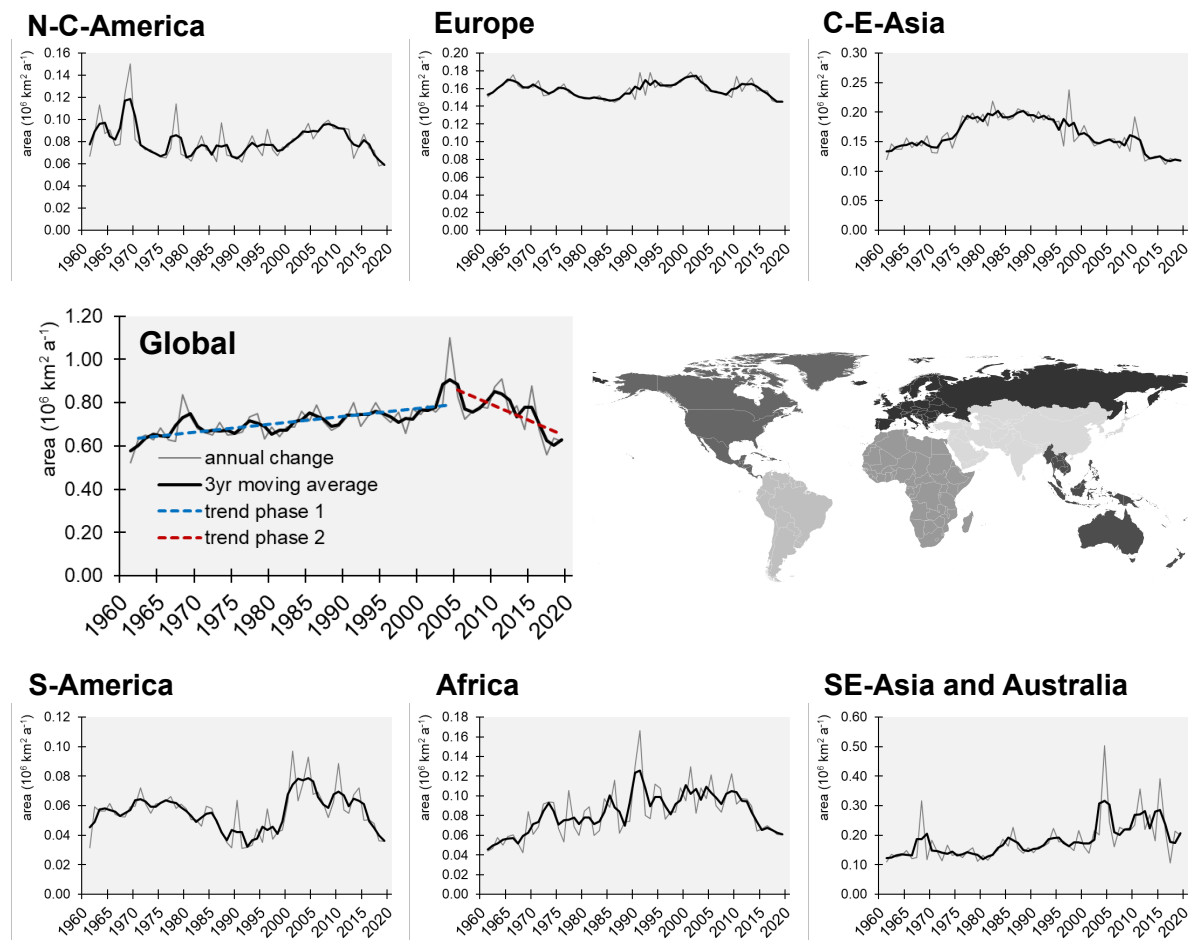


**Figure 2.7:** Rate of land use change: Annual rate of land use/cover change between 1960 and 2019 for different world regions and the globe. Global trends are depicted for phases 1: 1960-2004 and 2: 2005-2015. Grey lines show the annual change, black lines show the smoothed annual change based on a three-year moving average. The map shows the spatial extent of the presented world regions in different shades of grey.

found to be a major driver of land use change, particularly deforestation for commodity crops in the Global South (Ordway et al., 2017). This off-shoring of land use change from the Global North to the South is evident in the growing proportion of cropland in the countries of the Global South used for export and consumption outside of their territories (Yu et al., 2013).

However, the data suggest a rather abrupt change to decreasing rates of land use change in the period from 2005, which is most evident in Africa and South America (see Figure 2.7), regions of the Subtropics and Tropics (see Supplementary Figure 3). We hypothesise that the transition from accelerating to decelerating land use change is related to market developments in the context of the global economic and food crisis in 2007-2009. Before the crisis, rising demand for food, animal feed and biofuels as well as increasing oil prices (reaching an all-time high in 2008 at \$145.31 per barrel of Crude Macrotrends LLC (2010)

stimulated global agricultural production, which enhanced global land use change (Rajcaniova et al., 2014). In particular, high oil prices made bioenergy crops more competitive and profitable compared to fossil fuels. Increasing demand, mostly in the developed countries of the Global North, spurred bioenergy crop expansion in the Global South (e.g. production of oil crops in Ghana, Argentina, Brazil, and Indonesia, see Supplementary Figure 1). Biofuel policies, climatic extremes and export bans led to global food price spikes in 2007-2008 (Akram-Lodhi, 2012) and in 2010 (Bellemare, 2015; d'Amour et al., 2016), which raised concerns about food security in many import-dependent countries and rapidly growing economies (e.g. the EU, China or India). A wave of large-scale, transboundary land acquisitions and foreign investments in agriculture emerged, mostly targeting sub-Saharan Africa, Southeast Asia and South America (Arezki et al., 2015; Chen et al., 2017; Krausmann & Langthaler, 2019). This development is reflected in the sudden increase in the rate of land use change (during 2000-2005), ensuing fluctuations (during 2006-2010) and sharp decrease (after 2010) in countries of the Global South, e.g. Brazil, Argentina, or Ethiopia (see Supplementary Figure 4).

We find that the observed slowdown of global land use change after the economic crisis 2007-2009 is mainly caused by a decline in agricultural expansion in the countries of the Global South, particularly pronounced in Argentina, Ghana and Ethiopia (see Supplementary Figure 5). We postulate that the global deceleration of land use change is related to market mechanisms during the economic crisis. With the economic boom coming to an end during the Great Recession, the global demand for commodities dropped. Countries which focussed on the production of commodity crops for global markets prior to the crisis (e.g. Argentina, Brazil, Ghana, or Indonesia), no longer found buyers for their goods, reduced agricultural production and, thus, the rate of agricultural land expansion. The observed sharp decline in the rate of land use change, especially in Africa (see Figure 2.7), may be further caused by a decrease in the number and size of global land acquisitions after the financial crisis in 2007-2009. Since then, hedge funds in land became less common (Mechiche-Alami et al., 2019) and concerns were raised about unsustainable practices related to transboundary land acquisitions (e.g. land/water degradation and displacement of rural labour) (Akram-Lodhi, 2012; Mechiche-Alami et al., 2019). Resulting incentives from international organisations and exporting countries to limit land trade may have led to the recent decline in large-scale land acquisitions (Mechiche-Alami et al., 2019).

Aside from globalised trade, other important drivers of land change dynamics, which have increasingly influenced the rate of land use change during the deceleration phase, are climate change and its associated impacts such as extreme events, drought and floods. Agricultural land use has been affected by droughts in West (Henchiri et al., 2020) and Eastern Africa (Biazin & Sterk, 2013) during the 2000s, which can be observed in the strong decline in the rate of land use change in Ethiopia after the 2010/11 drought (see Supplementary Figure 2.8). Furthermore, land degradation, caused by both climatic variability and human activities, has often been associated with cropland abandonment,

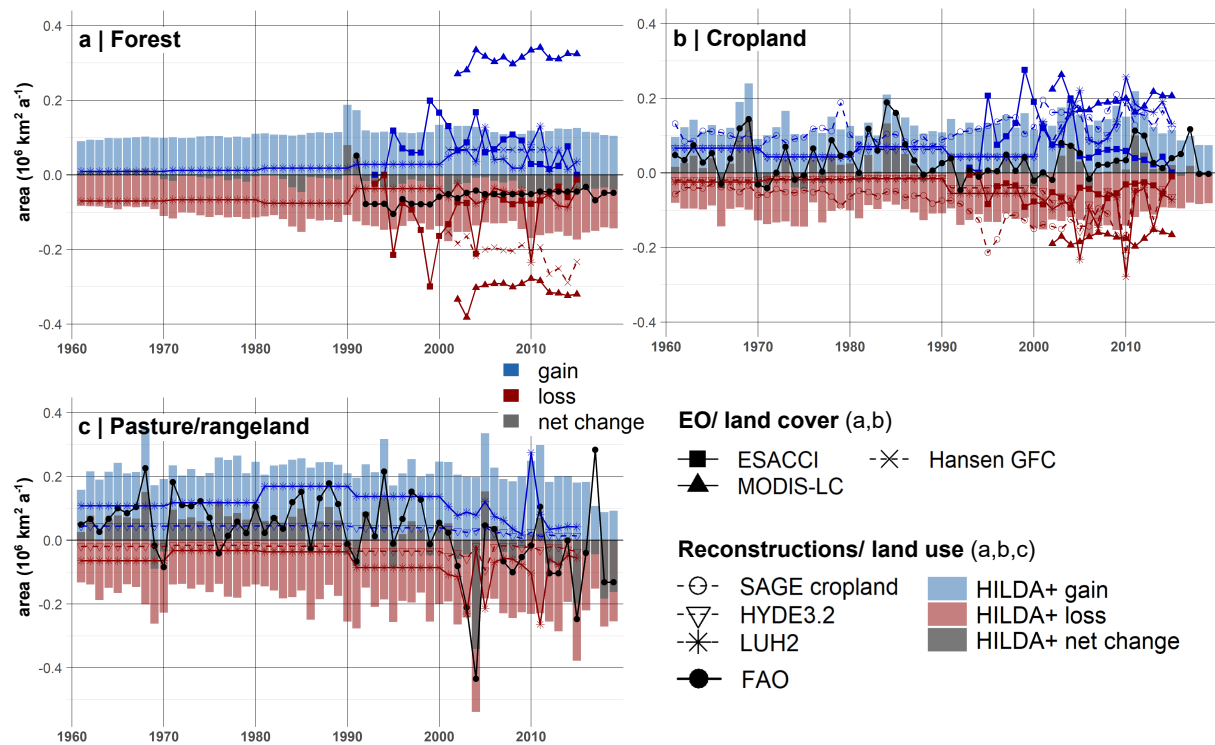


**Figure 2.8:** Comparison of forest, cropland and pasture/rangeland changes: Global comparison of annual change of a) forest, b) cropland, and c) pasture/rangeland (gain, loss and net change area per year) from HILDA+, different Earth Observation (EO)-based land cover datasets (ESACCI, MODIS LC, Hansen GFC), land use reconstruction models (SAGE cropland, HYDE3.2, LUH2) and FAO land use statistics.

subsequent expansion of agricultural land and deforestation elsewhere, as widely observed in tropical regions (Lambin et al., 2003).

When analysing the temporal dynamics of global land use change per land use/cover category, we find large annual variability in agricultural land use change. While global forest area shows a rather steady annual net decrease, which accelerated during the 1990s (see Figure 2.8a), croplands and pasture/rangeland show large fluctuations over time; about four times higher than observed for forests. This difference likely derives from a combination of the five-yearly reporting scheme of the FAO/FRA forest data and the quicker response times of agricultural land use change to socio-economic developments. In particular, the rate of agricultural land use change can be affected by political regime shifts (e.g. land abandonment after the collapse of the Soviet Union in 1990) (Schierhorn et al., 2013), disruptions in globalised supply chains (e.g. the US embargo on soybeans against Russia in 1980) (Fuchs et al., 2019; Zeimetz et al., 1987), nature conservation incentives (e.g. avoided deforestation as in REDD policies) (Lambin & Meyfroidt, 2011), natural hazards and extreme events such as droughts (Biazin & Sterk, 2013; Winkler et al., 2017). High inter-annual change dynamics in global agricultural land mainly emerged in

the 1990s after a long period of net expansion. This matches the period when major geopolitical shifts (particularly the collapse of the USSR) took place and market-driven food production gained in importance.

Whereas pasture/rangelands show a downward trend, which has been attributed to technology advances in the livestock sector (Blaustein-Rejto et al., 2019), global croplands, by contrast, experienced waves of increasing expansion since 2000 (see Figure 2.8b-c).

### 2.3.3 Comparing the rate of global land use change

Comparing the HILDA+ annual change rates with previous land use reconstructions (see Figure 2.8) demonstrates that the area affected by global land use change is nearly four (3.7) times greater than previously thought. A comparison of the rates land use change between HILDA+ and other land use datasets is presented in Figure 2.9. Corresponding annual change rates and considered periods are listed in Table 2.8. Specifically, the mean land use change rate from HILDA+ is 2.4 times as high as that of LUH2 (Hurt et al., 2020), 4.4 times as high as that of HYDE3.2 and 1.3 times as high as that of SAGE cropland, an update from Ramankutty & Foley (1999). This deviation is the effect of considering gross changes derived from Earth Observation data in HILDA+, which are not or only partially included in the other datasets.

Land cover change rates derived from higher-resolution remote sensing datasets such as Hansen GFC (Hansen et al., 2013), ESACCI (ESA, 2017) and MODIS (Friedl & Sulla-Menashe, 2019) are on average about the same order of magnitude (1.1 times) as for HILDA+. In particular, the HILDA+ annual change rate is on average 1.3 times greater than from remote sensing datasets, with MODIS (Friedl & Sulla-Menashe, 2019) deviating by +90% ESACCI (ESA, 2017) deviating by -60% and Hansen GFC (Hansen et al., 2013) deviating by 0% from HILDA+ change rates. These differences are most evident for annual forest change rates (see Figure 2.8a) and can be explained by different land cover classes on which the original datasets are based, their diverse semantics and delimitations (see Table 2.1 and 2.3).

Since HILDA+ is built on multiple heterogeneous datasets, errors inherent in single datasets are attenuated during the change allocation procedure. By harmonising multiple information in the change allocation procedure, we build on a confluence of evidence. Thus, HILDA+ can be seen as a synthesis product of quality-tested, recognised land use/cover datasets. To assess the uncertainty of HILDA+ maps of global land use change, we analysed the agreement of the used input datasets and the area fraction for each indicated land use/cover category on an annual basis (see Table 2.7, Figure 2.3 and Figure 2.4).

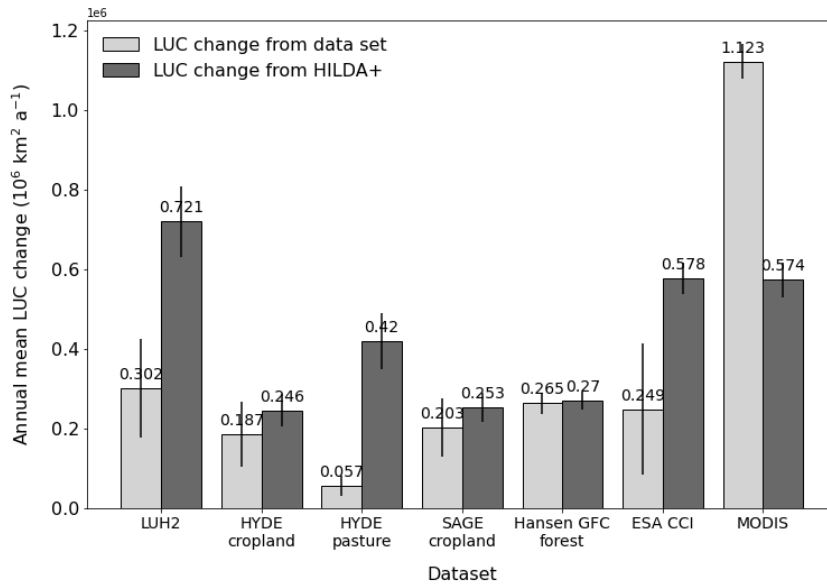


**Figure 2.9:** Comparison of change rates: Comparison of mean annual gross land use/cover change of different land use/cover change datasets (light grey bars) with HILDA+ (dark grey bars). Error bars represent the standard deviation.

**Table 2.8:** Comparison of annual gross land use/cover change (all transitions between included land use/cover categories or sum of gains and losses for individual land use/cover categories) of different datasets with HILDA+ for corresponding periods

Dataset	Categories included	Compared time period	Annual gross land use change (mean $\pm$ standard deviation in $10^3 \text{ km}^2 \text{ a}^{-1}$ )	
				HILDA+
LUH2	All	1960-2015	302 $\pm$ 125	721 $\pm$ 88
HYDE3.2 cropland	Cropland (2)	1960-2015	187 $\pm$ 82	246 $\pm$ 41
HYDE3.2 pasture	Pasture/rangelands (3)	1960-2015	57 $\pm$ 25	420 $\pm$ 71
SAGE cropland	Cropland (2)	1960-2011	203 $\pm$ 74	253 $\pm$ 37
Hansen GFC forest	Forest (4)	2000-2012*	265 $\pm$ 27	270 $\pm$ 21
ESA CCI	All with combined grassland (3+5)	1992-2015	249 $\pm$ 165	578 $\pm$ 40
MODIS	All with combined grassland (3+5)	2001-2015	1123 $\pm$ 44	574 $\pm$ 43

\*Hansen GFC covers forest gain only between 2000 and 2012 (no annual dynamics)

Dataset agreement differs per land use/cover category. Forests and areas with sparse/no vegetation show the highest agreements. On the other hand, dataset deviation is larger in agricultural land use/cover categories cropland and pasture/rangeland. Especially in heterogeneous landscapes, which hold a mix of managed and unmanaged lands, e.g. savannahs of Sub-Saharan Africa, rangelands in Australia or the grassy steppes of Central Asian, but also in the sparse taiga of eastern Siberia and the transition between Canadian boreal forest and tundra, land use/cover class coverage is ambiguous (lower area fractions) and, thus, dataset information deviates. The results of the HILDA+ land use change reconstruction show how synergistic information from Earth Observation data, reconstructions and national statistical inventories can be used to identify the spatial patterns and temporal dynamics of global land use change at unprecedented levels of detail. This study shows the benefit of using multiple, data-driven resources, which is needed for comprehensive land change assessment at a global scale. This gives more detailed insights into both the spatial patterns and the temporal dynamics of land use change across the Earth. We identify diverging processes of deforestation and agricultural expansion and demonstrate that the rate and extent of global land use change is responsive to socio-economic developments and disruptions such as the global economic crisis 2007-2009. The results suggest that global trade, affecting agriculture, has been one of the main drivers of global land use change over the last six decades.

The HILDA+ data have implications for the assessment of climate change, biodiversity loss and food security, especially in estimating carbon budgets, forest management and biomass. Due to its consistent and data-driven change allocation, HILDA+ is suited to global time series analysis. Although not free from potential data artefacts, inconsistencies of single datasets are attenuated through the use of multiple data sources. We aim to bridge the gap between long-term FAO-based land use trends, which lack spatial explicitness, and remote sensing-based observational land cover classifications, which lack long-term temporal consistency. Through the synergistic use of observational data and the provision of annual uncertainty measures, HILDA+ goes beyond conventional land use reconstructions that often rely on individual datasets, give an incomplete picture of land use/cover dynamics and lack information about uncertainty. HILDA+ provides a consistent time series of global land use/cover change that provides new possibilities for the analysis of global time series, the identification of possible drivers, impacts and correlations in the context of land use change. Thus, the HILDA+ data can contribute to better understanding the environmental impacts of land use change in the past by providing more detailed land change trajectories (e.g. affecting carbon pools) and their temporal classification. It can further improve the assessment of land use strategies in the future in support of policy, e.g. the Paris Climate Targets, the Sustainable Development Goals and the post-2020 agenda of the Convention on Biological Diversity.

## 2.4 Acknowledgements

This research has been supported by the European Commission, Horizon 2020 Framework Programme (VERIFY, grant no. 776810). K.W. was supported by the Open Science Fellows Programme of Wikimedia Deutschland e.V. (2019–2020). We acknowledge Christian Werner for helpful advices on developing the interactive map viewer to visualise our data.





## Chapter 3

# Expansion versus intensification of global agriculture

This chapter is based on:

Winkler, K., Fuchs, R., Rounsevell, M., & Herold, M. Expansion versus intensification of global agriculture. (in preparation).

*Landlords, like all other men, love to reap where they never sowed.*

Karl Marx

## Abstract

Population growth, changing consumption preferences, technological advances, and globalised trade have all shaped global agriculture. The growing demand has led to an increased agricultural production through either expansion (i.e. using more land) or intensification (i.e. increasing output per unit area). Yet the causes and interlinkage of global agricultural expansion and intensification remains unclear. Here we (1) analyse the spatio-temporal patterns of global changes in agriculture – particularly expansion, abandonment, intensification and extensification on croplands and pasture/rangelands – during six decades (1960-2020) and (2) explore the relationship between agricultural intensification and expansion at the country-scale. We hypothesise that when land is scarce and land prices are high, intensification is induced, but when land is abundant and thus relatively cheaper to purchase, land expansion occurs. We find that high-income countries have tended to pursue an intensification-abandonment trajectory in croplands and pasture/rangelands, whereas low-income countries have intensified less but substantially increased their agricultural area over time. Strikingly, emerging countries in tropical regions (e.g. Brazil, Indonesia, Thailand, Colombia, and Malaysia), show both the highest cropland intensification and expansion rates. Here we find evidence for a rebound effect of intensification of high-profit crops like soy bean, oil palm and sugar cane, stimulating further agricultural expansion into natural ecosystems. The expansion of tree crops is the underlying cause of more than half of the global deforestation for croplands. In contrast, pasture/rangeland changes in emerging countries may be subject to an induced intensification, when demand increases and land for further expansion becomes scarce. This supports the hypothesis of induced intensification due to land scarcity. Overall, the relationship of intensification and expansion on cropland and pasture/rangelands differs from region to region, but is affected to varying degrees by political intervention, global trade, technology transfer and climate change.

## 3.1 Introduction

Agriculture covers over one third of the global land surface (Ramankutty et al., 2008). With a rising world population, technological advances, changing consumption patterns and globalised trade, cropland and pasture areas have expanded and intensified their production during the last decades. A 300-year period of inexorable agricultural expansion has been replaced by the “Green Revolution” – a phase of technology-driven productivity increases in agriculture. In this context, high-yielding crop varieties have been developed through international programmes since the 1960s, with the aim of making new agricultural technologies available to farmers in the developing world (Qaim, 2020). The application of fertiliser, irrigation, pesticides, and new crop varieties, in combination with mechanisation has led to increasing crop production and yields (Evenson & Gollin, 2003; Kastner et al., 2022; Ramankutty et al., 2018).

Although agriculture produces more than enough food for all people, its global distribution is not equal and almost one billion people are suffering from insecure food supply. What is more, with increasing wealth, consumption is shifting towards diets that are more resource-intensive or of limited nutritional value, e.g. meat, refined fats and sugars compared to grains, legumes, fruits and vegetables (Ramankutty et al., 2018; Tilman & Clark, 2014). Already today, agriculture is under increasing pressure to meet the needs of a growing and more affluent population. To keep pace with estimated future demands, agricultural production would have to roughly double (Foley et al., 2011; Searchinger et al., 2019). However, agriculture already represents one of the greatest threats to the environment. Agricultural expansion and accompanying intensive management are major drivers of climate change, biodiversity loss, land and freshwater degradation (Foley et al., 2011; Power, 2010; Scott, 2020; Tilman et al., 2017; IPCC, 2019b; IPBES, 2019). Overall, agricultural land use has steadily become an arena of conflicting interests, as the demand for food, fodder and energy is balanced against climate change mitigation and biodiversity conservation (Egli et al., 2018; Thomas & Vazquez, 2022).

There are two main strategies to increase agricultural production: (1) expanding the area of croplands and pastures, concurrent with the loss of natural ecosystems, or (2) agricultural intensification by increasing the productivity (per unit area) of existing agricultural land (Licker et al., 2010). Agricultural intensification refers to an increase in agricultural land use intensity, which is a complex, multidimensional phenomenon that comprises three different dimensions: (1) input intensity including land, capital (e.g. technology, mechanisation, agrochemicals applied) and labour, (2) output intensity (relation of output to inputs of production, e.g. yields) and (3) system intensity such as the outcomes of production in form of altering system properties, e.g. biodiversity change, carbon loss (Erb et al., 2013; Kuemmerle et al., 2013).

In addition to land changes in agriculture such as agricultural expansion (increase in

agricultural land) and abandonment (decrease of agricultural land), we focus this study on agricultural land use intensity from an output perspective (e.g. crop yields and livestock production). We define agricultural intensification as increasing production per land area and time. In contrast, agricultural extensification (or “disintensification”) is the decrease in production per land area and time<sup>1</sup>.

Intensification is often regarded as sustainability pathway, since increasing the productivity on existing agricultural land is assumed to reduce pressure on land that can be returned to nature (land sparing) (Licker et al., 2010; Meyfroidt et al., 2018). However, this mechanism is controversial, as agricultural intensification can also lead to a rebound effect (Jevons paradox), where the adoption of intensification stimulates land use expansion by increasing the profitability of agriculture (Meyfroidt et al., 2018). Regarding the link between intensification and expansion, there is another concept, the theory of induced intensification. It states that intensification is a consequence of growing demand along with scarcity of available land for expansion, moderated by access to technology and institutional constraints (García et al., 2020). This concept of induced intensification fits the hypothesis of land supply, according to which intensification occurs when available land becomes scarce and consequently land prices rise. In this case, the costs of land conversion are high. If the demand of a product has a low elasticity to price (e.g. staple crops), land sparing is more likely. In contrast, when land for further agricultural expansion is available and land prices are low, agricultural land tends to expand (García et al., 2020; van Meijl et al., 2006).

Global analyses of the impacts of agricultural land use require spatial data on the evolution of the extent of agriculture, but also of agricultural land use intensity (Kastner et al., 2022). The spatio-temporal patterns of global agricultural land use change – expansion and contraction of agricultural areas – have frequently been studied (Hurt et al., 2020; Klein Goldewijk et al., 2017; Ramankutty & Foley, 1999; Taylor & Rising, 2021; Winkler et al., 2021), particularly in the context of tropical deforestation (Curtis et al., 2018; Ordway et al., 2017; Pendrill et al., 2022). However, the global patterns of agricultural land use intensity and the relationship between agricultural intensification and expansion have received less attention. Spatial data and analyses on agricultural land use intensity are often limited to specific crop types, selected regions, or narrow time spans (Gilbert et al., 2018; Grogan et al., 2022; Hu et al., 2020; Iizumi & Sakai, 2020; Kühling et al., 2016; Liu et al., 2021). Global data on agricultural management is scarce, thematically restricted (specific land use category or management type) and often comes with coarse spatial and/or temporal resolutions (Kuemmerle et al., 2013). This lack of consistent data leads to the fact that global land use change and agricultural management change are often analysed separately and rarely linked.

---

<sup>1</sup>Note that “extensification” is used here for “disintensification” and does not refer to expansion as sometimes used in the literature.

By using a data-driven approach of mapping past land use and intensity changes simultaneously at the global scale, we aim to (1) quantify the spatio-temporal patterns of global changes in agriculture, particularly expansion, abandonment, intensification and extensification on croplands and pasture/rangelands during the last six decades and (2) explore the relation of agricultural intensification and expansion at the country-scale. We hypothesise that agricultural intensification is induced after agricultural land expansion due to a scarcity of available land for further expansion and associated rising land prices.

## 3.2 Material and methods

### 3.2.1 Mapping cropland and pasture/rangeland area changes

We derived the changes in agricultural areas from the land use/cover maps of the Historic Land Dynamics Assessment+ (HILDA+), a data-driven reconstruction of global land use change from 1960 to 2020 at 1 km spatial resolution (Winkler et al., 2021). We used an updated version (version 2.0) of HILDA+ (to be submitted as an open data set to PANGAEA), which contains the following more detailed subcategories of the cropland class:

- Tree crops: Crops produced by trees, including the following FAO crop categories: Almonds, with shell; Apples; Apricots; Areca nuts; Apricots; Avocados; Cashew nuts with shell; Cashewapple; Cherries; Cherries, sour; Chestnut; Coconuts; Cocoa, beans; Coffee, green; Dates; Figs; Grapefruit (inc. pomelos); Grapes; Gums, natural; Hazelnuts, with shell; Jojoba seed; Kapok fibre; Kapok fruit; Kapokseed in shell; Karite nuts (sheanuts); Kiwi fruit; Kola nuts; Lemons and limes; Mangoes, mangosteens, guavas; Oil palm fruit; Oil, coconut (copra); Oil, olive, virgin; Oil, palm; Oil, palm kernel; Olives; Oranges; Peaches and nectarines; Pears; Pepper (piper spp.); Persimmons; Pistachios; Quinces; Rubber, natural; Tangerines, mandarins, clementines, satsumas; Tung nuts; Vanilla; Walnuts, with shell.
- Agroforestry: Crops grown among trees (mixture of cropland and tree cover)
- Annual crops: Crops that complete their life cycle within one year/growing season (all cropland which was not classified as tree crops or agroforestry).

In this updated HILDA+ version 2.0, additional cropland-related land use categories tree crops, agroforestry and annual crops were derived from a combination of remote sensing-based spatial datasets (see Table 3.1) and crop production statistics (tree crops defined as above) from the FAO (FAO, 2022b). Fractional information from the spatial data was used for a potential reallocation of HILDA+ version 1.0 land use categories cropland, pasture/rangeland, grass/shrubland or forests (not matching ESA CCI forest categories).

**Table 3.1:** Spatial datasets used for cropland mapping in HILDA+ version 2.0

Dataset	Variables used in this study	Spatial coverage/resolution	Reference time	References
SDPT 1.0	Tree crops	82 countries/ scale varies by country	2015	Harris et al. (2019)
Lesiv et al. Forest management	<ul style="list-style-type: none"> <li>• Oil palms</li> <li>• Agroforestry</li> </ul>	Global/ 100m	2015	Lesiv et al. (2022)
Descals et al. Oil palm map	<ul style="list-style-type: none"> <li>Oil palms</li> <li>• Industrial</li> <li>• Smallholder</li> </ul>	Global/ 10m	2019	Descals et al. (2021)
SPAM 2010	Tree crops: banana, cocoa, coconut, coffee, oil palm, plantain, tropical and temperate fruit	Global/ 5 arc min (~10km)	2010	Yu et al. (2020)
Agroforestry maps	Tree cover on agricultural land	Global/30 arc sec (~1km)	2000, 2010	Zomer et al. (2016)

The areas of cropland and pasture/rangelands as well as the areas of expansion and abandonment were mapped for global croplands and pasture/rangelands for the entire period of 1960-2020 and for each decade. For croplands, the HILDA+ land use categories annual crops, tree crops and agroforestry were merged. For pasture/rangelands, the HILDA+ land use/cover category pasture/rangelands was used. Based on this, we calculated the global and per-country net area changes in croplands and pasture/rangelands, respectively. This was done for the entire period of 1960-2020 and for each decade.

### 3.2.2 Mapping agricultural land use intensity changes

#### 3.2.2.1 Cropland intensity

For mapping and analysing changes in cropland intensity, we used the average crop yield (in tonnes per ha) as an indicator of the output intensity of croplands. With a data-driven approach, we generated a time series of global maps of mean crop yield at 1 km spatial resolution from 1960 to 2020. The crop yield maps were developed from a base map drawing on five spatial datasets, national crop yield statistics from the FAO and the annual trends in crop yields derived from four spatial datasets.

### 3.2.2.1.1 Base map of crop yields 2000

In a first step, we generated a harmonised base map of mean crop yield in the reference year 2000 based on five datasets containing yield as a variable (see Table 3.2).

**Table 3.2:** Spatial datasets used for crop yield mapping

Dataset	Variable	Crop types	Spatial resolution	Temporal resolution	References
Earthstat-M	Harvested area Yield	175 crops	5 arc min (~10km)	2000	Monfreda et al. (2008)
Earthstat-R	Harvested area Yield	4 crops: maize, soy bean, rice, wheat	5 arc min (~10km)	1995, 2000, 2005	Ray et al. (2012) based on Monfreda et al. (2008)
Earthstat-R-trend	Rate of yield change	4 crops: maize, soy bean, rice, wheat	5 arc min (~10km)	1961-2006	Ray & Foley (2013)
GAEZ	Harvested area Yield Production	26 crops	5 arc min (~10km)	2000, 2010 (v4); 2015 (v5)	Fischer (2021); Grogan et al. (2022)
GDHY	Yield	4 crops: maize, soy bean, rice, wheat	0.5 deg	annual 1981-2016	Iizumi & Sakai (2020)
SPAM	Harvested area Physical area Yield Production	42 crops (20 crops in 2000)	5 arc min (~10km)	2000, 2005, 2010	Yu et al. (2020)

For each of the datasets, the weighted-average crop yield from all available crop types was derived at the pixel level:

$$\overline{yield}_w = \frac{\sum_{i=1}^n yield_i * harvarea_i}{\sum_{i=1}^n harvarea_i}$$

with  $\overline{yield}_w$  as the weighted average crop yield,  $yield_i$  as the yield and  $harvarea_i$  as the harvested area for one crop type at a specific location (pixel). The weighting was based on the pixel-wise proportion of harvested area for each crop type to the total harvested area for all crop types. With this method, we aimed to account for the weight differences between crop types and to give higher weights to the yield of crops that occupy a larger

area within a pixel. Note that harvested area was not available for GDHY. Therefore, the average yield from all crops was calculated here without weighting.

The resulting maps of weighted average crop yield were resampled to a 1x1km grid and re-projected to the Eckert IV equal-area projection (EPSG:54012) to be consistent with the HILDA+ cropland maps. The weighted average of all contributing pixels was used as a resampling method (GDAL average). In addition, all non-cropland pixels (according to HILDA+) were masked out. The harmonised map of crop yields in the year 2000 was then calibrated to national crop yield statistics from the FAO (FAO, 2022). Again, a weighted average yield of all crop types was calculated at the country level (weighting based on harvested area, see above). We excluded all crop types within a country that were not covered as complete time series in the FAO statistics in order to avoid sharp yield fluctuations due to data gaps, abandoning or introducing certain crop types. The calibration was based on the mean of all yield values on cropland pixels at the country level:

$$yield_{p\ cal} = \overline{yield}_{FAO} + (yield_p - \overline{yield}_{all\ p})$$

with  $yield_{p\ cal}$  as the new calibrated yield value of an individual pixel;  $\overline{yield}_{FAO}$  as the national, weighted-average yield from the FAO;  $yield_p$  as the yield value of an individual pixel from the harmonised base map;  $\overline{yield}_{all\ p}$  as the mean yield from all cropland pixels within a country from the harmonised base map. The resulting FAO-calibrated map contains global mean crop yields in t/ha on cropland at a 1 km spatial resolution for the reference year 2000.

### 3.2.2.1.2 Data-derived reconstruction of crop yields 1960-2020

The national crop yield statistics from FAO (FAO, 2022) and the spatial datasets that cover multiple years (see Table 3.2) were used to dynamically reconstruct and map the mean crop yield over time from 1960 to 2020.

First, we prepared tables of FAO crop yields per country and year in 1960-2020. The country extents in the year 2015 were used to ensure a consistent country-specific reconstruction. Thus, yield values were completed for countries that have changed in area over the period of 1960-2015 (e.g. former Soviet Union countries) based on relative annual trends in the FAO recorded values for the predecessor country before the respective year of transition. In the transition year there is a data gap where we calculated an average of the trend of the first time step of the successor country and the trend of the last time step of the predecessor country. We extended the FAO time series (1961-2020) back to 1960 by linear trend extrapolation.

Second, maps of relative change in crop yield (trend maps) were derived for all datasets containing information on temporal dynamics: Earthstat-R, Earthstat-R-trend, GAEZ, GDHY and SPAM (see Table 3.2). For SPAM, only the yield changes from 2005 to 2010 were considered, as the data for 2000 refer to fewer crop types.

Finally, starting from the base map 2000, we reconstructed and mapped the mean crop yield globally from 1960 to 2020 at five-year time steps. The reconstruction model was run in a backward- and forward-mode starting from the year of the base map, 2000. For each time step and for each country, the relative changes from the spatially explicit trend maps were calibrated to the relative changes of national weighted-mean yields from FAO and added proportionally to the yield of the previous year.

$$yield_{y1} = yield_{y0} + (trend_{FAO} + [trend_{data_p} - \overline{trend_{data}}]) * yield_{y0}$$

with  $yield_{y1}$  as the per-pixel yield values in the year 1 (subsequent year),  $yield_{y0}$  as the per-pixel yield values in the year 0 (previous/base year),  $trend_{FAO}$  as the national relative FAO yield change from year0 to year1,  $trend_{data_p}$  as the per-pixel relative yield changes from the spatial datasets (if more than one dataset was available for the period, the average trend was derived), and  $\overline{trend_{data}}$  as the mean of all per-pixel relative yield changes from the spatial datasets. This iterative reconstruction of crop yields was only applied on HILDA+ cropland areas. Resulting maps show global crop yields in t/ha at a 1 km spatial and a 5-yearly temporal resolution from 1960 to 2020.

### 3.2.2.1.3 Analysing cropland intensity based on changes in crop yield

Based on the data-derived crop yield maps, we calculated the changes in crop yield for the entire period of 1960-2020 and for each decade both in absolute (t/ha) and relative (%) terms. The resulting maps were used to carry out global and per-country analyses of cropland intensification.

### 3.2.2.2 Pasture/rangeland intensity

To map and analyse changes in pasture/rangeland intensity, we use the meat and milk production in tonnes as an indicator of output intensity of livestock systems. With a data-driven approach, we generated a time series of global maps of meat and milk production at 1 km spatial resolution from 1960 to 2020. The livestock production maps were developed from a base map drawing on a spatial dataset of livestock density, national meat and milk production statistics from the FAO and annual trends of livestock density derived from spatial datasets.

#### 3.2.2.2.1 Base map of livestock production 2010

We generated a harmonised base map of meat and milk production for the reference year 2010. The spatial distribution at the subnational scale was based on GLW3, a spatial datasets of livestock density (see Table 3.3). From GLW3, we first summed up the per-pixel densities of grazing animals: cattle, sheep and goats. The resulting map of cattle, sheep and goat density in 2010 was then resampled to a 1x1km grid and re-projected

to Eckert IV equal-area projection (EPSG:54012) to be consistent with the HILDA+ pasture/rangeland maps.

**Table 3.3:** Spatial datasets used for crop yield mapping

Dataset	Variable	Livestock species	Spatial resolution	Temporal resolution	References
GLW3 GLW4	Livestock density	Buffaloes, cattle, chickens, ducks, horses, goats, pigs, sheep	5 arc min (~10 km)	2000 2015	Gilbert et al. (2018) data access *
GLW2	Livestock density	Cattle, chickens, ducks, goats, pigs, sheep	3 arc min (~5.65 km)	2006	Robinson et al. (2014) data access **

\* [https://dataverse.harvard.edu/dataverse/glw\\_3](https://dataverse.harvard.edu/dataverse/glw_3), [https://dataverse.harvard.edu/dataverse/glw\\_4](https://dataverse.harvard.edu/dataverse/glw_4)

\*\* <https://livestock.geo-wiki.org/Application/>

This grazing animal distribution was used as a base map to disaggregate national meat and milk production data from the FAO (FAO, 2022). For this, the sum of beef, sheep and goat meat as well as milk production in tonnes was derived from the FAO data at the country level. Although milk production most often outweighs that of meat in absolute terms, we considered the aggregated livestock production in combination with the spatial distribution of cattle, sheep and goats a valid measure of overall pasture/rangeland intensity. The national meat and milk production from FAO was distributed across the HILDA+ pasture/rangeland areas within a country based on the share of grazing animals (at the individual pixel level) in the total number of grazing animals (as the sum of all pixels):

$$lsprod_p\ cal = lsprod_{FAO} * \frac{gzanim_p}{gzanim_{all\ p}}$$

with  $lsprod_p\ cal$  as the new calibrated livestock production (meat and milk in tonnes) of an individual pixel;  $lsprod_{FAO}$  as the national aggregated sum of livestock production from the FAO;  $gzanim_p$  as the number of grazing animals of an individual pixel from the base map;  $gzanim_{all\ p}$  as the sum of numbers of grazing animals from all pasture/rangeland pixels within a country from the base map. The resulting FAO-calibrated map contains global meat and milk production from grazing animals in tonnes on pasture/rangelands at a 1 km spatial resolution for the reference year 2010.

### 3.2.2.2.2 Data-derived reconstruction of livestock production 1960-2020

The national statistics on meat and milk production from FAO (FAO, 2022) and the GLW datasets (see Table 3.3) were used to dynamically reconstruct and map the meat and milk production from grazing animals over time from 1960 to 2020.

We first prepared tables of FAO meat (beef, sheep and goat) and milk production per country and year in 1960-2020. The livestock production tables were processed in the same way as the crop yield data (see section above). Second, maps of relative change in numbers of grazing animals were derived from the GLW3 datasets.

Finally, starting from the base map 2010, we reconstructed and mapped the meat and milk production from grazing animals globally from 1960 to 2020 at five-year time steps. The reconstruction model was run in a backward- and forward-mode starting from the year of the base map, 2010. For each time step and for each country, the relative changes from the spatially explicit trend maps were calibrated to the relative changes of national sums of meat and milk production from FAO and added proportionally to the production value of the previous year.

$$lsprod_{y1} = lsprod_{y0} + (trend_{FAO} + [trend_{GLW_p} - \overline{trend_{GLW}}]) * lsprod_{y0}$$

with  $lsprod_{y1}$  as the per-pixel livestock production values in the year 1 (subsequent year),  $lsprod_{y0}$  as the per-pixel livestock production values in the year 0 (previous/base year),  $trend_{FAO}$  as the national relative FAO livestock production change from year0 to year1,  $trend_{GLW_p}$  as the per-pixel relative change in livestock numbers from GLW data, and  $\overline{trend_{GLW}}$  as the mean of all per-pixel relative changes in livestock numbers from GLW. This iterative reconstruction of crop yields was only applied on HILDA+ cropland areas. Resulting maps show global meat and milk production from grazing animals in t at a 1 km spatial and a 5-yearly temporal resolution from 1960 to 2020.

### 3.2.2.2.3 Analysing pasture/rangeland intensity based on changes in livestock production

Based on the data-derived livestock production maps, we calculated the changes in livestock production for the entire period of 1960-2020 and for each decade both in absolute (t) and relative (%) terms. The resulting maps were used to carry out global and per-country analyses of pasture/rangeland intensification.

## 3.3 Results and discussion

### 3.3.1 Cropland area changes

By analysing the changes in cropland areas that comprise annual crops, tree crops and agroforestry during the last six decades, we find that global cropland areas have expanded by a total of 4.09 million km<sup>2</sup> (ca. +27%), which is more than twice the size of Mexico. Of this gross expansion area, about 30% (1.25 million km<sup>2</sup>) is the result of deforestation. Another 30% (1.22 million km<sup>2</sup>) was at the expense of other natural vegetation areas. Globally, the largest areas of cropland expansion can be found in tropical regions, particularly in West Africa, the Amazon basin and Indonesia (see Figure 3.1 a,b,c,e). Cropland classes with the strongest expansion extent were annual crops (2.91 million km<sup>2</sup>; 71% of the expansion area), followed by tree crops (1.04 million km<sup>2</sup>; 25% of the expansion area). The expansion of agroforestry at 0.14 million km<sup>2</sup> was comparatively small (only 3% of the expansion area). It is striking that around 63% of the increasing tree crop areas have expanded into forests (0.66 million km<sup>2</sup>). This implies that more than half of the global deforestation for cropland (52%) is due to the expansion of tree crops (e.g. oil palm, cocoa, or rubber). Hence, tree crops can be regarded as the largest driver of global deforestation for cropland in the last 60 years.

However, croplands have also contracted in some regions, particularly in Europe (see Figure 3.1 a,d). Globally, 2.55 million km<sup>2</sup> of cropland areas were abandoned from 1960 to 2020 (ca. -17%). Of this gross cropland abandonment area, around 29% (0.75 million km<sup>2</sup>) was converted into forests, and another 29% (0.74 million km<sup>2</sup>) transitioned into other natural vegetation. Considering both gross expansion and abandonment areas, we find that the global net cropland change was an expansion of 1.53 million km<sup>2</sup> (+10%).

Countries with the largest gross cropland expansion are Indonesia (ca. 420,000 km<sup>2</sup>), India (257,000 km<sup>2</sup>), Brazil (228,000 km<sup>2</sup>), China (223,000 km<sup>2</sup>) and the US (215,000 km<sup>2</sup>). It is mainly tropical regions that have the largest deforested areas for crop production. Indonesia has the largest such change, with a deforestation area for cropland of ca. 327,000 km<sup>2</sup>. Indonesia is followed by Brazil (~90,000 km<sup>2</sup>), China (~70,000 km<sup>2</sup>), Nigeria (~60,000 km<sup>2</sup>) and Malaysia (~50,000 km<sup>2</sup>). In all of these countries except Brazil, tree crops are by far the most important cause of deforestation. In Indonesia, tree crops account for 89% of the total deforestation for cropland, in China for 76%, in Nigeria for 89% and in Malaysia even for 97% (see Figure 3.1). In contrast, the largest cropland abandonment can be found in the EU (ca. 430,000 km<sup>2</sup>), the US (270,000 km<sup>2</sup>), India (250,000 km<sup>2</sup>), Russia (220,000 km<sup>2</sup>) and China (140,000 km<sup>2</sup>). Apart from India, these are high-income or upper middle-income countries located in the Global North.

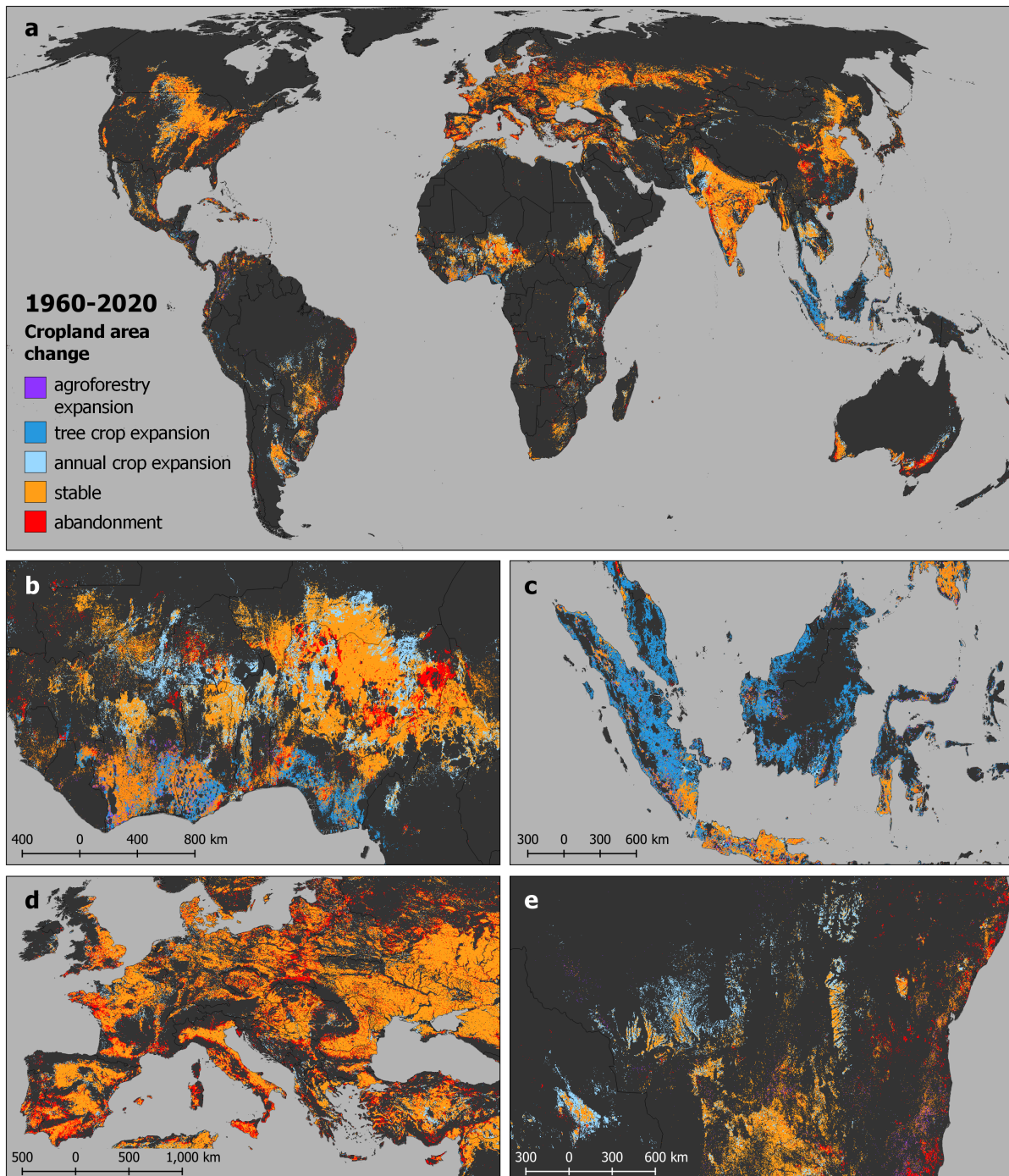


**Figure 3.1:** Map of cropland area change from 1960 to 2020 including areas of stable cropland, expansion, and abandonment. Expansion areas are further subdivided into the expansion of agroforestry, tree crops and annual crops. The maps have global (a) and regional (b: West Africa, c: Indonesia d: Europe, e: Brazil) extent.

In terms of the overall net change in cropland area from 1960 to 2020, the highest cropland increases are found in emerging countries of the Global South, particularly in tropical

regions (see Figure 3.2). Again, Indonesia has the largest increase, with a net cropland increase of around 410,000 km<sup>2</sup>, followed by Brazil (150,000 km<sup>2</sup>), Thailand and Argentina (130,000 km<sup>2</sup> each) as well as Malaysia (100,000 km<sup>2</sup>). We find that the share of tree crops on deforestation areas is remarkably high in countries of Southeast Asia (e.g. Indonesia 89%, Thailand 99%, Malaysia 97%) and Sub-Saharan Africa (e.g. Nigeria 91%, Côte d'Ivoire 53%, Uganda 73%), but comparably low in Latin America (e.g. Brazil 0%, Argentina 0%, Colombia 20%).

The largest net cropland decreases are mainly found for annual crops in the EU (ca. 320,000 km<sup>2</sup>) – particularly in Poland (60,000 km<sup>2</sup>), Italy (50,000 km<sup>2</sup>) and Spain (40,000 km<sup>2</sup>) – in Russia (160,000 km<sup>2</sup>), the US (60,000 km<sup>2</sup>) as well as in Australia (40,000 km<sup>2</sup>). It is striking that countries of the Global North, mostly high-income countries, are exclusively among the top net cropland abandoning countries (see Figure 3.2).

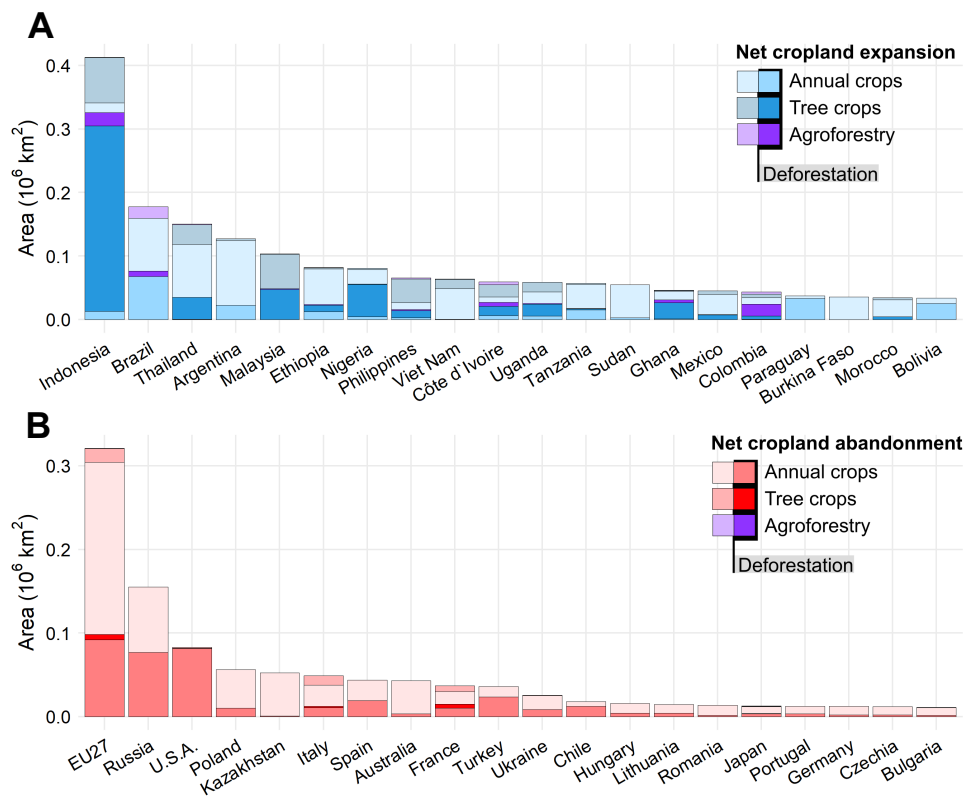


**Figure 3.2:** Top 20 net cropland expanding (top) and abandoning (bottom) countries: Stacked bars show the net expansion (top) and abandonment area (bottom) of cropland related to forest (deforestation or forest gain, respectively; in bold colours) and non-forest land use categories (in pale colours) per country.

### 3.3.2 Cropland intensification

By reconstructing the changes in mean crop yield for the last six decades as an output-based measure of cropland intensity, we find that the global crop yields have improved by 4.11 t/ha on average, which is an increase of around +2.4% per year.

Regions with the highest absolute increases in mean crop yield from 1960 to 2020 are located on the Arabian Peninsula (Kuwait +114t/ha or +9% per year, Oman +17t/ha or +7% per year, Jordan +16t/ha or +12% per year), in Central America (Costa Rica +27t/ha or +6% per year, Guatemala +25t/ha or +17% per year), the Netherlands (+26t/ha or +3% per year), Belgium (+15t/ha or +2% per year) as well as New Zealand (+20t/ha or +4% per year). The high yield change in Kuwait, however, seems rather unrealistic and strongly deviates from the other countries. The change in Kuwait is likely the consequence of an implementation of large-scale irrigation schemes for high-yielding crop types such as tomatoes (FAO, 2023). Apart from the Arabian Peninsula and Central America, we also find high relative yield improvements in Northern Africa (Libya, Algeria, Morocco; see Figure 3.3).

In contrast, the greatest declines in crop yield from 1960 to 2020 can be found on mostly

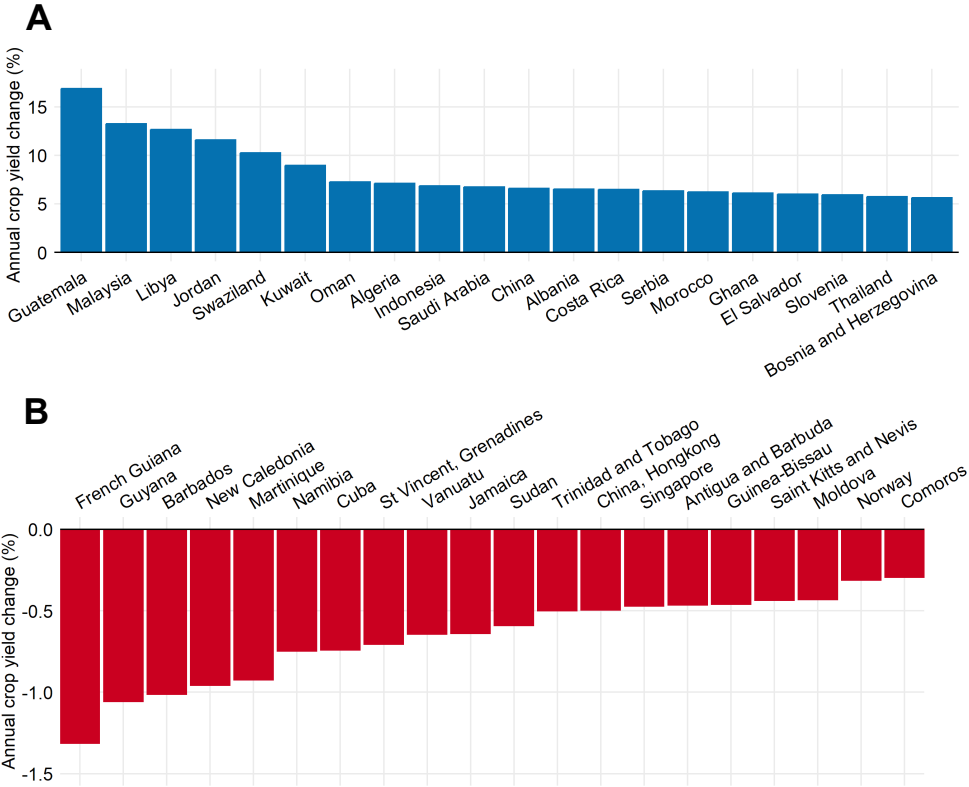


**Figure 3.3:** 20 countries with largest relative increases (A) and relative declines (B) in crop yield from 1960-2020. The bar charts show the mean annual yield change in relative terms (as % of the mean yield in 1960).

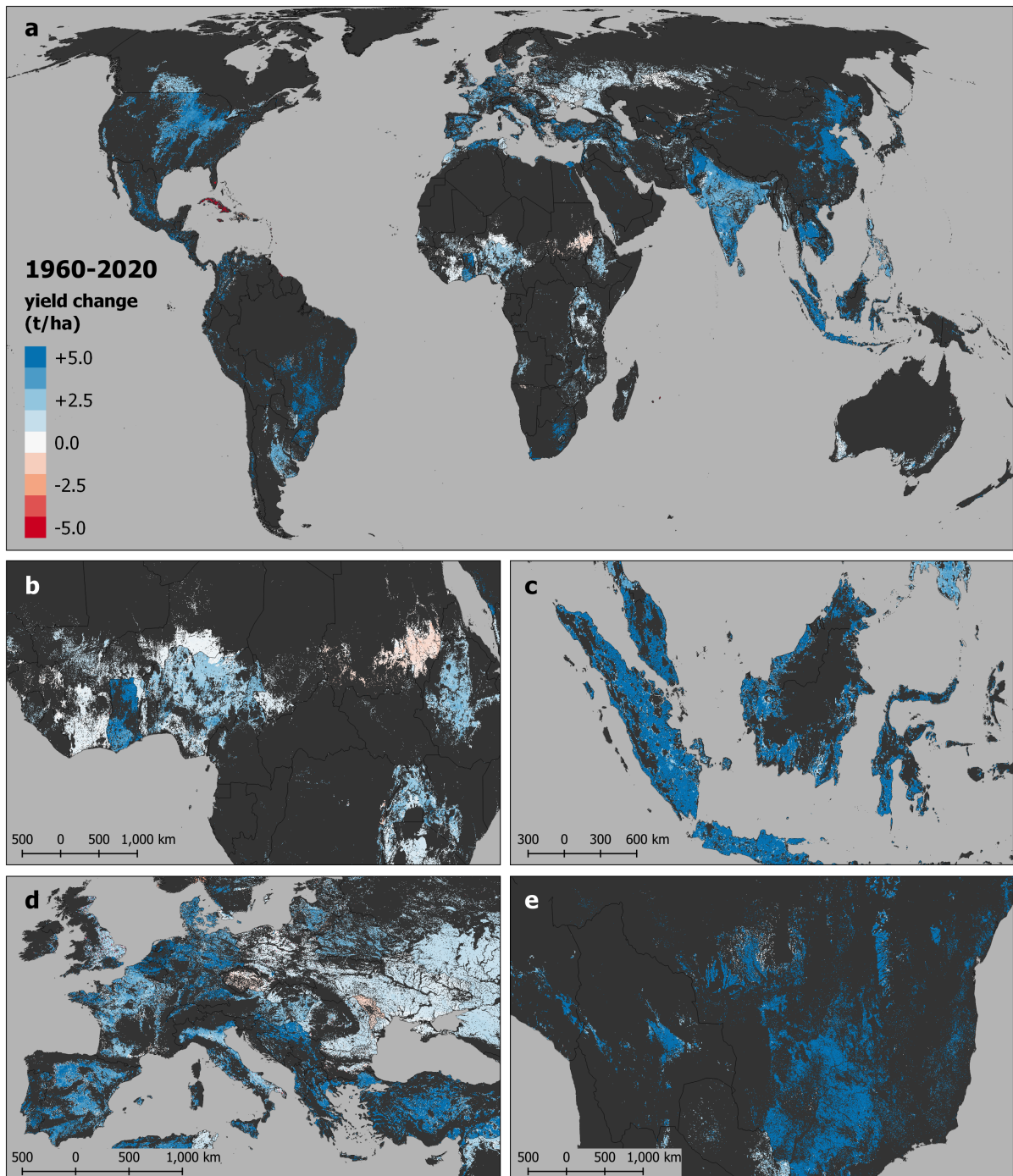


**Figure 3.4:** Yield change on croplands from 1960 to 2020: Global map of net absolute yield change in t/ha. The bar chart shows the mean absolute change in t/ha of the 30 countries with the largest cropland area.

island countries located in the Caribbean Sea, e.g. Martinique -45 t/ha (-0.9% per year), Barbados -40 t/ha (-1.0% per year), Cuba -14 t/ha (-0.7% per year), in the Indian (Singapore -7 t/ha or -0.5% per year, Réunion -5 t/ha or -0.1% per year) or the South-western

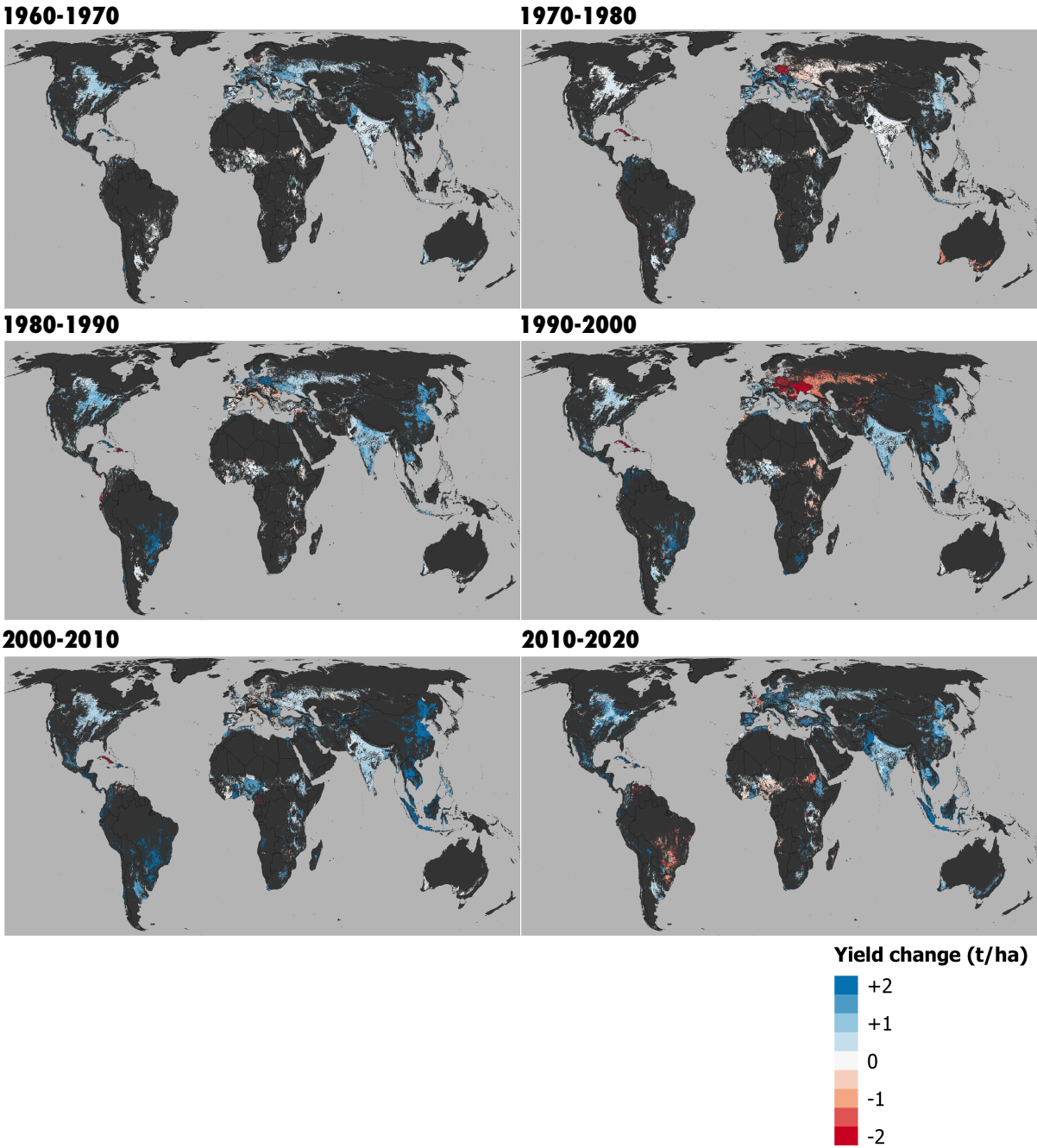


Figure 3.5: Decadal yield change (in t/ha) on croplands from 1960 to 2020

Pacific Ocean (New Caledonia -4 t/ha or -1.0% per year, Vanuatu -2 t/ha or -0.6% per year). Also, some countries in sub-Saharan Africa – Namibia (-0.8 t/ha or -0.8% per year), Sudan (-0.7 t/ha or -0.6% per year) and Guinea-Bissau (-0.4 t/ha or -0.5% per year) – show high relative yield declines. In Europe, overall crop yield decreases can only be observed in Norway (-1.4 t/ha or -0.3% per year), Moldova (-0.9 t/ha or -0.4% per year) and Czechia (-0.5 t/ha or -0.1% per year).

Many of these countries, however, have only a small share of cropland areas, which is why a focus on higher-yielding crops such as sugar crops (e.g. sugar cane in Guatemala, Nicaragua, Costa Rica), fruits and vegetables (such as bananas in Costa Rica, dates in Oman, tomatoes in Kuwait) has a greater influence on overall yield changes. Also, shifts in crop varieties towards higher-yielding varieties as well as the deployment of irrigation may cause large relative yield increases. In Saudi Arabia, maize recorded a +790% yield increase from 1970 to 2020. In Nicaragua, cassava (+164%) and potato (+384%) yields increased since the late 1970s, cocoa yields more than tripled from 2000 onwards (+350%). In Honduras, potato (+189%) and rice (+212%) yields have shown large increasing trends since 1961 (FAO, 2022c; Ritchie et al., 2022).

Focussing on the countries with the largest cropland areas, we identify large crop yield increases in Indonesia (+12.7 t/ha or +7% per year), Brazil (+10.5 t/ha or +4% per year), China (+8.7 t/ha or +7%), Thailand (+8.0 t/ha or +6% per year) and Mexico (+6.7 t/ha or +4% per year). Also, Pakistan (+5.7 t/ha) and Iran (+4.5 t/ha) show relative crop yield increases of ca. 5% per year. These emerging countries experienced major shifts in crop production. Rice (19% production and 40% area share in 1961) has been replaced by oil palm as the most produced crops in Indonesia, where oil palm accounts for 53% of the production and 33% of harvested area in 2020. Sugar cane (69% production but only 12% area share) and soy bean (11% production and 44% area share) lead the list in Brazil, whereas in 1961, hardly any soy beans were grown there (0.2% production and 0.1% area share). In China, production has shifted from sweet potatoes (22% production and 8% area share) and rice (17% production and 20% area share) in 1961 to maize (13% production and 23% area share) in 2020. In Thailand, rice (37% production and 74% area share in 1961) has been substituted by sugar cane (38% production but only 9% area share in 2020).

Whereas, in the past, these countries focused mainly on staple crops for domestic supply, today they grow large quantities of crops for the world market, often for animal feed. This becomes visible in crop production statistics from the FAO (FAO, 2022b). While the proportion of crops produced for food has decreased, the share of animal feed and that of exports have risen dramatically until the present. In Indonesia and Brazil, shares of food crops have halved from 1961 to 2019 (from 60% to 30% in Indonesia, from 29% to 14% in Brazil). At the same time, the proportion of exports has more than doubled in Indonesia and even increased seven-fold in Brazil. In China, where the population has more than doubled during that time, the share of food crops has been reduced from 75% to 68%, whereas fodder crops have augmented from 10 to 16% and that of exports from 0.8% to 2.3%. In Thailand, we see an even more drastic decrease in food production from 57% to 16% accompanied with a tripling of the feed (from 3% to 9%) and a slight increase of the exports (from 20 to 21%). Although the share of food crops increased from 38% to 47% in Mexico, the share of feed and that of exports have roughly quadrupled (4% to 15% and 3% to 13%, respectively; FAO, 2022b).

Eastern Europe as well as countries in the Sahel Zone show comparably lower yield increases than other countries with large cropland areas (see Figure 3.4 a,b,d). This is due to large fluctuation in crop yields over time (see Figure 3.5).

In Eastern Europe, political factors were the main drivers of yield declines from 1990 to 2000. The collapse of the Soviet Union caused a period of crop yield decreases and agricultural abandonment. From 1990 to 2000, investments in the Russian agricultural sector dropped by 95% (Prishchepov et al., 2013), the removal of subsidies for fertilisers let soil fertility and crop yields decline (Trueblood & Arnade, 2001; Prishchepov et al., 2013). Prishchepov et al. (2013) found that a decrease in yields from the late 1980s partially explained subsequent agricultural land abandonment in Eastern Russia. Eastern Europe faces nutrient limitation for wheat and maize production (Mueller et al., 2012). Added to this are drought conditions, which have repeatedly caused comparably low and fluctuating crop yields in the southern Russian bread baskets and will also become more important in the future as climate change progresses (Schierhorn et al., 2014). In the Ukraine, climate variations during the last decades, particularly in 2003, affected crop production and led to a loss of winter crops of up to 50% and summer crops of up to 75% (Adamenko & Prokopenko, 2011).

Furthermore, the African Sahel region has been affected by climatic extreme events, particularly severe drought conditions during the last decades. In Sudan, sorghum and millet yields have declined due to drought in at least 15 years during 1970-2006 (Elagib, 2014). Gibon et al. (2018) presented a close linkage between crop yields in the Sahel (Niger, Mali, Senegal, Burkina Faso) and climate variability, as soil moisture explained 81% of the millet yield variability during 1998-2014. Yields for most crop types in Ethiopia have decreased due to past climate variability within 35 years due to a negative relation between yield and temperature on highly productive croplands (Yang et al., 2020).

The recent decline in Brazilian crop yields in 2010-2020 (see Figure 3.5) may have resulted from decreases of sugar cane (-3.44 t/ha), which is Brazil's most produced crop accounting for 69% of the total crop production but only 12% of the total harvested area in 2020, wheat (-0.22 t/ha) and rapeseed (-0.26 t/ha) during this period (Ritchie et al., 2022).

### 3.3.3 Intensification versus expansion of global croplands

By comparing the cropland intensification with area expansion during the period of 1960-2020, we find that high-income countries have intensified while reducing their cropland, whereas low-income countries have intensified less but substantially increased their cropland area (see Figure 3.6). It is striking that middle-income countries belonging to the group of emerging markets, which are characterised by high rates of economic growth and mainly located in the tropics (e.g. Brazil, Indonesia, Thailand, Colombia, and Malaysia), show both the highest intensification and expansion rates.

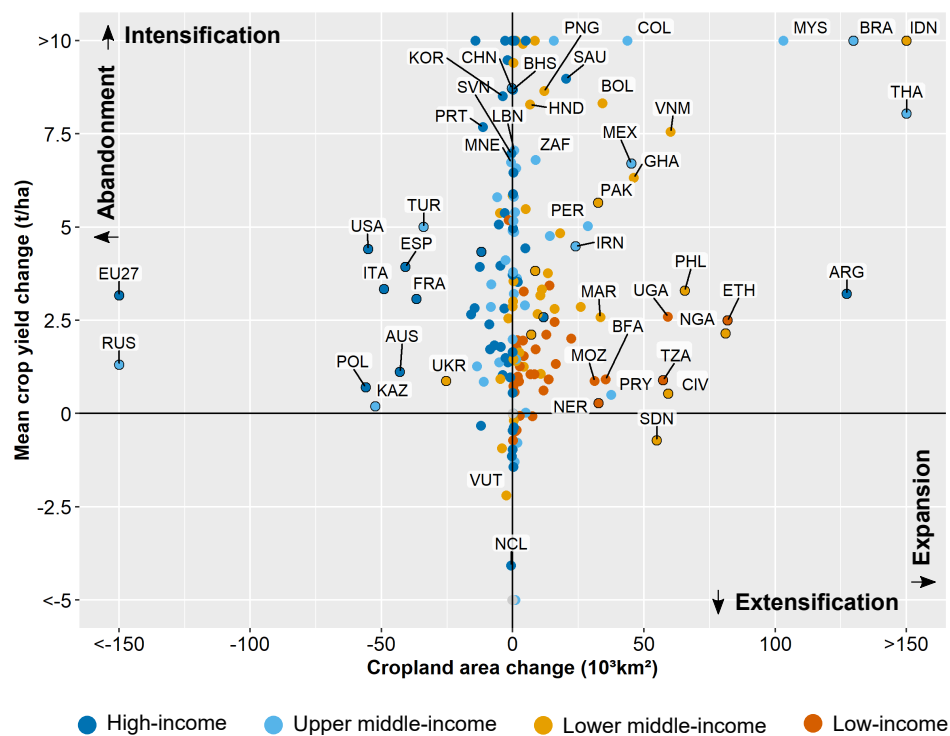


**Figure 3.6:** Relation of intensification (absolute crop yield change) and expansion (net area change) of croplands for all countries during 1960-2020. The coloured dots indicate the income group of the countries. Countries are labelled according to their ISO-3 Codes (some remain unlabelled for better readability).

However, the relationship between intensification and expansion has not always or everywhere been the same over time. Figure 3.7 shows the pathways of cropland intensity and area change for different countries over the last six decades.

Croplands in Indonesia, for example, went through a period of intensification without major expansion during 1960-1990, which was followed by a 10-year expansion phase and, finally from 2000 onwards, by both massive intensification and expansion. Growing international trade has been identified as a major driver of global agricultural land use change, particularly of large-scale oil palm and timber plantations at the expense of forests in Indonesia (Austin et al., 2019; Byerlee et al., 2014; Meyfroidt et al., 2013). Thereby, the relation between deforestation and oil palm expansion is often mediated by timber extraction (Byerlee et al., 2014). In addition, deregulation and expansionist policies, as pursued by the Indonesian government since the 1980s, paved the way for a market-driven palm oil expansion. The palm oil boom in Indonesia is an example for the rebound effect (Jevons paradox) of intensification causing further expansion (Varkkey et al., 2018). Thailand shows a similar cropland trajectory, where large expansion started after the onset of continuously high intensification.

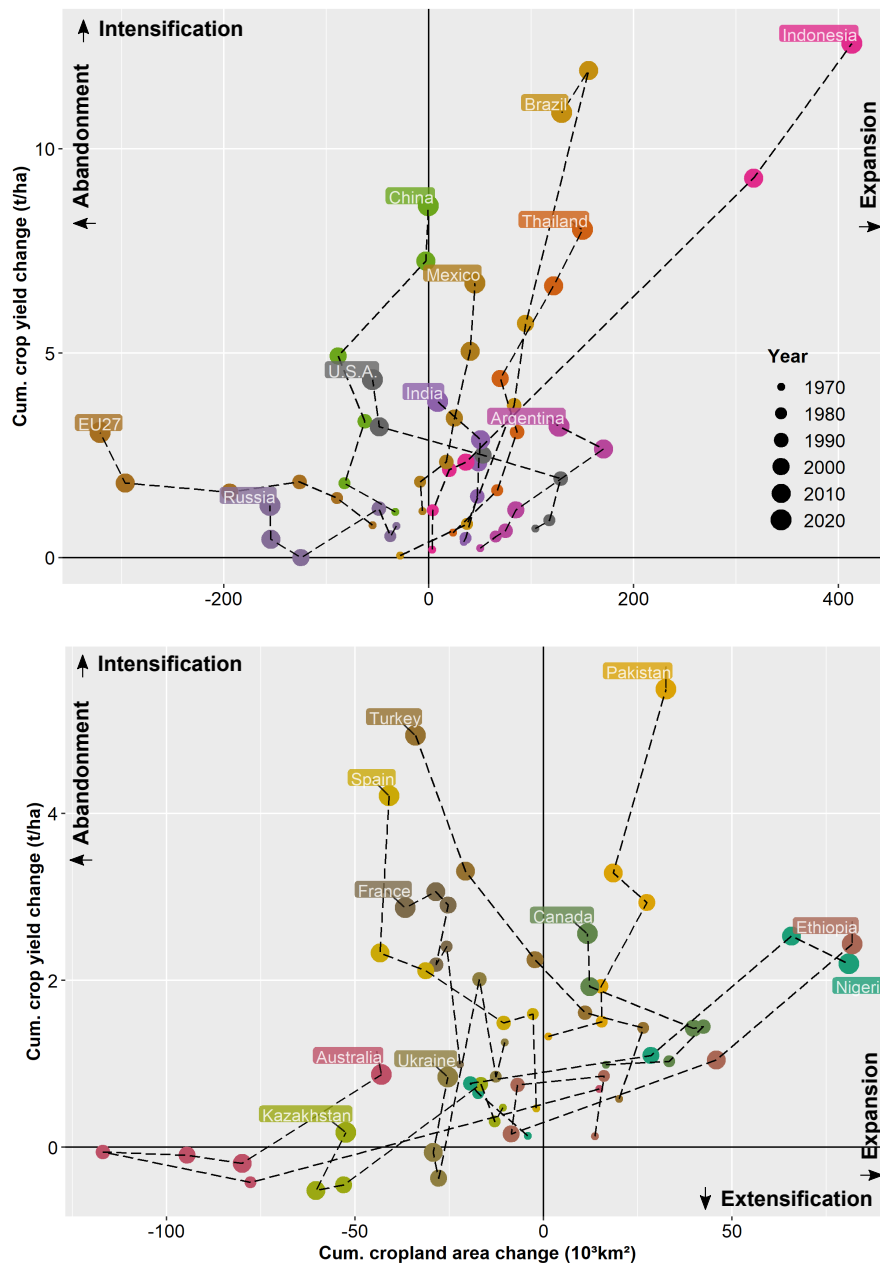


**Figure 3.7:** Trajectories of cropland change: Decadal intensification (absolute crop yield change) and expansion (net area change) of croplands for selected countries during 1960-2020. The 20 countries with the largest cropland areas are displayed.

Brazil experienced a sharp cropland intensification with high but declining expansion rates since the 1980. However, a decline in yields and cropland area is noticeable during the recent decade. Brazil was ranked among the top cropland-intensifying and cropland-expanding countries (Hu et al., 2020). As consistent with this study, Dias et al. (2016) found that cropland expansion in Brazil has slowed down and has been followed by a significant trend of intensification. Areas with great intensification were found in the

soy bean and coffee regions of the South (Hu et al., 2020)). The intensification of soy bean production often goes along with that of maize production, as they are cultivated in double cropping systems (e.g. in Mato Grosso) (Dias et al., 2016). Higher yields on soy bean expansion in Brazil were assumed to increase land rents and boost further soy bean expansion (Garrett et al., 2013). This suggests that the combination of high cropland intensification and expansion in Brazil may partly result from a rebound effect (Jevons paradox) of intensification of high-profit crops such as soy bean and sugar cane. The relation between land use intensity and area changes can also be vice versa. A recent study provides evidence that the ongoing deforestation of the Brazilian Cerrado negatively affects rain-fed maize production, as altered weather through less evapotranspiration reduces maize yields by 6-8% (Spera et al., 2020).

Also, Nigeria shows a highly dynamic trajectory, with 30 years of intensification and net cropland contraction followed by an enormous cropland expansion with low intensification rates and even extensification during 2010-2020. Our findings on this large cropland expansion are consistent with other studies (Hu et al., 2020; Nzabarinda et al., 2021). Cassava, the main crop produced in Nigeria (FAO, 2022c), is mainly grown for domestic consumption and experienced large production increases over the past decades. However, the growing cassava production in Nigeria was mainly the effect of expanding area harvested. Although they experienced a long-term increase, yields showed a pronounced decline after 2010 (Ikueomonisan et al., 2020), which may be the reason for the observed cropland extensification trend in Nigeria during 2010-2020.

China underwent a phase of cropland abandonment during 1960-1980, followed by high yield increases with cropland expansion. Our findings on the strong cropland intensification in China are in line with Hu et al. (2020) who associate crop productivity increases in China during 2000 and 2010 due to changes in management (crop mix, cropping frequency, fertiliser, irrigation, and paddy rice water management). However, the cropland area changes found here – while in line with FAO (FAO, 2022c) – differ from their findings on cropland abandonment in China for 2000-2010 (Hu et al., 2020). Cropland abandonment was generally balanced by expansion in China, not only temporally but also spatially, as shown likewise in a recent study (Zuo et al., 2018). In this context, it was demonstrated that, current regulations in China cause an offset of cropland loss with expansion elsewhere and, hence, drive cropland expansion on uncultivated lands (Zuo et al., 2018). Further, urbanisation is a major driver of land use intensity in China (Jiang et al., 2013). While the highly increasing crop production has become less environmentally impactful over time, the rising efficiency in crop production only partially compensated for the environmental pressures, which are spatially divergent (Zuo et al., 2018).

Interestingly, the US shows a shift from 30 years of cropland expansion to another 30 years of abandonment, particularly during 1990-2010, while cropland intensification was consistently high. Cropland expansion has mainly occurred in the West, cropland aban-

donment in the East of the United States up to 2002 (Ramankutty et al., 2010). Lin and Huang (2019) found that cropland expansion was less rapid than the increase of crop production in the corn belt of the Midwestern US from 1974 to 2008, which suggest a strong trend of intensification. However, higher crop prices and farm subsidies were found to be linked to agricultural expansion (Lin and Huang, 2019). Furthermore, crop production in the US was more responsive to crop diversity than to cultivated area (Burchfield et al., 2019). As a consequence of the biofuels boom in the late 2000s, the Midwestern US experienced a resurgence of cropland expansion mainly for maize and soy bean production at the expense of grasslands (Lark et al., 2015; Zhang et al., 2021).

The intensification-expansion trajectories of Russia, Ukraine and Kazakhstan are characterised by large fluctuations in crop yield changes and large-scale cropland abandonment. The disruptive effect of the collapse of the Soviet Union caused a U-turn from former intensification to an abrupt extensification alongside massive cropland abandonment during 1990-2000. Synergies between intensification and cropland expansion were found in these countries since the early 2000s (Meyfroidt et al., 2016). In addition, the intensification combined with cropland expansion in Russia, Ukraine and Kazakhstan may have resulted from investments and governmental support for widespread re-cultivation since 2000 (Meyfroidt et al., 2016). A reversal in the trends of cropland abandonment occurred in the Western Siberian grain belt in the early 2000s due to re-cultivation as well as rising fertiliser inputs and narrowing crop rotations (Kühling et al., 2016).

We find that the EU has followed a long-time trajectory of large net cropland abandonment with constant intensification, interrupted by a phase of stagnating yields during 1990-2010. Our findings suggest a sharp cropland intensification in recent years. This fits the recent agricultural land use history in Europe, which was shaped by a subsidy-driven intensification on productive versus extensification of marginal land as well as cropland abandonment and extensification in Central and Eastern Europe following the fall of the Soviet Union (van Vliet et al., 2015). The sharp intensification, however, could also be the result of a yield re-distribution rather than a real yield increase on croplands. When less productive land is abandoned, overall crop yields increase due to relatively more productive non-abandoned lands (with higher yields).

Whereas the land-sparing theory may apply for high-income, developed countries of the Global North, as seen in western EU or the US in recent decades, our findings suggest that it is rebutted in the low- to middle-income, emerging countries of the Global South such as Indonesia and Brazil. There, the rebound-effect (Jevons paradox) corresponds better to the spatio-temporal dynamics of cropland change.

Overall, our findings support the hypothesis that cropland intensification caused a rebound-effect and led to further land use expansion in emerging, middle-income countries. This particularly applies to crops with high price-elasticity of demand such as sugar cane, oil palm and soy bean (García et al., 2020).

### 3.3.4 Pasture/rangeland area changes

By analysing the global changes in pasture/rangeland areas, we find that global pasture/rangelands have expanded on 5.16 million km<sup>2</sup>, which is more than have the size of China and an increase of ca. 18% from 1960 to 2020. Around 27% of these expansion areas (ca. 1.5 million km<sup>2</sup>) have caused deforestation, whereas 20% (1.0 million km<sup>2</sup>) were at the expense of other natural vegetation. The largest areas of pasture/rangeland expansion can be found in Western China, Australia, and in the Amazon basin (see Figure 3.9 a,b,c,e).

It is noticeably that the global area of pasture/rangeland abandonment (ca. 5.29 million km<sup>2</sup>) outweighed that of expansion by 0.12 million km<sup>2</sup>. That implies that pasture/rangeland areas have experienced a slight net contraction of -0.42% in the last six decades. Particularly large extents of pasture/rangeland abandonment can be identified in North America, southern Chile and Argentina, Europe and Australia (see Figure 3.9a,c,d).

By comparing the gross pasture/rangeland expansion areas at the country level, we

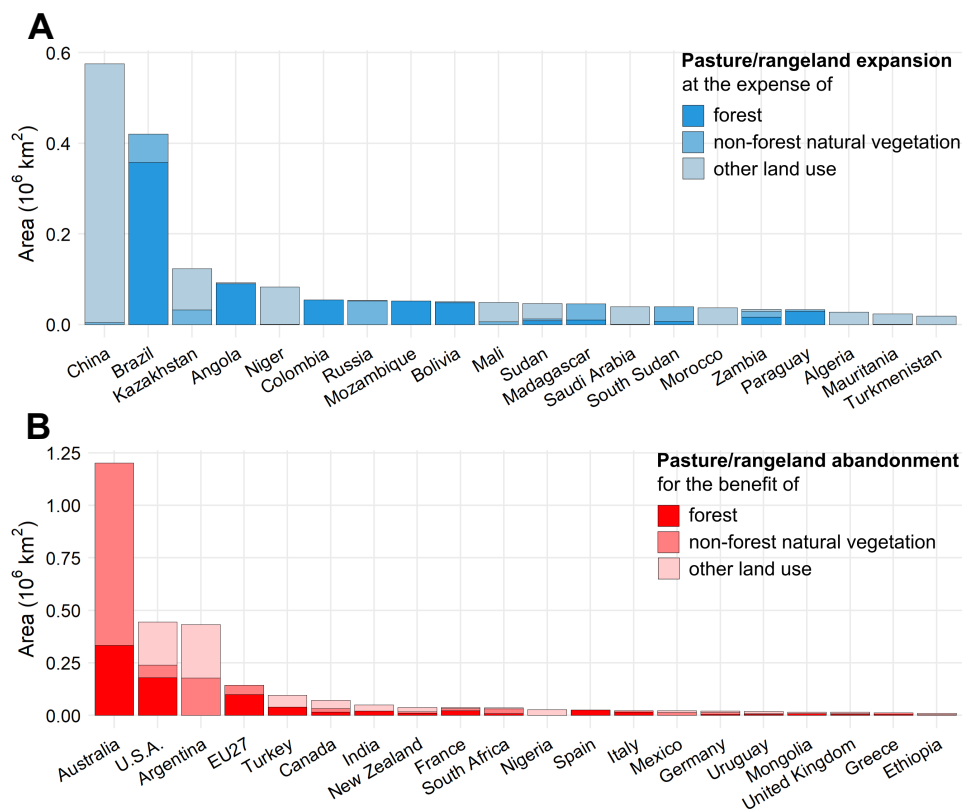


**Figure 3.8:** Top 20 net pasture/rangeland expanding (top) and abandoning (bottom) countries: Stacked bars show the net expansion (top) and abandonment area (bottom) of pasture/rangeland related to forest (deforestation or forest gain, respectively), non-forest natural vegetation and other land use categories per country.

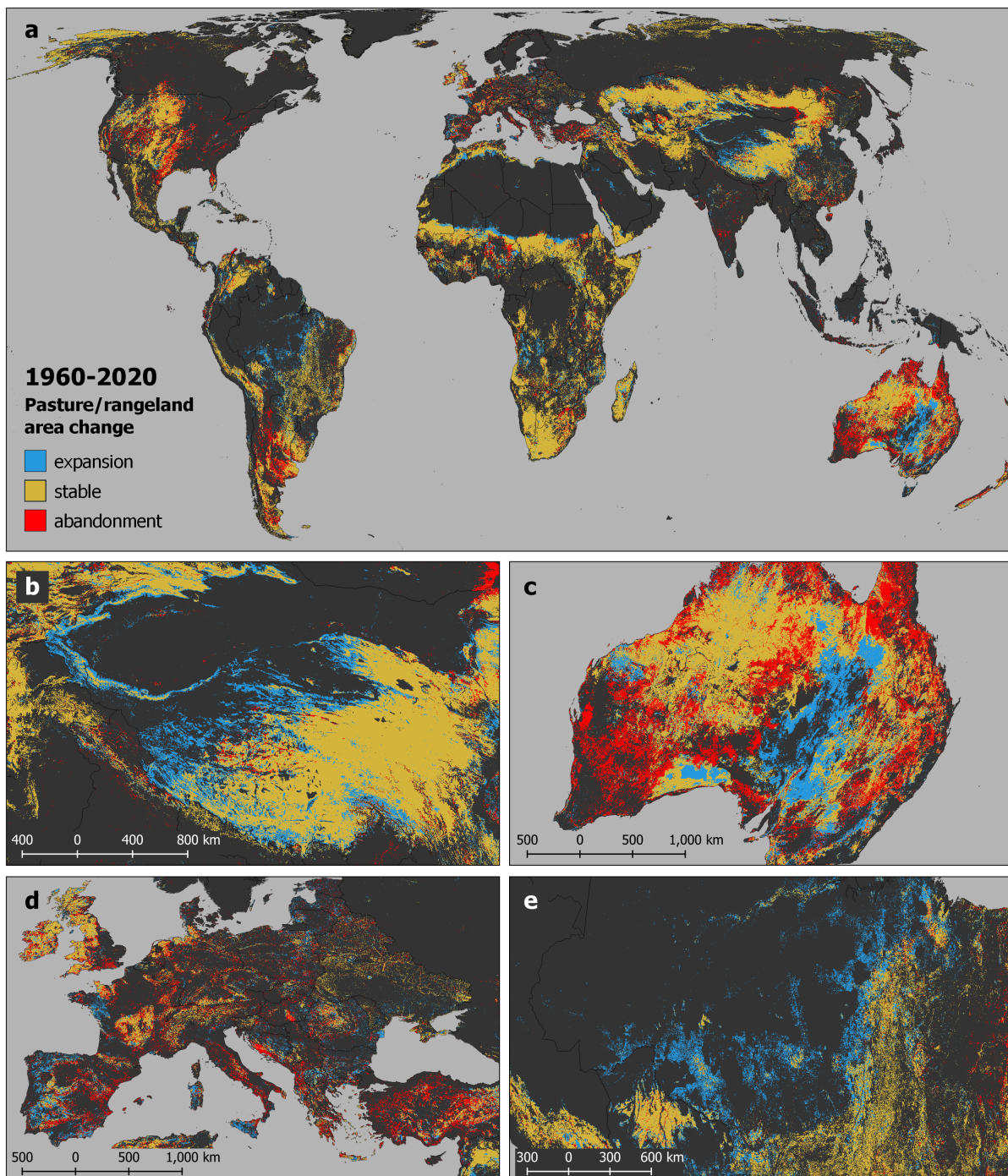


**Figure 3.9:** Map of pasture/rangeland area change from 1960 to 2020 including areas of stable pasture/rangelands, expansion, and abandonment. Maps have global (a) and regional (b: West China, c: Australia, d: Europe, e: Amazon basin) extent.

can observe the greatest expansions in Australia (ca. 910,000 km<sup>2</sup>, +23% of the pasture/rangeland area as in 1960), China (780,000 km<sup>2</sup>, +26%), Brazil (540,000 km<sup>2</sup>, +41%), the US (310,000 km<sup>2</sup>, +11%) and the EU (220,000 km<sup>2</sup>, +33%). Brazil is the coun-

try with the largest deforestation caused by pasture/rangeland expansion, as around 71% (ca. 380,000 km<sup>2</sup>) of its total pasture/rangeland expansion was at the expense of forests. Also, Angola (120,000 km<sup>2</sup>), the US (100,000 km<sup>2</sup>), China (90,000 km<sup>2</sup>), Mozambique (70,000 km<sup>2</sup>), Colombia, Indonesia and Bolivia (ca. 60,000 km<sup>2</sup> each) show large extents and shares of deforestation for pasture/rangelands.

The largest areas of pasture/rangeland abandonment can be found in Australia (ca. 1.59 million km<sup>2</sup>, -40% compared to pasture/rangelands of 1960), the US (760,000 km<sup>2</sup>, -25%), Argentina (470,000 km<sup>2</sup>, -40%), the EU (330,000 km<sup>2</sup>, -51%), and China (290,000 km<sup>2</sup>, -9%).

By aggregating pasture/rangeland expansion and abandonment areas, we find that, similar to croplands, the largest net pasture/rangeland expanding countries are lower- to middle-income countries of the Global South (e.g. Brazil, Kazakhstan, Angola, Niger), with the exception of China. In contrast, net abandoning countries are mainly high-income countries of the Global North (e.g. Australia, US, Argentina, EU; see Figure 3.8).

The largest forest losses due to pasture/rangeland expansion can be found in tropical regions, particularly in the Amazon (Brazil, Colombia, Bolivia, Paraguay) but also in the Miombo woodlands of Angola and Mozambique, whereas the largest forest increases after pasture/rangeland abandonment can be identified for Australia, the US, China, and the Mediterranean Europe.

### 3.3.5 Pasture/rangeland intensification

Globally, we find an intensification trend on pasture/rangelands during 1960-2020, as the production of meat and milk from grazing animals has increased by an average of 18 t/km<sup>2</sup> (+2.2% per year).

Remarkably large production increases can be found in countries of the EU (Cyprus: +10,000 t/km<sup>2</sup> from no production in 1960, Finland: +1,700 t/km<sup>2</sup> or +0.3% per year, Netherlands: +1,100 t/km<sup>2</sup> or +2.2% per year), southern and western Asia (India: +1,600 t/km<sup>2</sup> or +10% per year, Pakistan: +980 t/km<sup>2</sup> or 12% per year, Israel: +910 t/km<sup>2</sup> or +5% per year) as well as South Korea (+2,600 t/km<sup>2</sup> or +6% per year) and Japan (+1,000 t/km<sup>2</sup> or +2% per year). In contrast, the largest decreases can be noticed in Hongkong (-1,400 t/km<sup>2</sup> or -1% per year), Scandinavia (Norway: -900 t/km<sup>2</sup> or -0.7% per year, Denmark: -800 t/km<sup>2</sup> or -0.4% per year, Sweden: -410 t/km<sup>2</sup> or -0.7% per year), Eastern Europe (Lithuania -260 t/km<sup>2</sup> or -0.8% per year, Moldova -160 t/km<sup>2</sup> or -1.0% per year, Czechia: -140 t/km<sup>2</sup> or -0.5% per year) as well as in island countries of the Caribbean. Figure 3.10 shows the countries with the largest relative intensification and extensification on pasture/rangelands.

In general, Europe and America are the continents with the largest livestock production changes, as areas of high pasture/rangeland intensification as well as extensification are

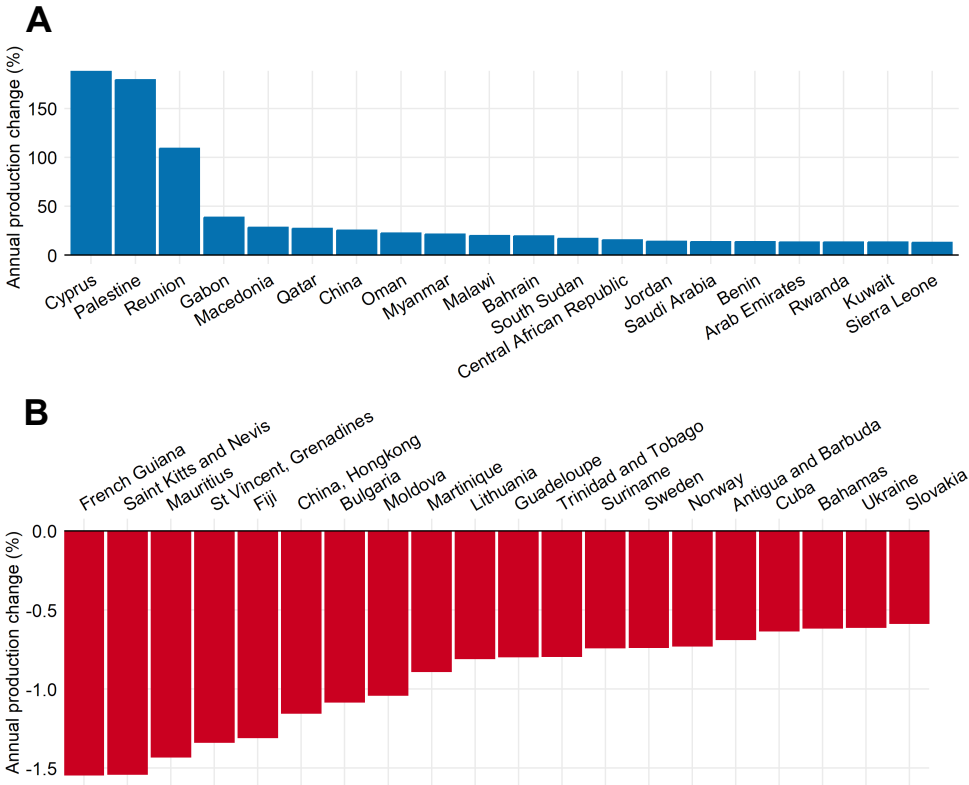


**Figure 3.10:** 20 countries with largest relative increases (top) and relative declines (bottom) in production from 1960-2020. The bar charts show the annual mean change of meat and milk production change in relative terms (as % of the mean production in 1960).

widespread (see Figure 3.11 and Figure 3.12). In comparison, Australia, central Asia (Kazakhstan and Mongolia) as well the western Sahel and Southern Africa shows very little changes. In these regions mean livestock density and production is relatively low, as they are characterised by extensive rangelands and thus low land use intensity. Interestingly, Africa seems to be divided by a NW-SE axis. While the West and the South show low pasture/rangeland intensities and also little changes, the North and the East have higher production levels and strong intensification trends (see Figure 3.11).

### 3.3.6 Intensification versus expansion of global pasture/rangelands

In the distribution of countries according to intensification versus expansion of pasture/rangelands, we can also see similar but not as pronounced patterns as in that of the croplands. Whereas upper middle- to high-income countries (e.g. EU, US, Turkey, Argentina, Canada or Australia) have intensified but abandoned their pasture/rangelands in the last six decades, low- to lower middle-income countries of Sub-Saharan Africa (Mali, Niger, Angola, Sudan) tended to intensify less but expand their pasture/rangelands over time. It has to be noted that, since the marginal (upland or arid) grassland areas are often abandoned first, pasture/rangeland abandonment can lead to higher yields of live-

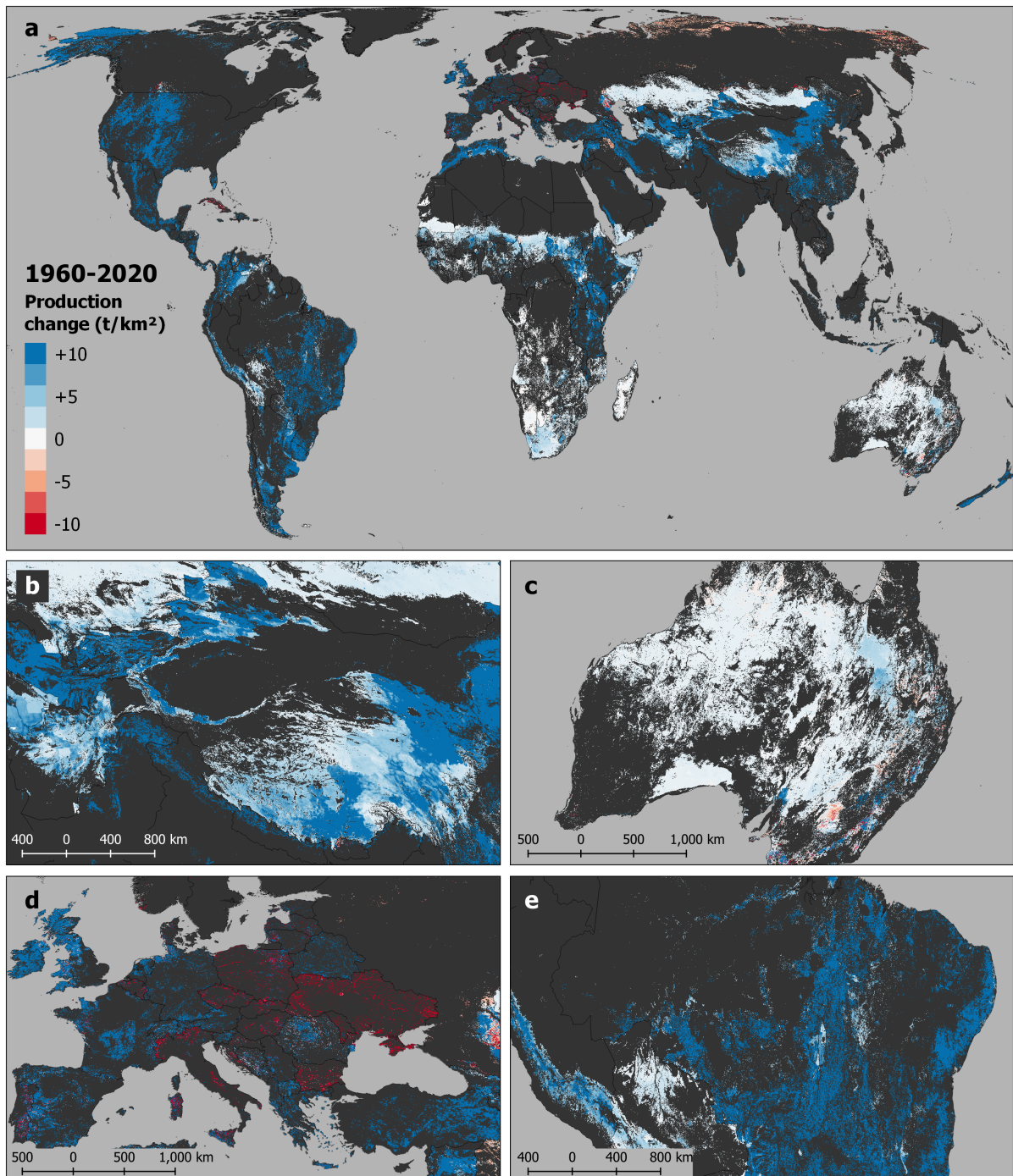


**Figure 3.11:** Map of mean change of meat and milk production in t/km<sup>2</sup> from 1960 to 2020. The bar chart shows the mean milk and meat production change in t/km<sup>2</sup> of the top 30 with the largest pasture/rangeland area.

stock systems through a re-distribution of productivity rather than a real intensification trend.

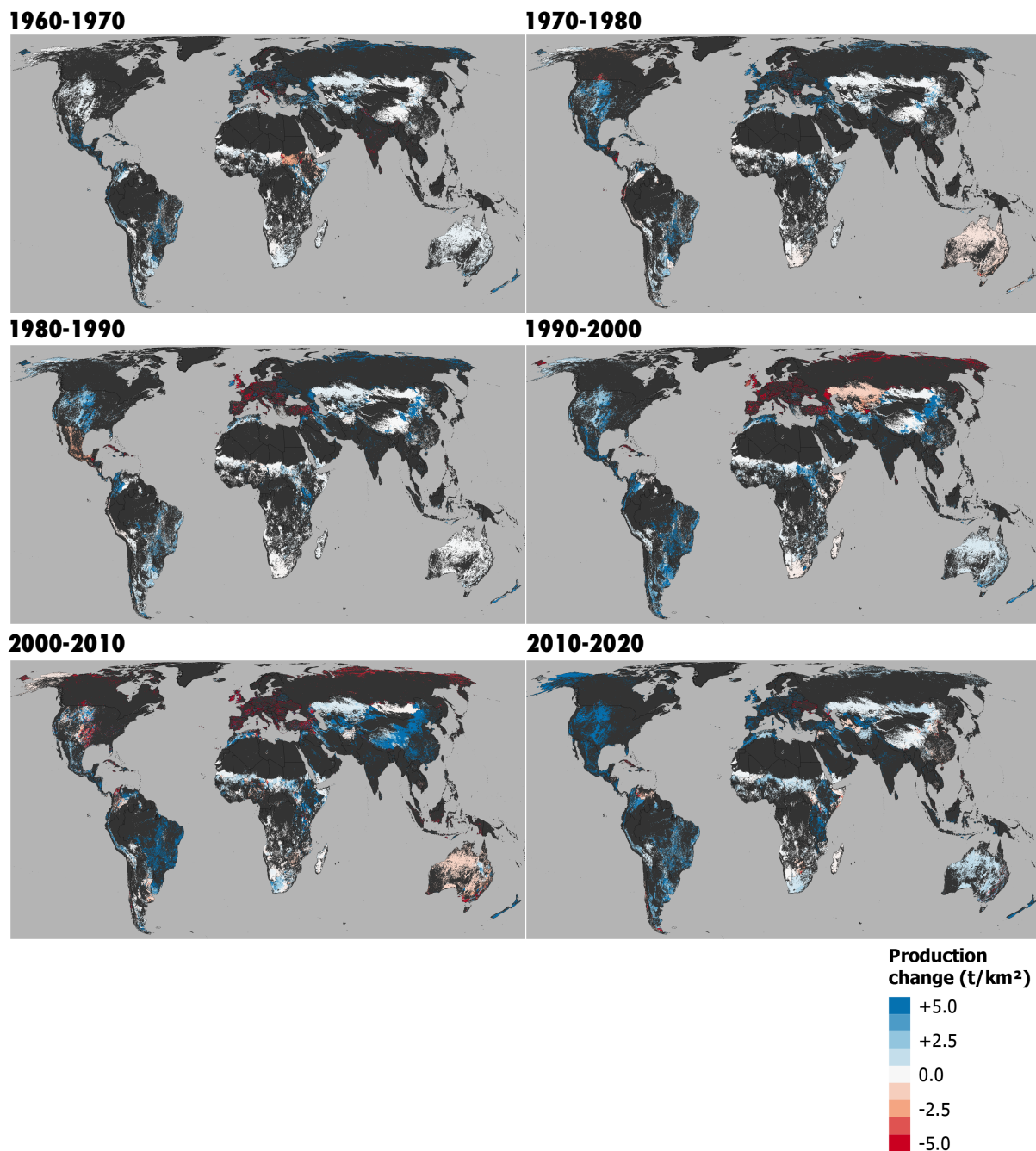


**Figure 3.12:** Decadal change in meat and milk production from grazing animals (in t/km<sup>2</sup>) on pasture/rangelands from 1960 to 2020

Again, we find emerging countries on the extreme ends of the intensification-expansion relation. Brazil, China and Saudi Arabia show both intensification and large expansion of pasture/rangelands, whereas Turkey, India and Mexico have followed a pathway of strong intensification and large abandonment of pasture/rangelands (see Figure 3.13).

Brazil followed a long-lasting pasture/rangeland expansion strategy from 1960 to 1990,

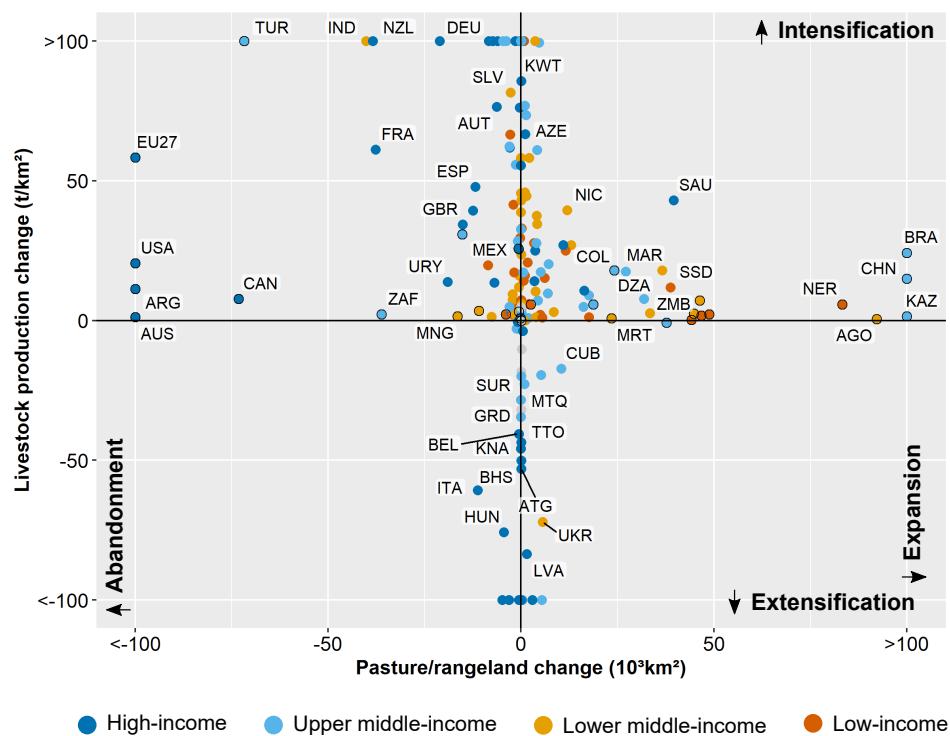


**Figure 3.13:** Relation of intensification (meat and milk production change) and expansion (net area change) of pasture/rangelands for all countries during 1960-2020. The coloured dots indicate the income group of the countries. Countries are labelled according to their ISO-3 Codes (some remain unlabelled for better readability).

followed by a turnaround with substantial intensification and area decline, to a resumption of expansion with further intensification from 2010 (see Figure 3.14). It is well known that a main driver of deforestation in Brazil is cattle ranging followed by soy bean cultivation (Song et al., 2021). The intensification of pasture/rangelands could not be directly linked to a decrease in deforestation. Rather, a positive correlation between pasture/rangeland area, deforestation and cattle growth rate has persisted in the Amazon (McManus et al., 2016). Moreover, livestock intensification was not equally distributed in Brazil, as cattle densities in Amazonia grew less strongly than in southern regions due to a lagged technology transfer (Dias et al., 2016). Walker et al. (2013) found that around 75% of the deforestation in the Brazilian Amazon was caused by cattle expansion, which is strongly spurred by exports. Whereas a small decline was registered for non-Amazon regions, the amount of cattle in the Amazon more than doubled during 1994-2009, with sharply rising exports of beef and leather.

We can observe a similar situation in Colombia. Here, a strong intensification trend with a declining area started in the 1980s after a period of expansion. In the recent decade, pasture/rangeland intensification in Colombia continued but expansion was readopted. It has been estimated that nearly half of the natural ecosystems in Colombia were transformed

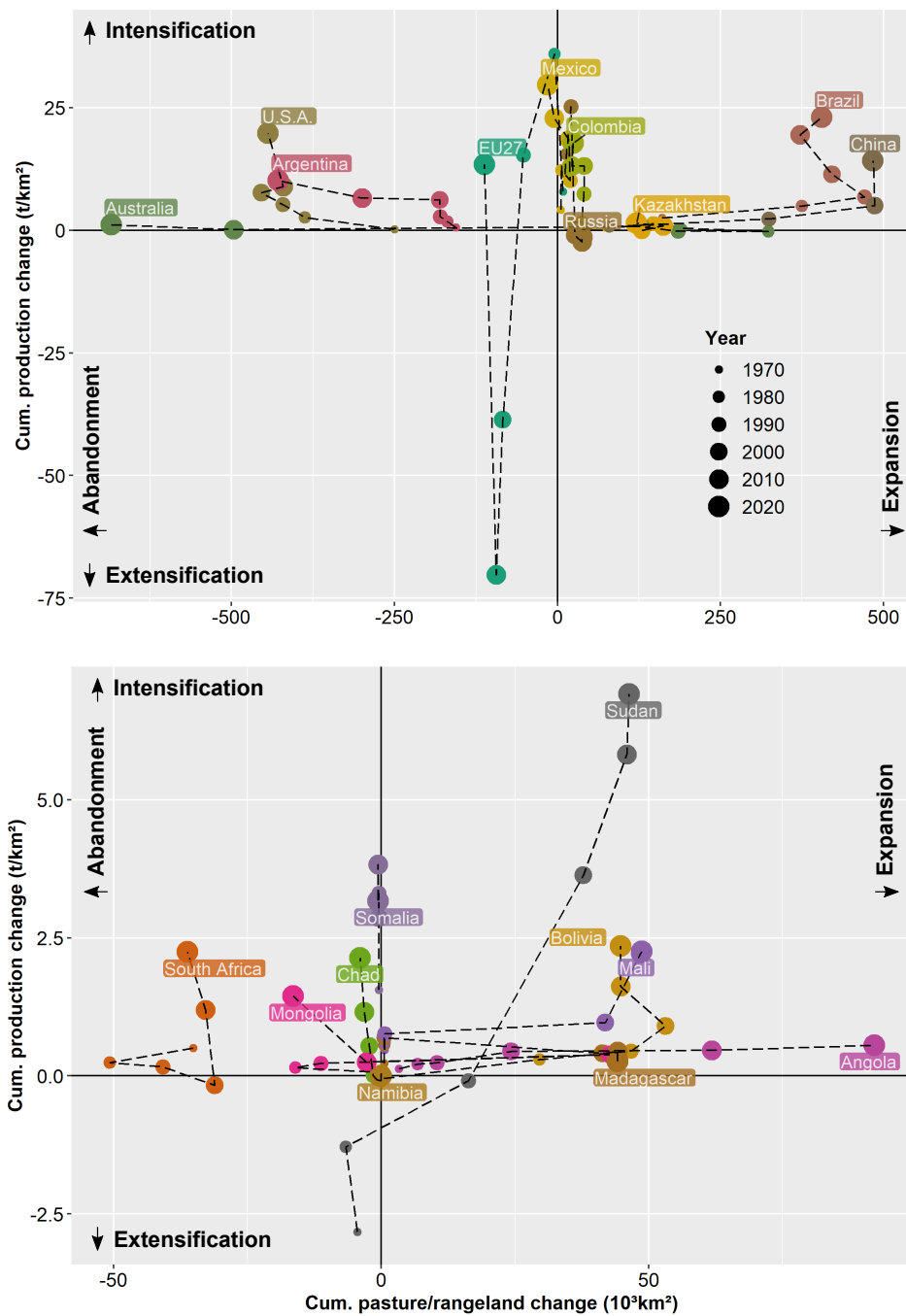


**Figure 3.14:** Trajectories of pasture/rangeland change: Decadal intensification (absolute meat and milk production change) and expansion (net area change) of pasture/rangelands for selected countries during 1960-2020. The 20 countries with the largest pasture/rangeland areas are displayed.

to mainly cattle pastures by 2000 (Lerner et al., 2017).

In Bolivia, the expansion phase lasted until 2000, after which the reversal began and an

intensification surge – however less intense than in Brazil or Colombia – accompanied by the abandonment of pasture/rangelands was initiated, without resuming expansion. Mexico showed high intensification rates and even shifted from net pasture/rangeland expansion to abandonment from 1990 onwards.

The onset of intensification after long-term expansion in Brazil, Colombia and Bolivia backs up the hypothesis of induced intensification that farmers tend to expand, while land is abundant, before they intensify due to higher land prices, when land becomes scarce (Kaimowitz & Angelsen, 2008).

China followed a pathway of immense expansion on pasture/rangelands with rather low but increasing land use intensities from 1960 to 2000. Afterwards, a very strong intensification with stagnating pasture/rangeland areas was initiated. This turnaround towards less land expansion and more intensive land use coincides with environmental policies. In the 2000s, nomad "sedentarisation" projects were launched by the Chinese government. They decreased the mobility of livestock herds of extensive pastoralists with the aim to improve household income and restore grasslands through reduced grazing pressure and additional fodder cultivation (Bryan et al., 2018; Hruska et al., 2017). As a consequence, livestock numbers more than doubled within just 10 years in Inner Mongolia (Briske et al., 2015). In addition, China's meat and dairy industries have experienced an immense growth and drastic revolutionary changes during the last 20 years, which were driven by political support, technological advances, availability of efficient feed and globalised trade (DuBois & Gao, 2017; Zhou et al., 2012). The drastic intensification in the Chinese meat and dairy sector goes along with large environmental costs. It caused greenhouse gas emissions that are ~50% higher than those in developed countries and led to ecosystem degradation due to unsustainable land use practices (Briske et al., 2015; Du et al., 2018).

In contrast, Argentina is one of the countries with a clear pathway towards pasture/rangeland intensification with area decline. The strongest intensification trend could be found during 1970-2000, followed by large-scale pasture/rangeland abandonment at stagnating production levels. Since 2010, production increased while pasture/rangeland area further decreased. In Argentina, deforestation for pasture/rangeland in the past has been replaced by strong intensification of grazing systems, which involves grassland conversion to other uses such as croplands in the Pampas region (Godde et al., 2018). It was suggested that further intensification involving the transformation of grazing land to cropland is likely to continue in the Argentinian Pampas and Chaco as long as agricultural demands and profits remain high (Piquer-Rodríguez et al., 2018). The soy bean expansion on former grasslands in the last 20 years has forced the displacement of grazing systems to marginal lands, which has often led to ecosystem degradation and a disappearance of grasslands (Busso & Fernández, 2018). Therefore, the observed pasture/rangeland abandonment in Argentina does not necessarily mean an increase of natural vegetation but rather an expansion of croplands.

Another example of an pasture/rangeland intensification and abandonment trajectory are the US, where long-term pasture/rangeland abandonment with increasing intensification rates has been replaced by a phase of strong intensification with relatively low area changes. The US has experienced a conversion of grazing systems to other uses (e.g. to maize and soy production in the Western Corn Belt) and progressively turned to landless livestock systems. This goes along with intensification due to high efficiencies in the grazing system. However the impacts of unsustainable intensification strategies (water contamination, greenhouse gas emissions, biodiversity reduction) have raised environmental concerns and even led to cases of extensification (Godde et al., 2018). Westward movement of dairy production in the US coincided with increasing farm sizes and outsourcing rather than own production of fodder (Gillespie et al., 2010).

Our findings show that countries of the EU also underwent a long period of massive pasture/rangeland abandonment, most pronounced during 1980-2000. Whereas grazing systems have been dis-intensified, as meat and milk production decreased from 1980 to 2010, a recent phase of intensification was induced only recently from 2010. The downward trend in livestock intensity during 1980-2000 may be the result of political upheavals in Eastern Europe, particularly the collapse of the Soviet Union, which caused an abrupt decline of meat and milk production in around 1990 (e.g. Germany, Poland, Czechia; FAO, 2022). The reduction of the agricultural area in many countries coincided with the establishment of the EU in around 1970. This went along with a decrease in livestock density (except for the Netherlands and Austria) (van der Sluis et al., 2016). Furthermore, political restrictions of milk production formed the development of the livestock sector in the EU and likely explain the extensification-abandonment trajectory observed here. During the 1970s, a policy of guaranteed high prices for agricultural products was pursued, which led to overproduction (primarily of butter). As a consequence, the EU implemented production limits in 1984 (Bórawski et al., 2020). Only recently, a political deregulation of the dairy sector occurred in the EU (Clay et al., 2020). The removal of milk production quotas in 2015 resulted in a rapid increase of European milk production (Bórawski et al., 2020; Clay et al., 2020). Yet, the increase in livestock numbers grew faster than the productivity (Bórawski et al., 2020). What is more, rising production costs and declining market prices due to overproduction and retailer control of supply chains have caused abandonment of farms during the last decades. Shifts from pasture-based to confinement feeding systems further revolutionised the dairy industry (Clay et al., 2020). Livestock systems in many regions experienced rapid increases in farm size (most pronounced in new EU member states Bulgaria, Slovakia and Poland) accompanied by a fast growth of megastables with 500 or more livestock units (notably in Germany, Poland, Sweden and France) (Debonne et al., 2022). In addition, agriculture in Europe has been shaped by regionally differing megatrends: climate change, demographic change, post-productivism shifts and risingly stringent environmental regulations. Therefore, many European regions have followed a dynamic rather than a stable trajectory (Debonne et al., 2022).

Overall, we find evidence of an induced intensification of pasture/rangelands in emerging middle-income countries such as Brazil, Colombia or China, where intensification begins when demand increases and land for further expansion becomes scarce (e.g. due to environmental constraints or over-exploitation). Further, political factors mediate the intensification-expansion trajectories of pasture/rangelands, as most pronounced in Europe. What is more, changes of pasture/rangelands are often interlinked with those on croplands (e.g. cattle ranging and soy bean cultivation in Brazil). Finally, the role of distant drivers such as demand in one world regions inducing agricultural changes in another region, was not addressed in depth and offer room for further research.





## Chapter 4

# Global land use transitions and their drivers

This chapter is based on:

Winkler, K., Fuchs, R., Rounsevell, M., & Herold, M. Global land use transitions and their drivers. *Scientific reports*, Collection: Anthropogenic modifications (in review).

*The truly unique trait of 'Sapiens' is our ability to create and believe fiction. All other animals use their communication system to describe reality. We use our communication system to create new realities. Of course, not all fictions are shared by all humans, but at least one has become universal in our world, and this is money.*

Yuval Noah Harari

## Abstract

We analyse global land use transitions and their drivers based on a novel land use reconstruction from 1960-2019, the Historic Land Dynamics Assessment+ (HILDA+), and a data-driven estimation of causal relationships. We find that agricultural expansion accounted for the largest share of land use change ( $\sim 7.6$  million km<sup>2</sup>); an area as large as Greece every year. Notably, the global expansion of agriculture into non-forested areas was over three times greater than expansion into forests. Agricultural expansion was the major land use transition in the Global South with strong links to globalised markets. Conversely, agricultural abandonment, forest expansion and intensive forestry dominated in the Global North, driven by economic growth, production and political factors. This supports the thesis that forest expansion in the Global North involves the displacement of land use, especially deforestation and agricultural expansion, to the Global South. Our driver analysis underlines the dominating role of humans, particularly, the importance of economic drivers and the (as yet) small influence of environmental factors on global land use transitions. Our findings highlight the significance of the indirect socio-economic drivers of land use change, and why acting on them is critical when defining and implementing sustainable, climate-adapted land use policies.

## 4.1 Introduction

The ways in which people use the land surface is critically important in contributing to solutions to global societal challenges, such as climate change (Friedlingstein et al., 2020; Jia et al., 2019), biodiversity loss (Haddad et al., 2015) and food security (Foley et al., 2011). To find sustainable pathways for future land use transitions, we need to learn from past land use dynamics.

The extent of past, global land use change has been evaluated in numerous studies (Hurtt et al., 2020; Klein Goldewijk et al., 2017; Winkler et al., 2021). Yet, little is known about the underlying causes of land use transitions at the global scale, reflected within the drivers of change and their interactions. New insights are still constrained by a lack of consistent spatial, temporal and thematic detail in available land use data. Despite increasing availability and accuracy, Earth Observation data such as ESA CCI Land Cover (ESA, 2017), Global Forest Change (Hansen et al., 2013), Copernicus Land Cover (Buchhorn et al., 2020) is still fragmented, detects land cover, but not necessarily land use, and does not provide continuous time series that are long enough to explore major land use transitions over several decades such as reforestation or cropland expansion and abandonment. A recent land use reconstruction, the Land-Use Harmonization 2 (LUH2) (Chini et al., 2021), provides a comprehensive land use database that is used as the state of the art for Earth system models, but LUH2 remains at a rather coarse spatial resolution ( $\sim 0.25^\circ$ ) and relies on only a few observational data streams with many assumptions about the allocation of land use types. Furthermore, LUH2 contains land use trends, which deviate from independent databases, e.g. the cropland trend since 2000 or the extent of shifting cultivation in the tropics (Ganzenmüller et al., 2022). Other studies have either addressed individual land use transitions in isolation, such as deforestation (Aide et al., 2013; Hansen et al., 2013; Sy et al., 2019) or cropland abandonment (Schierhorn et al., 2013; Yu & Lu, 2018), or lacks spatially-explicit mapping and quantification. Because of these limitations, LUH2 and other past land use/cover reconstructions cannot sufficiently inform understanding of the extent of land use transitions at the global scale. This led to the development of the Historical Land Dynamics Assessment+ (HILDA+) dataset (Winkler et al., 2021), of global land use change between 1960 and 2019. HILDA+ provides, for the first time, a comprehensive, data-driven analysis of the spatio-temporal dynamics of land use change at the global scale, with high spatial resolution over a long time period.

The underlying processes and complex interactions between the drivers of land use change have been analysed from different thematic, spatial or temporal perspectives. A distinction is often made between direct and indirect drivers, which is consistent with existing studies of land use and ecosystem change (Díaz et al., 2015; Kleemann et al., 2017; Lambin et al., 2003). Direct drivers have obvious and local impacts on the land surface, e.g. production, management as well as environmental and climatic factors. In contrast, indirect

drivers are the underlying anthropogenic (socio-economic) causes of land use change, e.g. demography, politics, economy/trade and consumption, and are often channelled through direct drivers at different scales. While there is much research on specific drivers of land use transitions for particular world regions (Munteanu et al., 2014; Plieninger et al., 2016; van Vliet et al., 2015), comprehensive global studies of the drivers of land use change remain scarce. The reason for this is probably a lack of data at high temporal, spatial and thematic resolutions, with global coverage. For a general study of the drivers of land use changes, it is suggested to focus on socio-economic, political, technological, natural and cultural driving forces and their spatial, temporal but also institutional dimensions (Bürgi et al., 2004). At the global scale, commodity production, forestry, shifting cultivation, and wildfires have been identified as drivers of forest loss (Curtis et al., 2018). Population expansion and changing consumption are considered to be strong indirect drivers of agricultural expansion for food, bioenergy, and waste production (Alexander et al., 2015). Many studies address wide-ranging drivers of land use change at the regional scale. For example, agricultural production for meat supply has been shown to drive land use change in the Global South (Hong et al., 2021). Policies (forest conservation or agricultural subsidies) and market opportunities have been shown to be the main drivers of land use transitions in tropical forest-agricultural frontiers (van Vliet et al., 2012). Mechanisation leads to displacement of land use, when deforestation for pasture is followed by commercial cropland in the Amazon (Arima et al., 2011; Piquer-Rodríguez et al., 2018; Sy et al., 2015). Global markets, changing consumption, increasing wealth and political incentives play an important role in the expansion of commodity crops such as rubber in Laos (Junquera et al., 2020), tobacco in Tanzania (Jew et al., 2017) and soy bean in South America (Reenberg & Fenger, 2011). In the EU, agricultural land use change has been strongly influenced by globalised agricultural markets, the transition from a rural to an urban society, and a regime shift to post-socialism (van Vliet et al., 2015). Energy production, in particular from biofuels, is an increasing driver of land use change, for example in the US (Trainor et al., 2016). Indicators of climate and environmental change such as precipitation, duration of the rainy season, or temperature have been identified as key drivers of land use change in arid regions, for example in Iran (Tahmasebi et al., 2020) or African savannahs (Wigley et al., 2010).

Hence, land use change is driven by the complex interplay of economic, technological, institutional, demographic, sociocultural, location, and environmental factors that operate at different spatial and temporal scales (Bürgi et al., 2022). Attempts to measure these drivers, and their role in causing land use change, comprehensively and consistently for the entire globe over several decades at high temporal and spatial resolution are currently lacking.

In this paper, we identify and quantify the main transitions of global land use change and their spatio-temporal patterns, as well as the main drivers as the underlying causes of change. We build on the HILDA+ dataset of global land use change between 1960

and 2019 (Winkler et al., 2021) to identify and classify the major global, land use/cover transitions. We correlate the rate of land use change with numerous indicators representing indirect drivers from demography, politics, and economy/trade as well as the direct drivers from production and environmental change.

By providing new data-driven and quantitative insights into the underlying drivers of global land use transitions, we aim to learn from the recent past, to identify trends and to understand how socio-economic and environmental factors affect the way humans use and change the land surface. This insight from the past is essential in guiding the implementation of measures and policies for future sustainable land use.

## 4.2 Material and methods

### 4.2.1 HILDA+ land use change dataset

We used the Historic Land Dynamics Assessment+ (HILDA+) dataset (Winkler et al., 2021), a synthesis dataset of global land use change covering six land use/cover categories between 1960 and 2019 (based on Earth Observation and statistical datasets), as the basis for this analysis. HILDA+ combines long-term, land use statistics with multiple satellite-based land cover products and contains annual transitions between six generic land use/cover categories: urban areas, cropland, pasture/rangelands, forests, unmanaged grass/shrubland, and areas with no/sparse vegetation. HILDA+ has a global coverage, high spatial resolution (1 km), annual temporal resolution, and a time span of several decades, which makes it suitable for the analysis of land use transitions. In this study, an updated version of the HILDA+ dataset was used (Winkler et al., 2020).

### 4.2.2 Classification of land use transitions

The annual HILDA+ land use/cover layers between 1960 and 2019 were used in the original Eckert IV projection, an equal-area pseudo-cylindrical map projection, where one pixel equals an area of 1 km<sup>2</sup>. Based on these land use/cover maps, we applied a rule-based classification of general land use transitions. Figure 4.1 gives an overview of the defined rules and land use/cover sequences describing the targeted land use transitions. By iterating through the annual maps of global land use/cover, the land use transitions were then classified according to these rules and mapped onto a global 1x1 km grid. This procedure was implemented in Python 3.7 with the GDAL package (<https://pypi.org/project/GDAL/>) and yielded a global map of land use transitions from 1960 to 2019 at a 1 km grid resolution.

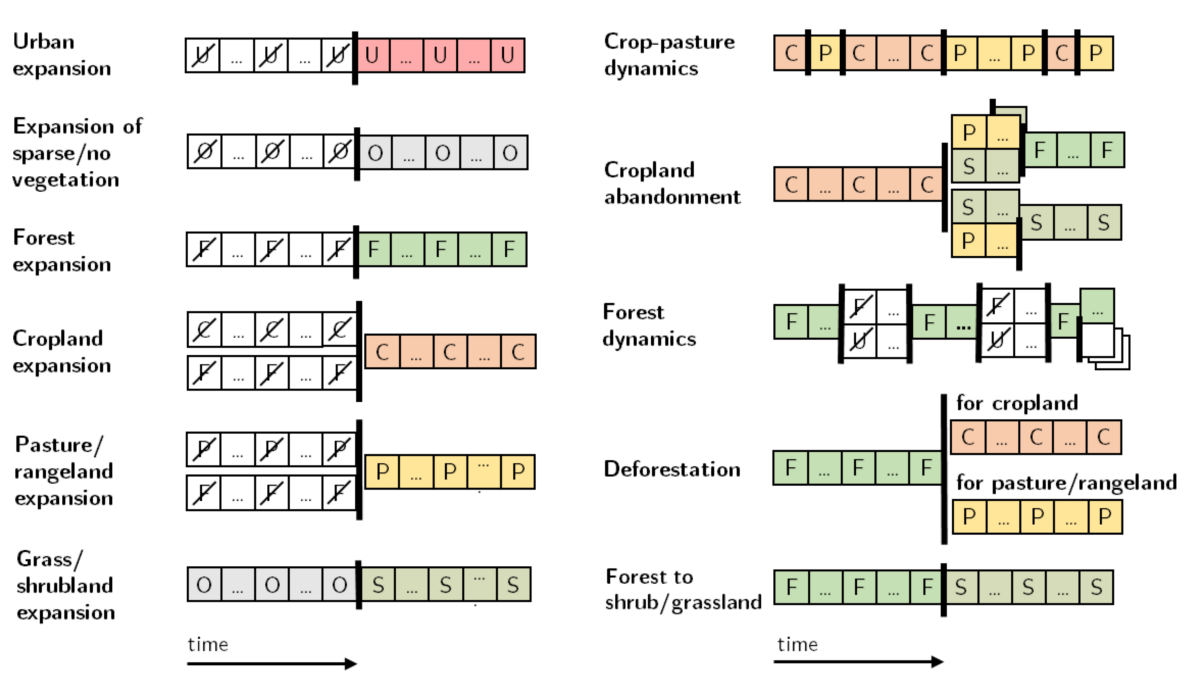


**Figure 4.1:** Land use transitions, their underlying land use/cover sequences and rules for classification. U: Urban, C: Cropland, P: Pasture/rangeland, F: Forest, S: Grass/shrubland, O: sparse/no vegetation

For each year and country (based on GADM 2.8 maps of administrative areas for all countries, <https://gadm.org/>), the number of pixels with a change in land use category on the annual HILDA+ transition maps were counted and attributed to one of the land use transitions. We assigned a new class code for each of the 12 land use transitions. With this data, the annual rate of change belonging to each land use transition was derived per country and stored in a data frame. The resulting data frame was used for the subsequent driver analysis.

### 4.2.3 Driver analysis

Selection of driver indicators Based on existing studies about the drivers of land use change from different perspectives (Alexander et al., 2015; Curtis et al., 2018; Hong et al., 2021; van Vliet et al., 2015), indicators were selected and classified into the following categories:

- **Indirect Drivers**

- **Demography:** Population and its structure
- **Economy:** Economic growth, trade, market, labour and consumption
- **Politics:** Institutional factors such as governance, environmental policies, conflicts

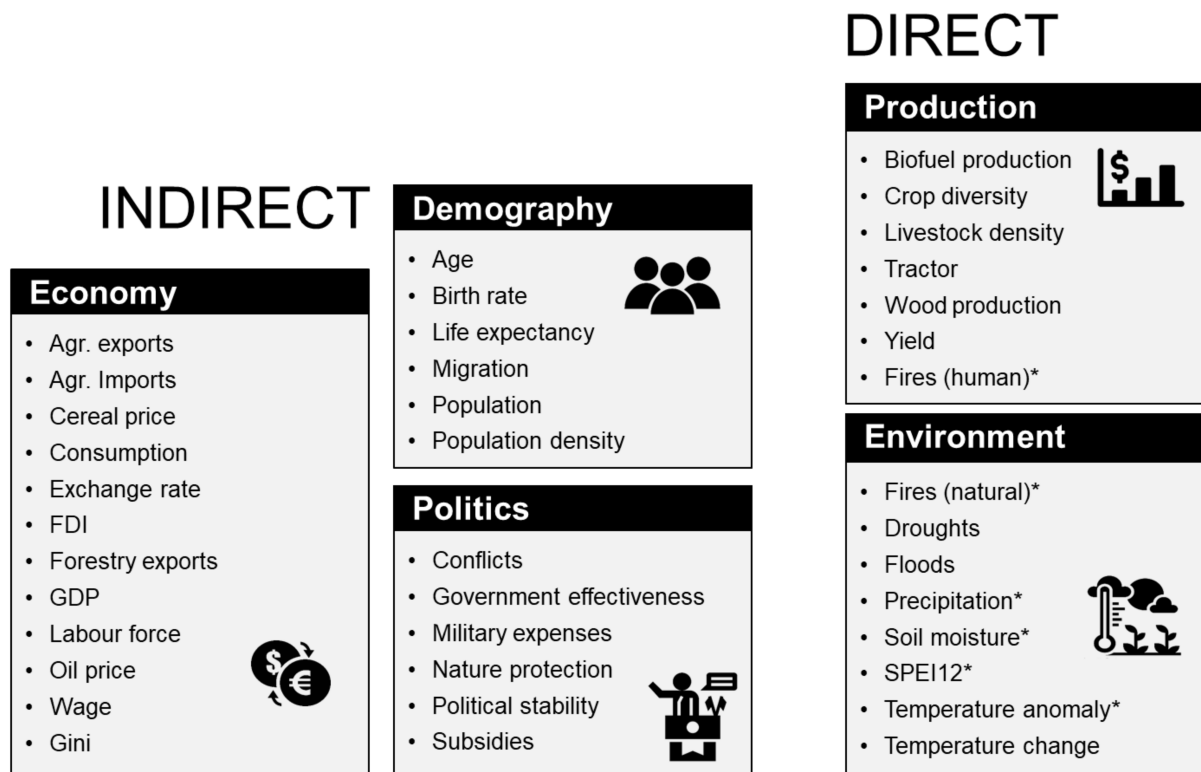


**Figure 4.2:** Indirect and direct drivers of global land use change: Selected categories and underlying indicators in alphabetical order. \*Indicators originating from spatial datasets are marked with an asterisk.

- **Direct drivers**

- **Production:** Agricultural production and technical land management
- **Environment:** Climate and environmental factors

The categories comprise 39 individual indicators, which were collected for as long and continuous an annual time series as possible. Indicators were selected based on relevant studies (as given above) and data availability (ideally national-scale, with global coverage, as annual time series from 1960 to 2019). A distinction was made between direct and indirect drivers based on existing work studying drivers of land use and ecosystem change (Díaz et al., 2015; Kleemann et al., 2017; Lambin et al., 2003).

With this ensemble of indicators (see Figure 4.2), we mapped a largely holistic spectrum of possible drivers of land use change. However, completeness and independence of the indicators cannot be assured, which is why absolute statements and causal relationships were derived with caution.

#### 4.2.4 Preparation of the indicator set

The annual and country-specific rates of land use change for the land use transitions were compiled with the 39 driver indicators as explanatory variables in a large table. Existing data gaps in the annual values were filled by temporal linear interpolation.

Some environmental indicators were acquired as spatial datasets (marked with an asterisk in Figure 4.2 and Table 4.1). Pre-processing of these datasets was done by first resampling and re-projecting both the land use transition map and the GADM country map to the original resolution and projection of the indicator dataset (see detailed data specifications in Table 4.1). Next, the annual mean value of each indicator was calculated only for the area covered by each of the land use transitions, respectively. This means that, for spatially explicit environmental indicators, each pair of land use transitions and driver indicators in a country refers to the same area, namely the area affected by the respective land use transition, and not to the entire country as for all other driver indicators. Note that oil price is the only driver indicator that is globally constant and not country-specific.

#### 4.2.5 Causal network estimation with PCMCI

As a method to identify possible drivers of land use change, we used the Peter and Clark Momentary Conditional Independence (PCMCI) algorithm for causal discovery in time series as integrated in Tigramite, a python package for causal time series analysis (Runge, 2022; Runge et al., 2019). PCMCI quantifies time-lagged and contemporaneous relations between variables. It has been successfully applied in studying the drivers of land surface variables in large river basins (Uereyen et al., 2022).

PCMCI consists of a two-step procedure to identify causal links between multiple variables. First, a version of the Peter and Clark (PC) algorithm is applied to select the conditions, i.e. extract potential time-lagged drivers for each input variable. Second, the momentary conditional independence (MCI) test is used. During the MCI step, causal links between the variables are tested given the discovered potential drivers from the first PC step. Here, p values and test statistic values were estimated for all links accounting for common drivers, indirect links, and autocorrelation (Runge, 2022).

We adapted the PCMCI algorithm to select only the significant causal links between the time series of the 39 driver variables (explanatory variable set) and the annual rate of land use change from each of the 12 land use transitions (response variables) in an iterative procedure for all countries. To meet the stationarity requirement for the PCMCI, we removed the linear trend in each of the time series of the indicators by a least square fit (signal de-trending). A maximum time lag of five years was used for the analysis. We applied ParCorr (partial correlation test) as a conditional independence test.

**Table 4.1:** Detailed specifications of selected indirect and direct driver indicators and their references.

Driver indicator	Used thematic coverage	Unit	Period	Driver group	Reference
Age	Median age of the total population	years	1960-2019 (5-year steps, interpolated)	demography	United Nations (UN) (2019)
Birth rate	Crude birth rate: Number of live births occurring during the year, per 1,000 population estimated at midyear	people	1960-2019	demography	World Bank (2019a)
Life expectancy	Life expectancy at birth, total: Number of years a new-born infant would live if prevailing patterns of mortality at the time of its birth were to stay the same throughout its life	years	1960-2019	demography	World Bank (2021c)
Migration	Net migration: Number of immigrants minus the number of emigrants, including citizens and non-citizens	people	1962-2017 (5-year steps, interpolated)	demography	World Bank (2019b)
Population	Total population	people	1960-2019	demography	FAO (2019b)
Population density	Population density	people/ km <sup>2</sup>	1960-2019	demography	World Bank (2021d)
Agr. exports	Export quantity of crops and livestock products (Cereals, bovine meat, dairy products, fodder and feeding stuff, oilseeds)	tonnes	1961-2019	economy	FAO (2020e)
Agr. imports	Import quantity of crops and livestock products (all items)	tonnes	1961-2019	economy	FAO (2020e)
Cereal price	Producer price index of cereals: Prices received by farmers for primary products as collected at the point of initial sale (prices paid at the farm-gate).	index (relative to 2014-2016)	1991-2019	economy	FAO (2020c)
Consumption	Food supply – Animal products potentially available for human consumption (total quantity produced added to the total quantity imported, exported and adjusted to any change in stocks per capita, divided by total population)	1000 tonnes per capita	1961-2019	economy	FAO (2021a)
Exchange rate	Price of one country's currency in relation to US dollar	standard local currency units per US\$	1970-2019	economy	FAO (2020a)
FDI	Foreign Direct Investments (FDI): Total FDI inflows: Investment which aims to acquire a lasting management influence (10% or more of the voting stock) in an enterprise operating in a foreign economy	million US\$ (2015 prices)	1991-2019	economy	FAO (2020b)
Forestry exports	Export quantity of round-wood	volume m <sup>3</sup>	1961-2019	economy	FAO (2021b)

Driver indicator	Used thematic coverage	Unit	Period	Driver group	Reference
GDP	Gross domestic product (GDP) per capita: Sum of gross value added by all resident producers in the economy plus product taxes and minus subsidies; total value created in the production of goods and services (two time series: World Bank and FAO)	US\$ per capita	World Bank: 1960-2019 (data gaps interpolated) FAO: 1970-2019	economy	World Bank (2021a); FAO (2021c)
Gini	Gini index (World Bank estimate): Measure of inequality, the extent to which the distribution of income within an economy deviates from an equal distribution.	index (0-100)	~1980-2019 (data gaps interpolated, different periods per country)	economy	World Bank (2021b)
Labour force	Labour force participation rate: Proportion of a country's working-age population that engages actively in the labour market (working or looking for work)	percentage	1990-2017	economy	International Labour Organization (ILO) (2020b)
Oil price (global)	Global crude oil prices	US\$ per barrel	1960-2019	economy	Our World in Data (2021b)
Wage	Mean nominal monthly earnings of employees	US\$	1992-2019 (data gaps interpolated, different periods per country)	economy	International Labour Organization (ILO) (2020a)
Conflicts	Number of armed conflicts from Armed Conflict Location & Event Data Project (ACLED) and Uppsala Conflict Data Program (UCDP) as two different time series	amount of conflicts	ACLED: 1997-2019 UCDP: 1989-2019	politics	ACLED (Raleigh et al., 2010) UCDP Version GED 20.1 (Pettersson et al., 2021)
Government effectiveness	Government effectiveness from Worldwide Governance Indicators (WGI): Perceptions of the quality of public services, policy formulation and implementation	index scale from -2.5 to +2.5	1996-2019	politics	World Bank and multiple sources (Kaufmann et al., 2010)
Military expenses	Military expenditure by country as proportion of government spending	percentage	1988-2019	politics	Stockholm International Peace Research Institute (SIPRI) (2020)
Nature protection	Environmental performance index (EPI): Terrestrial Biome Protection (national): Weighted proportion of each biome in a country that lies within a protected area	percentage	1995-2019	politics	Yale University (2020)

Driver indicator	Used thematic coverage	Unit	Period	Driver group	Reference
Political stability	Political stability and Absence of Violence/Terrorism from Worldwide Governance Indicators (WGI): Likelihood of political instability and/or politically-motivated violence including terrorism	index scale from -2.5 to +2.5	1996-2019	politics	World Bank and multiple sources (Kaufmann et al., 2010)
Subsidies	Subsidies and other transfers: All transfers on current account to private and public enterprises, governments, international organisations, other government units, social security, social assistance, and employer social benefits	current local currency	1988-2019	politics	World Bank (2021e)
Biofuel production	Biofuel energy production (includes both bioethanol and biodiesel)	TWh	1990-2019	production	Our World in Data (2021a)
Crop diversity	Gini coefficient, calculated from relative mean absolute difference in produced crops (area harvested in ha), higher values represent lower crop diversity (higher imbalance).	index scale from 0 to 1	1961-2019	production	FAO (2020d)
Fire*	Sum of burned area, derived from spatial dataset (0.25 ° resolution) linked with anthropogenic land use transitions (this study): cropland expansion, pasture/rangeland expansion, crop-pasture dynamics, deforestation for cropland or pasture/rangelands, urban expansion	pixels	1982-2018	production	ESA Fire CCI (Chuvieco et al., 2020)
Livestock density	Livestock number (cattle, buffalo, sheep, goats; in heads) per pasture area	heads/1000ha	1961-2019	production	FAO (2020d)
Tractors	Number of agricultural tractors in use	tractors	1961-2009	production	FAO (2016)
Wood production	Production quantity of round-wood	volume in m <sup>3</sup>	1961-2019	production	FAO (2021b)
Yield	Yield of cereals: Harvested production per unit of harvested area for cereals	hg/ha	1961-2019	production	FAO (2020d)
Droughts	Occurrence of disaster type "drought"	droughts	1961-2019	environment	EM-DAT (2021)
Floods	Occurrence of disaster type "flood"	floods	1961-2019	environment	EM-DAT (2021)
Precipitation*	Sum of monthly precipitation; derived from spatial dataset (~4 km resolution)	mm	1961-2019	environment	TerraClimate (Abatzoglou et al., 2018)
Soil moisture*	Mean of daily soil moisture, derived from spatial dataset (0.25 ° resolution)	ratio of volume m <sup>3</sup> /m <sup>3</sup>	1979-2019	environment	ESA Soil Moisture CCI (Dorigo et al., 2020)
SPEI12*	Standardised Precipitation Evapotranspiration Index (SPEI, multi-scalar drought index) for drought conditions with 12 months; derived from spatial dataset (1 ° resolution)	Index scale from 3 to 3	1961-2019	environment	SPEI Global Drought Monitor (2021)

Driver indicator	Used thematic coverage	Unit	Period	Driver group	Reference
Temperature anomaly*	Average of monthly land surface air temperature; derived from spatial dataset (1° resolution)	°C	1961-2019	environment	Earth (2020); Rohde & Hausfather (2020)
Temperature change	Temperature change: Mean surface temperature change by country and meteorological year	°C	1961-2019	environment	FAO (2021d)
Wildfires*	Sum of burned area, derived from spatial dataset (0.25° resolution) linked with non-anthropogenic land use transitions (this study) as transitions between unmanaged land use categories: forest dynamics, forest to shrub/grasslands, expansion of shrub/grassland, expansion of sparse/no vegetation	pixels	1982-2018	environment	ESA Fire CCI (Chuvieco et al., 2020)

\* Indicators were derived from spatially explicit datasets and computed only for the affected area of each land use transition, respectively.

In our study, partial correlation is estimated through linear ordinary least squares (OLS) regression and a test for non-zero linear Pearson correlation on the residuals. Here, a student's-t distribution at 95% confidence level was implemented. The resulting p-values and partial correlation coefficients, as test statistic values, give a qualitative measure of the uncertainty and the strength of the detected significant causal links.

#### 4.2.6 Driver mapping and analysis

Each land use transition was assigned a driver indicator with the highest partial correlation coefficient, i.e., the strongest causal link. Here, the strength of the causal links was defined as its absolute partial correlation coefficient. The associated driver category of this “winner” indicator was then mapped onto the geographic area affected by the respective land use transitions. This was done for the entire causal link dataset with 1) indirect and direct driver indicators, 2) only indirect driver indicators and 3) only direct driver indicators.

#### 4.2.7 Ranking of the driver indicators

To identify the driver indicators with the highest significance, we took two approaches. First, we ranked the driver indicators (“winner indicators”) by area of land use change. Thereby, we assumed that the driver indicators linked to a large area affected by land use transitions were more important than those related to only small areas of land use

transitions. This approach assumes that large-scale land use changes are more significant than small-scale changes, which is not always the case. Urban expansion for example, although very small in global extent, has a strong impact on land use changes in the surrounding area. To take this into account, in the second approach, the ranking of the driver indicators (“winner indicators”) was done by correlation coefficient. In doing so, we took the strength of the causal link as the partial correlation coefficient into account and assumed that driver indicators with stronger correlations to land use transitions were more important than those yielding weaker correlations. Note that the ranking does not distinguish between positive and negative correlations. However, negative correlation results were displayed as dark shaded bars (in terms of area in the first and in terms of relative occurrence in the second approach).

#### 4.2.8 Uncertainty of the driver analysis

The driver analysis presented here has limitations and includes uncertainties of various sources. First, the utilised data itself represents a source of uncertainty. Uncertainties in the land use dataset HILDA+ arise from deviation of input datasets (remote sensing-based maps of land use classifications) due to different definitions, classification methods and resolutions, and from the methodology owing to the extrapolation of land use trends, particularly for the period before 1982, when no spatially explicit data were available (Winkler et al., 2021). In addition, the driver analysis relies on numerous indicators from different databases (e.g. FAO, World Bank, United Nations). These do not all cover the full period of 1960-2019, are not all provided as continuous annual values, have not all been obtained under the same methodology (e.g. statistical data vs. Earth Observation data) and are not all available for all countries of the world. Information on the temporal and spatial data gaps are given in Table 4.1. These deviations in temporal and spatial coverage or resolution imply that not all indicators are equally represented in the driver analysis. Because of this, the results of the driver analysis for individual indicators and their ranking by area should be treated with caution. Second, the configuration of the driver analysis is constrained by the selection of the driver indicators and some model assumptions. The ensemble of driver indicators used here does not represent a complete outline of the structure of drivers of land use change and their reciprocal effects. Data availability and interdependencies of indicators are clear limitations of the driver analysis. Another important aspect of uncertainty is the breakdown of the indicators into driver groups. Although our classification is drawn from existing studies about drivers of land use change (Alexander et al., 2015; Curtis et al., 2018; Hong et al., 2021; van Vliet et al., 2015), the classification sometimes has ambiguities, which makes the group assignment difficult. The demarcation of driver groups is often fuzzy and can therefore be challenged. Moreover, they are not equally represented based on the number of indicators. Thus, when comparing the driver groups, not all drivers are equally represented based on the availability, number and temporal reference of their indicators.

Nevertheless, we attempted to overcome these limitations by aggregating the results spatially and thematically. The comparison of the driver configurations by world region and land use transitions gives an overarching picture of the driver framework of land use change.

Even though the method targets the identification of causal links, correlation does not always mean causality. Here, we analysed the causal links between driver indicators and land use transition on an annual basis by means of PCMCI. The method accounts for time-lagged causal links, interdependencies, and (undirected) contemporaneous links. Note that the causal analysis assumes that all relevant variables in a specific system are included and no hidden variables exist. Therefore, the results and interpretations are only valid with respect to the generated feature space.

## 4.3 Results and discussion

### 4.3.1 Land use transitions

The distribution of 12 major land use transitions reveals a complex pattern of global land use change (see Figure 4.3). In terms of area, agricultural expansion dominated the land use transitions over the last six decades. Adding up the transitions in agricultural land use (pasture/rangeland expansion, cropland expansion, deforestation for pasture, deforestation for cropland), an area of about 7.6 million km<sup>2</sup> was affected from 1960 to 2019. Thus, agricultural land has expanded at a rate equivalent to the area of Greece every year. The expansion of agricultural land, either pasture/rangeland or cropland, into non-forest areas was the largest land use transition during that time. This expansion affected about 5.9 million km<sup>2</sup> of land, which is almost twice the size of India.

Strikingly, agricultural expansion at the expense of non-forested areas, namely natural grass, shrub- or non-vegetated land, affected  $\sim 6.0$  million km<sup>2</sup> of land and is over three times as large as deforestation for agriculture ( $\sim 1.7$  million km<sup>2</sup>). While the climatic and environmental impact of deforestation arising from agricultural expansion has been highlighted and recognised by many studies, public media and political decision-making bodies (Aleixandre-Benavent et al., 2018; Gibbs et al., 2010, 2007; IPCC, 2019a), the expansion of cropland and pasture/rangelands into non-forested natural areas has received relatively less attention.

Among all the transitions of agricultural expansion, the expansion of pasture/rangeland accounts for the largest global land area. Around 64% of agricultural expansion into non-forested land comes from the spread of pasture/rangeland. However, a large affected area does not mean uniformly intensive land use practices. Areas of pasture/rangeland expansion mainly contain low-intensity and often nomadic forms of pastoral land use that have spread in arid, semi-arid or high-mountain regions. In China and Central Asia, the

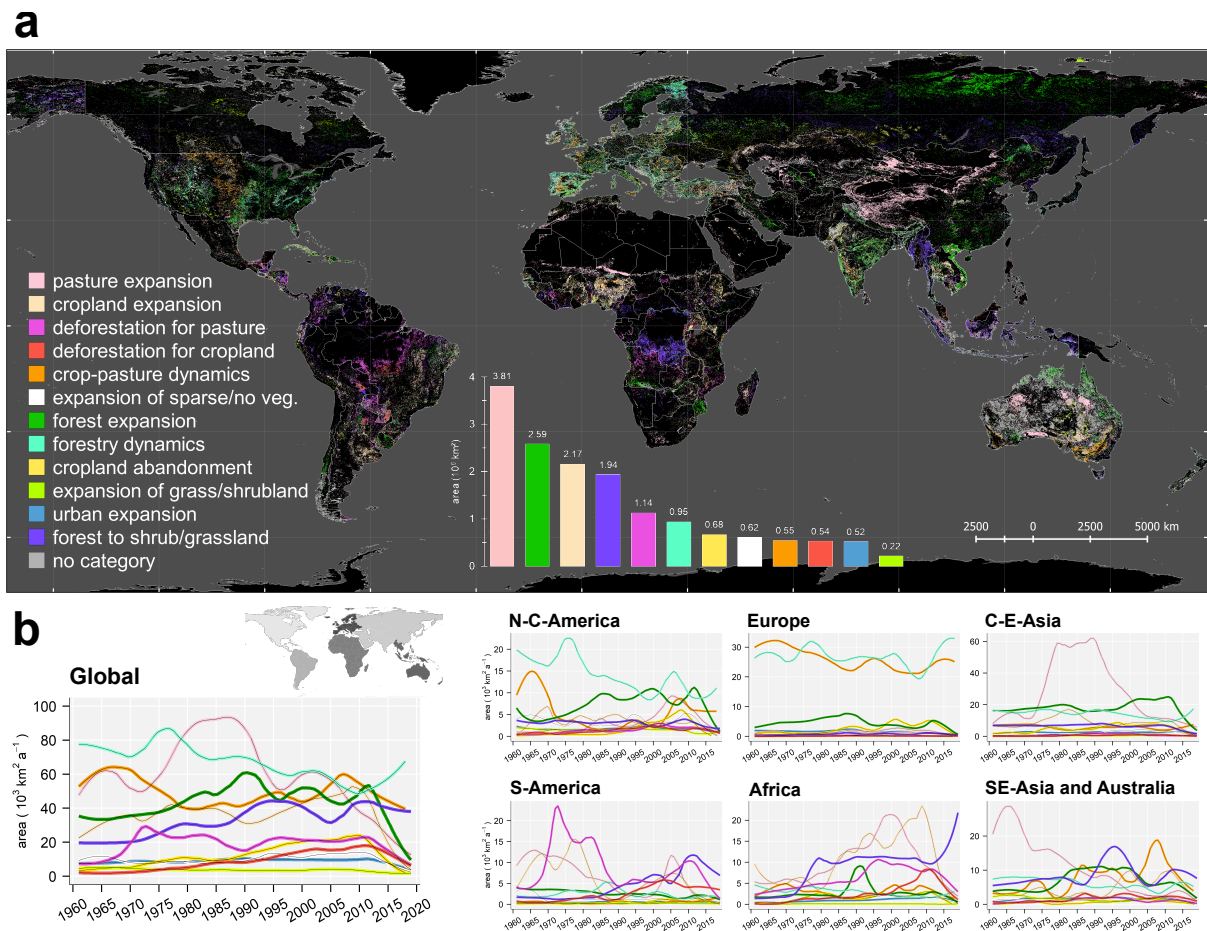


**Figure 4.3:** Spatio-temporal patterns of global land use transitions. a) Spatial extent of categorised global land use transitions in 1960-2019 b) Annual rate of land use transitions for different world regions. Extents are displayed in small world map. Lines of annual area were smoothed with a 3 year moving average.

Sahel zone, and Australia, pasture/rangelands have expanded into former unmanaged land, i.e. sparsely/non-vegetated, grass- or shrubland areas.

In Africa, the rate of pasture/rangeland expansion more than quadrupled between 1970 and 2000, but sharply decreased since 2000 as the expansion of cropland accelerated and eventually overtook that of pasture/rangeland (see Figure 4.3 b). This development can be observed in the Sahel area of West Africa, where interlinked pressures of rapid cropland expansion, increased livestock numbers, land degradation, and climate change-induced rainfall variability has led the nomadic pastoral grazing system and its mobility to decline (Holechek et al., 2017; Rahimi et al., 2021; Turner et al., 2005).

China's extensive area of pasture/rangeland expansion is located in the Northwest such as in Xianjiang, a region of traditional nomadic pastoralism, where herders follow wide-ranging seasonal migration routes (Dong, 2016). We find that the rate of pas-

ture/rangeland expansion has risen steeply in the late 1970s, then remained consistently high throughout the 1980s and fell sharply from 1990 until the early 2000s (see Figure 4.3 b, C E Asia). The transition from a fast and long increase to a significant slowing down of pasture/rangeland expansion coincides with political reform programmes accompanying a paradigm shift in Chinese land use organisation. The Collective Era, characterised by state-directed collectivisation from 1958-1984, was replaced by a period of privatisation (Household Land Contract, HLC) after 1984 as part of the Reform and Opening Policy (Bryan et al., 2018; Li et al., 2019). The re-privatisation from communes to households led to an increase in national agricultural production but caused unsustainable land use practices associated with rangeland fragmentation and overgrazing, leading to ecosystem and land degradation (Hua & Squires, 2015).

In Australia, rangeland has expanded into former grass/shrubland areas. The expansion of pasture/rangeland however significantly slowed down during the period 1960-2019. Rangelands in Australia have experienced a ‘post-productivist’ transition arising from agricultural overcapacity, and a change in societal values, which led to the displacement of pastoralism in marginal lands (Holmes, 2002). Furthermore, woody encroachment, the spread of shrubs at the cost of herbaceous vegetation, has also led to a decline in the expansion of Australian pasture/rangelands (Godde et al., 2020).

The main areas of cropland expansion during 1960-2019 were located in the Global South, especially in South America (Argentina, Brazil), Africa (Ethiopia, Nigeria, Uganda, and Kenya), India and Thailand. Furthermore, agricultural expansion (deforestation for pasture, cropland and pasture/rangeland expansion) shifted from South America to Africa since the late 1980s. In Africa, a long period of a high and increasing rates of agricultural expansion was followed by a decreasing rate of pasture/rangeland and of cropland expansion from ~2000 and 2010, respectively. This shift is also consistent with greenhouse gas emissions from agricultural production. Whereas, in South America, emissions increased from ~2000 after a long-term decline, in Africa, an earlier, fast and extensive increase in agricultural production caused an upward trend in emissions during the entire period of 1961-2017 (Hong et al., 2021). In line with our findings, an accelerating rate of global cropland expansion was mainly attributed to increasing cropland expansion rates in Africa during the 2000s (Potapov et al., 2022). As shown in another recent publication (Dornelles et al., 2022), Sub-Saharan Africa stands out for its rapid agricultural expansion during the period 1995-2015. The global area of forest loss is larger than that of forest expansion during the last six decades. Overall, forest expansion accounts for ~2.8 million km<sup>2</sup> while ~3.8 million km<sup>2</sup> of global forests were lost either through deforestation for agriculture or forest degradation to shrub/grasslands during 1960-2019. This long-term net forest loss is in line with satellite-based analyses of recent decades (Hansen et al., 2013) and the officially reported Global Forest Resources Assessment (Keenan et al., 2015).

We find that the transition of forests to shrub/grassland takes up most of the global forest

loss area ( $\sim 1.9$  million km<sup>2</sup>) and the rate of conversion has accelerated over time. The conversion of forest to shrub/grassland can include various land use/cover changes. In the Congo, for example, there is evidence of shifting cultivation and smallholder agricultural activity (Turubanova et al., 2018), but also the production of tree crops such as coffee and cocoa that has led to forest loss (de Beule et al., 2014; Pendrill et al., 2019). Furthermore, increased human pressure on forests during periods of political instability has led to forest degradation (Nackoney et al., 2014). As reported by several studies (Bodart et al., 2013; Mitchard & Flintrop, 2013; Sikuzani et al., 2020), a large loss in forest cover occurred in the Miombo woodlands in southern Congo, Angola and Zambia. There, dense woodland was converted into fragmented, open woodland due to high demographic pressure, associated agricultural expansion, fuel wood (firewood, charcoal) extraction, and anthropogenic fires (Syampungani et al., 2009). In Myanmar, rubber plantations (Nomura et al., 2019) and rice agriculture (Richards & Friess, 2016) are the dominating drivers of forest loss. Long-term selective logging in production forests, but also shifting cultivation and illegal logging, charcoal, and fuelwood extraction are drivers of forest degradation (Mon et al., 2012), which is a larger cause of forest loss than direct deforestation (Naing Tun et al., 2021). In Indonesia, forests have been cleared for oil palm and timber plantations at large scales (Austin et al., 2019; Koh & Wilcove, 2008). Furthermore, large areas of forest degradation are located in Russia, where increased fire frequency (particularly in Siberia), insect outbreaks, and forestry, especially clear cuts and selective logging with high intensity, have been identified as major drivers of primary forest loss (Achard et al., 2006; Curtis et al., 2018).

In contrast, the global rate of forest expansion, consisting mainly of forests in North America and Russia, has increased until  $\sim 2010$ , when a sudden slowdown occurred. This global decrease in forest expansion rates is in line with a reported decrease in the expansion of planted forests for the US, Canada, and Russia during 2010-2015, potentially due to increasing climate impacts, population pressure and competition for land (Payn et al., 2015). The slowdown in forest expansion in the Global North is confirmed by the work presented here, indicating a possible stabilisation of forest areas in recent decades (FAO, 2020f; Palmero-Iniesta et al., 2021). The reasons for this decrease in forest expansion rates at the global level are not entirely clear, but could be due to globalisation that caused timber self-sufficiency through planted forests to become less important, the expansion of settlements and infrastructure into forests or increasing societal benefits from forestry, as observed in Europe in earlier decades (Gold et al., 2006). It is striking that land use transitions with very high inter-annual dynamics (multiple change events) have predominated in the Global North, while one-time land use transitions (single change events) have mainly taken place in the Global South (Winkler et al., 2021). In Europe and North America, these highly dynamic land use transitions are, on the one hand, forest and crop-pasture dynamics as indicators of intensive agricultural and forestry activity, and on the other hand, cropland abandonment, which implies a cessation of land use. In South America,

Africa, and Southeast Asia, land use transitions, predominantly agricultural expansion, can be clearly assigned to a single year.

In North and Central America, crop-pasture dynamics were highest during the 1960s (see Figure 4.3), a period of high agricultural production and intensification driven by agrotechnological progress during the Green Revolution, leading to North America becoming the main exporter of cereals and oilseeds (Krausmann & Langthaler, 2019). Afterwards, the rates of crop-pasture transitions decreased and remained relatively stable. From 2000, crop-pasture dynamics and the rate of cropland abandonment increased sharply and peaked at  $\sim 2008$ , followed by a decline. Similarly, this prominent peak in  $\sim 2008$  and abrupt decrease afterwards can be found in the rates of crop-pasture dynamics in Australia. The peak in highly dynamic land use transitions is concurrent with an observed transition from globally accelerating to decelerating land use change (Winkler et al., 2021) and coincides with the global economic crisis 2007-2009. Europe, however, shows consistently high rates of crop-pasture and forest dynamics, which follow a wave-like development over time.

#### 4.3.2 Drivers of land use change

By estimating the causal links in the time series of driver indicators from five thematic groups (demography, politics, economy, production, environment) with the land use transitions for all countries of the globe, we find that, globally, economic factors are the most land-intensive and therefore most important drivers of land use change (affecting an area of  $\sim 5.5$  million  $\text{km}^2$ , see Figure 4.4 a). Labour force and wages are most important in Central and Eastern Asia, Gross Domestic Product (GDP) in South America, and forestry exports in Africa and Europe, which are combined with agricultural imports (see Figure 4.5).

Ranked by correlation, economic factors such as GDP and wages dominate as indirect economic drivers of land use transitions in the Global North (see Figure 4.6), where it is mainly linked with cropland abandonment, crop-pasture dynamics and forest expansion (see Figure 4.7). In the Global South, highly correlated economic drivers relate to global markets and trade (agricultural exports, exchange rate, global oil price, see Figure 4.6). Agricultural exports and the global oil price show strong links to deforestation for cropland, and exchange rates to the transition of forest to shrub/grassland and cropland expansion (see Figure 4.8).

In the Global South, political factors such as conflicts and nature protection policies as well as demographic indicators such as population density are among the key drivers of land use change (see Figure 4.6). These are mainly related to deforestation and agricultural expansion, but also to grass-/shrubland expansion (see Figure 4.8).

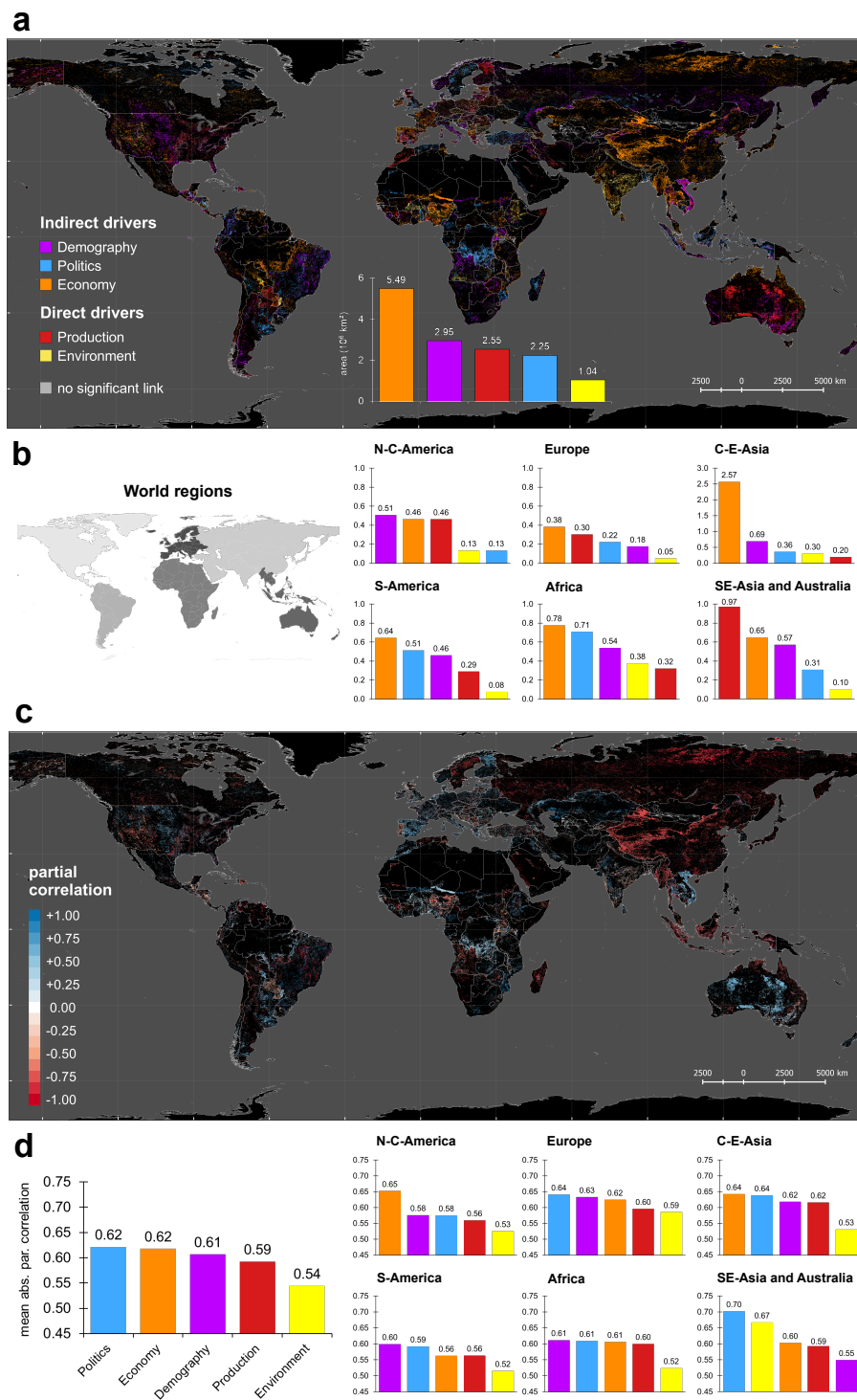


**Figure 4.4:** Driver groups of land use transitions in 1960-2019: a) Spatial distribution b) Comparison across world regions ranked by affected area c) Spatial distribution of partial correlation coefficients d) Comparison across world regions ranked by absolute partial correlation. Driver groups were assigned to the driver indicator with the significant link of the highest causal strength (partial correlation) to each land use transition and country.

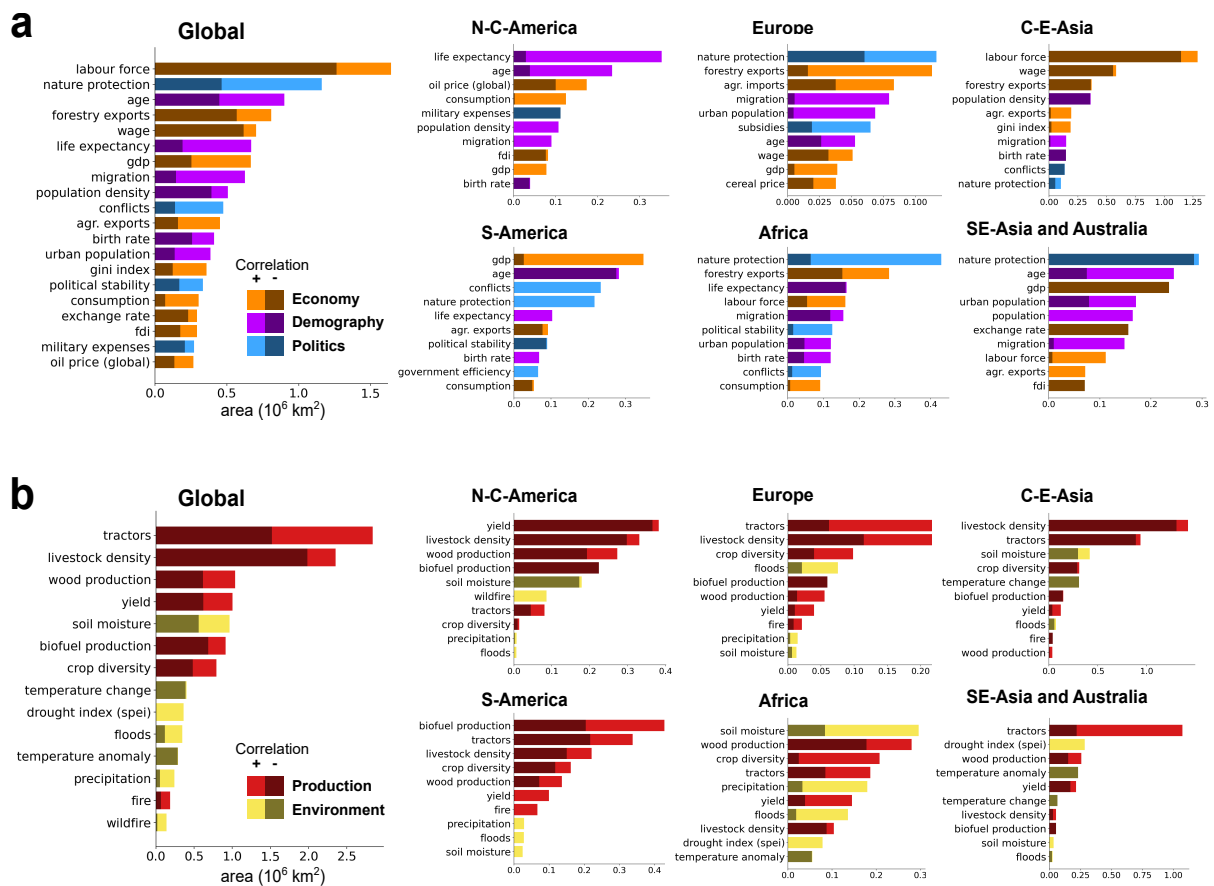


**Figure 4.5:** a) Indirect and b) direct driver indicators with the strongest causal link (as of partial correlation) to land use transitions, ranked by area affected by land use change for different world regions. The displayed indicators represent the top 10 for each world region and the top 20 for the global dataset. Dark shaded areas indicate the proportion (by area) with a negative correlation to land use transitions.

The findings underline the importance of, on the one hand, economic growth for land use dynamics in the Global North (Taylor & Rising, 2021), and on the other hand, global markets for the agricultural sector in the Global South. The large effect of globalised markets, especially of cash crops, on the expansion of agricultural land use in the Global South has been highlighted, e.g. as indicated by the prices of beef and soy bean in the Brazilian Amazon (Barona et al., 2010), rubber in Laos (Junquera et al., 2020), coffee (Gaveau et al., 2009) and palm oil (Wicke et al., 2011) in Indonesia, and clove and vanilla in Madagascar (Llopis et al., 2019).

Ranked by affected area, a strong link can be observed between economic indicators and global deforestation for agricultural land and agricultural expansion, as well as forest expansion and forest dynamics (see Figure 4.9). In summary, economically strong, wealthy countries in the Global North show forest expansion and intensive forestry (as indicated by high within-forest dynamics), while in the Global South, the dependency of global

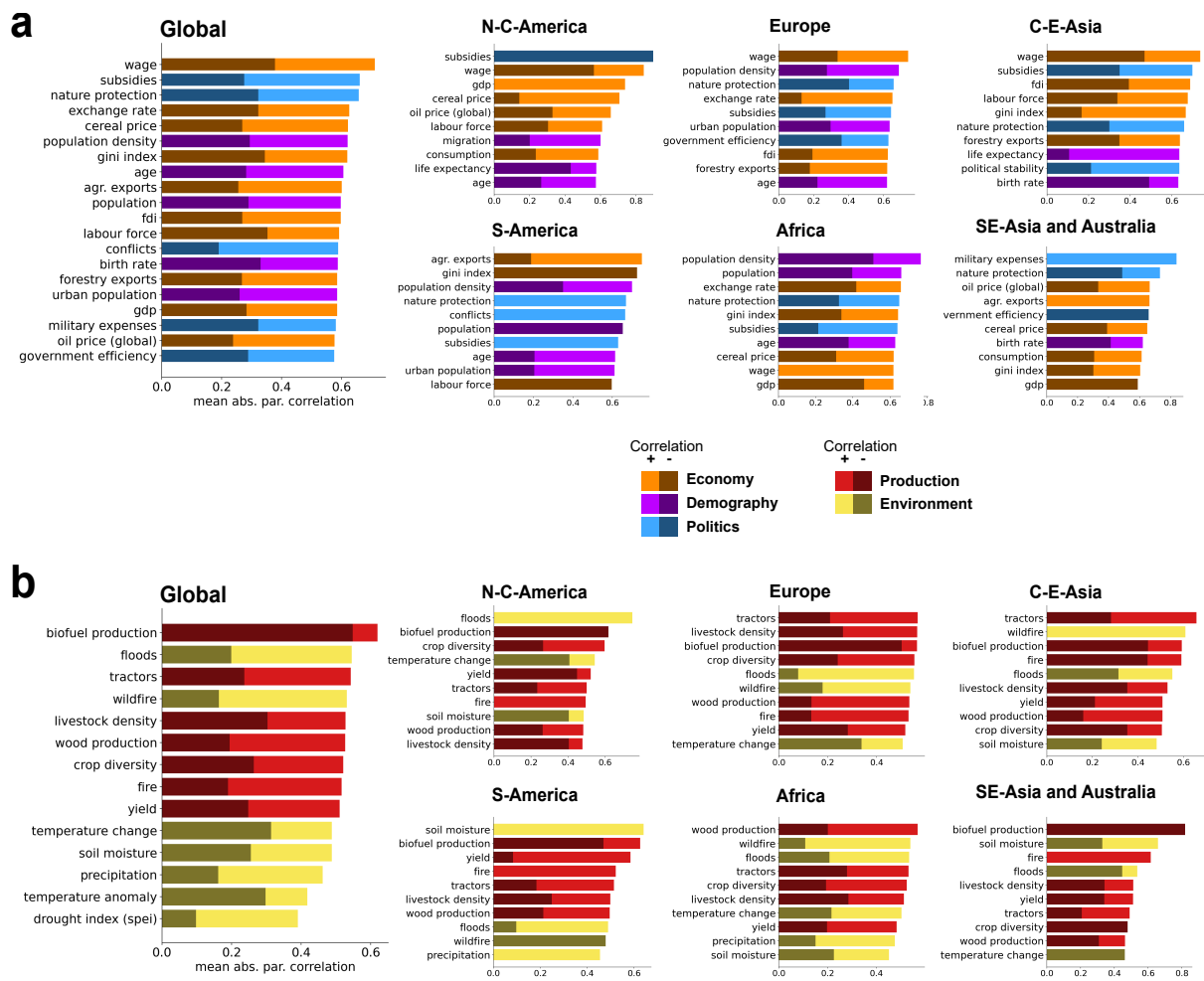


**Figure 4.6:** a) Indirect and b) direct driver indicators with strongest causal link (as for partial correlation) to land use change, ranked by absolute partial correlation for different world regions. The displayed indicators represent the top 10 for each world region and the top 20 for the global dataset. Dark shaded areas indicate the proportion (by number of occurrence) with a negative correlation to land use transitions.

trade causes agriculture to expand further into (semi-)natural areas. This supports the thesis that forest expansion in the Global North involves the displacement of land use, especially deforestation and agricultural expansion, to the Global South (Fuchs et al., 2020; Meyfroidt et al., 2013; Pendrill et al., 2019).

Ranked by correlation, political factors are the strongest drivers of global land use transitions (see Figure 4.4 d). They affect large areas of cropland expansion but also cropland abandonment (conflicts) as well as land degradation such as forest to shrub/grassland (nature protection policies) and expansion of sparse/no vegetation (military expenses) (see Figures 4.9 and 4.10). We observe that political indicators show larger areal importance in the Global South than in the North, except from subsidies and nature protection policies, which are also strong drivers of forest expansion and cropland abandonment in Europe

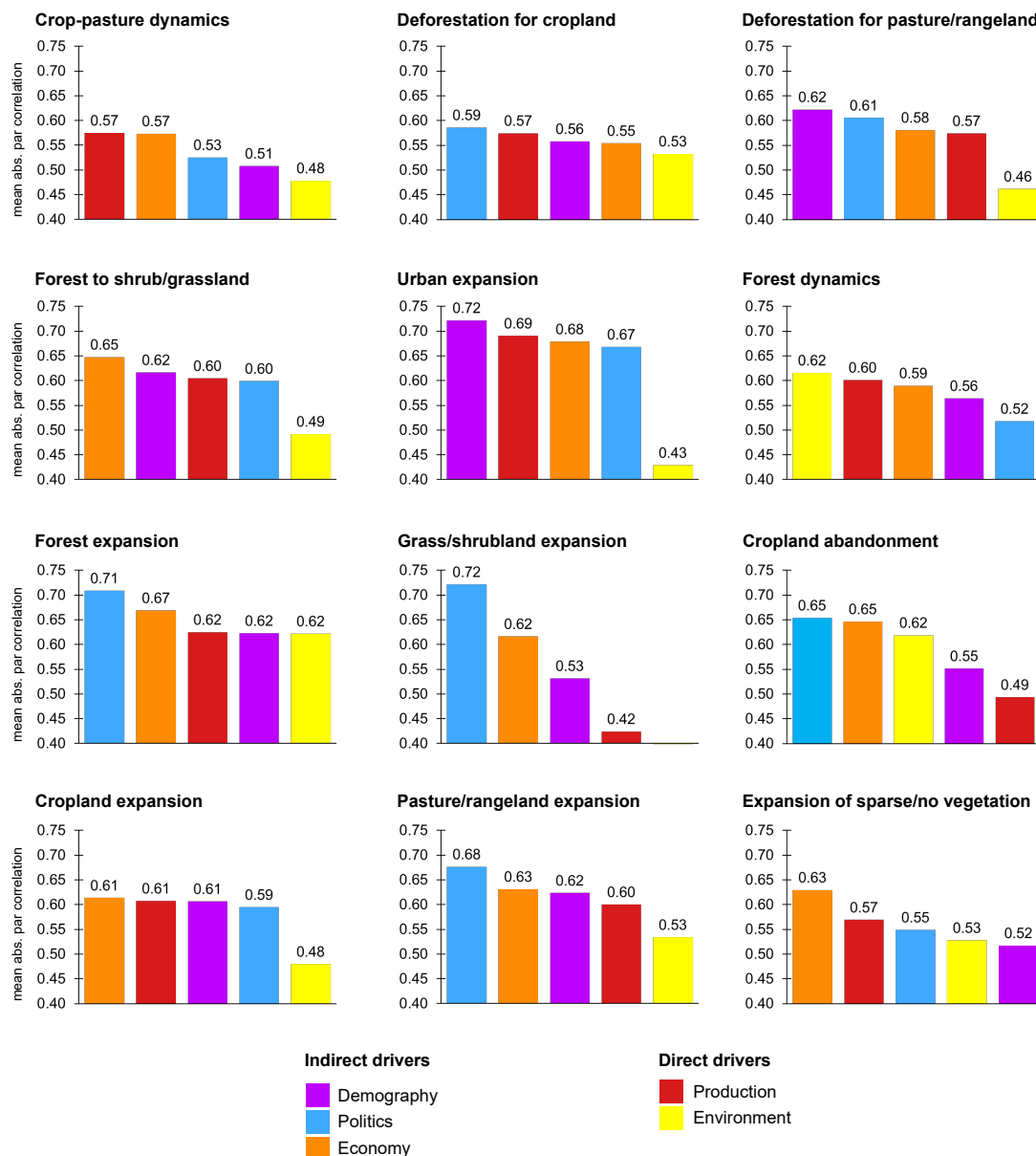


**Figure 4.7:** Driver groups of different land use transitions in 1960-2019 ranked by mean absolute partial correlation. Driver groups were assigned to the driver indicator with the strongest causal link (as for partial correlation) to each land use transition and country.

(see Figure 4.4 and Figure 4.5). This is underpinned by high correlations for nature protection policies (e.g. in Argentina and Brazil), political stability (e.g. in Mozambique), conflicts (e.g. in Brazil, Colombia, Tanzania, and Zimbabwe) and military expenses (e.g. in Cambodia and Thailand). Political and institutional factors have been demonstrated as drivers of long-term land use changes in many regional studies, e.g. smallholder farming systems in Uganda (Ebanyat et al., 2010), conflict-caused deforestation in Colombia (Landholm et al., 2019), and Post-Soviet institutional disruption leading to land degradation in the agro-pastoral transition zone of Kazakhstan (Yan et al., 2020).

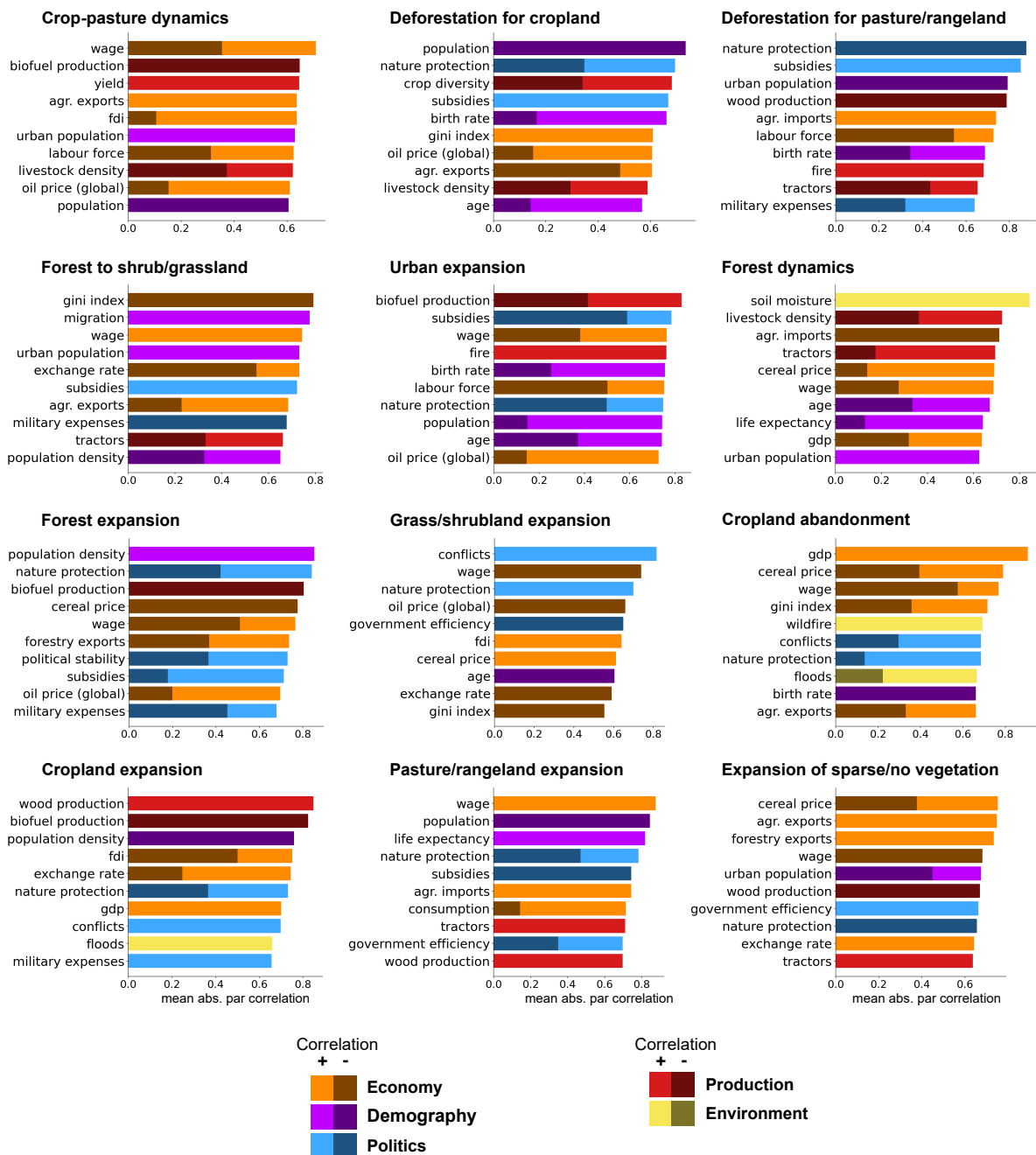


**Figure 4.8:** Top 10 driver indicators of different land use transitions in 1960-2019 ranked by mean absolute partial correlation. Driver groups were assigned to the driver indicator with the strongest causal link (as for partial correlation) to each land use transition and country. Dark shaded areas indicate the proportion (by number of occurrence) with a negative correlation to land use transitions.

Our analysis demonstrates that demographic drivers are the second most important cause of land use change ranked by area (see Figure 4.4 a). In Europe, the most land-intensive demographic driver is migration and urban population. In Africa and the Americas, age

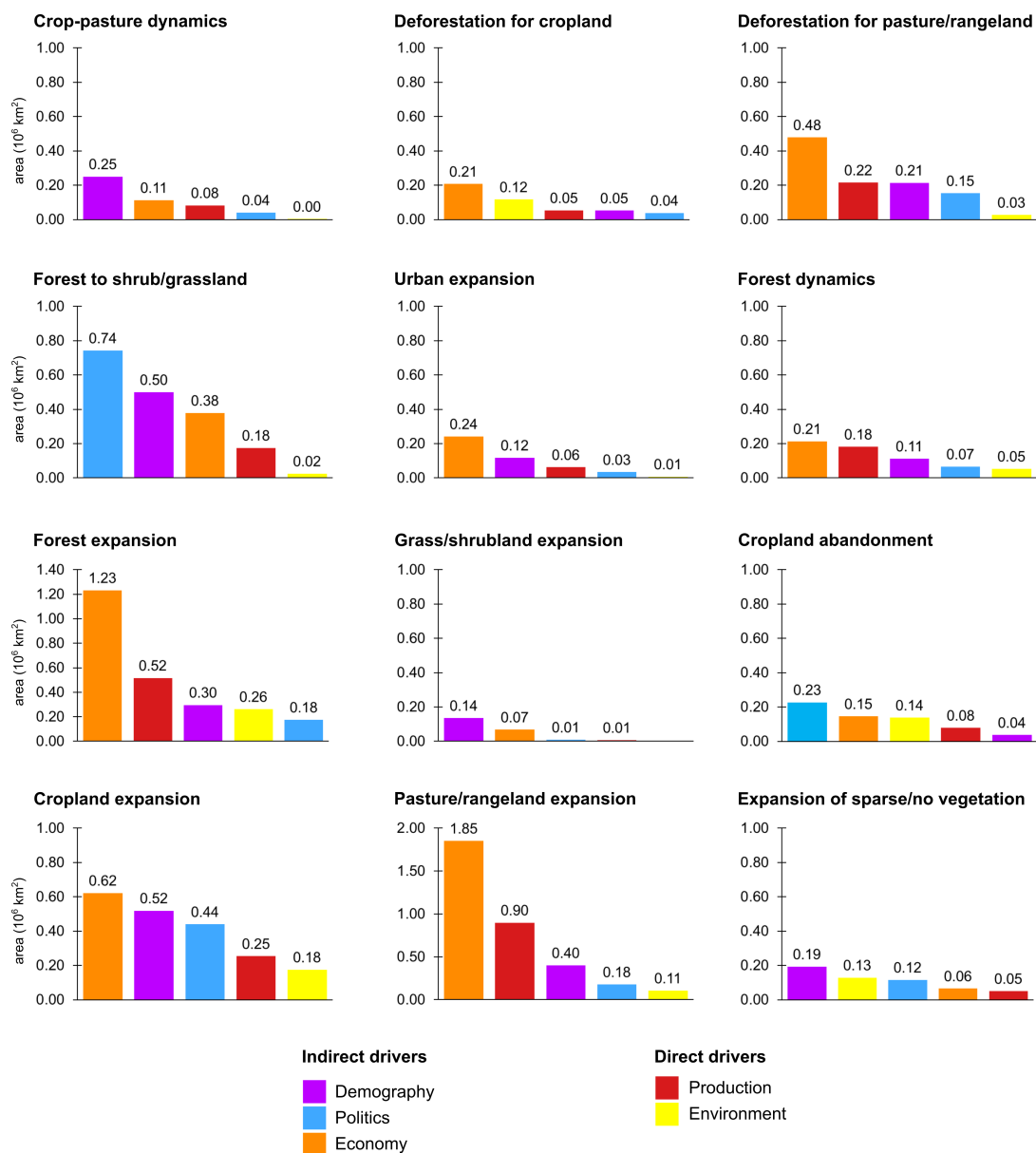


**Figure 4.9:** Driver groups of different land use transitions in 1960-2019 ranked by area affected by land use change. Driver groups were assigned to the driver indicator with the strongest causal link (as for partial correlation) to each land use transition and country.

and life expectancy are the most important (see Figure 4.5). When ranked by correlation coefficients, demographic indicators become the most important indirect drivers for South America and Africa (see Figure 4.4 d).

In these regions of the Global South, demographic factors show particularly high correlations with urban and agricultural expansion as well as with forest loss (as forest to shrub/grassland and deforestation for pasture/rangeland). Overall, we find a strong linkage between demographic drivers and urban expansion (see Figure 4.7). This provides a

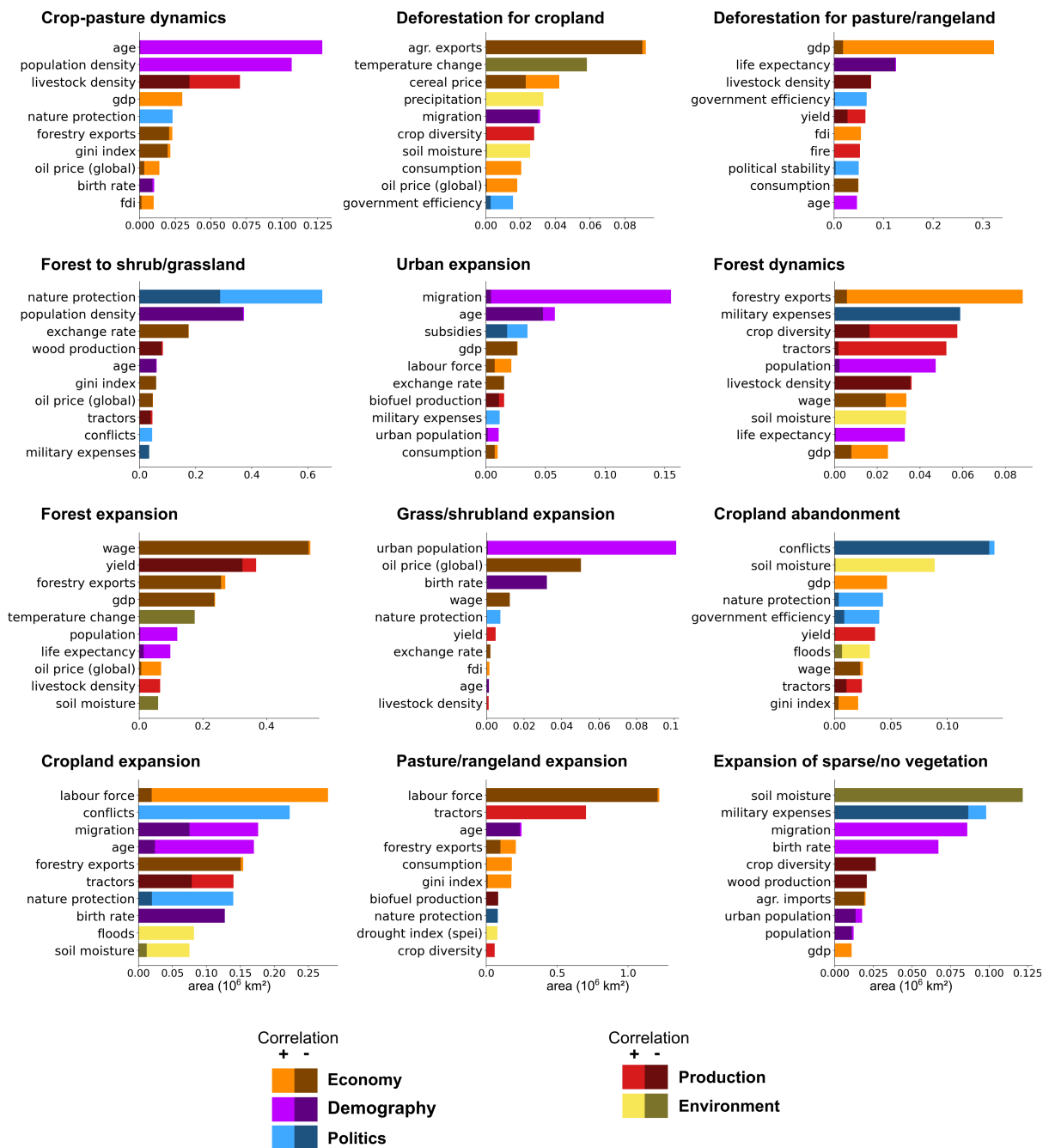


**Figure 4.10:** Top 10 driver indicator with the strongest causal links (partial correlation) to different land use transitions ranked by area affected by land use change. Dark shaded areas indicate the proportion (by area) with a negative correlation to land use transitions. From all driver indicators (direct and indirect), only one was selected as winning driver for each land use transition and country.

data-driven confirmation of the well-known theoretical assumption – taken into account in many land use models (Kaplan et al., 2010; Klein Goldewijk et al., 2017; Pongratz et al., 2008) – that population dynamics are a principal global driver of land use change.

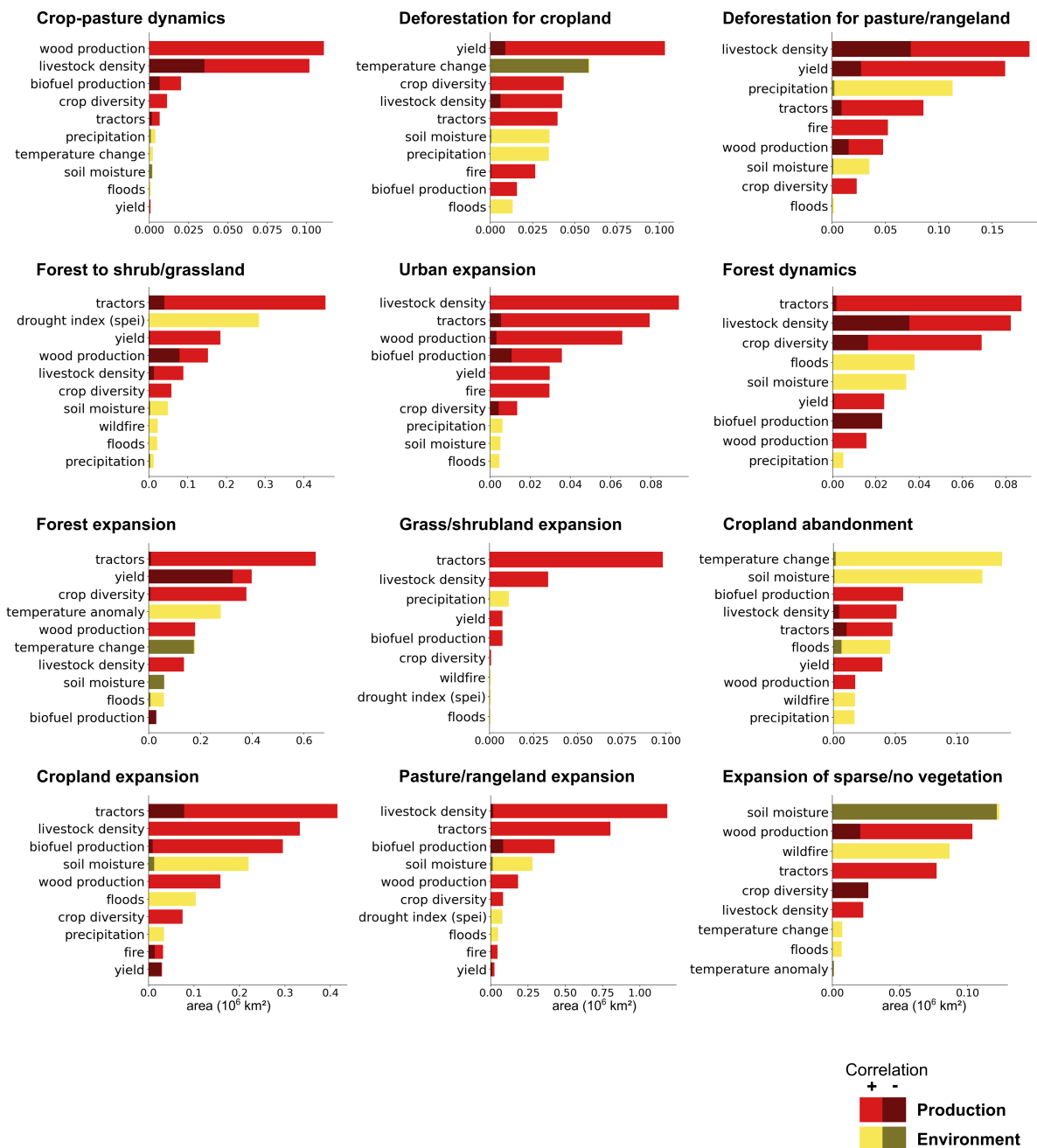


**Figure 4.11:** Top 10 direct driver indicator with the strongest causal links (partial correlation) to different land use transitions ranked by area affected by land use change. Dark shaded areas indicate the proportion (by area) with a negative correlation to land use transitions. From the direct driver indicators, only one was selected as winning driver for each land use transition and country.

Globally, production is the most extensive direct driver (~2.6 million km<sup>2</sup>), while environmental factors tend to have relatively weaker causal links to the rate of land use change and affect smaller areas (see Figure 4.4). This is because production factors such as yields,

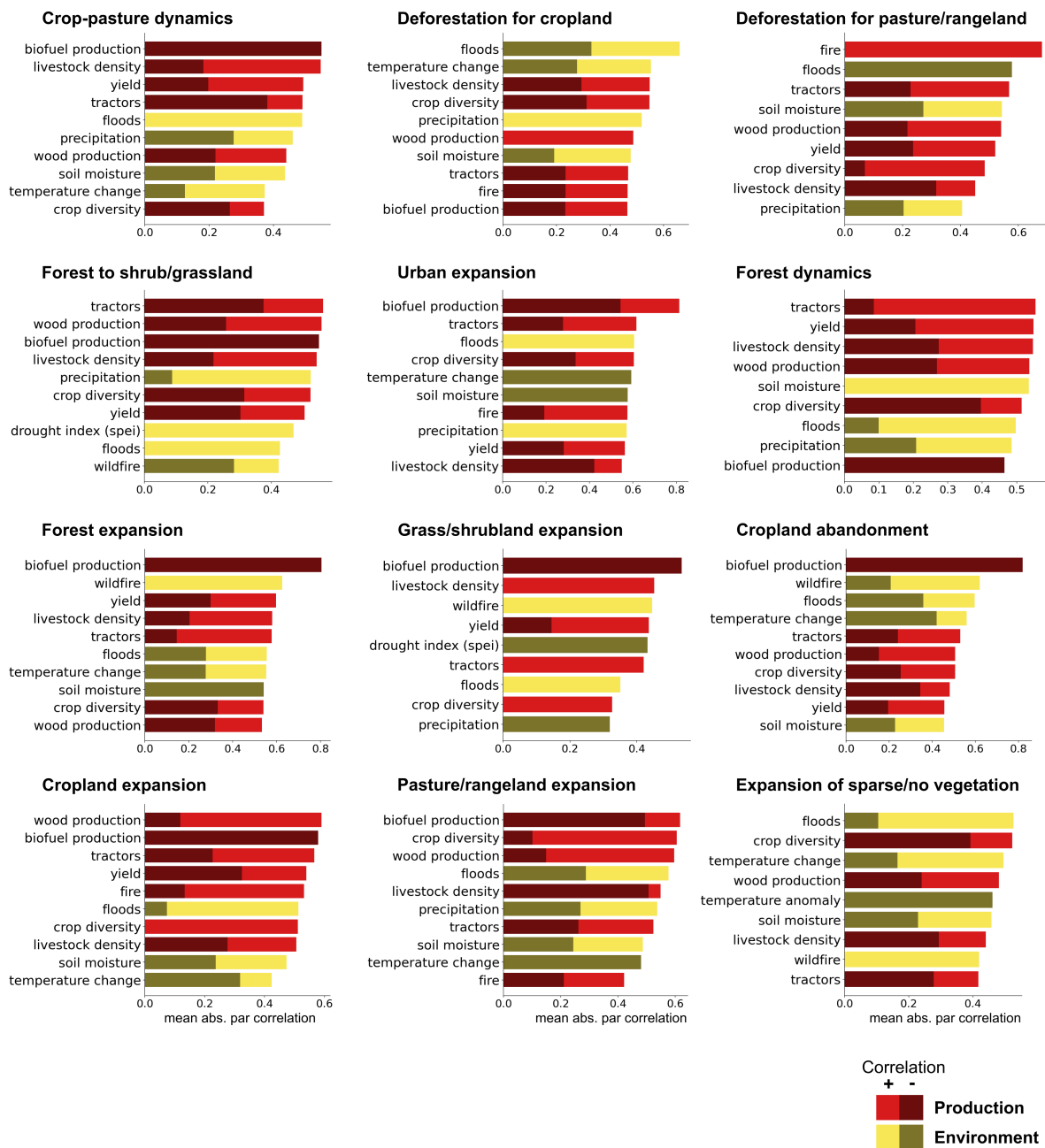


**Figure 4.12:** Top 10 direct driver indicators with the strongest causal link to different land use transitions ranked by mean absolute partial correlation. Dark shaded areas indicate the proportion (by number of occurrence) with a negative correlation to land use transitions. From the direct driver indicators, only one was selected as winning driver for each land use transition and country.

tractors, biofuel production are more immediately interlinked – in terms of space and time – with land use transitions affecting e.g. cropland and pasture/rangeland, whereas environmental factors have a more complex relationship with land use. Production factors are often not only a driver but also an outcome of land use transitions, which allows us

to identify more causal connections, but complicates their assignment and interpretation. Ranked by affected area, production indicators dominate as direct drivers for most land use transitions (see Figure 4.9). Production indicators related to land management such as tractors, livestock density, or yield are linked to large areas of agricultural expansion, crop-pasture dynamics, and forest transitions (see Figure 4.10 and Figure 4.11).

It is worth noting that biofuel production is the top direct driver indicator for land use change, as it has the highest (but mostly negative) lagged correlations to agricultural land transitions (cropland and pasture expansion, crop-pasture dynamics, cropland abandonment), but also to forest and grassland expansion (see Figure 4.8 and Figure 4.12). The linkage between biofuels and cropland dynamics has been illustrated by other studies. In the Brazilian Amazon, biofuels are associated with extensive indirect deforestation, as a replacement for rangelands that have been converted to cropland for sugarcane ethanol and soy bean biodiesel (Lapola et al., 2010). Similar effects of land use displacement have been shown in the US, where biofuels lead to further cropland expansion and an increase in carbon emissions (Lark et al., 2015; Searchinger et al., 2008). However, the negative correlation of biofuel production with both the expansion of natural vegetation and agricultural transitions appears contradictory and could be indicative of a data artefact. Data for biofuel production, as used in this study, was only available from 1990 onwards and, thus, the driver analysis is only able to describe the potential causal link between biofuel production and land use transitions for the second half of the study period.

The weaker causal relationships between environmental variables and land use change possibly stem from large time lags, insufficiently scaled data or the interplay with other environmental variables. Environmental factors have higher temporal, e.g. inter-annual, and spatial variabilities, but were considered here as annual and national-scale mean values. Thus, the spatio-temporal heterogeneity of environmental indicators was, to some extent, under-represented in this approach, including the effect of extreme events such as droughts or floods. In order to better explore the influence of environmental factors on land use, future studies could consider not only land use changes but also management changes.

Although we find a relatively low causal link between environmental indicators and land use change globally, environmental factors have a greater influence on land use change in the Global South than in the Global North (see Figure 4.4). In (semi-)arid regions such as the Sahel, land use transitions are more responsive to environmental factors, e.g. fires, floods and droughts. We find that environmental factors are linked to deforestation for cropland, land degradation or desertification (as expansion of sparse/no vegetation) in the Global South, whereas in the North, they are predominantly linked to forest expansion, forest dynamics and cropland abandonment (see Figure 4.4 and Figure 4.7).

## 4.4 Conclusions

Providing new data-driven and quantitative insights, this study reveals the complexity of global land use transitions, their patterns and interrelated drivers. We find that agricultural expansion into non-forested areas such as grass- and shrubland is over three times greater than deforestation for agricultural land use. Given the large areal footprint and the value of grass- and shrubland ecosystems, the role of agricultural land expansion into natural, non-forested areas and its impact on biodiversity and climate needs further consideration in research and policy. Our findings support the forest transition theory and associated land use displacement through globalisation. Economically strong countries of the Global North experienced a forest transition from net forest loss to net forest expansion. We found a relationship between large forest expansion in the Global North with economic growth, particularly with wages and GDP. In contrast, the main transitions in the Global South are deforestation for agriculture and agricultural expansion into non-forested areas, which are highly correlated with globalised markets (e.g. agricultural exports, cereal prices). There are related implications of these observations.

First, the results suggest that the distribution of land use transitions strongly depends on a country's stage in its economic development, which can be determined by analysing how employment changed among sectors in the economy, but also by other indicators of human development such as wealth (e.g. as income) and public health affecting demographic indicators (e.g. age and life expectancy). Second, we found a striking influence of global markets on the global distribution of land use transitions. In developed countries of the Global North that have experienced forest transitions, displacement of land use demand abroad is concurrent with domestic forest expansion (Lambin & Meyfroidt, 2011; Meyfroidt et al., 2010). As land use changes are affected by globalised movements of commodities, information, capital and people, land has increasingly become the arena of many competing interests and hence has become another global commodity. Hence, telecoupling between distant land use transitions and their globally networked drivers will be an important topic for further study.

The small role of environmental factors as drivers for land use change, as presented in this study, confirms that global land use transitions have mainly occurred in a production- and market-oriented system during the last six decades. However, the land and food system has recently and will likely become more vulnerable to changing environmental conditions such as climate extremes (Asseng et al., 2015; Godfray et al., 2010; Wang et al., 2014). In light of the major crises we are facing – climate change, biodiversity loss, food insecurity – such a globally dependent system might face re-configuration in times of de-globalisation.



# Chapter 5

## CO<sub>2</sub> emissions based on high-resolution land use data

This chapter is based on:

Ganzenmüller, R., Bultan, S., Winkler, K., Fuchs, R., Zabel, F., Pongratz, J. (2022). Land use change emissions based on high-resolution activity data substantially lower than previously estimated. *Environmental Research Letters* 17, 064050. DOI: <https://doi.org/10.1088/1748-9326/ac70d8>.

Supplementary material can be found in the online publication.

*Models without data are fantasy. Data without models are chaos.*

Patrick Crill

## Abstract

Land use and land cover changes (LULCCs) contributed around one third to the cumulative, anthropogenic CO<sub>2</sub> emissions from 1850 to 2019. Despite its great importance, estimates of the net CO<sub>2</sub> fluxes from LULCC (ELUC) have high uncertainties, compared to other components of the global carbon cycle. One major source of uncertainty roots in the underlying LULCC forcing data. In this study, we implemented a new high-resolution LULCC dataset (HILDA+) in a bookkeeping model (BLUE) and compared the results to estimates from simulations based on LUH2, which is the LULCC dataset most commonly used in global carbon cycle models. Compared to LUH2-based estimates, results based on HILDA+ show lower total ELUC (global mean difference 1960-2019: 541 TgC a<sup>-1</sup>, 65%) and large spatial and temporal differences in component fluxes (e.g. CO<sub>2</sub> fluxes from deforestation). In general, the congruence of component fluxes is higher in the mid-latitudes compared to tropical and subtropical regions, which is to some degree explained with the different implementations of shifting cultivation in the underlying LULCC datasets. However, little agreement is reached on the trend of the last decade between ELUC estimates based on the two LULCC reconstructions. Globally and in many regions, ELUC estimates based on HILDA+ have decreasing trends, whereas estimates based on LUH2 indicate an increase. Furthermore, we analysed the effect of different resolutions on ELUC estimates. By comparing estimates from simulations at 0.01° and 0.25° resolution, we find that component fluxes of estimates based on the coarser resolution tend to be larger compared to estimates based on the finer resolution, both in terms of sources and sinks (global mean difference 1960-2019: 36 TgC a<sup>-1</sup>, 96%). The reason for these differences are successive transitions: these are not adequately represented at coarser resolution, which has the effect that—despite capturing the same extent of transition areas—overall less area remains pristine at the coarser resolution compared to the finer resolution.

## 5.1 Introduction

The net CO<sub>2</sub> flux from land use and land cover change (ELUC) is a key component of the global carbon cycle (Friedlingstein et al., 2020). ELUC includes the carbon transfer from soil and biomass to the atmosphere through e.g. deforestation, harvest activities, and pasture to cropland conversions as well as the uptake and storage of carbon from the atmosphere in biomass and soil through e.g. afforestation and regrowth of vegetation after abandonment of agricultural land or harvest (Pongratz et al., 2014). These land use and land cover change (LULCC) activities can be targeted as means to reduce emissions or to re-sequester carbon (often called carbon dioxide removal or negative emissions technologies in the latter case) and will be essential for meeting the 1.5°C target (Goldstein et al., 2020; Crippa et al., 2021). Especially, halting deforestation and forest degradation on the one side (Maxwell et al., 2019; Roe et al., 2019; Gatti et al., 2021) and supporting afforestation and regeneration of natural forests on the other side are widely discussed, available, and effective measures for climate mitigation (Hoegh-Guldberg et al., 2019; Lewis et al., 2019; Roe et al., 2019). The implementation of these also greatly influences national abilities to reach net zero emissions (van Soest et al., 2021).

Compared to fossil CO<sub>2</sub> emissions, estimates of ELUC are subject to high relative uncertainties (Arneth et al., 2017). In the Global Carbon Budget 2020 (GCB2020), the uncertainty in ELUC estimates was specified to be, with a likelihood of at least 68% ( $\pm 1\sigma$ ), in the range of  $\pm 0.7 \text{ GtC a}^{-1}$  based on a best-value judgement (Friedlingstein et al., 2020). In relative terms, this translates to an uncertainty of 43.8% (in comparison, fossil CO<sub>2</sub> emissions: 5.2%). The high uncertainty of ELUC estimates has various reasons as summarised by Pongratz et al. (2021): different terminologies and definitions (Pongratz et al., 2014; Grassi et al., 2018; Malins et al., 2020; Obermeier et al., 2021), different model assumptions and parameters (Bastos et al., 2020; Gasser et al., 2020; Hartung et al., 2021), and different considerations of management processes (Stocker et al., 2014; Arneth et al., 2017; Hartung et al., 2021). Furthermore, several studies have attributed major parts of this uncertainty to underlying LULCC datasets. From a set of sensitivity experiments based on the high, low, and baseline LULCC scenarios, Hartung et al. (2021) estimate that about 22% of the sensitivity in cumulative ELUC stems from LULCC inputs. Similarly, Gasser et al. (2020) find substantial differences between ELUC estimates based on different versions of LUH2, LUH1 and Global forest resources assessments (FRAs). Houghton & Nassikas (2017) use different versions of FRA to highlight differences in ELUC estimates after 1950, while Peng et al. (2017) compile multiple historical plant functional type (PFT) maps and conclude that different transition rules result in large differences in ELUC estimates. Moreover, different regional studies (Yu et al., 2019; Kondo et al., 2022; Rosan et al., 2021) discuss the influence of underlying LULCC forcing data on ELUC estimates.

For this study, we implemented the new LULCC dataset HHistoric Land Dynamics Assess-

ment + (Winkler et al., 2021, hereafter HILDA+) in the bookkeeping of land use emissions model (Hansis et al., 2015, hereafter BLUE). HILDA+ is a global high-resolution data product with a spatial resolution of  $0.01^\circ \times 0.01^\circ$ , covering common LULCC classes and a decent time period (1900/1960-2019), which makes it suitable as LULCC forcing for carbon cycle models. BLUE is one of three bookkeeping models in the yearly global carbon budgets (GCBs) (Friedlingstein et al., 2020, 2021). Within the high uncertainties climate target (Griscom et al., 2017; Harper et al., 2018) associated with ELUC, BLUE is generally in line with other bookkeeping model and dynamic global vegetation model (DGVM) estimates, such that we use it here as a representative state-of-the-art model to quantify ELUC and expect our qualitative conclusions to be robust against the choice of model. Detailed comparisons of BLUE to other models can be found in Bastos et al. (2021); Friedlingstein et al. (2021); Obermeier et al. (2021). The implementation of HILDA+ in BLUE opens up the novel possibility to compare and evaluate ELUC based on two spatially explicit and independently derived LULCC datasets. Given the high uncertainty arising from LULCC inputs, the verification of ELUC estimates based on HILDA+ with estimates based on other LULCC forcings is an important step to identify causes of the ELUC uncertainty. We take this opportunity to investigate mechanisms beyond the specific LULCC data and ELUC model used and investigate the relevance of initialisation time and, for the first time, the sensitivity of results to spatial resolution, highlighting a previously under-appreciated role of successive transitions in global carbon cycle modeling.

By using BLUE, we make use of the computationally efficient design of the model that enables us to estimate ELUC at the original resolution of HILDA+ at  $0.01^\circ$ . In the past, ELUC has been estimated globally at  $0.25^\circ$  resolution (Le Quéré et al., 2018a,b; Friedlingstein et al., 2019, 2020; Bastos et al., 2021; Hartung et al., 2021), at  $0.5^\circ$  resolution (Hansis et al., 2015), at country level (Houghton & Nassikas, 2017; Le Quéré et al., 2018b; Friedlingstein et al., 2019; Le Quéré et al., 2018a; Friedlingstein et al., 2020; Bastos et al., 2021), and at regional and biome level (Friedlingstein et al., 2020; Gasser et al., 2020). Thus, ELUC estimates based on HILDA+ have an at least 25 times higher information content than any previous studies. The high resolution of HILDA+ allows us a spatially more precise detection of LULCC events and consequently a better location of ELUC sinks and sources. Nevertheless, subgrid-scale omissions of transitions can still not be completely avoided, for which a field-scale resolution of roughly 1 ha would be needed (Wilkenskjeld et al., 2014). An example of such subgrid-scale transitions are transitions from shifting cultivation (also called swidden agriculture/cultivation or slash-and-burn), which are small-scale land use systems with rotational cycles of shorter cultivation phases of annual crops and longer natural fallow phases of woody regrowth, separated by fire clearances (Mertz et al., 2009). Using LULCC data of less than 100 m resolution, studies such as Spawn et al. (2020) and Feng et al. (2021) might be able to account for subgrid-scale transitions. However, these studies are restricted in their spatial extent (Tropics,

US), do not cover legacy fluxes due to their temporal limitation, and provide only specific component fluxes of ELUC. The latter is a general problem of ELUC estimates based on satellite-derived data of vegetation dynamics, such as forest cover changes (Hansen et al., 2013): since land use dynamics coincide with natural disturbances (e.g. natural wildfires or insect outbreaks), satellite-derived data of vegetation cover changes, although increasingly available at high resolution, cannot be used directly as input to carbon cycle models (Pongratz et al., 2021). Typically, only component fluxes such as from cropland expansion of specific types of land use-induced forest cover losses can be derived directly from satellite data. Due to the increasing availability of time series from satellite products, there is a clear tendency towards spatially higher resolutions of LULCC datasets and ELUC estimates, but research on the influence of the resolution of underlying LULCC reconstructions on ELUC estimates is limited.

HILDA+ provides annual data for the time period 1960-2019 and based on that data interpolated trends for the time period 1900-1960 (Winkler et al., 2021). In comparison, LUH2 (Hurtt et al., 2020; Chini et al., 2021) covers a LULCC history dating back to AD 850 with data provided every 100 years until 1700, every 10 years between 1700 and 2000, and annually afterwards. To create annual LULCC maps, the data before 2000 is linearly interpolated between the above-mentioned time steps (Hurtt et al., 2020). The importance of the starting year of a model simulation is analysed by Hartung et al. (2021) for cumulative LULCC fluxes. Accordingly, based on simulations starting in AD 850, 1700, and 1850, the uncertainty introduced by the initialisation year amounts to 15% for estimates of cumulative ELUC in the time period 1850 to 2014. However, it remains unclear to what degree the starting year influences estimates of the more recent years, which are most important, e.g. as reference years or for the global stocktake, and if an initialisation in 1900 is sufficient for estimating emissions from 1960 onwards.

The goal of this study is to highlight spatial and temporal uncertainties in ELUC estimates related to (a) LULCC reconstructions, (b) the resolution of the LULCC forcing, and (c) the initialisation year.

## 5.2 Material and methods

For this study, HILDA+ is implemented in a bookkeeping model (BLUE) and results are compared to estimates of simulations based on LUH2, which is the LULCC dataset most commonly used in global ELUC models. In simulations of BLUE, ELUC fluxes from transitions between natural vegetation, cropland, and pasture, as well as from wood harvesting are considered (Hansis et al., 2015). Vegetation and soil carbon densities for each combination of LULCC states and eleven PFTs are based on literature values and provided in Hansis et al. (2015). Response curves derived from literature represent the carbon dynamics of different carbon pools following land use changes and describe the

decay and accumulation of vegetation and soil carbon. This includes the transfer of carbon to product pools of different lifetimes or the increase of carbon in different vegetation and soil pools due to regrowth of natural vegetation (Hansis et al., 2015).

BLUE simulations with three different LULCC inputs (HILDA+ at 0.25° and at 0.01°, and LUH2 at 0.25°) were initialised. Four BLUE simulations were carried out based on HILDA+ at 0.25° with different initialisation years (1900, 1920, 1940, 1960), and six simulations with the HYDE3.2 based LUH2 data that was used for the BLUE estimates in the GCB2020 (initialised in 1700, 1850, 1900, 1920, 1940, 1960). The runs with different years of initialisation are important to identify the minimum required starting year for robust ELUC estimates. The initialisation year 1700 corresponds to pre-industrial times, the year 1850 marks the approximate beginning of the industrial era, and the years 1900, 1920, and 1940 relate to the time period of interpolated trends of HILDA+, while 1960 is the first data-driven year of HILDA+. The simulation with HILDA+ at 0.01° was initialised in 1900.

Unlike LUH2, HILDA+ does not provide information on wood harvest and does not distinguish primary and secondary land, which is both required to capture important aspects of the carbon cycle. Thus, HILDA+ had to be processed and complemented before implementing it in BLUE. A detailed description of the processing of the data as well as a comparison of HILDA+ and LUH2 in terms of total area, spatial patterns, and annual change rates of LULCC states is provided in the supplementary materials (sections A and B) (available online at [stacks.iop.org/ERL/17/064050/mmedia](https://stacks.iop.org/ERL/17/064050/mmedia)).

## 5.3 Land use change emissions based on HILDA+ and LUH2

### 5.3.1 Differences in global estimates

Global ELUC estimates based on HILDA+ and LUH2 differ in size and trends (Figure 5.1 and Figure 5.2). Total ELUC estimates from the simulations with HILDA+ alternate around 1.0 PgC a<sup>-1</sup> and decrease from 1.3 PgC a<sup>-1</sup> in 2012 to 0.8 PgC a<sup>-1</sup> in 2019. Contrary, ELUC estimates based on LUH2 decrease from 2.3 PgC a<sup>-1</sup> in 1960 to about 0.9 PgC a<sup>-1</sup> in 1999 and increase afterwards to 2.0 PgC a<sup>-1</sup> in 2019. Gross source and sink fluxes are greater in estimates based on LUH2 compared to the one based on HILDA+. Trends in the last two decades are dominated by emissions from cropland expansions, with increasing tendencies for LUH2-based estimates and decreasing tendencies for estimates based on HILDA+.

Overall cropland emission estimates are on average almost three times higher, and the sink from abandonment of agricultural land is more than twice as big in the simulation with LUH2 compared to the one based on HILDA+ (Figure 5.2). The differences in cropland

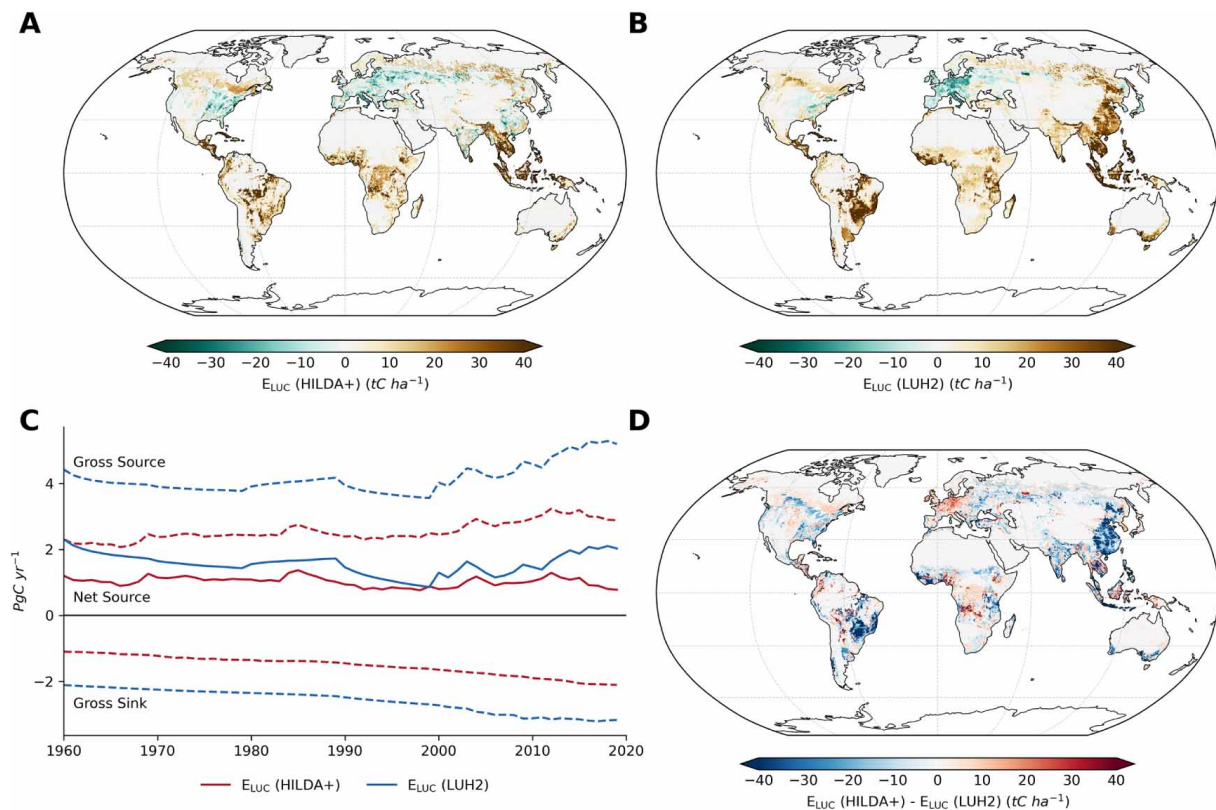


**Figure 5.1:** Global estimates of net CO<sub>2</sub> fluxes from LULCC (ELUC) at 0.25° resolution between 1960 and 2019. (A) Cumulative ELUC based on HILDA+, (B) cumulative ELUC based on LUH2, (C) ELUC based on HILDA+ and LUH2 over time (dashed: gross sink and source fluxes), (D) difference between cumulative ELUC estimates based on HILDA+ and LUH2. Global estimates of total ELUC are lower, and gross sources and sinks are smaller based on HILDA+ compared to estimates based on LUH2. The largest differences in total ELUC estimates exist in tropical regions, China, and Europe.

expansion and agricultural land abandonment estimates are connected to differences in the annual change rates of the LULCC input datasets. Due to the implementation of shifting cultivation in LUH2, gross gains and losses in cropland and secondary land area are higher in LUH2 compared to HILDA+, resulting in higher cropland emissions and a larger sink from agricultural land abandonment (Figure 5.3). Compared to cropland expansion and agricultural land abandonment, emission estimates from pasture expansion and wood harvest are of similar magnitudes on a global level. However, larger regional differences exist for pasture emission estimates.

### 5.3.2 Differences in regional estimates

Regional total ELUC estimates based on HILDA+ and LUH2 have different levels of agreement (Figure 5.4). The highest agreement in terms of mean total ELUC for 1960-2019 is found for Canada, Central and northern South America, Southern Africa, Mideast,

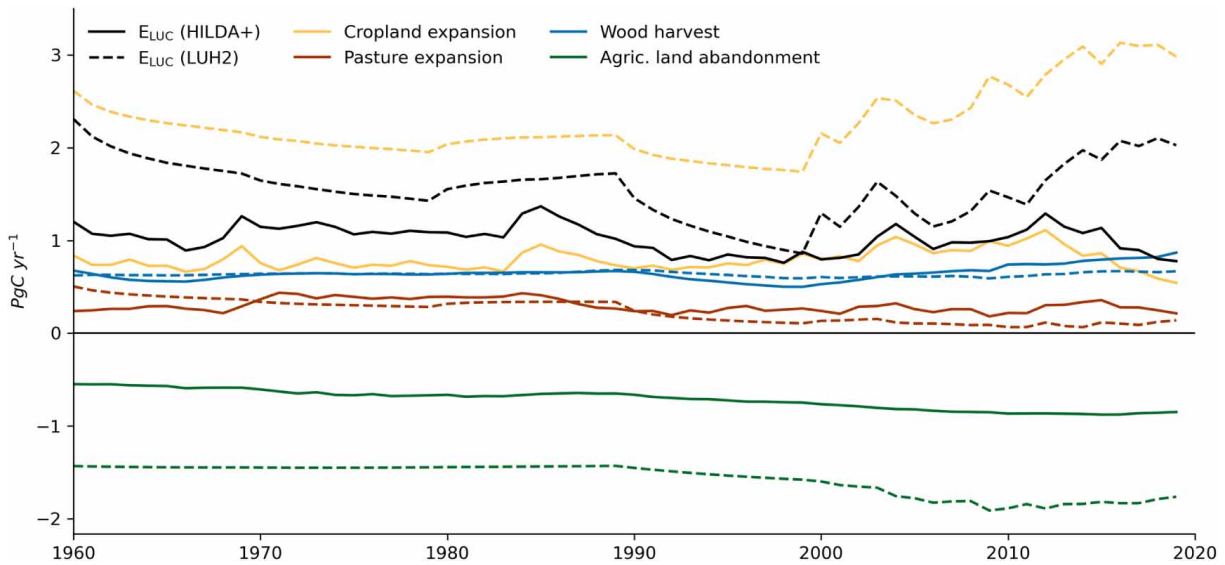


**Figure 5.2:** Global estimates of total and component CO<sub>2</sub> fluxes from LULCC (ELUC) based on HILDA+ and LUH2 at 0.25° resolution between 1960 and 2019. ELUC estimates based on LUH2 are higher than estimates based on HILDA+, mainly due to much higher emissions from cropland expansion. Also note the different dynamics since 2000 with increasing trends of LUH2-based estimates and decreasing trends with estimates based on HILDA+.

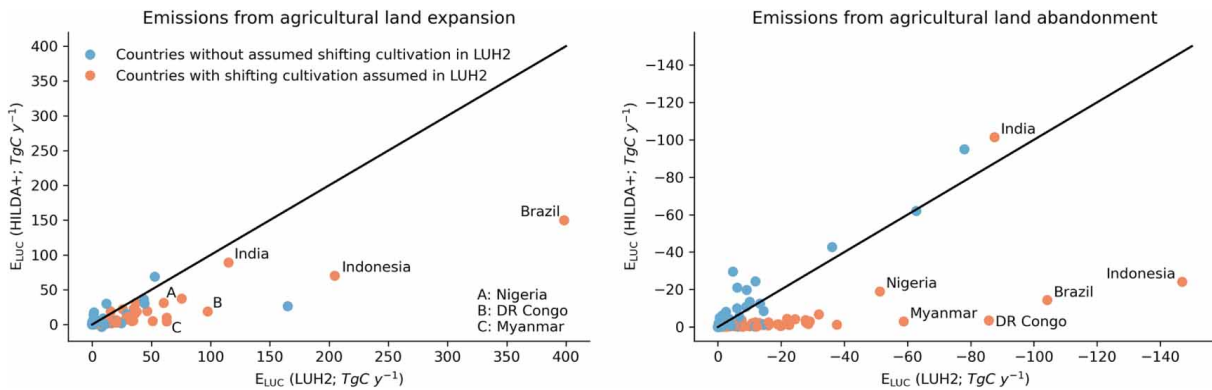


**Figure 5.3:** National estimates of yearly mean CO<sub>2</sub> fluxes (1960-2019) from expansion and abandonment of agricultural land based on HILDA+ and LUH2 (both at 0.25° resolution). Countries with shifting cultivation according to Heinimann et al. (2017) are highlighted in red. The estimates based on LUH2 of countries with shifting cultivation are mostly much higher compared to the ones based on HILDA+, while the estimates of countries without shifting cultivation coincide more. India is the only exception, which can be explained by the small area of shifting cultivation relative to the size of the country.

and ‘Korea and Japan’ with less than 10 TgC a<sup>-1</sup> difference. However, some of these regions have far less total ELUC emissions compared to other regions or estimates differ substantially in certain time periods. The largest differences in total ELUC estimates exist in China and Brazil (mean differences: 159 resp. 148 TgC a<sup>-1</sup>).

Individual component fluxes show further regional differences (Figure 5.4). Mostly in tropical and subtropical regions, emissions from cropland expansion are higher and the sink from abandonment is larger, with estimates based on LUH2 compared to HILDA+. As mentioned above, the magnitude of these differences originates from the implementation of shifting cultivation in LUH2. In the study by Heinemann et al. (2017), which is underlying LUH2 shifting cultivation assumptions, it is particularly the tropical and subtropical regions on all three continents that are affected by shifting cultivation in varying intensity. In the case of Central America, northern South America and Southern Africa, mean total ELUC estimates based on HILDA+ and LUH2 might have a high agreement despite large differences in component fluxes from cropland expansion and agricultural abandonment. Only in Europe and the Mideast, cropland emissions are mostly higher and abandonment emissions lower in the simulation based on HILDA+. Emissions from pasture expansion are higher or similar in the simulation with HILDA+ in most regions, except for Central Asia, China, and in some years Brazil. Emissions from wood harvest differ greatly in the US, Canada, Brazil, Equatorial Africa, Russia, and Southeast Asia due to a depletion of biomass to harvest over the years in the simulations based on HILDA+. The HILDA+ version used in BLUE contains less primary land area compared to LUH2, which can lead to a concentration of harvesting events. In regions, where this is not the case, harvest emissions of the two simulations are similar.

Another substantial difference between estimates of the two simulations are opposing ELUC trends within the last two decades in many regions, namely Southwest South America, Northern and Equatorial Africa, China, Southeast Asia, and to a certain degree also Oceania (Figure 5.4). While total ELUC in the run based on LUH2 is increasing in these regions, it is decreasing in the run based on HILDA+. The increase in ELUC in these regions is mostly driven by an increase in emissions from cropland expansion. Thus, the increase resp. decrease of cropland area in recent years is one crucial difference between HYDE3.2 based LUH2 and HILDA+.

Furthermore, regional ELUC plots reveal for some regions the occurrence of extreme ELUC changes in one or multiple years (Figure 5.4). Especially, emission spikes, where emission estimates strongly increase in one year and drop again to previous levels in the following years, are striking. This phenomenon, being present in estimates based on HILDA+ and LUH2, is apparent in the ELUC time series of the US, Canada, Russia, China, Oceania, and others. In all regions, these spikes can be attributed to extreme increases and soon after decreases in the annual change of single land cover states. It seems unlikely that these extreme changes reflect the actual development in the specific years, but rather originate from inconsistencies or misclassifications in the underlying datasets of LUH2 and HILDA+, especially since they do not occur in the same region and years in the two BLUE simulations.

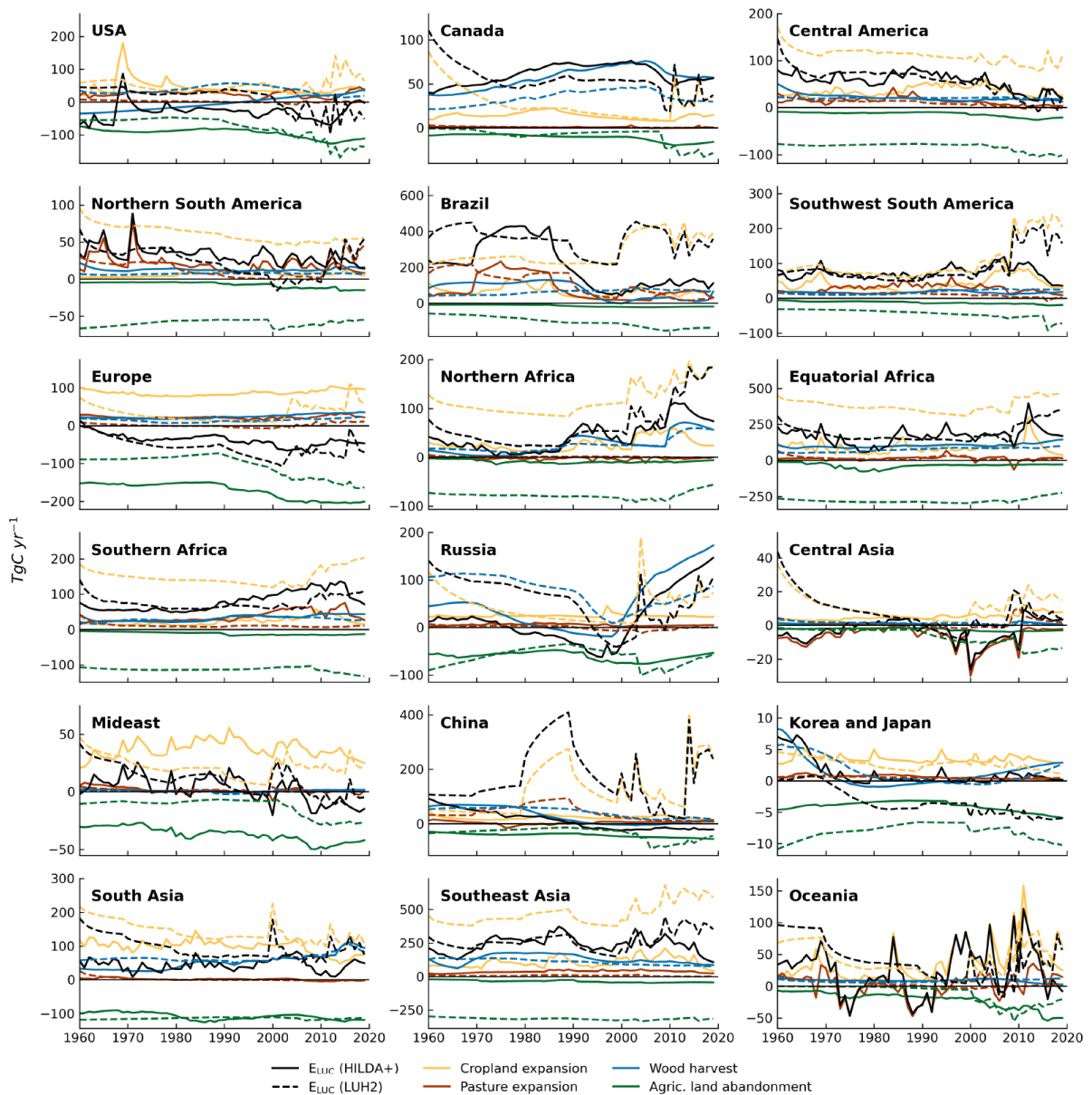


**Figure 5.4:** Regional net CO<sub>2</sub> fluxes from land use and land cover change (ELUC) estimates based on HILDA+ and LUH2 (both at 0.25° resolution).

### 5.3.3 Influence of spatial resolution

BLUE simulations, when forced with HILDA+ at 0.01° and 0.25° resolution (original HILDA+ resp. LUH2 res.) as LULCC input, reveal substantial differences mainly in component fluxes (Figures 5.5). Globally, the mean difference between the two simulations is 36 TgC a<sup>-1</sup> for the time period 1960-2019. The highest differences in component fluxes are observed in Europe, South Asia, and the Mideast. In general, emission estimates from cropland and pasture expansion tend to be larger and the sink from abandonment of agricultural land tends to be greater at 0.25° resolution.

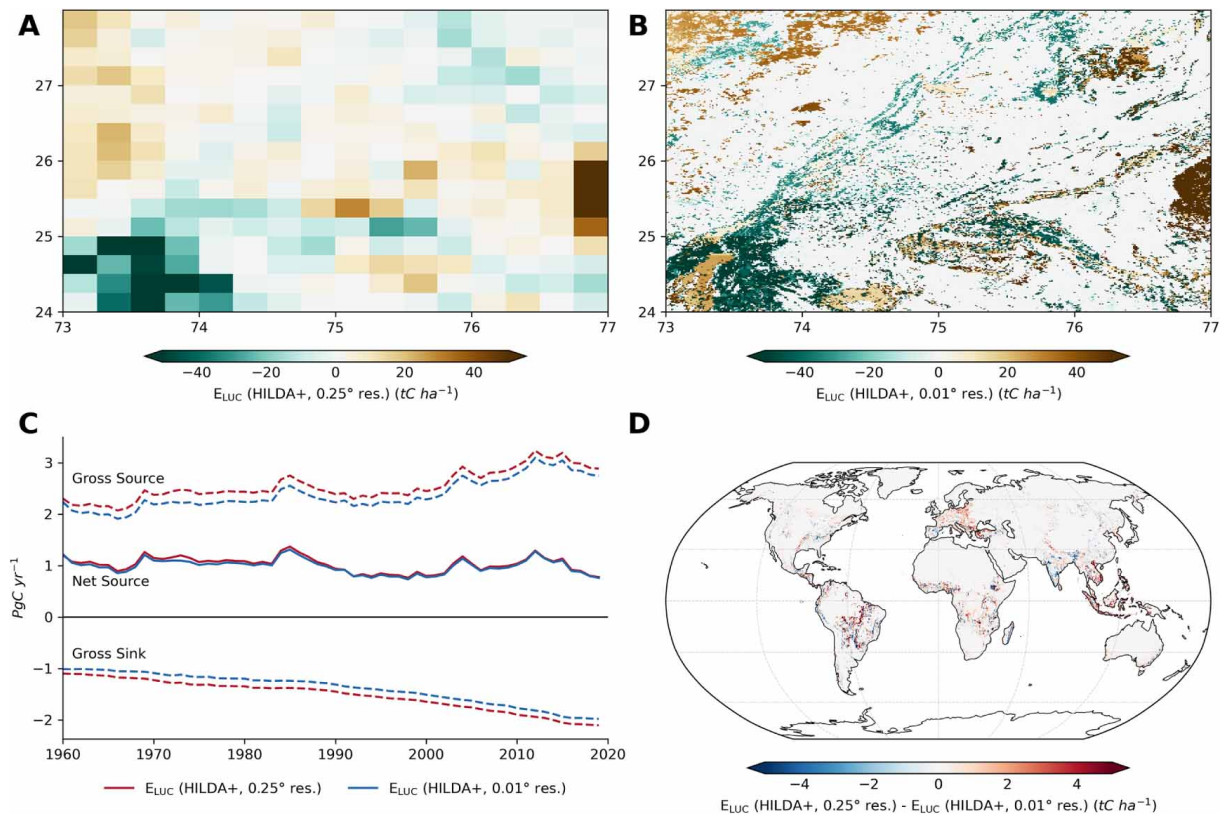


**Figure 5.5:** Global estimates of net CO<sub>2</sub> fluxes from LULCC (ELUC) based on HILDA+ at 0.25° and 0.01° resolution between 1960 and 2019. (A) Map extract of cumulative ELUC estimates based on the LULCC input at 0.25° for an exemplary area south-west of New Delhi, India with high positive and negative ELUC fluxes, (B) map extract of cumulative ELUC estimates based on the LULCC input at 0.01° for the same area as (A), (C) ELUC based on HILDA+ at 0.25° and 0.01° resolution over time (dashed: gross sink and source fluxes), (D) difference between cumulative ELUC estimates based on HILDA+ at 0.25° and 0.01° resolution. Total ELUC estimates based on the LULCC input at 0.25° resolution are slightly higher than estimates based on 0.01°. Gross sources and sinks are larger at the coarser resolution.

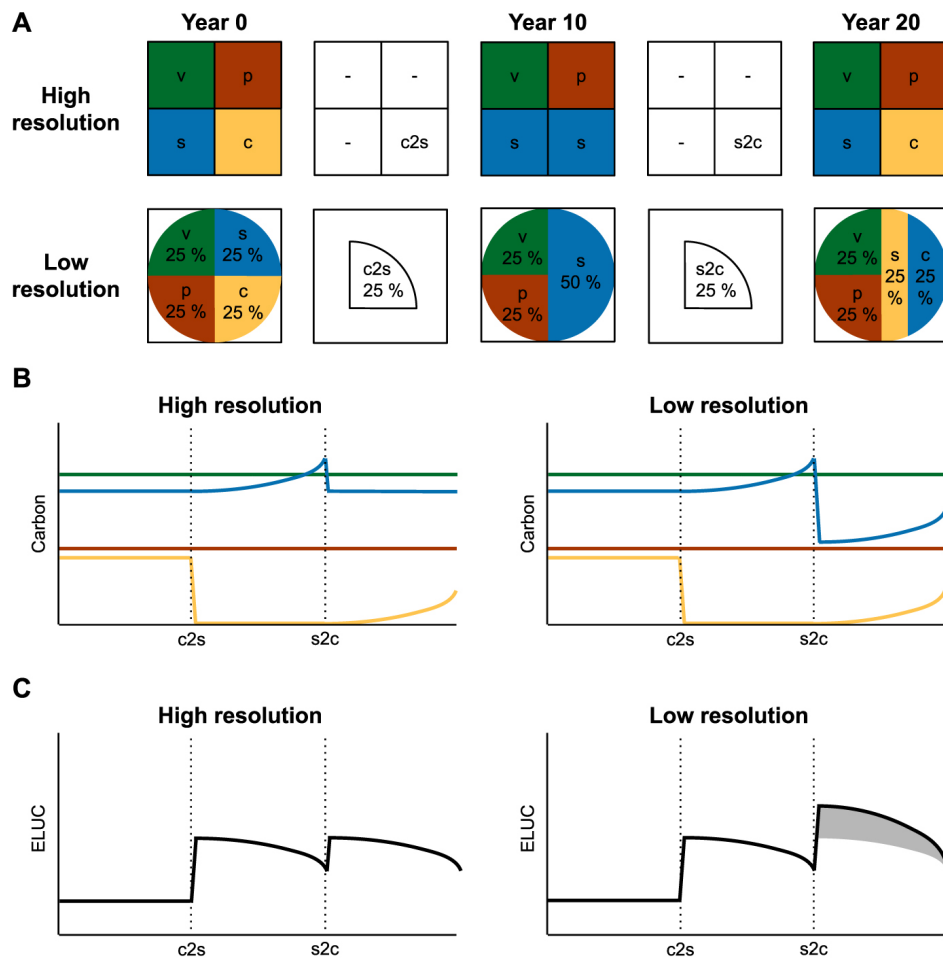


**Figure 5.6:** Illustration of the resolution dependent 'effect of successive transitions' on estimates of the CO<sub>2</sub> flux from LULCC (ELUC). (A) Exemplary land use and land use cover change data as used in BLUE (c: cropland, p: pasture, s: secondary land, v: primary land). The area of four grid cells at high resolution (e.g. 0.01°) corresponds to one grid cell at low resolution (e.g. 0.25°). In three out of the four grid cells at high resolution, LULCC does not change in the selected time period. Only the grid cell with cropland at the beginning is abandoned in year 10 and then transitions back to cropland in year 20. States and transition areas are exactly the same at low resolution, but are expressed as fractions of the grid cell area. Less area remains unchanged at low resolution compared to the land cover at high resolution. (B) The carbon pools of the four state types, shown in a simplified way. Carbon pools, are the same before and after the first transition from cropland to secondary land (c2s) at both resolutions. However, with the second transition (secondary land to cropland; s2c) the carbon pool of secondary land drops by half at low resolution, while at high resolution it 'only' descends to the level that corresponds to one grid cell of secondary land in equilibrium. At low resolution the carbon pools are affected proportionally by transitions, which results in less area being in equilibrium, when there are successive transitions. (C) ELUC at high and low resolution. The gray area marks the higher emissions at low resolution compared to the emissions at high resolution shown on the left. Additional BLUE experiments and explanations on the 'effect of successive transitions' are provided in the supplementary materials (section G).

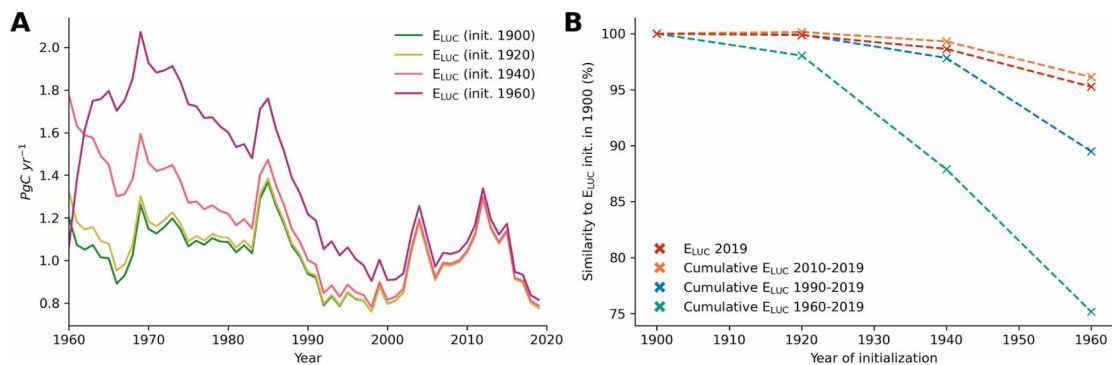


**Figure 5.7:** Comparison of BLUE simulations with different initialisation years based on HILDA+ (res.  $0.25^\circ$ ). (A) The net  $\text{CO}_2$  fluxes from LULCC (ELUC) with different initialisation years converge over time. At the end of the time period, differences between runs initialised in 1900, 1920, and 1940 are marginal. (B) The larger the difference between the initialisation years and the larger the time period of interest, the higher is the difference in cumulative ELUC estimates. The difference in cumulative ELUC estimates is less than 2% for the time period 1960 to 2019 between simulations initialised in 1900 and 1920.

Additional idealised BLUE simulations with artificial LULCC input data (section G in supplementary materials) revealed that these differences are related to the occurrence of successive transitions in grid cells, i.e. these grid cells experience at least two, but mostly more transitions in the covered time period. In the prepared HILDA+ dataset at  $0.01^\circ$  resolution, 84% of the global land grid cells do not undergo any transition between 1900 and 2019, 10% experience one transition and 5% have more than one transition. In comparison, in Europe 21%, in South Asia 15%, and in the Mideast 7% of the grid cells have two or more transitions. Oceania (34%) and US (9%) have high numbers of grid cells with successive transitions as well. However, the differences in component fluxes in these two regions are rather small, balancing out spatial differences. Also other regions have substantial amounts of successive transitions, but relative to the total transitions less than Europe, South Asia or the Mideast. Figure 5.6 illustrates the effect of successive transitions at different resolutions.

### 5.3.4 Influence of initialisation

ELUC estimates of simulations with different initialisation years show relatively small differences when the initialisation year is at least 60 years prior to the analysed time period (Figure 5.7).

The difference in cumulative ELUC estimates of the time period 1960-2019 for the simulation based on HILDA+ (res.  $0.25^\circ$ ) and initialised in 1900 versus the simulation based on HILDA+ (res.  $0.25^\circ$ ) and initialised in 1920 is less than 2%. For simulations based on LUH2 and initialised in 1700 and 1900, the difference in cumulative ELUC estimates (1960-2019) is less than 0.1%. The difference of cumulative ELUC emissions of later

time periods such as 1990-2019 or 2010-2019 is even smaller, since ELUC estimates with different years of initialisation converge with increasing time.

## 5.4 Discussion

The alignment of ELUC emission estimates based on different underlying LULCC forcing data differs globally, between regions and in certain regions depending on the time periods. Comparing ELUC estimates from the BLUE model based on HILDA+ with estimates based on LUH2, the highest agreement for the total ELUC is reached for Europe and Central America, while estimates for Brazil, China, and Oceania disagree substantially (Figure 5.4). For other regions, the level of agreement varies over time. For Europe, a high consensus among estimates based on different LULCC forcing data and models is confirmed by several studies (Gasser et al., 2020; Bastos et al., 2021; Petrescu et al., 2021). For Brazil, similar to our analysis, Rosan et al. (2021) find little agreement of ELUC emission estimates based on HYDE3.2, the newer HYDE3.3 version, and a national LULCC forcing. However, the suggested decline of total ELUC emission estimates based on HYDE3.3 by Rosan et al. (2021) in the last two decades cannot be reproduced by our estimates based on HILDA+ due to increasing emissions from pasture expansion. The change in trend in the global ELUC estimates that occurred in the GCB2020 as compared to the GCB2021 (Friedlingstein et al., 2021) and that resulted from the change from a HYDE3.2 to a HYDE3.3 based LULCC forcing as described by Rosan et al. (2021) is thus not confirmed by our simulations based on HILDA+ for Brazil. The decreasing trend in global emissions described in section 3.1 (Figure 5.1 C) for the last two decades in ELUC based on HILDA+ in contrast to LUH2 is instead strongly attributable to Southeast Asia, where cropland emissions are revised down in our simulations using HILDA+. For Southeast Asia, a regional study (Kondo et al., 2022) that uses DGVMs and bookkeeping models with different LULCC forcing data concludes a higher reliability of estimates based on LUH1 (Chini et al., 2014) compared to the ones based on LUH2 for the region. The estimates based on HILDA+ confirm decreasing ELUC emissions in Southeast Asia since the 2000s, although they suggest a later peak than Kondo et al. (2022). For the US, Yu et al. (2019) reason that ELUC emission estimates based on LUH2 overestimate the carbon sink, when comparing it to estimates based on a national land cover dataset. Contrary, our estimates based on HILDA+ do not suggest such a substantial overestimation compared to estimates based on LUH2 for the US. These regional examples highlight a lack of agreement between different LULCC datasets and the implementation of LULCC dynamics in different models, in particular on regional level. Newer estimates do not necessarily converge. Given the fact that the most recent years are most important for tracking mitigation efforts such as policies to halt deforestation or reforestation programs, the disagreement of LULCC datasets since 2000 urgently needs to be resolved.

Another major difference in ELUC estimates, mainly in tropical regions, are much higher

emissions from cropland expansion and a larger sink from abandonment of agricultural land (cropland and pasture) in estimates based on LUH2. As explained in section 3.1, this is connected to the implementation of shifting cultivation in LUH2 and the omission of it in HILDA+. According to Heinemann et al. (2017), the area influenced by shifting cultivation is spatially limited to roughly 280 Mha in the tropics between 30° S and 30° N. The inclusion of shifting cultivation in models, usually treated as a net vs. gross transition issue, is reported to lead to higher ELUC estimates (Stocker et al., 2014; Wilkenskjeld et al., 2014; Hartung et al., 2021). Arneeth et al. (2017) estimate an increase by 20%-30% when considering processes such as shifting cultivation. Furthermore, Bastos et al. (2021, 2020) and Gasser et al. (2020) highlight substantial differences due to the implementation of gross transitions in estimates based on LUH2 compared to estimates based on other LULCC datasets. We do not find considerably higher ELUC estimates based on LUH2 and HILDA+ that can be attributed to shifting cultivation as long as we consider the total ELUC. Despite much higher annual area gross changes of cropland and secondary land in certain tropical regions in LUH2 compared to HILDA+, which we ascribe to the implementation of shifting cultivation in LUH2, the component fluxes of cropland expansion and agricultural land abandonment mostly compensate for each other, and as a consequence total ELUC estimates match fairly well in most of the affected regions (at least before the increase in the last two decades, which is not connected to shifting cultivation). Similarly, Gasser et al. (2020) note that shifting cultivation has a long-term effect of zero net emissions in the OSCAR model. Based on our findings, we argue that (a) gross transitions and shifting cultivation should be treated differently and (b) the implementation of shifting cultivation in LULCC reconstructions and carbon cycle models needs to be reconsidered. As described in section 3.3, in LULCC reconstructions with low resolution more area is assumed to be under transition compared to the same data at high resolution ('effect of successive transitions'), which shows that the rotational cycles of shifting cultivation cannot accurately be represented at 0.25° resolution, neither can they at 0.01° resolution, since patches of shifting cultivation are usually maximum a few hectares in size (Villa et al., 2020; Bruun et al., 2021). Moreover, several case studies (Bruun et al., 2009; McNicol et al., 2015; Terefe & Kim, 2020) point out substantial differences in the carbon fluxes of the expansion and abandonment cycles of shifting cultivation compared to other expansion or abandonment transitions (e.g. clearing of former shifting cultivation areas for palm oil plantations), due to different regrowth rates and soil carbon dynamics. It remains unclear, if these drawbacks of current implementations in models can fully explain the large influence that shifting cultivation has on global and regional ELUC component fluxes according to simulations based on LUH2 or if the implementation of shifting cultivation in LUH2 leads to an additional overestimation.

The spatial resolution of the LULCC input data has a significant influence on ELUC component fluxes. Our estimates based on gross transitions of HILDA+ at 0.01° and 0.25° resolution and the BLUE experiments with artificial LULCC input revealed that com-

ponent fluxes are smaller at higher resolutions, which can lead to overall higher or lower total ELUC estimates. As described above, these differences are caused by successive transitions. According to Winkler et al. (2021), successive transitions were prevailing in the Global North (US, Europe, Australia) and rapidly growing economies such as India, Nigeria, and Turkey. Most of the transitions in these regions were changes between managed and unmanaged land (crop/pasture to secondary land or reverse) (Winkler et al., 2021). However, potential explanations are needed for these diverse and region-specific high land use dynamics: in the US cropland abandonment was driven over time by federal policies and changes in commodity prices among others (Chen & Khanna, 2018; Hendricks & Er, 2018; Lark et al., 2022), in Mediterranean Europe and Australia certain pasture-shrubland dynamics were influenced by climatic and socio-economic changes (Eldridge & Soliveres, 2015; Rolo & Moreno, 2019), in Eastern Europe the agricultural sector experienced massive changes following the breakdown of the former Soviet Union (Prishchepov et al., 2013; Schierhorn et al., 2019), in Turkey a mix of industrialisation, urbanisation, and migration led to rapid changes in land use practices (Tanrivermis, 2003), in India the heavy usage of irrigation and fertiliser enabled agricultural intensification (Ambika et al., 2016; Chen et al., 2019), and in Nigeria conversions to cultivated land dominated LULCC dynamics (Arowolo & Deng, 2018). Moreover, crop rotation or mixed croplivestock systems may also be linked to the observed successive transitions in Australia, the US, and Europe (Peyraud et al., 2014; Rosenzweig et al., 2018; Ghahramani et al., 2020).

The resolution-dependent ‘effect of successive transitions’ has not been described in the literature so far, although different studies discuss the importance of spatial resolution and transition types for ELUC estimates in other respects. For example, Wilkenskjeld et al. (2014) point out that a coarser resolution of net LULCC data leads in a reduction in area affected by LULCC and thus affects ELUC estimates. Several studies highlight the importance of using gross over net LULCC transitions to account for the actual area changes (Hansis et al., 2015; Arneth et al., 2017; Bayer et al., 2017; Bastos et al., 2020, 2021). However, Yue et al. (2018) conclude from simulations with sub-grid secondary forests of different age classes that the contribution from gross transitions to overall ELUC estimates tend to be overestimated due to the non-consideration of age classes in most models. The findings from Yue et al. (2018) go in a similar direction as our observation that successive transitions are not adequately represented in gross transitions at coarse resolution (nor with net transitions), and consequently different land areas are affected by successive transitions, when compared to the same LULCC data at high-resolution. It is likely that the ‘effect of successive transitions’ is also of greater importance for DGVMs and other bookkeeping models.

Our simulations starting at different years showcase the importance of a prudent choice for the year of initialisation. ELUC estimates of simulations based on HILDA+ for 2019 differ by more than 5% when initialised in 1960 compared to simulations with the same LULCC forcing but initialised in 1900. Further, the results indicate that the influence decreases

over time and differences between simulations with earlier and later starting years become marginal after a few decades. The simulations highlight that (a) the initialisation year needs to be well before the satellite era to capture present-day fluxes accurately (at least 95% similarity in cumulative emission estimates compared to simulations starting 20 years earlier), (b) a lead time of 60 years seems sufficient (95% similarity criterion, see above) and (c) the time period covered by HILDA+ starting in 1900 is suitable for the estimation of ELUC after 1960 without introducing large uncertainties due to the initialisation year.

## 5.5 Conclusions

ELUC estimates have high uncertainties, which are partly caused by underlying LULCC datasets among other drivers and parameters. The implementation of a new LULCC reconstruction dataset (HILDA+) in a bookkeeping model (BLUE) enabled us to evaluate and compare ELUC estimates based on HILDA+ to ELUC estimates based on the widely-used default LULCC dataset LUH2. Results show that global ELUC estimates based on HILDA+ are substantially lower than estimates based on LUH2. Regionally, a pattern of higher ELUC emissions from cropland expansion and a larger sink from agricultural land abandonment in estimates based on LUH2 can be observed in most tropical regions. The larger sources and sinks can partly be explained by the inclusion of shifting cultivation in LUH2, which raises questions about the influence of shifting cultivation on the global carbon cycle and the implementation of shifting cultivation in LULCC datasets and carbon cycle models. Another significant difference are opposing trends of ELUC estimates globally and in many regions in the last two decades. These substantial differences highlight the need for more reliable LULCC reconstructions for more accurate and robust ELUC estimates. Independent estimates for the evaluation of LULCC dynamics, including knowledge of regionally specific LULCC activities, component-specific evaluations, and complementing default global runs, such as in the GCBs, by alternative LULCC data could increase the understanding of differences and provide better estimates of uncertainties. Furthermore, we run simulations based on LULCC data at different spatial resolutions ( $0.01^\circ$  vs.  $0.25^\circ$ ) and find significant differences in ELUC component fluxes. The reason for this phenomenon are successive transitions. These cannot adequately be represented at the coarse resolution, which has the effect that at the coarser resolution overall a larger area is affected by LULCC events. Moreover, a lead time of at least 60 years has been found crucial to account for legacy emissions and retrieve robust ELUC estimates. This rather long lead time to capture legacy emissions, together with the need for ancillary data or methods to split anthropogenic from natural drivers of land use dynamics, challenges the application of purely satellite-based LULCC datasets, although their often high spatial resolution could provide an important step forward to capture successive transitions. Both the sensitivity to spatial resolution and initialisation year

are qualitatively independent of the concrete LULCC dataset, such that we recommend accounting for these issues in future studies with other LULCC activity data and carbon cycle models.

## 5.6 Acknowledgements

R.G. and K.W. acknowledge support from the European Commission through Horizon 2020 Framework Programme (VERIFY, Grant No. 776810). S.B. was supported by German Stifterverband für die Deutsche Wissenschaft e.V. in collaboration with Volkswagen AG. This work used resources of the Deutsches Klimarechenzentrum (DKRZ) granted by its Scientific Steering Committee (WLA) under Project ID bm0891.

## 5.7 Author contributions

KW and RF formed the HILDA + framework and KW developed the HILDA+ model. KW processed the HILDA+ data and adapted HILDA+ to the needs of the BLUE model. RG carried out the pre- and post-processing for the BLUE model and the model runs, with support from SB, FZ, and JP. RG prepared the manuscript, created all figures and maps. All authors interpreted and discussed the results. All authors were involved in critical revision of the manuscript, and commented on the paper.





# Chapter 6

## Impacts of land use and environmental change on the Eastern European land carbon sink

This chapter is based on:

Winkler, K., Yang, H., Ganzenmüller, R., Fuchs, R., Ceccherini, G., Duveiller, G., Grassi, G., Pongratz, J, Bastos, A. Shvidenko, A. Araza, A., Herold, M. & Ciais, P. Decline of the Eastern European land carbon sink – analysing the contribution of land use, management and environmental change. *Communications Earth & Environment*, (in review).

*We can't solve problems by using the same kind of thinking  
we used when we created them.*

Albert Einstein

## Abstract

Land-based mitigation is essential in reducing carbon emissions. Yet, the attribution of land carbon fluxes to their sinks and sources remains highly uncertain, in particular for the forest-rich but data-poor region of Eastern Europe. Here we integrate various data sources to show that Eastern Europe accounted for an annual aboveground biomass (AGB) carbon sink of  $\sim 0.49$  Gt C in 2010-2019, or about 75% of the entire European carbon uptake. We find that the overall sink is declining, mainly driven by changes in land use and land management, but also by increasing natural disturbances. Despite the high overall importance of environmental factors such as soil moisture, nitrogen and CO<sub>2</sub> for enhancing the land sink, we find indicators of a saturation effect of the regrowth in abandoned former agricultural areas, combined with an increase in wood harvest, particularly in European Russia. Our results contribute to better understand the role of land management for climate mitigation.

## 6.1 Introduction

Carbon sequestration from the terrestrial biosphere can contribute significantly to climate change mitigation. Globally, the terrestrial biosphere absorbs almost one third of the total anthropogenic CO<sub>2</sub> emissions (Friedlingstein et al., 2020; IPCC, 2022). This has been taken up after the Paris Agreement. Many countries proclaimed ambitious plans to achieve neutral net greenhouse gas emissions (Deng et al., 2022) – a target that can only be reached by reducing emissions in combination with increasing “negative” emissions from land-based carbon uptake (Griscom et al., 2017).

However, despite the societal relevance of land-based mitigation, there are still large uncertainties when measuring both the amount of carbon that is currently taken up by the land surface and estimating the additional carbon the land could potentially further take up (Friedlingstein et al., 2020; Petrescu et al., 2021). These uncertainties stem from the use of diverse methodologies, differences in underlying land use/cover datasets and divergent representation of processes within models (Friedlingstein et al., 2020).

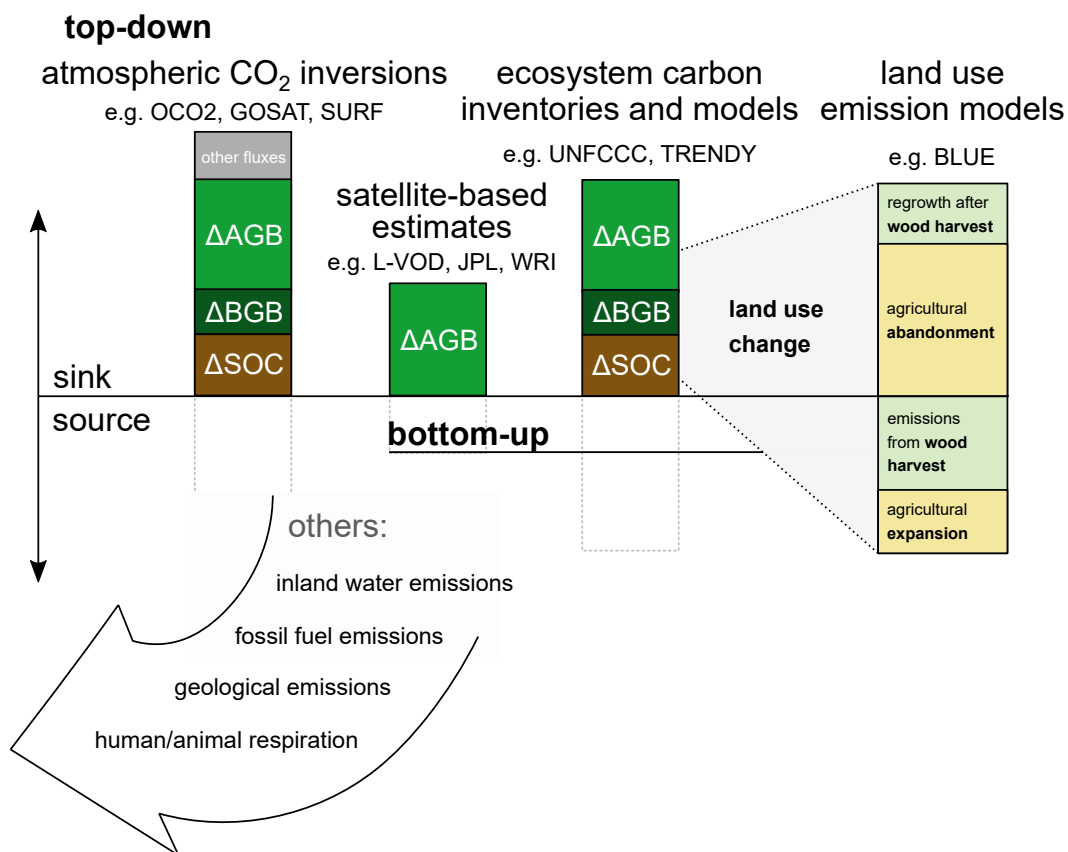


**Figure 6.1:** Overview of carbon flux components ( $\Delta$ AGB: Above-ground biomass,  $\Delta$ BGB: Below-ground biomass,  $\Delta$ SOC: Soil organic carbon) as addressed by different datasets and models.

According to global atmospheric inversions that account for land use impacts and environmental factors but do not separate them, managed lands account for a global sink of  $\sim 1.3 \text{ Gt C a}^{-1}$  (Deng et al., 2022), while in national inventories, which do not systematically account for environmental factors, they represent a sink of only  $\sim 0.3 \text{ Gt C a}^{-1}$  (Grassi et al., 2021). A new data compilation of national inventories, however, clarifies existent discrepancies and calculates a new net global sink of  $\sim 1.6 \text{ Gt C a}^{-1}$  (Grassi et al., 2022).

Although the Northern Hemisphere plays a dominant role as a carbon sink (Ciais et al., 2019) and operational measurement as well as modelling approaches are numerous, in Europe, there is no consent about the magnitude of the current carbon uptake of the terrestrial biosphere between inventories and research-based methods including atmospheric inversions, ecosystem models and satellite based biomass carbon storage (Petrescu et al., 2021; Reuter et al., 2014). Deviation between estimates are large and remain poorly understood (Reuter et al., 2017), especially in regions with few observational data. Studies focussing on the European carbon balance have found a large spread in the continental carbon sink:  $\sim 0.20 \text{ Gt C a}^{-1}$  for 2006-2015 (based on inversions) (Monteil et al., 2020),  $\sim 0.30 \text{ Gt C a}^{-1}$  for 2010-2015 (based on in-situ  $\text{CO}_2$  and passive microwave measurements) (Scholze et al., 2019) or  $\sim 0.95 \text{ Gt C a}^{-1}$  for 2003-2010 (based on inversions) (Reuter et al., 2014).

A particularly under-investigated area is Eastern Europe due to the lack of available observation sites and measurements. For the scope of this study, the region consists of 13 countries: Belarus, Bulgaria, Czech Republic, Estonia, Hungary, Latvia, Lithuania, Moldova, Poland, Romania, Slovakia, Ukraine, and western Russia (up to the Ural mountains). Eastern Europe is not only an extensively forested area, which indicates a potentially large carbon uptake. It also has been affected by major land use and management changes through a history of political and institutional upheaval. The collapse of the Soviet Union generated land tenure changes, a transition to open-market economies and several economic crises, all of which has triggered dramatic changes in forest disturbances and recovery rates (Potapov et al., 2015) but also in agricultural land management (Estel et al., 2015). Furthermore, Eastern European forests are prone to natural disturbance and weather extremes, which lead to fires, storms and insect outbreaks (Bellassen & Luyssaert, 2014; Lindroth et al., 2009). What is more, forests across Russia have acted as a larger carbon sink than previously reported during the last decades (Schepaschenko et al., 2021).

To find land use and climate mitigation strategies, measuring and attributing the land carbon uptake to its drivers is needed. In this paper, we aim to take stock of new observation-based approaches and improved models to quantify the land-based carbon uptake in Eastern Europe in the last decade, identify spatial and temporal patterns and finally attribute possible underlying drivers from land use, management and environmental change.

## 6.2 Material and methods

Methods for estimating land-based carbon fluxes are divided into two principal approaches: top-down and bottom-up. Top-down approaches such as satellite-based CO<sub>2</sub> inversions rely on the analysis of atmospheric CO<sub>2</sub> concentrations, which represent the accumulated effect of all CO<sub>2</sub> sources and sinks after removing fossil CO<sub>2</sub> emissions (Petrescu et al., 2021). Bottom-up approaches cover ground-based inventories, satellite-based estimates of biomass carbon changes, and vegetation growth models. Inventories are performed in regular multi-year periods by national agencies and form the base of UNFCCC reporting (Eggleston et al., 2006). However, they differ on e.g. how natural disturbances are considered (Deng et al., 2022). Satellite-based estimates are limited to the monitoring of biomass changes (Harris et al., 2021; Liu et al., 2015; Wigneron et al., 2020). Models are wide-ranging. Data-driven models (Bloom et al., 2016) compute carbon fluxes using biomass and soil carbon changes, and time-varying maps of carbon input to ecosystems from gross or net primary productivity. Process-based models such as Dynamic Global Vegetation Models (DGVMs) (Sitch et al., 2003) simulate carbon input from plant productivity, turnover in various ecosystem carbon pools, mortality and decomposition and can to some extent separate anthropogenic from natural drivers by including or excluding land use and land management in their simulation protocol (Friedlingstein et al., 2022). Some models are specialised in certain components of the terrestrial carbon balance: Most notably, emissions and removals from land use change and land management are commonly assessed by semi-empirical bookkeeping models (Friedlingstein et al., 2022). The various observation- and model-based estimates differ concerning how comprehensively anthropogenic and natural drivers are separated from each other (including the question of where synergistic terms are attributed to) and therefore care has to be taken when component fluxes from different methods are compared to each other (Pongratz et al., 2021). Figure 6.1 gives an overview of the different components of the land carbon flux as assessed by different approaches and datasets. In the following, the datasets and models used in this study are described.

## 6.2.1 Carbon flux datasets

### 6.2.1.1 CO<sub>2</sub> inversions

We used the annual CO<sub>2</sub> flux data at a spatial resolution of 1.875° latitude × 3.75° longitude from the atmospheric inversion of the Copernicus Atmosphere Monitoring Service inversion (CAMS). We compared the CO<sub>2</sub> flux data from CAMS constrained by surface air sample measurement (referred to as SURF) and by CO<sub>2</sub> column retrievals from two satellites (referred to as OCO2 and GOSAT). SURF was released in 2019 and results from the assimilation of CO<sub>2</sub> surface air-sample measurements in a global atmospheric transport model over the period from 1979–2018. We used version v18r3 of SURF inversion data (CAMS, 2020). OCO-2 is a satellite from NASA that was launched in July 2014, providing spatially dense and fine-resolution CO<sub>2</sub> column retrievals. The OCO2 data assimilates OCO-2 retrieval data into atmospheric inversion models. OCO-2 infers atmospheric CO<sub>2</sub> mixing ratios from solar radiation in the near-infrared that has reflected from the Earth's surface and atmosphere. From these measurements, the mixing ratio as a function of altitude (or pressure) is inferred using inverse methods. We used OCO2 data version FT18r1 (CAMS, 2020). GOSAT is a Japanese satellite that was launched in January 2009, and the column retrievals from GOSAT have relatively coarse-resolution data and low spatial density. The GOSAT data used in this study is a special product of the RECCAP-2 project (ESA) with LMDZ6A, the Atmospheric Component of the IPSL Climate Model. In this study, the temporal coverage of SURF, OCO2 and GOSAT was 2010-2018, 2015-2018 and 2010-2016, respectively.

### 6.2.1.2 TRENDY global models

TRENDY is an ensemble of dynamic global vegetation models (DGVMs) in support of the Global Carbon Budget (GCB) annual assessment (Sitch, 2022; Sitch et al., 2015). In this study, we used the following 15 DGVMs of the TRENDY project: CABLE-POP, CLASSIC, CLM5.0, ISAM, ISBA-CTRIIP, JSBACH, JULES-ES-1p0, LPJ-GUESS, LPX-Bern, ORCHIDEE, ORCHIDEE-CNP, ORCHIDEEv3, SDGVM, VISIT, YIBs. We use the "S3 simulation" with time-varying CO<sub>2</sub>, climate and land use forcing, as this is the simulation that captures both natural and anthropogenic dynamics.

In order to extract the AGB carbon, we obtained the gridded variable of cVeg (carbon in vegetation) from all 15 models. Additionally, the variable cRoot (carbon in roots) was used, however, it was only available for ten DGVMs. For those models without cRoot (JSBACH, JULES-ES-1p0, ORCHIDEEv3, VISIT, YIBs), we generated cRoot with the help of gridded above/below-ground biomass ratios derived from Spawn et al. (2020). As a next step, we computed AGB carbon ( $C_{AGB}$ ) as

$$C_{AGB} = C_{Veg} - C_{Root}$$

with  $C_{Veg}$  as carbon in vegetation (above-ground) and  $C_{Root}$  as carbon in roots (below-ground).

In this way, we calculated the change between AGB carbon of 2010 and that of 2019 for each of the 15 models. We re-sampled the maps from  $1^\circ$  to  $0.25^\circ$  resolution using bilinear interpolation. In order to synthesise the information, we calculated the average across all 15 models.

### 6.2.1.3 Satellite-based estimates of AGB carbon

#### *L-VOD*

Vegetation optical depth, which represents vegetation attenuation properties, has been widely used to monitor the dynamics of vegetation above-ground carbon and water content (Liu & Yang, 2015; Moesinger et al., 2020). In this study, we used the low frequency (1.4 GHz) passive microwave satellite data of L-band vegetation optical depth (L-VOD) derived from the Soil Moisture and Ocean Salinity (SMOS) with ascending (ASC) and descending (DESC) orbits, providing global measurements at a spatial resolution of 25 km with re-visiting time of 1-3 days since 2010 (Wigneron et al., 2021). The L-VOD product is available at <https://ib.remote-sensing.inrae.fr/>. To avoid the effect of Radio Frequency Interference (RFI), we filtered the L VOD data based on the root mean square of the measured and simulated brightness temperature (RMSE-TB). After that, the filtered “best quality” data from ASC and DESC orbits were merged, and they were fitted and reconstructed using a method from Thoning et al. (1989). The reconstructed de-seasonalised long-term trend data were used to calculate the yearly value, which is the average of May, June, July and Aug (i.e., July 1st – centred averages). Next, the yearly values of above-ground biomass (AGB) were calculated using yearly L-VOD and the regressed relationship between AGB and L-VOD. Such regressed relationship was built using three existing reference maps, namely GlobBiomass product (Santoro et al., 2021), ESA CCI Biomass product (Santoro & Cartus, 2021) and AGB map by Avitabile et al. (2016). The uncertainty of the AGB changes was estimated by the standard deviation of the estimates using different reference maps.

#### *JPL*

Xu et al. (2021) from the Jet Propulsion Laboratory (JPL) provided annual estimates of the live biomass of the global terrestrial ecosystems between 2000 and 2019, which are based on a bottom-up framework using machine learning techniques to synthesise ground-based forest inventories with airborne and satellite data (Xu et al., 2021). We refer to the dataset here as JPL. We used the maps referred of global live woody vegetation carbon density, which are at around 10 km ( $0.1^\circ$ ) spatial resolution, calculated the annual changes and derived the mean annual change for the period of 2010-2019. We re-sampled the map of biomass carbon density change to  $0.25^\circ$  resolution using bilinear interpolation.

Since the carbon density refers to both the above-ground and the below-ground biomass, we extracted the above-ground biomass with the help of the gridded above-/below-ground biomass ratio derived from Spawn et al. (2020).

### *WRI*

The carbon flux model of Harris et al. (2021) developed at the World Resources Institute (WRI) was modified to obtain the fluxes attributed to above-ground biomass (AGB) and carbon from 2010 to 2019. We refer to the dataset here as WRI. Net flux in this context is defined as the difference between the carbon emitted and removed by woody vegetation, set as areas with  $> 30\%$  tree cover of the global forest change data by Hansen et al. (2013). Note that in contrast to L-VOD and JPL, which consider AGB from all vegetation, WRI refers to forests only. In particular, we modified the AGB map input, using the 2010 CCI Biomass map (Santoro & Cartus, 2021) adjusted for potential systematic differences when compared with plot-based reference data (Araza et al., 2022). We also changed all inputs and variables originally set for 2000 into our baseline year 2010 such as the primary forest and tree cover datasets. We further modified the original model to exclude fluxes from other gases aside from  $\text{CO}_2$  and remove carbon components from below-ground and soil. The resulting carbon flux was divided by a factor of 0.49 to derive the AGB.

The tool Plot2Map (<https://github.com/arnanaraza/PlotToMap>) which implements the AGB map assessment framework (Araza et al., 2022) was used to adjust for the systematic differences in the 2010 CCI Biomass map. The framework implements a model-based approach that makes use of a worldwide database of reference AGB with uncertainty estimates as basis for modelling spatial uncertainties of the AGB map at aggregated levels i.e., 1 km.

#### **6.2.1.4 UNFCCC inventories**

The United Nations Framework Convention on Climate Change (UNFCCC) provides data from the national greenhouse gas (GHG) inventories submitted by countries that are Parties to the Convention. For comparing the land carbon uptake of the countries in Eastern Europe, we used GHG inventories referring to net  $\text{CO}_2$  emissions/removals from land use, land use change and forestry (LULUCF). We collected the data from the national inventories submitted to the UNFCCC. We acquired a complete time series from 1990 to 2019 (annual emissions) for Annex I countries Belarus, Bulgaria, Czech Republic, Estonia, Hungary, Latvia, Lithuania, Poland, Romania, Slovakia, and Ukraine from the UNFCCC website (UNFCCC, a). For Moldova (Annex II country), inventory data was only available up to the year 2013. In order to obtain the GHG inventory data for the region of European Russia, we acquired the national inventory reports (NIR) of Russia for all years from 2010 to 2019 (UNFCCC, b), extracted and summed up the AGB carbon balance of managed forests from UNFCCC data for 54 Russian districts belonging to European Russia (Ural mountains as the eastern border).

### 6.2.1.5 EFISCEN

The European Forest Information SCENario Model (EFISCEN) is a large-scale model for estimating forest resource development in Europe. The model uses National Forest Inventory data as a main input. By using biomass expansion factors, stem wood volume is converted into biomass and subsequently to carbon stocks of trees. It includes a detailed dynamic growth module, while natural mortality and harvesting are included as regimes, depending on the region. For this study, EFISCEN data for 2010-2018 was acquired and used in the same version as from the European VERIFY project (Petrescu et al., 2021).

### 6.2.1.6 CBM

The Carbon Budget Model developed by the Canadian Forest Service (CBM-CFS3) simulates the forest carbon dynamics under different scenarios of harvest and natural disturbances (fires, storms). The CBM has been validated by the Joint Research Centre of the European Commission (JRC) and adapted to forests in Europe. Forest stands are described by area, age and land use classes, and other parameters. Yield tables specify the merchantable volume production for each species, while allometric equations convert merchantable volume production into above-ground biomass at the stand level. The model provides annual data on net primary production (NPP), carbon stocks and fluxes, as the annual C transfers between pools and to the forest product sector. For this study, CBM data for 2010-2015 was acquired from and used in the same version as in the European VERIFY project (Petrescu et al., 2021).

## 6.2.2 Estimating the land-based carbon sink

We estimated the average land carbon flux (in  $\text{Gt C a}^{-1}$ ) from inversions (SURF, GOSAT, OCO2), AGB sink estimates (L-VOD, JPL, WRI), forest ecosystem models and inventories (EFISCEN, CBM, UNFCCC) and land use bookkeeping model BLUE for different regions in Europe between 2010 and 2019. For this, we derived the annual land carbon flux estimates and calculated a multi-year average. The standard deviation was used as a measure of uncertainty and displayed as error bars in Figure 6.2. For AGB biomass estimates available as annual maps, we first computed the annual AGB changes between two years. Then, the multi-year average AGB change was derived. Again, the standard deviation was used as an uncertainty measure. This was performed for different regions of Europe, defines as:

- EUR-North: Denmark, Finland, Iceland, Norway, Sweden
- EUR-West: Austria, Belgium, France, Germany, Ireland, Liechtenstein, Switzerland, United Kingdom of Great Britain and Northern Ireland, Luxembourg, Netherlands

- EUR-South: Croatia, Cyprus, Greece, Italy, Malta, Monaco, Portugal, Slovenia, Spain
- EUR-East: Belarus, Bulgaria, Czechia, Estonia, Hungary, Latvia, Lithuania, Moldova, Poland, Romania, Slovakia, Ukraine
- European Russia: Russia up to Ural mountains as eastern border

For the scope of this study, Eastern Europe consists of EUR-East and European Russia.

### 6.2.3 Mapping AGB carbon change

We calculated the agreement of AGB carbon changes in 2010-2019 between L-VOD, JPL, and WRI. TRENDY was excluded from the analysis due to its coarser spatial resolution, large inter-model deviations and relative distance to observational data streams. The level of agreement was derived pixel-wise for either a carbon source or sink across Eastern Europe. Sources are defined by AGB below  $-0.05 \text{ Mg C ha}^{-1} \text{ a}^{-1}$ , sinks by AGB above  $0.05 \text{ Mg C ha}^{-1} \text{ a}^{-1}$ .  $\Delta\text{AGB}$  values that are between  $-0.05$  and  $0.05 \text{ Mg C ha}^{-1} \text{ a}^{-1}$  were treated as no change. Levels of agreement represent the number of agreeing datasets. By including levels of agreement from 2 to 3, the average AGB carbon change was derived on the basis of the agreeing datasets only.

### 6.2.4 Datasets used as driver indicators of AGB carbon change

#### 6.2.4.1 Land use-based carbon fluxes (BLUE)

The Bookkeeping of Land-Use Emissions model (hereafter BLUE; see (Hansis et al., 2015), for documentation) is one of three bookkeeping models used in the Global Carbon Budget 2020 (Friedlingstein et al., 2020) for estimating the net  $\text{CO}_2$  flux from land use/cover change. In BLUE, transformations of natural vegetation to agriculture (cropland, pasture) and back, including gross transitions at the sub-grid scale, are considered as well as degradation from rangeland dynamics and wood harvesting. The temporal evolution of carbon gains or losses after transformations or harvesting events is based on response curves derived from literature. These response curves describe the decay of vegetation and soil carbon, including the transfer to product pools of different lifetimes, the carbon uptake due to regrowth of vegetation, and the subsequent refilling of soil carbon pools. Response curves in BLUE depend on literature-based carbon densities, which are implemented for 11 different plant functional types.

For this study, BLUE estimates based on HILDA+ have been used as described by Ganzenmüller et al. (2022). We used the net carbon sink from BLUE (BLUE net) as the total of all emissions from agricultural expansion (carbon source), wood harvest (carbon source) and agricultural land abandonment (carbon sink). Additionally, we used

gross carbon sink from BLUE (BLUE gross), which refers to the carbon uptake by agricultural land abandonment only.

#### 6.2.4.2 Forest harvest (JRC)

The dataset represents a forest harvest annual time-series from 2001 to 2019 (Ceccherini et al., 2020). Forest harvest is expressed as the percentage of forest area affected by management practices per year in a  $0.2^\circ$  grid cell ( $\sim 20$  km), excluding forest losses due to fires, major windstorms and areas with sparse forest cover. The dataset relies on the Global Forest Change (GFC) (Hansen et al., 2013) product (version 1.8), a time-series analysis of the Landsat archive characterizing tree cover extent in the year 2000 and annual forest loss with a spatial resolution of  $\sim 30$  m. Due to the spatial scale of the GFC dataset, small-scale silvicultural practices such as thinning or selective logging that may not be seen by the satellite could not be fully detected as forest loss.

First, a tree-cover threshold of 20% was used to define a ‘forest’ from the GFC tree cover product. Then, a spatial aggregation to  $0.2^\circ$  was performed and the annual forest harvest was computed as the ratio between the area of forest loss and the area of forest cover, within each grid cell. Areas with sparse forest cover – that is, where forest cover in a grid cell of  $0.2^\circ$  is less than 10% – were excluded. Regions affected by forest fires, as detected by the ESA Fire Climate Change Initiative (Fire CCI version 5.1) (Chuvieco et al., 2018) dataset collection, were masked out from the analysis. In the same way, in regions where the annual percentage of forest loss is greater than a given threshold, the forest loss was attributed to wind-throw and masked out. This was done under the assumption that major windstorms generally cause larger losses than those caused by forest management. The forest harvest dataset was generated using Google Earth Engine. To account for and harmonise different forest definitions in datasets used in this study (e.g. 20% tree cover threshold here but 30% in WRI-based AGB), we used the land use/cover map of 2010 from the HILDA+ dataset (Winkler et al., 2021), which is based on the 30% tree cover definition. We set forest harvest to 0 outside the HILDA+ forest areas.

#### 6.2.4.3 Cropland abandonment

The cropland abandonment dataset we used for this study is a synthesis map from three different data sources:

1. Abandoned arable land by Lesiv et al. (2018): The dataset covers the former Soviet Union, refers to the year  $\sim 2010$  and has a spatial resolution of 10 arc-seconds. Abandoned arable land is defined as the land that was previously cultivated (agricultural land) but has not been utilised for more than 5 years.
2. Farmland abandonment by Estel et al. (2015): Abandoned areas were classified based on MODIS Normalized Differenced Vegetation Index (NDVI) time series in 2001–2012. The dataset has a spatial resolution of 232 m and covers Europe, includ-

ing European Russia. We utilised the map of abandonment based on the following definition: At least three active cropland years during 2001-2006 were followed by five or six fallow years during 2007-2012.

3. HILDA+ cropland abandonment map: All areas where cropland has been converted into unmanaged grass/shrubland or forests during 2010-2019 have been classified as abandoned cropland based on HILDA+ annual land use/cover transitions maps (Winkler et al., 2021). The dataset has global coverage and a spatial resolution of  $\sim 1$  km.

All three maps were reclassified to binary mask format, with 1 representing abandoned cropland and 0 representing all other areas. The binary masks were re-sampled to  $0.25^\circ$  resolution using bilinear interpolation and converted to floating point values. The resulting maps depict the fractions of abandoned cropland, respectively. Finally, we derived the mean fraction of abandoned cropland per pixel from all available datasets (for former Soviet Union: Lesiv et al., Estel et al., HILDA+; for non-former Soviet Union: Estel et al., HILDA+). The resulting map of abandoned cropland represents the maximum fraction of a grid area affected by cropland abandonment during 2010-2019. It should not be used to measure abandonment in absolute terms.

#### 6.2.4.4 Fire

FireCCI51 from the ESA CCI Fire project was used to derive the change in burned area/fire between 2010 and 2019. This is based upon data from the MODIS instrument on-board the TERRA satellite at 250 m resolution for the period 2001-2020 (Chuvieco et al., 2018). Burned area represents the sum of area (in  $\text{m}^2$ ) of all pixels detected as burned within each grid cell and period. From this data, we cannot distinguish whether fires are naturally induced or anthropogenic. As next step, we derived the annual sums of the monthly gridded data and derived the mean annual change of burned area during 2010-2019. Finally, we re-sampled the map to  $0.25^\circ$  resolution using bilinear interpolation.

#### 6.2.4.5 Soil moisture

Estimates of soil moisture from the Copernicus Climate Change Service (C3S) v20201 are based on the ESA Climate Change Initiative soil moisture version 03.3 and represents the current state-of-the-art for satellite-based soil moisture climate data record production (Copernicus Climate Change Service, 2021). We extracted the monthly maps of volumetric soil moisture in  $\text{m}^3 \text{m}^{-3}$ , converted them to annual means and derived the annual change between 2010 and 2019. Subsequently, we re-sampled the map to  $0.25^\circ$  resolution using bilinear interpolation.

#### 6.2.4.6 Precipitation

We used gridded monthly precipitation from the TerraClimate data of monthly climate and climatic water balance for global terrestrial surfaces from 1958-2019 ( $\sim 4$  km spatial resolution) (Abatzoglou et al., 2018). From this, we derived the difference of the annual precipitation sums in 2010 and 2019 (in mm) and re-sampled the map to  $0.25^\circ$  resolution using bilinear interpolation.

#### 6.2.4.7 Temperature

We acquired the Berkeley Earth gridded monthly surface air temperature at  $1^\circ$  spatial resolution (Earth, 2020; Rohde & Hausfather, 2020) to account for temperature as a potential driver of AGB carbon change. We derived the difference of the mean annual temperature from 2019 and 2010 and re-sampled the map to a  $0.25^\circ$  resolution using bilinear interpolation.

#### 6.2.4.8 CO<sub>2</sub> concentration

To address the potential effect of CO<sub>2</sub> fertilisation, we acquired monthly gridded data of the atmospheric CO<sub>2</sub> concentration as column-mean molar fraction from CAMS global greenhouse gas reanalysis (EGG4) (CAMS, 2021), which covers the period of 2003-2021. We first derived annual means from the monthly column-mean molar fraction of CO<sub>2</sub> (in ppm) for the period of 2010-2019. Second, we calculate the mean annual change in CO<sub>2</sub> flux for the entire period and re-sampled the map from a  $0.75^\circ$  to a  $0.25^\circ$  resolution using bilinear interpolation.

#### 6.2.4.9 Nitrogen deposition

We acquired global estimates of inorganic nitrogen deposition for six individual years in the periods of 2004-2006 and 2014-2016 ( $2.0^\circ \times 2.5^\circ$  grid resolution) simulated with GEOS-Chem (Ackerman et al., 2019). The spatially explicit information provided in tables containing values of inorganic nitrogen deposition in  $\text{kg km}^{-2}$  was first converted to point shape files and subsequently transformed into geotiff raster files. For each 3 year-period, the multi-year mean was derived. The difference between the nitrogen deposition maps of  $\sim 2015$  and  $\sim 2005$  was calculated and transformed into an annual rate of nitrogen deposition change in  $\text{kg ha}^{-1} \text{a}^{-1}$ . The map was re-sampled to a  $0.25^\circ$  resolution using bilinear interpolation. Note that the map of nitrogen deposition change, as used for the driver analysis, does not exactly cover the period from 2010 to 2019 and, thus, the effect of nitrogen deposition on ABG carbon change cannot be analysed in its full details.

### 6.2.5 Driver analysis

In order to identify the major drivers of AGB carbon change in Eastern Europe, we carried out a driver analysis in two steps.

#### 6.2.5.1 Trend pattern matching

In a first step, we used the standardised trends – the change between 2010 and 2019 – of each of the potential driver indicators (carbon fluxes attributed to agriculture BLUE-agr, abandonment BLUE-aban and wood harvest BLUE-harv; fraction of cropland abandonment; wood harvest; fire; soil moisture; precipitation; temperature; CO<sub>2</sub> concentration; nitrogen deposition). Note that for cropland abandonment, not the change but the maximum fraction of abandoned land during ~2000-2019 (see Cropland abandonment) was used to account for the effect of formerly abandoned cropland, since carbon sequestration can persist for several years after abandonment (Foote & Grogan, 2010). In order to assign a major driver indicator to each grid cell, assumptions about the relationship between the driver indicators and AGB carbon change were used (see Table 6.1).

A raster stack was built from the driver indicator layers, each for AGB carbon sink and source. The values of each driver indicator were standardised to a range between -1 and +1, with the exception of abandonment ranging from 0 to 1. According to the assumed relations, the values of driver indicators with a negative relationship were inverted (multiplied by -1). When the relationship was unclear, as for temperature, precipitation and soil moisture, the absolute value from the values was taken so that both negative and positive changes were considered. In both the AGB carbon sink and the AGB source stack, the driver indicator with the maximum value was identified for each grid cell. This driver indicator was assigned to the respective grid cell. As a consequence, for each AGB carbon sinks and sources (based on the average AGB carbon change from L-VOD, JPL, and WRI), the driver indicators that showed the strongest trend constrained by its relation could be identified and mapped across Eastern Europe.

#### 6.2.5.2 Random forest model

In a second step, we applied a random forest regression model in order to derive the importance of the driver indicators in explaining the distribution of the AGB carbon change of Eastern Europe. All the eleven driver indicators (see above) were used as predictors, the average AGB carbon change from L-VOD, JPL, and WRI agreement (see Mapping AGB carbon change) was used as target variable. The random forest regression model was applied using scikit-learn, a machine learning library in Python 3.9. The random forest regression was run for three different subsets based on the target variable. Subset 1: AGB carbon source only, Subset 2: AGB carbon sink only, Subset 3: All AGB change values (including grid cells of agreement but classified as “no change”).

**Table 6.1:** Assumed relationship between change of driver indicators and AGB carbon change, either sink (positive change) or source (negative change). Negative relations are displayed as -, positive relations are displayed as +, unclear relations are displayed as +/-.

Driver indicator	Relation to AGB carbon sink	Relation to AGB carbon source	Description
BLUE-agr	-	+	Agricultural expansion leads to carbon emissions (source).
BLUE-aban	+	-	Agricultural land abandonment leads to enhanced woody biomass (carbon sink).
BLUE-harv	-	+	Wood harvest removes biomass (carbon source).
harvest	-	+	See BLUE-harv.
abandonment fraction	+	-	See BLUE-aban.
fire	-	+	Fires lead to biomass removal and carbon emissions (sink).
soil moisture	+/-	+/-	Unclear relation
precipitation	+/-	+/-	Unclear relation
temperature	+/-	+/-	Unclear relation
CO <sub>2</sub>	+	-	CO <sub>2</sub> fertilization effect enhances biomass production (sink).
nitrogen	+	-	Nitrogen deposition enhances biomass production (sink).

For all runs, the dataset was split into test and train subset, where the test subset was set as 0.25 of the dataset. The values of all predictors were standardised and scaled between -1 and 1. To derive the optimal number of decision trees used by the model, we iteratively trained the model by using 10 to 200 trees in a 10-tree interval. The number of trees in the model yielding the best performance was taken and implemented in the final model run. Performance of the model was measured with the R-Squared ( $R^2$ ) as the proportion of variance in the target variable that can be explained by the predictors.

We used cross-validation to rank the importance of the driver variables. We estimated the importance of the driver variables as by the decrease in the model performance (as the  $R^2$ ) if the values of a variable are randomly permuted. This has the effect of removing all the predictive power for that driver variable. The accuracy is computed from the out-of-bag data (test subset). We cross-validated the importance scores (performance decrease) on both different numbers of decision trees (optimal number  $\pm 50$  in a 10-tree interval) and on 10 different random splits of the dataset (10x10-fold cross-validation). The mean absolute decrease of the model performance as the  $R^2$  was taken as measure of the importance of each driver variable (see Figure 6.6 b).

## 6.3 Results

### 6.3.1 The role of the Eastern European carbon sink

By comparing estimations of land-based carbon uptake from different data sources – satellite-based biomass change, CO<sub>2</sub> inversions, land use emission models, and inventories (see Figure 6.1) – we find that Eastern Europe holds the largest share ( $\sim 80\%$ ) of the total European carbon sink based on all data streams (see Figure 6.2). According to L-VOD-based above-ground biomass (AGB) estimates, the annual carbon uptake of the Eastern European region is  $\sim 0.45 \text{ Gt C a}^{-1}$  during 2010-2019 – around three times as much as taken up by Northern, Western and Southern Europe together. AGB estimates from WRI indicate a land carbon sink of  $\sim 0.36 \text{ Gt C a}^{-1}$ . Considering only the areas of annual carbon increase (gross carbon sink), we obtain a JPL-derived carbon sink of  $\sim 0.32 \text{ Gt C a}^{-1}$  (see Table 6.2). This is in line with the carbon sink estimated from inversions (SURF, GOSAT, OCO2), ranging from  $\sim 0.32$  to  $\sim 0.52 \text{ Gt C a}^{-1}$  and suggests that most of the net carbon sink from inversion lies in an increasing AGB. Based on UNFCCC reports, we note a significantly smaller mean carbon sink from national inventories of the land use, land use change and forestry (LULUCF) sector ( $\sim 0.20 \text{ Gt C a}^{-1}$ ) compared to the inversion- and L VOD-based biomass carbon increase. In addition, the LULUCF sink of Eastern Europe is ten times larger than the net sink caused by land use change alone as indicated from the land use emission model BLUE ( $\sim 0.02 \text{ Gt C a}^{-1}$ ). The gross carbon increase caused by land use change (agricultural abandonment) in BLUE, however, adds up to  $\sim 0.11 \text{ Gt C a}^{-1}$ , around half of the reported carbon sink from LULUCF in Eastern Europe (see Figure 6.2).

Overall, the deviations between the carbon sink estimates from different data streams can be explained by four aspects. First, the datasets differ in terms of methodology and incorporate different definitions (e.g. regarding land cover), cover different carbon components (soil organic carbon, above-ground or total vegetation biomass) and different conceptual constraints (top-down vs. bottom-up) (Petrescu et al., 2021; Pongratz et al., 2021). Second, deviating time periods lead to discrepancies due to high inter-annual variability of net carbon fluxes. Third, the models are tailored to different drivers of carbon change such as altering climate and environmental factors, land use, or land management. Fourth, whether focus is laid on calculating gross or only net fluxes, can cause major deviations, as shown in BLUE (see Figure 6.2). Taking into account observation-based datasets, JPL and WRI gross and L-VOD-based estimates, we find that the overall AGB carbon sink of Eastern Europe is on average  $\sim 0.38 \text{ Gt C a}^{-1}$  ( $\pm 0.07 \text{ Gt C a}^{-1}$ ). From this, LULUCF contributes with  $\sim 53\%$  and land use change with  $\sim 29\%$  (when gross carbon sink estimates are considered).

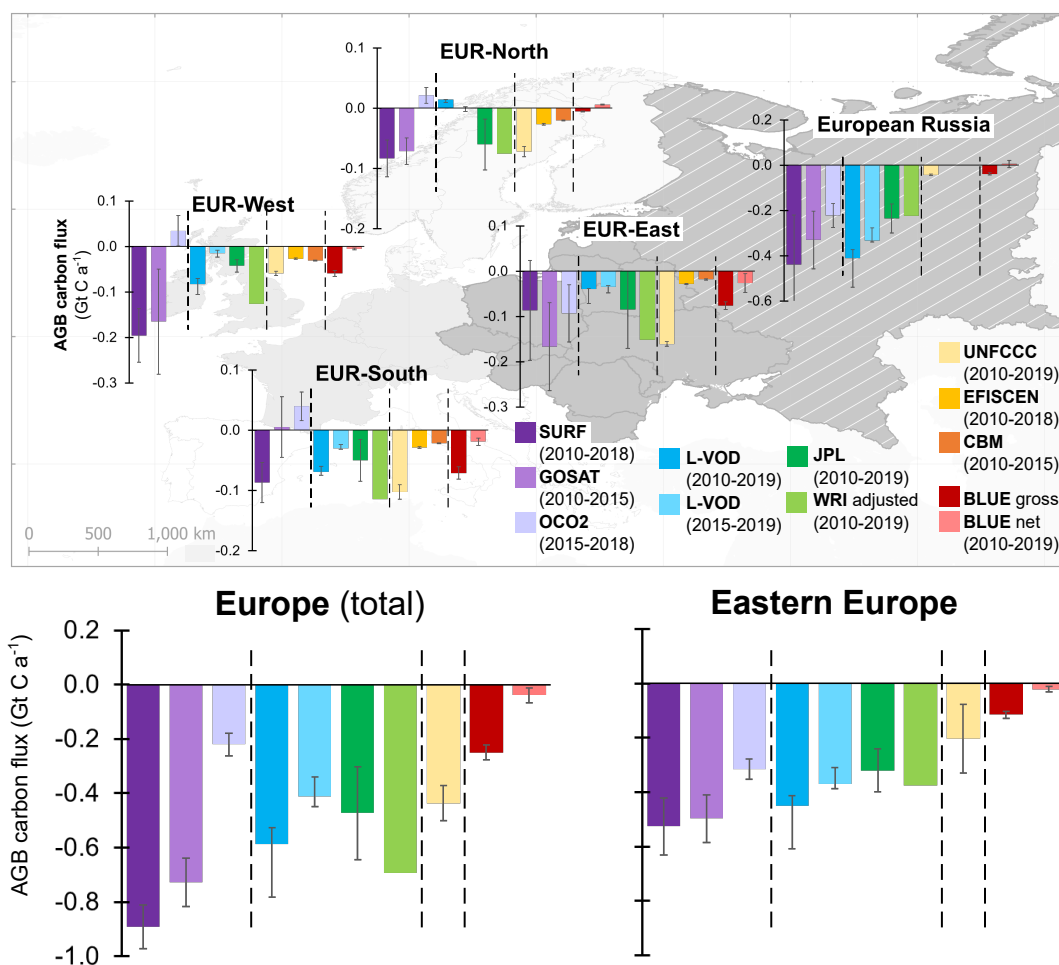


**Figure 6.2:** Average land carbon flux (in  $\text{Gt C a}^{-1}$ ) from inversions (SURF, GOSAT, OCO2), AGB sink estimates (L-VOD, JPL\*\*, WRI\*\*), forest ecosystem models and inventories (EFISCEN, CBM, UNFCCC) and land use bookkeeping model BLUE for different regions in Europe between 2010 and 2019. Negative values represent a land carbon sink, positive values a land carbon source. Eastern Europe comprises EUR-East and European Russia. Error bars display the standard deviations of the estimates. \*\* refers to gross carbon sink estimates.

### 6.3.2 Decline of the Eastern European carbon sink

We find that the land-based carbon uptake in Eastern Europe declined over the period of 2010-2019. Mean annual carbon uptake from L-VOD is almost 20 % lower in 2015-2019 ( $\sim 0.37 \text{ Gt C a}^{-1}$ ), compared to 2010-2019 ( $\sim 0.46 \text{ Gt C a}^{-1}$ ). This declining trend is also indicated from satellite inversions. The OCO-2 inversion, which refers to the period 2015-2019, shows a significantly lower carbon sink ( $\sim 0.32 \text{ Gt C a}^{-1}$ ) than SURF and GOSAT inversions ( $\sim 0.51 \text{ Gt C a}^{-1}$ ), which cover the periods 2010-2018 and 2010-2015, respectively.

According to UNFCCC annual reports of Eastern Europe (see Figure 6.3), Russia, Belarus,

**Table 6.2:** Average land carbon flux (in  $\text{Gt C a}^{-1}$ ) from different datasets (see Figure 6.2) for European regions.

Data Period	<b>SURF</b> 2010-18	<b>GOSAT</b> 2010-15	<b>OCO2</b> 2015-18	<b>L-VOD</b> 2010-19	<b>JPL**</b> 2010-19	<b>WRI**</b> 2010-19	<b>UNFCCC</b> 2010-19	<b>BLUE<sup>°</sup> **</b> 2010-2019
North	-0.28	-0.07	0.02	0.02	-0.06	-0.08	-0.07	-0.01
West	-0.20	-0.17	0.04	-0.08	-0.04	-0.13	-0.06	-0.06
South	-0.09	0.01	0.04	-0.07	-0.05	-0.11	-0.10	-0.07
East	-0.09	-0.17	-0.09	-0.04	-0.09	-0.15	-0.16	-0.08
Russia	-0.44	-0.33	-0.22	-0.41	-0.24	-0.22	-0.04	-0.04
EE	-0.53	-0.50	-0.32	-0.45	-0.32	-0.38	-0.20	-0.11
<i>EE share</i>	<i>59%</i>	<i>68%</i>	<i>143%</i>	<i>77%</i>	<i>68%</i>	<i>54%</i>	<i>47%</i>	<i>46%</i>
Europe	-0.89	-0.73	-0.22	-0.59	-0.47	-0.69	-0.44	-0.25

<sup>°</sup> includes not only AGB, but also below-ground biomass (BGB) and soil organic carbon (SOC).

\*\* refers to gross carbon sink estimates.

and Poland are the biggest contributors to the land carbon sink. Overall, the annual land carbon sink from the LULUCF sector has decreased during the last decade (-52% decrease relative to 2010). The highest rates of decrease can be found in Czechia (-283%), Ukraine (-100%), and Poland (-65%). Czechia even turned from a net carbon sink to a net source in the last five years.

A declining trend can also be found in the net carbon flux from land use change, as derived from the BLUE model. The Eastern European net carbon sink from land use change decreased by  $\sim 92\%$  ( $\sim 34 \text{ Mt C}$ ) during 2010-2019. This includes increasing emissions from wood harvest (+47%) and agricultural expansion (+12%) as well as decreasing carbon sequestration from agricultural land abandonment (-11%). This suggests that changes in land use and management have substantially contributed to the decreasing AGB carbon sink in Eastern Europe during the last decade.

Our observations are consistent with other studies. Deng et al. (2022) compared global inversion models with UNFCCC inventories and found a decreasing land carbon sink in the EU-27 and UK (Deng et al., 2022). Early signs of a carbon sink saturations in European forests have been observed (Nabuurs et al., 2013). However, the declining trend of the Eastern European carbon sink was only evident until the early 2000s. In 2010, a significant negative anomaly of net primary productivity of forests in European Russia was observed due to the effects of a strong heatwave (Bastos et al., 2014). The drought of 2010 caused an enormous rise of forest fires in European Russia, a substantial source of carbon emissions (Schaphoff et al., 2016). In addition, an increasing rate of wood harvest and disturbances by forest fires have found to cause a decrease of the forest carbon sink in Russia since 2008 (Zamolodchikov et al., 2017). More frequent temperature extremes and days without precipitation have been linked to lower growing stock in forests of southern European Russia (Schepaschenko et al., 2021).

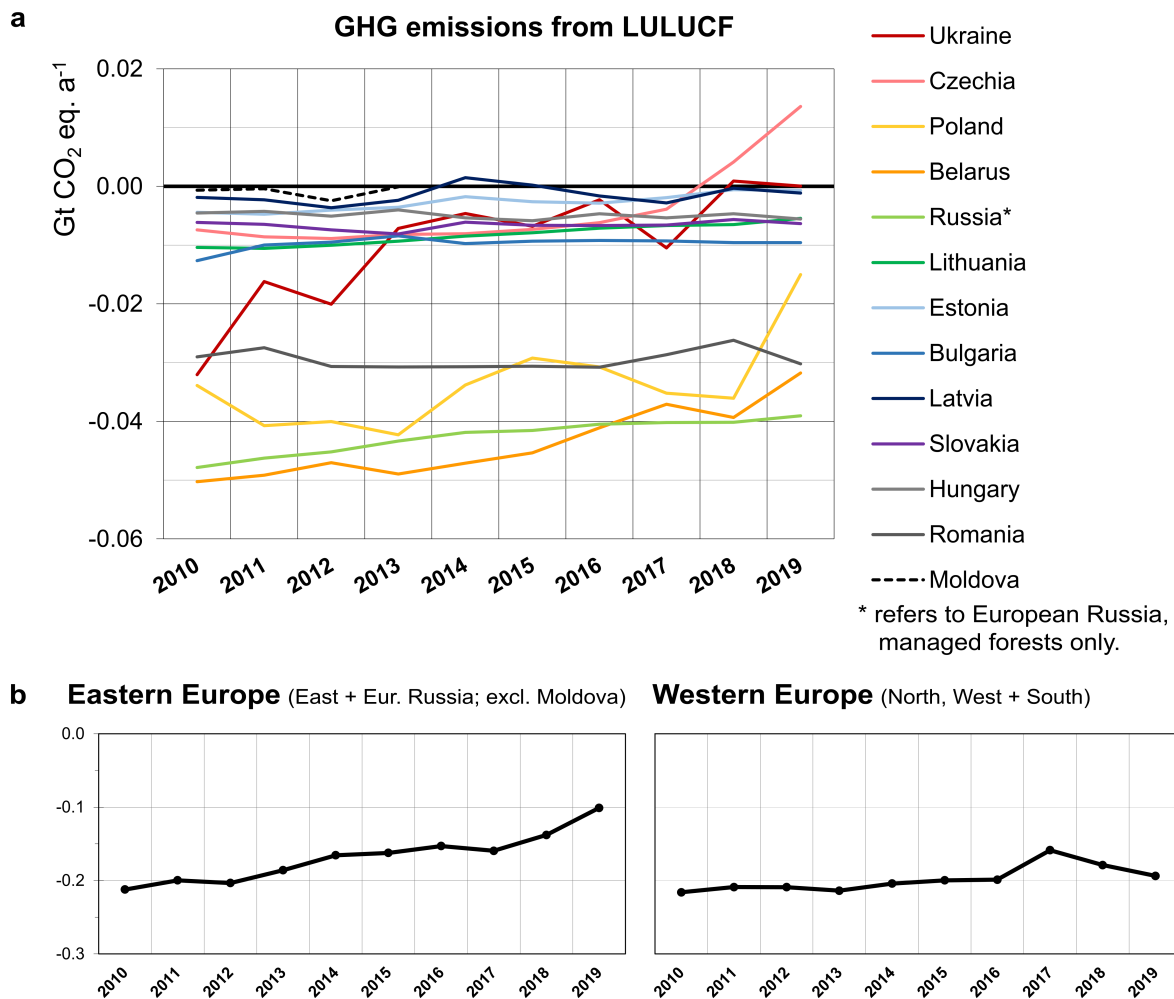


**Figure 6.3:** Annual greenhouse gas (GHG) emissions from land use, land use change and forestry a) by country in Eastern Europe during 2010-2019 b) for regions of Eastern and Western Europe from aggregated country data (UNFCCC). Negative values represent a land carbon sink, positive values represent a land carbon source. \*Values for European Russia contain carbon fluxes from forestry only (National Inventory Reports).

### 6.3.3 Spatial patterns of the Eastern European carbon sink

By comparing the spatial patterns of AGB carbon change in Eastern Europe from JPL (Xu et al., 2021), satellite L-VOD, and bias-adjusted WRI (Harris et al., 2021) (see Figure 6.4a), we find high agreement on a carbon sink along the Ural mountains, in the border between Belarus, Ukraine and Russia as well as on the Kola peninsula in north-western Russia (see Figure 6.4b). Considering both the level of agreement and the strength of the carbon sink from agreeing data sources (see Figure 6.4 b and c), we find that the southern Ural mountains and the border region of Russia, Belarus and Ukraine were hot spots of the Eastern European carbon uptake during 2010-2019. At the same

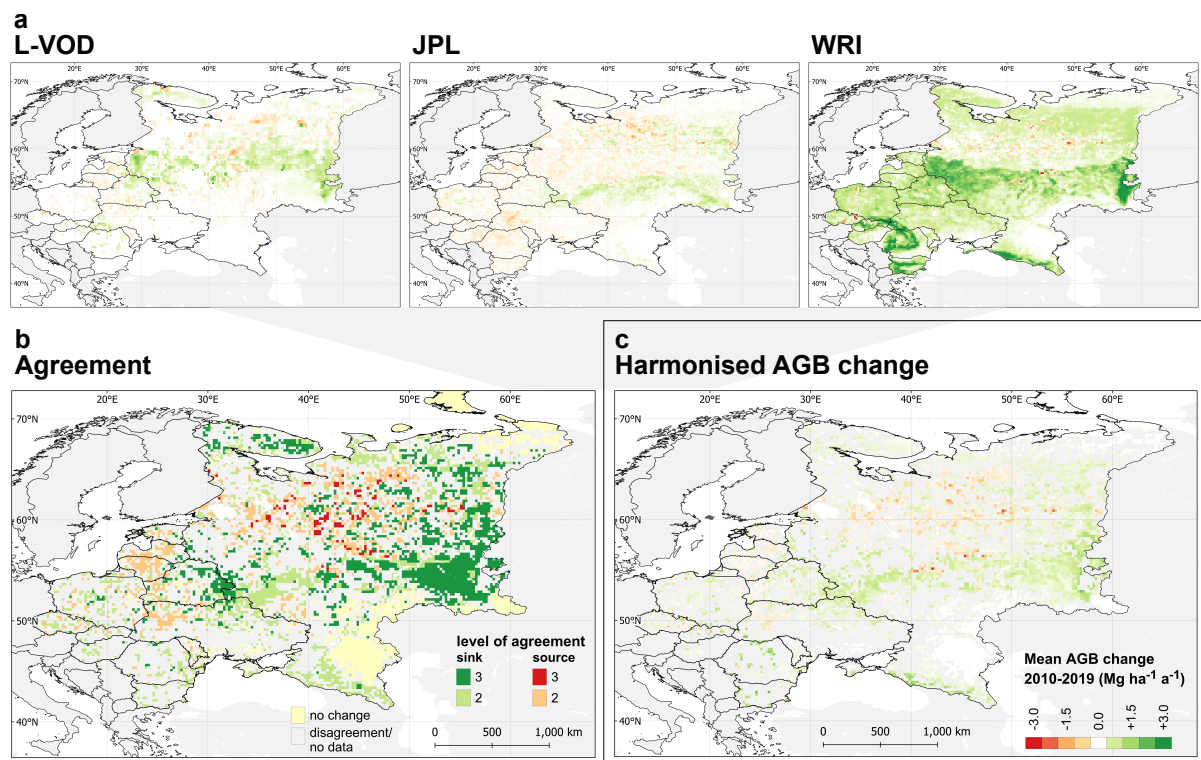


**Figure 6.4:** Spatial patterns of AGB change in Eastern Europe during 2010-2019. a) Individual datasets: L VOD, JPL, and bias-adjusted WRI. b) Data agreement on carbon gains (source) and losses (sink). Sources are defined by  $\Delta\text{AGB} < -0.05 \text{ MgC ha}_1\text{a}_1$ , sinks by  $\Delta\text{AGB} > 0.05 \text{ MgC ha}_1\text{a}_1$ . Levels of agreement represent the number of agreeing datasets. c) Harmonised mean AGB change from agreeing datasets. Areas of disagreement are displayed in grey.

time, scattered hot spots of carbon sources are located in central to northern European Russia, north of  $55^\circ\text{N}$ . Reuter et al. (2017) suggested the largest carbon sink area to be further north in European Russia, where we locate scattered carbon sources. However, their findings referred to a previous period and are therefore not directly comparable (Reuter et al., 2017). A recent satellite-based study on the carbon budget of the top five  $\text{CO}_2$  emitters shows that European Russia comprises a large carbon sink, whose location corresponds to the hot spot regions presented in this study (Jiang et al., 2022).

### 6.3.4 Underlying drivers of the Eastern European carbon uptake

Land-based carbon uptake and above-ground biomass changes are influenced on the one hand by land use change (the conversion of one land use class to another) and management changes (within one land use class), and by changes in environmental conditions on the other. To find out where exactly which factors have caused land carbon changes in Eastern Europe during recent years, we analysed the trends of individual possible drivers of AGB changes and compared them with the harmonised map of AGB change. As

possible land use and management drivers of AGB changes we consider land use-based carbon fluxes from BLUE (including agricultural expansion, wood harvest and agricultural land abandonment), forest harvest change and the fraction of cropland abandonment. Environmental and climate factors are changes in land surface temperature, precipitation, soil moisture, fires, atmospheric CO<sub>2</sub> concentration, and nitrogen deposition. The trends of all possible driving factors of AGB change in Eastern Europe during 2010-2019 are displayed in Figure 6.5.

By matching the trends of the driver indicators to AGB change, we find that land use change, in particular cropland abandonment and subsequent regrowth processes, coincide with the hot spot areas of the Eastern European carbon sink (see Figure 6.6a). The fraction of formerly abandoned land is high in the carbon sink hot spot region of the border between Russia, Belarus and Ukraine and in central European Russia. As very well explored by other studies, cropland abandonment has mainly occurred in the early 1990s after the fall of the Soviet Union (Schierhorn et al., 2013; Vuichard et al., 2008). Thus, abandoned lands have already sequestered considerable quantities of carbon before 2010. Nevertheless, carbon storage on formerly abandoned areas still plays a significant role for the Eastern European carbon budget and, in fact, is yet to happen as large parts of abandoned lands convert to full-grown forests (Kuemmerle et al., 2015). Based on this study, abandoned land is still a significant contributor to the Eastern European carbon uptake during 2010-2019 ( $\sim 0.11 \text{ Gt C a}^{-1}$  from BLUE), contributing about 1/3 to 1/5 to the net carbon exchange.

The decreasing trend of the carbon sink shown above from satellite records and land use inventories are partly explicable by the decreasing trend in the abandonment sink as observed from the BLUE model (see Figure 6.7). This may be attributable to a saturation of the effects of the carbon sequestration following land abandonment. A decrease of the carbon sequestration in soils from around 15 years after agricultural abandonment in Russia has been reported by several studies (Dolman et al., 2012; Kurganova et al., 2015; Wertebach et al., 2017). Further, as regrown forests on formerly abandoned land turn to a mature state of higher age classes, first signs of a saturation effect of the carbon accumulation – a decreased carbon absorption – has been registered (Nabuurs et al., 2013; Zamolodchikov et al., 2018, 2017). Under these circumstances, the carbon sink on abandoned areas is expected to further decrease in the future.

Interestingly, abandoned lands, although widely encroached by woody vegetation, often still have a legal designation for crop production and could be recultivated any time in the near future. A partial revival of agricultural production has occurred on abandoned areas in Russia during 2006-2009. And even after that, Russian government demonstrated a substantial willingness to support the recultivation of abandoned lands (e.g. by banning agricultural imports from the EU in 2014) (Meyfroidt et al., 2016).

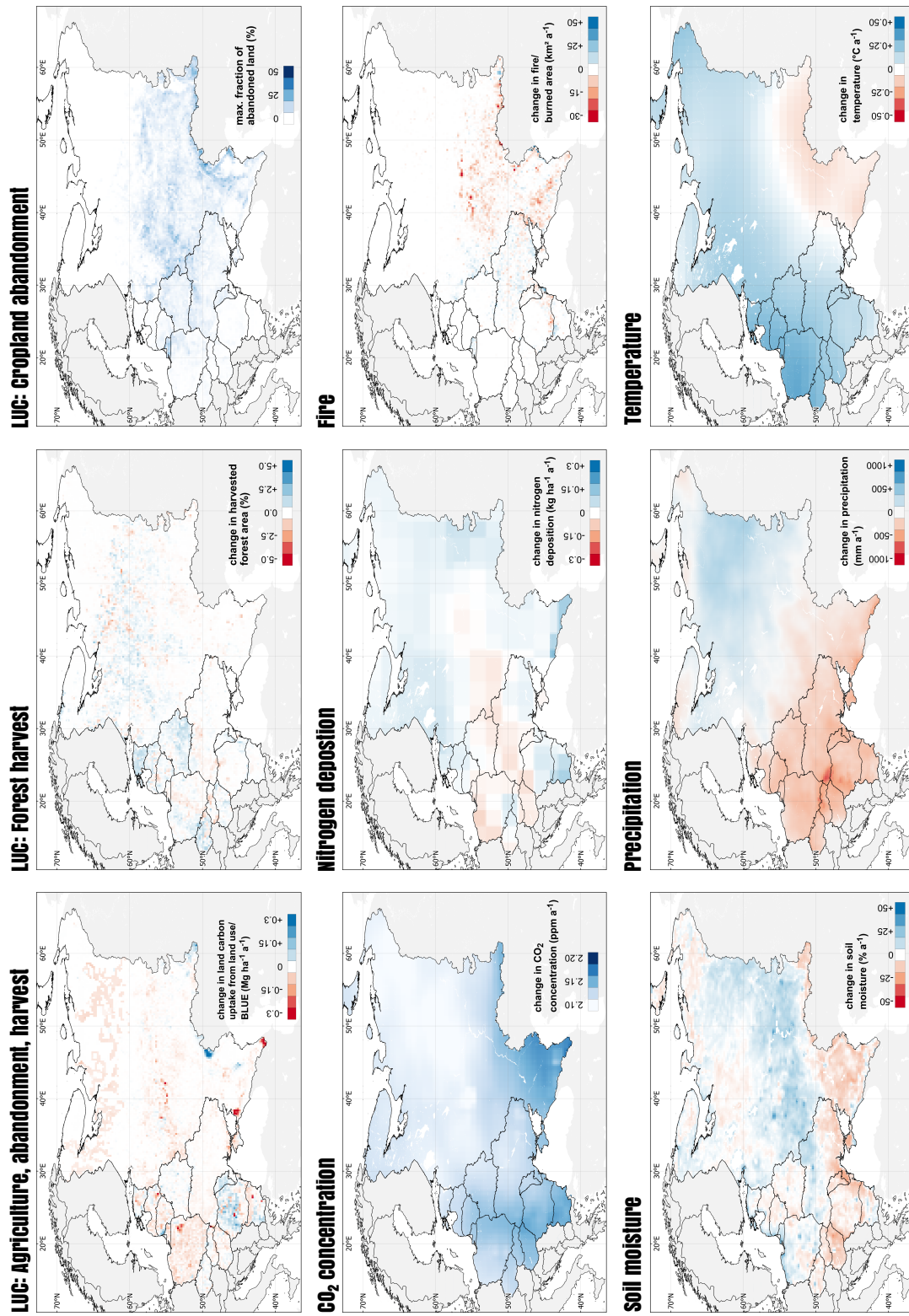
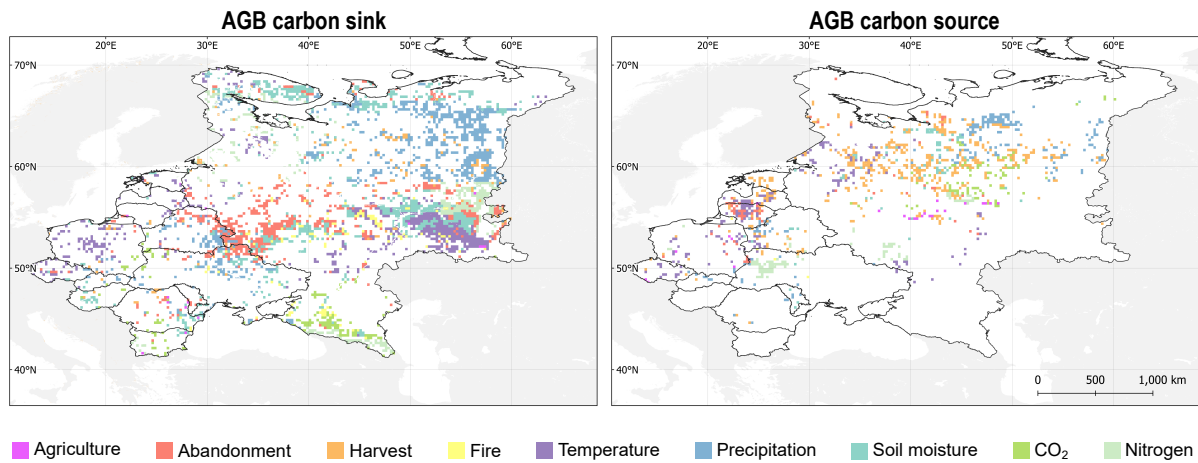


**Figure 6.5:** Spatial trends of possible underlying drivers and influencing factors of AGB carbon change in Eastern Europe during 2010–2019. Values are normalised to a mean value of 0 (except from cropland abandonment).

## a Trend pattern matching



## b Variable importance from random forest model

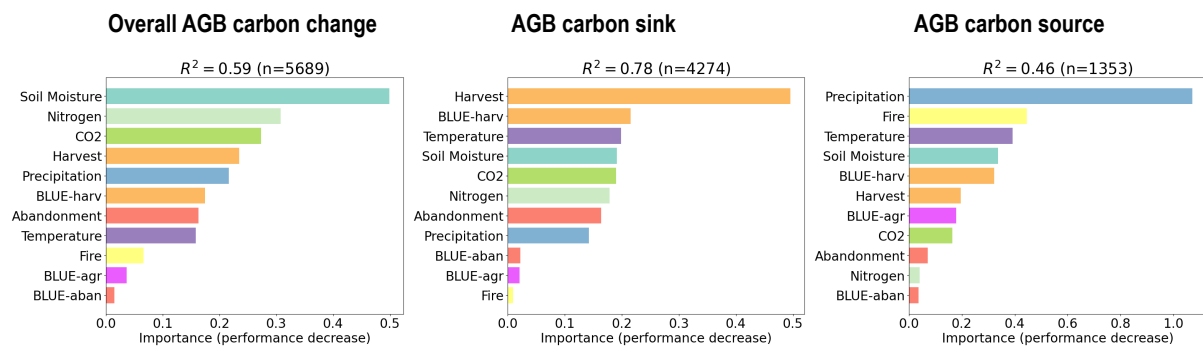


**Figure 6.6:** Possible drivers of AGB carbon change in Eastern Europe during 2010-2019. a) Trend pattern matching: Factors with the highest/lowest standardised trend during 2010-2019 were selected and classified as possible drivers. b) Random forest regression model: Relative feature importance for all areas with AGB carbon change, AGB sink and source areas.

The currently ongoing war between Russia and Ukraine, however, could lead to large-scale cropland abandonment, reduce the rate of recultivation and thus increase the carbon sink in areas of the conflict region. Such effects of conflicts on agricultural land use could already be observed during the Chechen wars in Russian north Caucasus (Yin et al., 2019). In contrast, the current rise in food prices and sanctions being placed on trade (Wegren, 2022) could urge the Russian government to boost domestic agricultural production and, thus, lead to massive recultivation of abandoned areas in Russia. This scenario would have a significant impact on the Eastern European carbon budget and would lead to a continuation of the declining trend of the land carbon sink in the near future.

The trend in the net carbon flux from land use change goes from a notable sink of  $0.04 \text{ Gt C a}^{-1}$  towards near neutral (see Figure 6.7). In BLUE, besides the declining car-

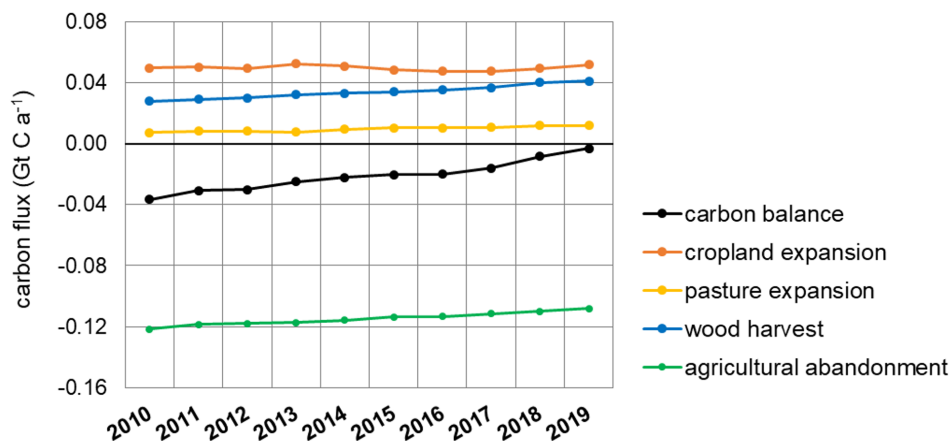


**Figure 6.7:** Annual net carbon flux from land use change (carbon balance), derived from the BLUE model using the HILDA+ land use forcing (Winkler et al., 2021), and its component fluxes from cropland and pasture change, wood harvest (net flux of release from product and slash decay and uptake by regrowth), and agricultural abandonment in Eastern Europe in 2010-2019. Negative values represent a carbon sink.

bon uptake from agricultural abandonment, an increase in the net emissions from forest harvest contributes to the overall decreasing trend. This underlines the importance of land management in addition to the often better investigated land-use-induced land cover changes and stresses the need for monitoring of land management in addition to land cover changes (Pongratz et al., 2017). Based on a random forest regression model, we find that forest management (harvest) is the most important anthropogenic cause of land carbon changes in European Russia during 2010-2019 (see Figure 6.6b). A growing harvest rate in European Russia and Baltic countries has also been noted by other studies (Ceccherini et al., 2020; Potapov et al., 2015). UNFCCC data shows that carbon losses (net carbon sources) due to clear-cutting in forests of European Russia have increased by around 34 % (from 16.0 to 21.5 Mt C a<sup>-1</sup>, see Figure 6.8).

Not only increasing carbon losses due to felling and rising logging volumes in European Russia in particular in Volga and north-western districts, have led to a decreasing carbon sink. Also, the changing age structure in the forest stands after 2008 (older stands) has decreased the carbon sink due to reduced carbon absorption (Zamolodchikov et al., 2018).

Our findings suggest that the rising rates of wood harvest, together with saturation effect from agricultural abandonment, have been the main driver for the declining carbon sink in Eastern Europe during 2010-2019. The biomass loss due to wood harvest, however, might be compensated by the enhanced carbon absorption of young deciduous (or mixed-species) forest after wood harvest compared to former mature coniferous forest. This stand replacement associated with wood harvest can not only lead to an increased

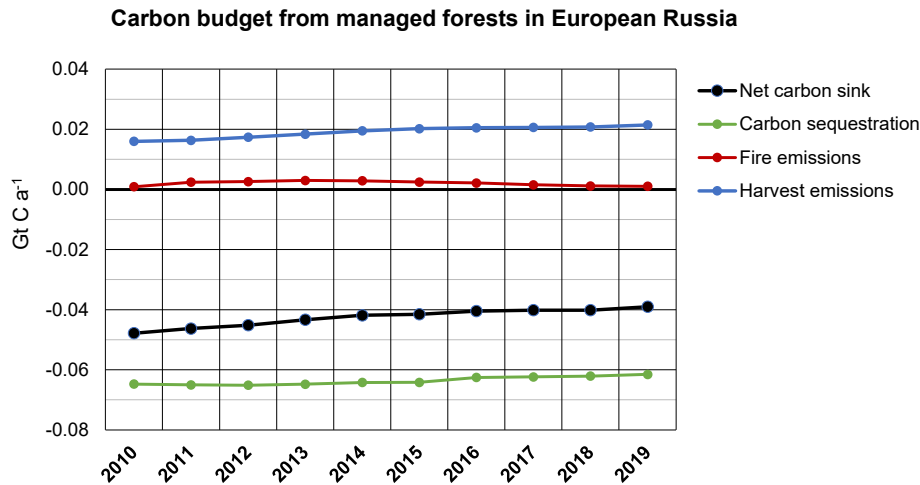


**Figure 6.8:** Carbon budget from managed forests in European Russia and its components: Emissions from wood harvest and fire; carbon sequestration (based on Russian National Inventory Reports, UNFCCC).

carbon sequestration rate, it goes along with a reduction of fire risk and albedo and could have further consequences on the energy balance (Duveiller et al., 2018) and cloud cover (Duveiller et al., 2021).

The relatively small fraction of the carbon sink explained by land use (agricultural abandonment) and management change (wood harvest) implies that other factors such as environmental changes are more dominant drivers on regional level. This is consistent with other large-scale studies on attributing the carbon sink in Europe (Bellassen et al., 2011). Environmental factors such as soil moisture, precipitation, nitrogen deposition and CO<sub>2</sub> concentration influence the carbon sink, especially in northern European Russia and along the Ural mountains. The results from the driver analysis based on a random forest regression model highlight the importance of these environmental drivers (see Figure 6.6). We find that soil moisture is identified as indicator of high importance for explaining the AGB carbon change in Eastern Europe (see Figure 6.6 b). In accordance with this, it has been shown that soil moisture variability and trends largely influences the global terrestrial carbon sink (Green et al., 2019; Humphrey et al., 2021). At the same time, an increase in agricultural inputs – cropland intensification in Ukraine, and southern Russia – has affected the land-based carbon balance in terms of an increased nitrogen deposition, which in turn stimulates vegetation productivity (Tharammal et al., 2019). However, increased CO<sub>2</sub> concentrations have explained the rising global terrestrial carbon sink during the last three decades to a much higher extent than increased nitrogen deposition (Tageson et al., 2020). The effect of CO<sub>2</sub> fertilisation – enhanced vegetation productivity due to increased CO<sub>2</sub> concentration – is well described as an important negative feedback on climate warming (Schimel et al., 2015). Recently, a global decline in the CO<sub>2</sub> fertilisation

effect has been discovered, mainly affecting European forests (Wang et al., 2020). The currently ongoing decrease in nitrogen deposition may still contribute to the saturation of the Eastern European forest carbon sink (Nabuurs et al., 2013).

The overall climate effect on the Eastern European carbon uptake is ambiguous. Warmer and wetter conditions due to climate change in Russian boreal forests favour forest growth in the North, whereas an increasing influence of precipitation anomalies (especially drought conditions) in southern agricultural areas, which act as a carbon source, contributes to the declining trend of the carbon sink. Future climate change projections show an ongoing decrease of precipitation in southern European Russia (European Forest Institute, 2020).

What is more, climate change and accompanied extreme events have led to a substantial increase in forest fires and other forest disturbances. The frequency of extreme events and hydrological hazards amplified nearly three-fold in Russian forests during 2000-2018 (European Forest Institute, 2020). In this context, extensive drying out of forests as well as insect outbreaks have been registered in the North-East of the region and are likely to increase in the future (Shvidenko & Schepaschenko, 2013). Forest fires have been listed as second largest contributor of the declining carbon sink of Russian forests after wood harvest (Zamolodchikov et al., 2017). Findings of our random forest-based driver analysis support the strong importance of precipitation and fires for Eastern European carbon source areas. In recent years (2018-2020), exceptionally high level of disturbances have been registered and are expected to cause a significant decrease of the Russian forest carbon sink (European Forest Institute, 2020).

An adapted forest management with a reliable monitoring system as well as more effective forest protection under future disturbance regimes are highly needed. A stable and large carbon sink of Eastern European forests is essential for the European attempt to achieve net zero emissions in the future.





# Chapter 7

## Synthesis

*Change will not come if we wait for some other person or some other time. We are the ones we've been waiting for. We are the change that we seek.*

Barack Obama

## 7.1 Data-driven reconstruction of global land use change

This thesis presents a **data-driven** approach for reconstructing the global land use change of the past six decades (1960-2019/1960-2020). Central aspects are both the use of freely available data sources from remote sensing and statistics and the subsequent publication of the resulting maps as open data. The global land use reconstruction model HILDA+ (Historic Land Dynamics Assessment+), which was developed and analysed in this thesis, uses the synergies of heterogeneous data streams from multiple sources by harmonising this information consistently. Unlike other land use reconstructions, HILDA+ is purely based on empirical data and avoids assumptions about the distribution of land use changes on the global grid. HILDA+ land use/cover maps are published as open data (openly accessible, exploitable, editable and shared by anyone for any purpose) on a public data repository (Winkler et al., 2020) along with an interactive map viewer showing the results (<https://landchangestories.org/hildaplus-mapviewer/>). Further improvements and updated versions of the HILDA+ dataset (with e.g. extended time period or integration of new datasets) are in preparation and will be published in the same repository.

With the **reconstruction** of global land use change, this thesis provides a retrospective view on the human influences on the land surface from 1960 to 2019/2020. Land use reconstructions are an essential input variable for climate and Earth system models in order to better understand the interaction between humans and the environment and to assess potential future land use pathways. So far, humans and their interactions with the land system are underrepresented in those models, as land use data often originates from only a single source and does not provide sufficient level of detail to encompass land use changes in its full dynamics. In this thesis, a backward-looking, iterative procedure is applied to allocate land use changes on the global land surface on an annual basis. This procedure is guided by temporally and spatially explicit input data from both remote sensing and statistical inventories. It is important to note that such a reconstruction is also a model and, thus, does not claim to match reality on all scales but to come closer to it through the use of empirical data.

**Global land use change** is the core theme of this thesis. We aimed at a global-scale analysis of land use changes, because, on the one hand, land use dynamics differ by world region and, yet, are spatio-temporally interlinked. On the other hand, we aimed to meet the research needs of the global Earth system modelling community. We hypothesized that, only through globally consistent data with sufficient spatial, temporal and thematic resolution, land use changes could be comprehensively captured and represented in Earth system models. A higher level of detail in all dimensions (space, time and theme) was the prerequisite for studying the spatio-temporal dynamics, the underlying drivers and the environmental impacts of global land use change in the course of this thesis.

## 7.2 Main findings

In the following, we discuss the main findings of this thesis on the subject of the three central research questions.

### **A. What can synergistically and consistently combined open data reveal about the spatio-temporal dynamics of global land use change over the past six decades?**

This thesis provides comprehensive findings on the spatio-temporal dynamics of global land use change in the past six decades. Chapter 2, 3 and 4 focus on the dynamics of global use change. All findings were based on the data-driven land use reconstruction HILDA+, which was developed and updated in the course of this thesis.

Chapter 2 studies global land use dynamics by synergistically combining multiple open data streams (remote sensing, reconstructions and statistics) to create the first version of HILDA+ at a spatial resolution of 1km, a temporal resolution of yearly time steps, and a temporal coverage of six decades (1960-2019). With this, we estimated that land use changes have affected almost a third (32%) of the global land surface. Compared to previous land use reconstructions, land use change is around four times greater in extent. Further, we identified geographically diverging land use change processes, with afforestation and cropland abandonment in the Global North versus deforestation and agricultural expansion in the Global South. By analysing the temporal evolution of global land use change, we observed a transition from accelerating to decelerating land use change, mainly caused by a decrease of agricultural expansion in the Global South after 2005. This decrease in agricultural expansion was likely related to the economic crisis, trade in commodities and land.

Chapter 3 illuminated the spatio-temporal patterns of global changes in agriculture - particularly expansion, abandonment, intensification and extensification of croplands and pasture/rangelands - during six decades (1960-2020). For this, an updated version of HILDA+ (with extended time series, more input data and improved cropland categories) was presented and analysed. Furthermore, the relation of agricultural intensification and expansion was explored for all countries across the globe. We found that high-income countries pursued an intensification-abandonment trajectory in croplands and pasture/rangelands, whereas low-income countries intensified less but substantially increased their agricultural area over time. Strikingly, middle-income countries showed both large cropland expansion and high rates of intensification. These findings indicate the occurrence of a so-called rebound effect, which implies that the intensification of high-profit crops, such as oil palm or soy bean, stimulated further agricultural expansion in emerging middle-income countries. This led to a large expansion of tree crops (e.g. oil palm, rubber, cocoa) which were found to be the underlying cause of more than half of

the global deforestation in the past six decades.

Chapter 4 analysed the global land use transitions from 1960 to 2019 based on the first version of HILDA+. We found that agricultural expansion accounted for the largest share of global land use change ( 7.6 million km<sub>2</sub>), which is an area as large as Greece every year. Notably, the global expansion of agriculture into non-forested areas was over three times greater than expansion into forests in that period. Agricultural expansion was the major land use transition in the Global South with strong links to globalised markets. Conversely, agricultural abandonment, forest expansion and intensive forestry dominated in the Global North, driven by economic growth, production and political factors. This supports the hypothesis that forest expansion in the Global North goes along with the displacement of land use, especially deforestation and agricultural expansion, to the Global South.

All three chapters demonstrated that a combination of multiple heterogeneous open data sets is able to reveal the dynamics of global land use changes with an unprecedented level of detail. Further, they conclude that the spatio-temporal dynamics of global land use change includes geographically diverging patterns, which are temporally related to each other.

### **A.1 The spatial dimension of global land use change**

Overall, this thesis reveals unprecedented details about the spatial extent of global land use change. We find evidence to support our hypothesis of a more detailed assessment of global land change dynamics through the synergistic and consistent combination of multiple open data streams compared to previous studies for two reasons. First, the HILDA+ land change model includes gross changes both in their spatial and temporal dimension. Second, the integration of high-resolution remote sensing products facilitated a reconstruction of land use change at higher spatial resolution (1 km) than previous global land use reconstructions (up to 0.25° or around 30 km). By including high-resolution gross changes in the calculation of the magnitude of land use change, we found that almost a third (32%) of the global land surface was subject to land use conversion during just six decades (Chapter 4). The comparison of the change rates with those from previous land use reconstructions (Hurtt et al., 2020; Klein Goldewijk et al., 2017; Ramankutty & Foley, 1999) demonstrated that the area affected by global land use change was around four times greater than previously assumed. The comparison of HILDA+ with long-term remote sensing products (ESA CCI, MODIS or the GFC global forest change) revealed that the extent of land use change matched the average value from these data. However, deviations between remote sensing products were substantial.

Whereas global forest areas have overall declined, agricultural areas – cropland as well as pasture/rangeland - have increased over time (Chapter 2). The expansion of agriculture denotes the largest land use transition during the past six decades (Chapter 2 and 4). Re-

markably, about one third of the cropland expansion caused deforestation, with more than half attributable to the spread of tree crops such as cocoa, coffee or oil palm (Chapter 3). Though, only around 22% of the global agricultural expansion encompasses deforestation. Globally, agricultural expansion at the expense of non-forested areas was over three times larger than deforestation for agriculture. The bulk of this area is the expansion of pasture/rangelands (Chapter 4). The observed spatial patterns of global land use change were shown to be in line with land use inventories (FAO, 2022a, 2019), statistics of agricultural production (FAO, 2020) as well as numerous regional studies (Chapter 2, 3 and 4).

### **A.2 The temporal dimension of global land use change**

Furthermore, this thesis gives new insights into the temporal dynamics of global land use change. We found that land use has not changed continuously over the past six decades. Strikingly, a long phase of accelerating land use change ( $\sim 1960$ -2005) was followed by a recent period of decelerating land use change ( $\sim 2006$ -2019). The slow-down of land use change was mainly due to a decrease of agricultural expansion in the Global South (Chapter 2 and 4). While agricultural and forest expansion slowed down, forestry dynamics and forest conversions to shrubland increased their speed in recent decades (Chapter 4). By extending the input database and providing more information on agricultural sub-categories (Chapter 3), we found that a major part of these transitions from forest to shrubland was in fact related to deforestation for oil palms.

The increased detail in the land use data allowed land use changes to be studied with such high temporal frequency for the first time. It even enabled linking land use transitions to socio-economically or politically disruptive events (e.g. collapse of the Soviet Union in 1990, trade embargoes, E.U. agricultural policy reforms or the global financial crisis in 2007-2009), but also to climatic extremes (e.g. severe droughts in East Africa in 2010/2011).

We also identified temporal shifts between different land use transitions during the past six decades. For instance, we found a shift from accelerating to decelerating expansion of pasture/rangeland followed by a speeding up of cropland expansion in Africa, a transition from increasing to decreasing rates of pasture/rangeland expansion in China as well as a trend from deforestation for agricultural expansion to increasing forest conversion to shrubland in South America and Africa (Chapter 4).

### **A.3 Spatio-temporal interlinkage of global land use change**

Moreover, this thesis finds that the spatio-temporal dynamics of global land use change during the past six decades differ geographically. We noted strong differences between higher-income countries of the Global North and lower-income countries of the Global South (Chapter 2, 3 and 4). While high-frequency land use transitions with multiple change events were mainly located in the Global North, single-change events predomi-

nantly occurred in tropical regions of the Global South (Figure 2.5 in Chapter 2). While forests expanded due to cropland abandonment, afforestation or climate effects in the Global North, large-scale deforestation or forest degradation due to agricultural expansion prevail in the Global South (see Figure 2.6 in Chapter 2 and Figure 4.3 in Chapter 4). While high-income countries of the Global North pursued a trajectory of agricultural intensification along with area abandonment, low-income countries of the Global South show lower intensification but substantial agricultural expansion over the past six decades (Chapter 3).

However, the regionally divergent patterns do not stand alone but are related to a certain degree. Our findings suggest that forest expansion in the Global North displaces land use, particularly deforestation and agricultural expansion, to the Global South (Chapter 4). Such global land use displacements are widely recognised and discussed in research (Meyfroidt et al., 2020; Weinzettel et al., 2013). We also observed spatio-temporal shifts of land use transitions, that is, the displacement of agricultural expansion (including deforestation) from South America to Africa since the late 1980s (Chapter 4).

Additionally, this thesis addresses another correlation, which is inherent in global land use change: the links between intensification and expansion in agriculture. Again, we recognise large North-South disparities. Whereas the land-sparing concept (intensification that leads to decreasing expansion; Meyfroidt et al., 2018) may apply for high-income countries of the Global North, our findings suggest that it is rebutted in the low- to middle-income, emerging countries of the Global South. There, market-driven intensification of high-profit crops like soybean, oil palm and sugar cane encouraged large-scale cropland expansion (Dias et al., 2016; Spera et al., 2020; Varkkey et al., 2018), which fits the concept of the rebound effect (intensification that leads to increasing expansion; Meyfroidt et al., 2018). Pasture/rangeland dynamics in emerging countries indicate that intensification was pursued when demand for products increased but land for further expansion became scarce. This matches the concept of induced intensification (first expansion then intensification due to scarce land and high land prices; García et al., 2020).

#### **A.4 The thematic depth of global land use change**

This thesis demonstrates how the integration of open data leads to an increasing thematic depth of global land use change assessments. In the course of the thesis, two versions of the HILDA+ global land use reconstructions were developed. HILDA+ version 1.0 (see Chapter 2, 4, 5 and 6) comprises six major land use/cover categories: urban, cropland, pasture/rangeland, forest (with subclasses), unmanaged shrub/grassland, no/sparse vegetation (published as Winkler et al., 2020). As a follow-up, HILDA+ version 2.0 provides more details regarding agricultural land use by including the following additional land use categories: annual crops, tree crops and agroforestry (publication in preparation; see Chapter 3). The effect of the higher thematic detail in HILDA+ version 2.0 can be ob-

served in the case of tropical deforestation in Indonesia (see Figure 7.1). While deforestation areas were mainly classified as transitions from forest to grass/shrubland in HILDA+ version 1.0 (Figure 7.1 a), the same areas were found to comprise tree crops rather than grass/shrubs in HILDA+ version 2.0 (Figure 7.1 b). Maps of HILDA+ version 1.0 show misclassifications that are typical to remote sensing data, as tree crops are commonly confused with shrubs or forest due to similar land cover characteristics. Such misclassifications led to the delineation of large-scale transitions from forest to grass/shrubland in Indonesia, which are in fact transitions from forest to tree crops (see Chapter 4 and 3).

Overall, the improvements in thematic depth, that is, the implementation of more detailed land use categories due to an integration of recent, high-resolution data sets, entails more insights into and, hence, a better understanding of global land use change processes.

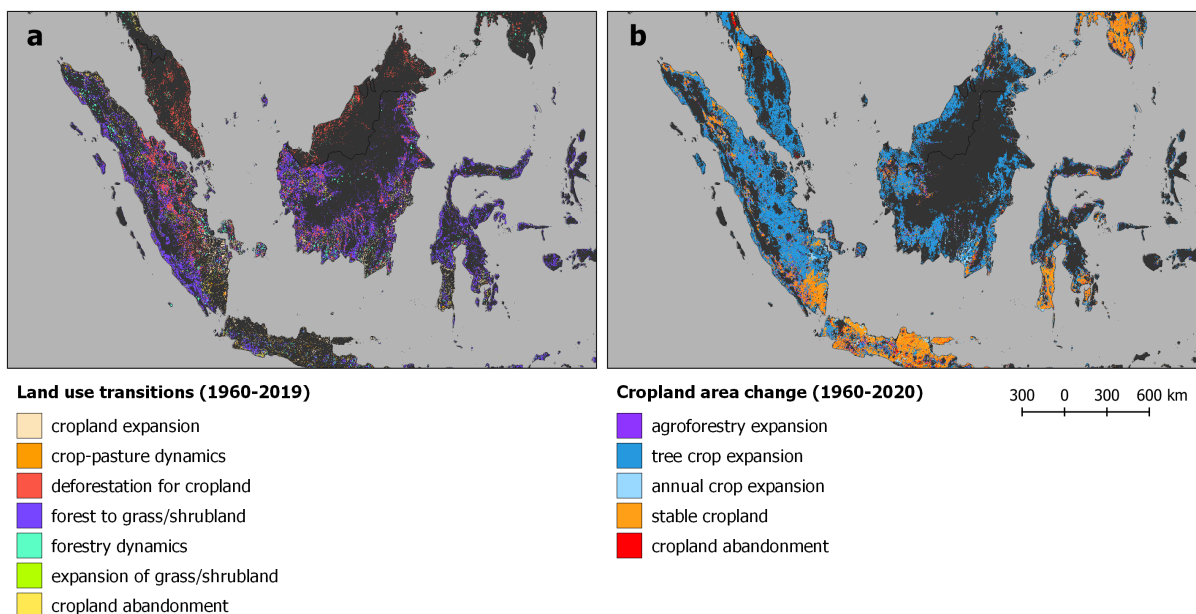


**Figure 7.1:** Land use change in Indonesia over six decades: a) Land use transitions as derived from HILDA+ version 1.0 related to cropland, forest and grass/shrubland (see Chapter 4), b) Cropland area change as derived from HILDA+ version 2.0 related to croplands as annual crops, tree crops, and agroforestry (see Chapter 3).

## **B. What were the main drivers of global land use transitions in the past six decades?**

This thesis provides new insights into the underlying drivers of global land use change. The drivers of global land use transitions were suggestively discussed in Chapter 2 and 3 and explored in more detail in Chapter 4 of this thesis.

In Chapter 2, the effects of economic crises, trade of commodities and of land were discussed as drivers for agricultural expansion in the Global South. Findings from Chapter 3 suggest that the relationship of agricultural intensification and expansion was affected by varying degrees of political intervention, global trade, technology transfer and climate change. Chapter 4 offers a comprehensive, explorative analysis of the causal relations between land use transitions and their drivers at the global scale. Our findings underline the dominating role of humans, particularly, the importance of economic drivers and the (as yet) small influence of environmental factors on global land use transitions in comparison to that. Economic development is suggested as a significant driver of global land use change. This underscores that acting on socio-economic systems is crucial when defining and implementing sustainable, climate-adapted land use policies.

Overall, this thesis highlights that the spatio-temporal dynamics of global land use change are interlinked through a complex interplay of socio-economic and environmental drivers acting at different scales.

Economic factors were found to be the most land-intensive drivers of land use change. Strikingly, we once more identified geographically differing patterns between the Global North and the Global South by mapping major drivers of land use transitions. Gross domestic product and wage dominated as indirect economic drivers for land use transitions in the Global North, mainly linked to cropland abandonment, crop-pasture dynamics and forest expansion, whereas, in the Global South, major economic drivers relate to global markets and trade (agricultural exports, exchange rate, global oil price). Our findings emphasise the importance of, on the one hand, economic growth for land use dynamics in the Global North, and on the other hand, global markets for the agricultural sector in the Global South. This supports the forest transition theory (from long-term decrease to increase of forest area; Barbier et al., 2017). The findings also suggest that globalisation displaces land use, particularly deforestation, from the Global North to the Global South (Pendrill et al., 2019).

Furthermore, political factors showed the strongest correlations to overall land use transitions. They affected large areas of cropland expansion but also cropland abandonment (conflicts) as well as transitions from forest to shrub/grassland (nature protection policies) and expansion of sparse/no vegetation (military expenses). We also found that political indicators have a larger importance in the Global South than in the North, except from subsidies and nature protection policies, which were identified as drivers of forest expansion and cropland abandonment in Europe. The importance of political and institutional

factors for land use dynamics was underpinned by numerous regional studies focussing on the role of political instability, conflicts as well as institutional disruptions (Ebanyat et al., 2010; Landholm et al., 2019; Yan et al., 2020).

In addition, population dynamics were revealed as another major global driver of land use change. Particularly in the Global South, demographic factors showed high correlations with urban spread, agricultural expansion and forest loss. The importance of population dynamics for global land use evolution is a well-known concept that is included in many land use reconstruction models (Kaplan et al., 2010; Klein Goldewijk et al., 2017; Pongratz et al., 2008). However, our findings suggest that population dynamics are rather channelled through economy and politics, which generally showed stronger links to global land use transitions.

We found that production indicators related to land management were closely linked to global agricultural expansion, crop-pasture dynamics, and forest transitions. The fact that land management indicators emerge as strong drivers of these agriculture- and forestry-related land use transitions matches our expectations, as they are closely linked to agricultural production and direct drivers of land use dynamics. This higher level of detail in land use dynamics is the merit of the synergistic data combination in HILDA+. However, this relationship is of complex nature, since production factors could not only be a driver but also an outcome of land use transitions. Because we could not distinguish these differently directed compounds in our methodology, the strong causal links between production indicators and land use change, as revealed in our study, should be treated with caution.

Although the causal link between environmental indicators and global land use change was relatively low, environmental factors demonstrated a greater influence on land use change in the Global South than in the Global North. This implies that global land use transitions during the past six decades mainly responded to a production- and (global) market-dominated system. However, our findings imply that agricultural land and production systems have recently and will likely become more vulnerable to altering environmental conditions such as climate extremes (Asseng et al., 2015; Godfray et al., 2010; Wang et al., 2014).

The reversal in the speed and trends of land use change after the global economic crisis (2007-2009), which was demonstrated in this thesis, indicates the high sensitivity of the global land system to socio-economic disruptions. The sudden impact of the COVID-19 pandemic in 2020 disrupted the economy and global supply chains. A high demand for energy in a phase of rapid post-pandemic economic rebound that outpaced energy supply led to a recent global energy crisis in 2021, which was exacerbated by the Russian invasion of Ukraine in 2022. Such events once again contribute to an awareness of the vulnerability of the globally interconnected agricultural system to crises. In the face of such upheavals, patterns of off-shoring of food production to the Global South (as found in this thesis) could be reversed and consequently a new on-shoring, a bringing back of

agricultural production to the Global North, could take place.

A shortcoming of this driver analysis is that it provides insights into the existence of causal links but hardly any information on their underlying mechanisms (e.g. effects of specific policies). Further, the selection of driver indicators strongly depends on data availability. Therefore, the generated feature space of drivers could encompass gaps due to missing information. Although we cannot claim to be completely exhaustive, the results of this study does shed new light on the important role of globally interconnected socio-economic systems in the distribution of global land use change.

### **C. What are the climate impacts of land use change and what role do high-resolution land use dynamics play in the carbon cycle?**

This thesis contributes to better understanding the climate impacts of land use change. Global and regional carbon fluxes resulting from land use change were focussed in Chapter 5 and 6.

#### **C.1 High-resolution land use change data for global carbon modelling**

Chapter 5 analyses the global carbon emissions from land use change by implementing the HILDA+ land use change dataset, developed in this thesis, in the Bookkeeping of Land Use Emissions (BLUE) model. A particular focus lies in the impact that the use of novel land use change data with high resolution has on carbon modelling. For that matter, land use/cover data from HILDA+ was used as a replacement of the state-of-the-art dataset LUH2, which is commonly used in global Earth system models.

Overall, global land use change during the past six decades accounted for a net carbon source of around  $1.0 \text{ PgC a}^{-1}$ , as modelled from HILDA+ land use change. Carbon emissions show a recent decrease from  $1.3 \text{ PgC a}^{-1}$  in 2012 to  $0.8 \text{ PgC a}^{-1}$  in 2019. In contrast, emission estimates based on LUH2 land use change data reduced from  $2.3 \text{ PgC a}^{-1}$  in 1960 to about  $0.9 \text{ PgC a}^{-1}$  in 1999 and increased afterwards to  $2.0 \text{ PgC a}^{-1}$  in 2019.

Our findings demonstrated that the use of high-resolution land use data instead of the default dataset as input for modelling land use-based carbon emissions has several implications:

First, it was shown that overall land use emissions based on HILDA+ were on average 65% lower than LUH2-based estimates. The agreement of gross carbon fluxes from land use change was higher in the mid-latitudes compared to tropical and subtropical regions. This was partially caused by different implementations of shifting cultivation in the forcing data. While LUH2 relies on prescribed rates of shifting cultivation in the tropics (assumptions based on Heinimann et al., 2017; Hurtt et al., 2020), the HILDA+ land use reconstruction does not incorporate shifting cultivation rates in its land use transitions at all. HILDA+, however, includes global but region-specific gross changes between all land

use/cover categories that were derived from data.

Second, opposing trends were found in emissions from global cropland expansion during the last decades. Emissions estimated from HILDA+ had decreasing trends, whereas estimates based on LUH2 indicated an increase. This deviation was strongly attributable to Southeast Asia, where a decreasing trend in carbon emissions was also observed by Kondo et al. (2022), along with overall large regional uncertainties between different carbon models.

Lastly, carbon fluxes of estimates based on the coarser resolution (LUH2) tend to be larger compared to estimates based on the finer resolution (HILDA+) due to an underrepresentation of successive transitions with coarser resolutions.

The lower amount of carbon emissions, revealed from replacing LUH2 with the higher-resolution HILDA+ land use data, likely comes from an offsetting effect of gross changes as well as successive multiple land use transitions that were previously unrecognised. This suggests that carbon in the land system is overestimated by LUH2-based modelling. This would have a huge impact, given the important role that LUH2 plays in current climate and Earth system modelling for international scientific-political communication (e.g. via the IPCC).

In conclusion, our findings suggest that the current implementation of shifting cultivation, successive transitions, and, above all, the spatial resolution in land use datasets used for carbon models needs to be reconsidered. Successive land use transitions and rotational cycles of shifting cultivation cannot be accurately captured in current land use reconstructions due to insufficient spatial resolutions (Bruun et al., 2021; Villa et al., 2020). Moreover, the influence of complex land use transitions, such as shifting cultivations, on the carbon cycle still remains unclear (Bruun et al., 2021; McNicol et al., 2015; Terefe & Kim, 2020). Therefore, we argue that complementing default runs of global emission models by alternative land use data, as demonstrated in this study, could increase the understanding of differences and provide better estimates of uncertainties in estimates of land use-based emissions.

## C.2 Climate impacts of land use and environmental change in Eastern Europe

Chapter 6 studied the dynamics of carbon fluxes from above-ground biomass in Europe, with a particular focus on Eastern Europe and the influence of possible underlying drivers from land use, management and environmental change during the last decade (2010-2019). This was done by integrating various data sources – satellite-based biomass estimates, CO<sub>2</sub> inversions, land use emission models, and inventories with data of land use change-related and environmental drivers.

It was shown that the carbon sink from aboveground biomass (AGB) in Eastern Europe accounted for 75% of the entire European carbon uptake during the last decade (2010-

2019). Strikingly, we found a declining trend in the overall carbon sink from AGB from both satellite-based estimates and land use inventories. The declining AGB carbon sink in Eastern Europe was likely driven by changes in land use and land management, along with increasing natural disturbances. Environmental change such as soil moisture variability, nitrogen deposition and CO<sub>2</sub> fertilization showed an overall higher importance for the net AGB carbon sink. Nevertheless, our findings indicate that the current decline of the Eastern European carbon sink was driven by land use and management change – both effects from past land use change and current land management activities. In this context, a saturation effect of the regrowth on formerly abandoned agricultural areas concurs with an increase in wood harvest, particularly in European Russia.

Our observations of the declining AGB carbon sink in Eastern Europe were shown to be consistent with other studies (Bastos et al., 2014; Deng et al., 2022; Nabuurs et al., 2013). It is likely that the concurrence of increased climate variability (leading to droughts and forest fires) (Schaphoff et al., 2016; Schepaschenko et al., 2021; Zamolodchikov et al., 2017), saturated or decreasing regrowth on abandoned agricultural land (Nabuurs et al., 2013; Zamolodchikov et al., 2018, 2017) and increasing wood harvest (Ceccherini et al., 2020; Zamolodchikov et al., 2017) caused the Eastern European land carbon sink to decline in the recent decade. The temporal development of AGB carbon fluxes due to the abandonment of croplands in the region is particularly interesting. Based on this study, abandoned areas were still a significant contributor to the Eastern European carbon uptake by contributing up to one third to the net carbon sink during 2010-2019. However, in the face of ongoing climate change and political unrest affecting the Eastern European region, the carbon sink on abandoned areas is expected to further decrease in the future.

Overall, our findings contribute to a better understanding of the role of land use and management for climate mitigation in Eastern Europe and – given its large contribution to the land-based carbon sink – in the whole of Europe.

## 7.3 Discussion and outlook

### 7.3.1 Added value versus limitations

The added value of this thesis lies in the creation and provision of an open dataset on global land use change with unprecedented spatial, temporal and thematic detail. This dataset, HILDA+, is based on a consistent data-driven methodology, which uses a synergistic combination of high-resolution remote sensing products and long-term land use inventories. It entails an approach that is consistent across regions, time periods, and land use/cover categories. The fusion of higher spatial (1 km), temporal (annual) and thematic (gross changes; transitions between six land use categories) resolution than previously known land use change data makes HILDA+ the first global land use reconstruction of its

kind. It gives new insights into the spatio-temporal dynamics of global land use change, but also enables further studies on underlying drivers and environmental impacts of land use change.

It was shown within this thesis that higher level of detail in land use reconstructions uncovers patterns of human influence on the land surface, which were previously unseen. It was shown how multiple, successive transitions, e.g. between cropland and pastures or between forest and shrubland, revealed areas with high agricultural or forestry land use intensities. It was demonstrated that the annual rate of land use changes relates to far-reaching socio-economic events such as political disruptions or economic crises. What is more, new insights into more complex processes of land use change such as forest regrowth after agricultural abandonment could be gained. Overall, the findings of this thesis proved how the combination of a higher spatial, temporal and thematic detail in land use maps helps uncovering the full dynamics of land use change.

The higher detail in land use change assessments translates into new findings about the global and regional carbon cycle (as shown in this thesis). This can set new opportunities for Earth system and climate modelling, because land use inputs and, as a result, land use-based emissions still represent a large uncertainty in the models (Friedlingstein et al., 2022). In addition, the inherent high-resolution in the HILDA+ data lays the foundation for numerous follow-up studies, such as time series analyses for analysing the interaction between land use change and socio-economic development and climate change. With this, even an attribution of land use dynamics responding to single socio-economic events or climate anomalies becomes possible.

However, the HILDA+ land use reconstruction approach also holds some limitations. One downside of this data-driven method is the dependence on the different technical capabilities, diverse classification uncertainties, or varying definitions of land use/cover categories of the input data. This is particularly evident in the demarcation of managed and unmanaged grasslands. As remote sensing products can only distinguish between different land covers and not necessarily land uses, they fail to differentiate between pasture/rangeland and unmanaged grassland. Uncertainties due to large disagreement of the input datasets on agricultural land use categories, especially pasture/rangelands were shown in Chapter 2. Remote sensing products used for the first HILDA+ version deviate the most in heterogeneous landscapes, holding a mix of managed and unmanaged lands, e.g. savannahs of Sub-Saharan Africa, rangelands in Australia, the grassy steppes of Central Asia, the sparse taiga of eastern Siberia, the transition between Canadian boreal forest and tundra. Another example is that remote sensing products commonly misclassify tree crops due to similar land cover as forest or shrubland. Here, additional observational data that specifically focusses on tree crops or mixed forest-cropland classes could compensate the error in an updated version of the HILDA+ land use change data (see Chapter 3 and maps in Figure 7.2 and Figure 7.3).

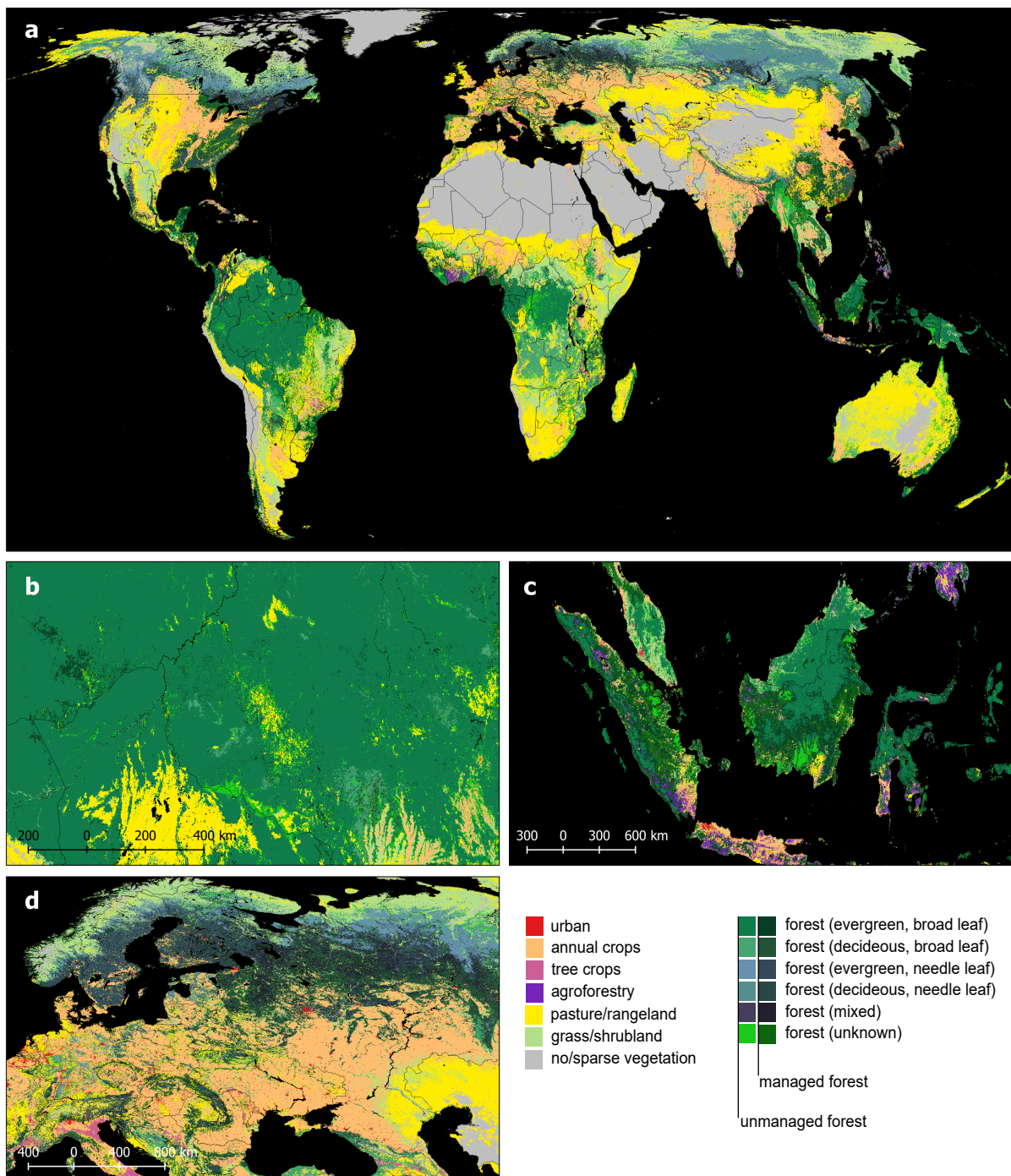


**Figure 7.2:** Land use/cover map of 1960 from HILDA+ version 2.0 (updated version of Winkler et al., 2020, ; publication under preparation). Maps show different geographical extents: a) Global b) Amazon (Brazil) c) Indonesia d) Central and Eastern Europe.

In addition to the land cover focus of the remote sensing products, another shortcoming of the HILDA+ approach lies in the choice of six discrete land use/cover classes. Mixed land uses, as they occur in reality, cannot be accurately captured in this way. This may

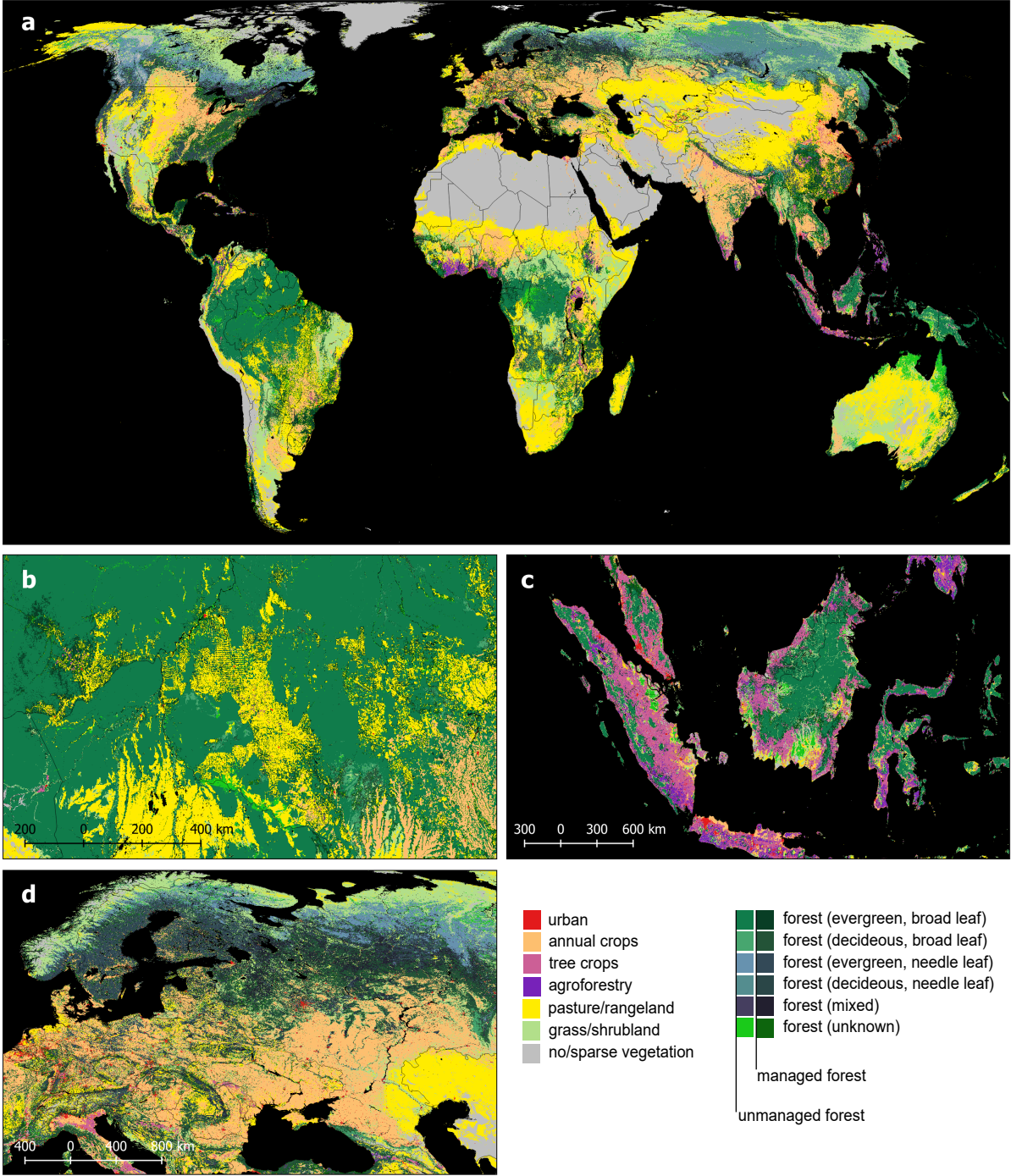


**Figure 7.3:** Land use/cover map of 2020 from HILDA+ version 2.0 (updated version of Winkler et al., 2020, ; publication under preparation). Maps show different geographical extents: a) Global b) Amazon (Brazil) c) Indonesia d) Central and Eastern Europe. Extents are the same as in Figure 7.2.

cause artefacts in form of multiple changes between two similar land use/cover categories, e.g. between forest and grass/shrubland. It remains unclear how much of the observed

high-frequency changes represent real land use conversions, result from management activities, or are artefacts from the input data. Nevertheless, improvements were made in the updated HILDA+ version 2.0 (see Chapter 3), which contains additional subcategories of cropland (annual crops and tree crops) and agroforestry. However, it is important to note that the 25-fold increase in resolution (compared to standard land use data used for Earth system modelling) is much closer to a realistic representation of the land use processes.

Another aspect is the incomplete consideration of land management in the land use reconstruction. It should be noted that agricultural land use categories in HILDA+ entail a wide range of management intensities. This becomes particularly evident from the large area of pasture/rangeland expansion, which was found in HILDA+ studies (see Chapter 2-4). It was discussed that the large affected area does not comprise uniformly intensive land use practices. The observed pasture/rangeland expansion mainly entails low-intensity and often nomadic forms of pastoral land use that spread in arid, semi-arid or high-mountain regions of China and Central Asia (Dong, 2016), the Sahel zone (Holechek et al., 2017; Rahimi et al., 2021; Turner et al., 2005), and Australia (Godde et al., 2020; Holmes, 2002). A first approach of incorporating land management information in HILDA+ version 2.0 was undertaken recently by reclassifying forest areas into managed and unmanaged forests (see maps in Figure 7.2 and Figure 7.3). This version of the dataset was used in Chapter 3, but without a focus on forest areas. The reconstruction of forest management was based on a combination of a high-resolution remote sensing-based dataset (Lesiv et al., 2022) with wood production statistics from the FAO (FAO, 2022a). However, there is still potential for improvement and further integration of land management information into HILDA+ is intended.

### 7.3.2 Societal and political implications

#### 7.3.2.1 News and media digest

The findings of this thesis have raised broad societal interest around the spatial extent, the underlying drivers as well as the environmental impacts of global land use change. Our study on the spatio-temporal dynamics of global land use change (Chapter 2) was picked up by a wide range of regional to global news outlets. These are selected themes that were most discussed in the news:

- Land use change has affected more area than previously estimated.  
"Land-use change has affected 'almost a third' of world's terrain since 1960". In: Carbon Brief (Viglione, 2021), reposted via e.g. EcoWatch (2021), Eco-Business (2021)  
"Nearly a fifth of Earth's surface transformed since 1960". In: CTVNews Hood (2021), reposted via e.g. The Hindu (2021), The Taipei Times (2021)  
"Weltweite Landnutzung ändert sich viel stärker als gedacht" In: BR24 (Westram,

2021)

"Humanidade mudou 17% do solo terrestre em 60 anos" In: Olhar Digital (Albuquerque, 2021)

"Uso del suolo: l'uomo ha modificato il 32% della superficie terrestre dal 1960" In: Rinnovabili (Rinnovabili.it, 2021)

"Global snapshot of land use reveals humanity's massive impact", In: Stuff (Griffin, 2021)

"Landnutzungsänderungen größer als gedacht" In: Bild der Wissenschaft (Podbregar, 2021)

"Area impacted by land use change four times higher than previously thought". In: Mongabay (Alberts, 2021)

- Food systems are a primary driver of global land use change and deforestation. "Farming the future: Transforming the ownership of food systems research & data" Policy document In: Common Wealth (Booth, 2021)  
"We are asking for more than food from our farms. A new cropping option may help meet the demand" In: Forbes (Savage, 2022)
- Globalised trade of agricultural commodities is a main driver of land use change in the Global South. "Deforestation is driven by global markets" In: The Conversation (Valbuena & Lovejoy, 2021)
- Global forest loss covers an area larger than the island of Borneo. "Study tracks global forest decline and expansion over six decades" In: Mongabay (Cannon, 2022)
- Land use change contributed to the loss of bee habitats. "Bees face many challenges – and climate change is ratcheting up the pressure" In: The Conversation (Durant, 2022)

### 7.3.2.2 Enforcing deforestation-free supply chains

Findings on North-South disparities in global land use transitions and their interconnect- edness through global trade, as presented in this thesis, have political relevance. They indicate that drivers and impacts of land use change are globally interlinked and can spill over to distant locations (Meyfroidt et al., 2022).

New light is shed on policy proposals such as the European Green Deal that was released in 2020 in order to make the E.U. carbon neutral by 2050. Fuchs et al. (2020) argued that the Green Deal could lead to a further outsourcing of environmental damage to other world regions, as long as it does not sufficiently account for the displaced deforestation and environmental impacts embedded in external trade (mainly through imports of agricultural commodities). In this context, the afforestation in the EU was as large as the deforestation outsourced to other world region during the last decade (Fuchs et al., 2020). A combined analysis of high-resolution land use transitions, provided by datasets

such as HILDA+, and additional information on trade patterns and associated supply chains could help to further disentangle such land use displacements related to political targets.

In general, more and more public and private policies promote deforestation-free international supply chains (Garrett et al., 2013; Lambin et al., 2018). Governments such as the EU or the US propose legislations to limit imports of forest-risk commodities to companies (Babbit et al., 2021; European Commission, 2021). However, the impacts of such private and public policy commitments are limited due to leakage effects, lack of transparency, traceability or incomplete adoption (Lambin et al., 2018; Villoria et al., 2022). Again, more information on land use transitions, as gained from the findings of this thesis, when studied in relation to imports and exports of trade partners, could contribute to better estimating the effects of such policies. More emphasis on public–private policy mixes that complement each other would be required to increase the effectiveness of supply-chain initiatives (Lambin et al., 2018). A recent study by Pendrill et al. (2022) suggests that demand-side supply-chain policies, including zero-deforestation commitments, need to look beyond their direct impacts and support large-scale governance change. This is confirmed by Villoria et al. (2022) who find that an up-scaling of zero-deforestation regulations holds the potential of reducing domestic leakage effects. Demand-side policies, trade regulations and broad international coordination that considers teleconnections and displaced environmental impacts can help ensure that conservation policies have a positive effect (Lewis et al., 2019). Meyfroidt et al. (2022) suggests that policy instruments in the land systems need to consider distant connections, such as spill-overs across spatial and temporal scales, and prevent environmental impacts rather than restore damaged land afterwards. In the context of deforestation-free supply chains, an engagement of the public sector in both exporting and importing regions is essential in order to reduce deforestation and enforce ecosystem restoration (Garrett et al., 2022). To inform policy makers, more studies about the interconnection of land use and trade should be carried out. For this, more data on both sides of the paradigm would be needed: comprehensive data on land use dynamics, for which a first step was taken in this thesis, and more insights into trade relations (e.g. matrix of harvested area of imported and exported commodities, stages in the supply chain, land ownership).

### 7.3.2.3 Verifying greenhouse gas emissions

This thesis was supported by VERIFY (VERIFYing greenhouse gas emissions), a Research and Innovation project funded by the European Commission under the H2020 programme. The aim of VERIFY was to estimate greenhouse gas emissions in order to support countries' emission reporting to the UN Climate Change Convention Secretariat. The emissions are estimated based on land, ocean and atmospheric observations. The project focuses on the three major anthropogenic greenhouse gases responsible for global warming: carbon dioxide (CO<sub>2</sub>), methane (CH<sub>4</sub>) and nitrous oxide (N<sub>2</sub>O) (see Figure 7.4).

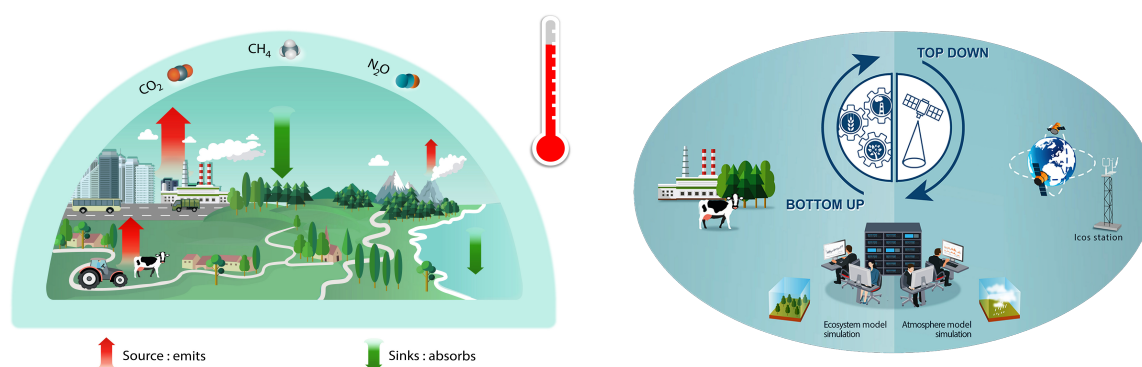


**Figure 7.4:** Overview of greenhouse gas emissions targeted (panel on the left) and methods used (panel on the right) in the VERIFY project. Greenhouse gas fluxes are represented as carbon sources and sinks (infographic adapted from VERIFY, 2018).

Measuring the effectiveness of climate policies against agreed-upon international targets require accurate and precise estimates of emissions and their trends. These estimates need to be established and regularly updated using transparent methods, traceable to international standards. VERIFY proposed to quantify more accurately carbon stocks and the fluxes of carbon dioxide (CO<sub>2</sub>), methane (CH<sub>4</sub>), and nitrous oxide (N<sub>2</sub>O) across the EU based on independent observations in support of inventories that rely only on statistical data (VERIFY, 2018).

This thesis contributed to WP3 of the VERIFY project, which covered data collection and development of advanced algorithms (including bottom-up and top-down models) for the estimation of terrestrial CO<sub>2</sub> sources and sinks as well as carbon stocks. The prerequisite for the provision of accurate estimates on carbon fluxes and its attribution to land use, management intensity and climate drivers was the collection of input data for ecosystem models. This involved the development of new high-resolution gridded climate data, land cover changes, management intensity and carbon stocks (biomass and soils). This thesis yielded new high-resolution data of global land use/cover change (HILDA+). With this, it contributed to deliverable D3.1 and D3.2 on building a first and a second state-of-the-art database, respectively. For this project, the land use/land cover data from HILDA+ (in a preliminary version before publication) were provided over an extended period back to 1900. To generate land use/cover maps before 1960, a spatio-temporal extrapolation of trends from subsequent data was applied. HILDA+ data were then fed into the book-keeping model of land use change emissions BLUE. As a result, a consolidated synthesis of the CO<sub>2</sub> emissions and removals for the EU and the UK over the past three decades was given (Petrescu et al., 2021).

In addition, findings from HILDA+ contributed to deliverable D3.14 on national forest inventories and high-resolution forest cover for Eastern Europe. This contribution consisted of the analysis of major land use/cover changes across Europe, with particular focus on

Eastern Europe. Finally, the study on the Eastern European carbon fluxes (Chapter 6) was emerged from the VERIFY project and contributed to deliverable 3.16 on the analysis of net ecosystem exchange and the carbon balance of Eastern Europe.

The findings of the VERIFY project are strongly relevant for policy makers. VERIFY contributed, e.g., to COP26 in Glasgow and to the assessment of the Global Carbon Budget (Friedlingstein et al., 2022). Initiatives like VERIFY support the provision of more accurate information on greenhouse gas emissions, particularly carbon fluxes and their attribution to its drivers – transport and energy, land use, land management and/or climate change. This enables a better understanding of the climate impacts that sector-related policies may have. The large uncertainties of land use or management-based emissions over Europe that still remain (due to different definitions and model set ups Petrescu et al., 2021) show that more such scientific initiatives are urgently needed to strengthen the knowledge base on land-based greenhouse gas emissions. This is the way to lay a good scientific foundation for informed political decisions.

#### **7.3.2.4 From the past to the future: Land-based carbon dioxide removal (CDR)**

Another topic that is gaining popularity in recent political debates is carbon dioxide removal (CDR) (Schenuit et al., 2021). To reach greenhouse gas neutrality - a goal that many governments have put on their political agenda - a balance between the sources and sinks of greenhouse gases is required (CDRterra, 2022; Schenuit et al., 2022). As shown in this thesis, land use change processes such as cropland abandonment or afforestation can absorb CO<sub>2</sub> from the atmosphere and act as a regional carbon sink. Thus, such land use transitions can be regarded as CDR measure.

Ongoing and further research on the data-driven assessment of land use change, which emerged and follows from this thesis, will contribute to a project about land-based CDR in Germany. STEPSEC (Scrutinizing the feasibility of TERrestrial CDR Potentials under Socio-Ecological Constraints) is embedded in the BMBF funding measure CDRterra on researching terrestrial CDR methods in Germany. STEPSEC specifically focusses on the land use and management processes that increase the carbon sink: afforestation and reforestation, forest management, and bioenergy with carbon capture and storage (BECCS). The STEPSEC project aims to provide more accurate estimates of how much CO<sub>2</sub> these measures will remove from the atmosphere, what side-effects they have and what societal processes present barriers to their implementation in Germany (CDRterra, 2022).

Methods and data from the work on this thesis will contribute to modelling the future of the German land system under consideration of different CDR measures (afforestation, reforestation, forest management, BECCS) within the STEPSEC project. For this, an agent-based land use modelling framework CRAFTY (Competition for Resources between Agent Functional Types; Brown et al., 2022a; Murray-Rust et al., 2014) will be applied and

refined for the context of land-based CDR measures in Germany. The development of the German application of the model, CRAFTY-DE, also includes a stakeholder engagement as well as the checking of the model baseline against the historical land use data from HILDA+. In doing so, maps of the land use dynamics of the past should seamlessly fade to the modelled paths of the future.

Overall, modelling of future land use pathways always requires knowledge about the current land system that results from land use dynamics of the past. Land use can play its role on actively absorbing carbon from the atmosphere. However, it is worth adding that policymakers should prioritise reducing greenhouse gas emissions from all sectors (e.g. energy, transport, land use) in the first place and focus on “negative” emissions from CDR measures in the second place.

### 7.3.3 The role of humans in Earth system models

The findings of this thesis suggest that the role of humans on the land surface, namely land use and management dynamics, is currently underrepresented in global Earth system models. This is due to a lack of spatial, temporal and thematic detail in long-term land use change assessments on the one hand and the reliance of Earth system models on often only a single dataset on the other hand. It is therefore not surprising that land use change is still one of the biggest uncertainties in modelling the global carbon cycle (Di Vittorio et al., 2020; Friedlingstein et al., 2022). As also acknowledged in recent studies (Calvin & Bond-Lamberty, 2018; Franzke et al., 2022; Verburg et al., 2019), there is an urgent need to increase the integration of research on human land use and Earth system science.

Further research should focus on decreasing the uncertainties in land use forcing and stop the dependence on one single dataset. A first step in this direction could be made by using more empirically supported and higher-resolution land use/cover datasets, such as the HILDA+ data presented here, in Earth system models.

Current initiatives in the Earth system modelling community, such as the TRENDY project (Sitch, 2022) in support of the Global Carbon Project’s (GCP) annual global carbon budget assessment, and its recent regional initiative, the Regional Carbon Cycle Assessment and Processes project (RECCAP2), have already started using the high-resolution HILDA+ land use data (developed in this thesis) as input for modelling the carbon budget (Bastos et al., 2022). Thereby, first studies replaced the standard land use dataset LUH2 with the new HILDA+ data and provided promising new insights into carbon dynamics from land use change (Bastos et al., 2022; Petrescu et al., 2021). Many more such initiatives are needed. The initial results suggest that the time has come for a more detailed representation of land use dynamics in Earth system models. To this end, LUH2 could be increasingly compared with higher-resolution datasets such as HILDA+ for its effect in Earth system models and, if necessary, even replaced with such datasets in the long term. For a long-term embedding of HILDA+ in global concerted Earth system

modelling initiatives such as the GCP, regular updates of HILDA+ would be necessary. Basically, the HILDA+ approach can easily be updated annually, whenever new data from Earth Observation and FAO land use inventories become available. However, such regular improvement and publication of HILDA+ data can be better ensured through long-term financial support.

An important point in favour of a greater representation of land use dynamics in Earth system models is the essential role of people in transforming the land system. Many of our global challenges (climate change, biodiversity loss, food insecurity) are human-made. However, the solutions emerge from political decisions, which in turn emerge from society. Sustainable land use pathways are walked by people and depend on socio-economic constraints. If the human impact is not sufficiently parametrised, Earth system models will fail to provide a better understanding of the interaction of humans with ecosystems and climate. One thing is clear: Land use and management will be ever more important for climate mitigation, climate adaptation and nature protection strategies. More interdisciplinary research is needed to synthesise research advances on anthropogenic land systems with those in Earth system modelling. This would take a major step towards a better understanding of the human-environment relationship.

#### **7.3.4 Ongoing developments in Earth Observation**

Advancements in satellite remote sensing have revolutionised the monitoring of the Earth's surface. In recent years, Earth Observation has seen drastic improvements - in terms of data availability, advances in spatial, temporal and spectral detail as well as innovative approaches in data managing and processing (Phiri et al., 2020; Sudmanns et al., 2020; Vali et al., 2020). More and more remote sensing products for global land use change detection are becoming freely available (Belward & Skøien, 2015; Sudmanns et al., 2020). Along with an increasing application of Deep Learning for land cover classification, the trend in Earth Observation moves progressively towards ever higher spatio-temporal resolution, process automation, and near real-time change detection (Klein et al., 2017; Sudmanns et al., 2020).

Particularly the ESA Sentinel missions coordinated by the Copernicus Programme, opened up new possibilities for mapping the global dynamics of the land surface (Phiri et al., 2020). This gave rise to the recently released ESA WorldCover, which is the first global land cover product for 2020 and 2021 at 10 m spatial resolution, developed and validated in near-real time from Sentinel-1 and Sentinel-2 data (ESA, 2023). Another innovation in the Earth Observation domain arose from a private-public cooperation between Google and the World Resources Institute. Dynamic World is another near real-time 10m resolution global land use/land cover dataset leveraging Deep Learning on 10 m Sentinel 2 imagery (Brown et al., 2022b). Compared to WorldCover, which is only available at an annual basis (currently 2020 and 2021), Dynamic World includes an automated approach

that provides regular updates at intervals of 2-5 days depending on location since July 2015 (Brown et al., 2022b; Google & World Resources Institute, 2023).

These major advances in both spatial and temporal resolution of global satellite-based land cover maps lay the foundation for a more detailed mapping of land use change. The improvements in Earth Observation are an essential building block for the evolution of data-driven land use reconstructions such as the HILDA+ framework presented in this thesis, as they allow not only the mapping of land use categories and their annual changes, but also the integration of smaller-scale management activities such as changes in crop types on cropland, mowing frequencies on grassland or logging practices in forests. Current developments in the field of Earth Observation (automated algorithms, private-public initiatives, open data sets and applications, near real-time mapping and ever higher spatial resolution) indicate that future land surface data will target an ever higher thematic level of detail in land use/cover classes. This development leads towards the derivation of individual vegetation types - crop types or tree species - but also of individual management regimes in agriculture and forestry (cropping cycles, harvesting rates, etc.). Already today, there are more and more global studies with a finer subdivision of land use/cover categories related to management of croplands (Descals et al., 2021; Liu et al., 2021; Ray et al., 2022) or forests (Hanan & Anchang, 2020; Lesiv et al., 2018; Santoro et al., 2021). The call for a better representation of land management in land change assessments (Erb et al., 2017; Gormley-Gallagher et al., 2022; Pongratz et al., 2017) could thus soon be answered by exploiting upcoming Earth Observation products.

### 7.3.5 More research opportunities

In this thesis, we addressed the climate impacts of land use change, particularly regarding the carbon cycle, but not the impacts on biodiversity. Impacts of land-use change on biodiversity are hard to measure as they often depend on location, research methods, and taxonomic focus, with recent global meta-analyses reaching contrasting conclusions (Davison et al., 2021). However, research advances on land use dynamics can contribute to a better understanding of how land use change affects biodiversity (Davison et al., 2021). The destruction and modification of natural habitats due to land use change are among the most important threats to biodiversity (Newbold et al., 2015). In this regard, effects from historic land use are as strong as the effects of current management (Le Provost et al., 2020). Therefore, more research should focus on the interaction between land use, management and biodiversity (Davison et al., 2021; Titeux et al., 2016). Better data on the spatio-temporal dynamics of land use change (as provided by the work of this thesis) can help to investigate the impact of land use and management on habitats and to explore the interactions between humans, climate and biodiversity.

Another interesting field of research is the study of telecoupling or teleconnections in global land use dynamics. From the findings of this thesis it becomes evident that investigating

how land use transitions in one place are interlinked with land use transitions in another place is important to better understand the global land system. Land use displacements, rebound effects between agricultural intensification and expansion, the prominent role of global trade as driver of land use change have been discussed in this thesis. Distant drivers (drivers located outside the country) could not be addressed so far in the explorative driver analysis presented in Chapter 4 of this thesis. However, further studies analysing global tele-coupled drivers of land use change are likely to emerge from the HILDA+ land use change assessment.

Finally, linking land use change with land management dynamics is of major importance in order to advance research on global land system change. A first linkage of agricultural land use change with land use intensity was undertaken in Chapter 3 of this thesis. The newly developed version 2.0 of the HILDA+ land change assessment provides the basis for a further linkage of management to land use/cover categories. There are further plans to integrate more and more data-derived information on land management in the form of agricultural inputs (crop varieties, cropping frequency, fertilizer and pesticide application, irrigation schemes, livestock type and density), forestry activities and land use intensity levels into the HILDA+ framework. Research on this is currently ongoing and aims to provide deeper insights into the complex interactions between land use and management changes over the last six decades. Moreover, this would lay an important foundation for the analysis of climate and biodiversity impacts caused by global land use dynamics.





# References

- Abatzoglou, J. T., Dobrowski, S. Z., Parks, S. A., & Hegewisch, K. C. (2018). TerraClimate, a high-resolution global dataset of monthly climate and climatic water balance from 1958–2015. *Scientific Data*, *5*, 170191. DOI: <https://doi.org/10.1038/sdata.2017.191>.
- Achard, F., Mollicone, D., Stibig, H.-J., Aksenov, D., Laestadius, L., Li, Z., Popatov, P., & Yaroshenko, A. (2006). Areas of rapid forest-cover change in boreal Eurasia. *Forest Ecology and Management*, *237*, 322–334. DOI: <https://doi.org/10.1016/j.foreco.2006.09.080>.
- Ackerman, D., Millet, D. B., & Chen, X. (2019). Global Estimates of Inorganic Nitrogen Deposition Across Four Decades. *Global Biogeochemical Cycles*, *33*, 100–107. DOI: <https://doi.org/10.1029/2018GB005990>.
- Adamenko, T., & Prokopenko, A. (2011). Monitoring Droughts and Impacts on Crop Yield in Ukraine from Weather and Satellite Data. In F. Kogan, A. Powell, & O. Fedorov (Eds.), *Use of Satellite and In-Situ Data to Improve Sustainability* NATO Science for Peace and Security Series C: Environmental Security (pp. 3–9). Dordrecht: Springer Netherlands. DOI: [https://doi.org/10.1007/978-90-481-9618-0\\_1](https://doi.org/10.1007/978-90-481-9618-0_1).
- Aide, T. M., Clark, M. L., Grau, H. R., López-Carr, D., Levy, M. A., Redo, D., Bonilla-Moheno, M., Riner, G., Andrade-Núñez, M. J., & Muñiz, M. (2013). Deforestation and Reforestation of Latin America and the Caribbean (2001–2010). *Biotropica*, *45*, 262–271. DOI: <https://doi.org/10.1111/j.1744-7429.2012.00908.x>.
- Akram-Lodhi, A. H. (2012). Contextualising land grabbing: Contemporary land deals, the global subsistence crisis and the world food system. *Canadian Journal of Development Studies / Revue canadienne d'études du développement*, *33*, 119–142. DOI: <https://doi.org/10.1080/02255189.2012.690726>.
- Alberts, E. C. (2021). Area impacted by land use change four times higher than previously thought. <https://news.mongabay.com/2021/06/area-impacted-by-land-use-change-four-times-higher-than-previously-thought/>.
- Albuquerque, K. (2021). Humanidade mudou 17% do solo terrestre em 60 anos.
- Aleixandre-Benavent, R., Aleixandre-Tudó, J. L., Castelló-Cogollos, L., & Aleixandre,

- J. L. (2018). Trends in global research in deforestation. A bibliometric analysis. *Land Use Policy*, *72*, 293–302. DOI: <https://doi.org/10.1016/j.landusepol.2017.12.060>.
- Alexander, P., Brown, C., Arneth, A., Finnigan, J., & Rounsevell, M. D. (2016). Human appropriation of land for food: The role of diet. *Global Environmental Change*, *41*, 88–98. DOI: <https://doi.org/10.1016/j.gloenvcha.2016.09.005>.
- Alexander, P., Rounsevell, M. D., Dislich, C., Dodson, J. R., Engström, K., & Moran, D. (2015). Drivers for global agricultural land use change: The nexus of diet, population, yield and bioenergy. *Global Environmental Change*, *35*, 138–147. DOI: <https://doi.org/10.1016/j.gloenvcha.2015.08.011>.
- Ambika, A. K., Wardlow, B., & Mishra, V. (2016). Remotely sensed high resolution irrigated area mapping in India for 2000 to 2015. *Scientific Data*, *3*, 160118. DOI: <https://doi.org/10.1038/sdata.2016.118>.
- Anderson, K. (2010). Globalization's effects on world agricultural trade, 1960–2050. *Philosophical Transactions of the Royal Society B: Biological Sciences*, *365*, 3007–3021. DOI: <https://doi.org/10.1098/rstb.2010.0131>.
- Araza, A. et al. (2022). A comprehensive framework for assessing the accuracy and uncertainty of global above-ground biomass maps. *Remote Sensing of Environment*, *272*, 112917. DOI: <https://doi.org/10.1016/j.rse.2022.112917>.
- Arezki, R., Deininger, K., & Selod, H. (2015). What Drives the Global “Land Rush”? *The World Bank Economic Review*, *29*, 207–233. DOI: <https://doi.org/10.1093/wber/lht034>.
- Arima, E. Y., Richards, P., Walker, R., & Caldas, M. M. (2011). Statistical confirmation of indirect land use change in the Brazilian Amazon. *Environmental Research Letters*, *6*, 024010. DOI: <https://doi.org/10.1088/1748-9326/6/2/024010>.
- Arneth, A., Brown, C., & Rounsevell, M. D. A. (2014). Global models of human decision-making for land-based mitigation and adaptation assessment. *Nature Climate Change*, *4*, 550–557. DOI: <https://doi.org/10.1038/nclimate2250>.
- Arneth, A., Denton, F., Agus, F., Elbehri, A., Erb, K., Osman Elasha, B., Rahimi, M., Rounsevell, M., Spence, A., & Valentini, R. (2019). Framing and Context. In P. Shukla, J. Skea, E. Calvo Buendia, V. Masson-Delmotte, H.-O. Pörtner, D. Roberts, P. Zhai, R. Slade, S. Connors, R. van Diemen, M. Ferrat, E. Haughey, S. Luz, S. Neogi, M. Pathak, J. Petzold, J. Portugal Pereira, P. Vyas, E. Huntley, K. Kissick, M. Belkacemi, & J. Malley (Eds.), *Climate Change and Land: An IPCC Special Report on Climate Change, Desertification, Land Degradation, Sustainable Land Management, Food Security, and Greenhouse Gas Fluxes in Terrestrial Ecosystems*. IPCC.
- Arneth, A. et al. (2017). Historical carbon dioxide emissions caused by land-use changes are possibly larger than assumed. *Nature Geoscience*, *10*, 79–84. DOI: <https://doi.org/10.1038/ngeo2250>.

- org/10.1038/ngeo2882.
- Arowolo, A. O., & Deng, X. (2018). Land use/land cover change and statistical modelling of cultivated land change drivers in Nigeria. *Regional Environmental Change*, *18*, 247–259. DOI: <https://doi.org/10.1007/s10113-017-1186-5>.
- Asseng, S. et al. (2015). Rising temperatures reduce global wheat production. *Nature Climate Change*, *5*, 143–147. DOI: <https://doi.org/10.1038/nclimate2470>.
- Austin, K. G., Schwantes, A., Gu, Y., & Kasibhatla, P. S. (2019). What causes deforestation in Indonesia? *Environmental Research Letters*, *14*, 024007. DOI: <https://doi.org/10.1088/1748-9326/aaf6db>.
- Avitabile, V. et al. (2016). An integrated pan-tropical biomass map using multiple reference datasets. *Global Change Biology*, *22*, 1406–1420. DOI: <https://doi.org/10.1111/gcb.13139>.
- Babbitt, B., Eizenstat, S., Loy, F., Reilly, W., Stern, T., Wirth, T., & Whitman, C. (2021). Amazon Protection Plan: Policy Recommendations for U.S. Action for Amazon Forests. <https://climateprincipals.org/amazon-plan/>.
- Ballantyne, A. P., Andres, R., Houghton, R., Stocker, B. D., Wanninkhof, R., Anderegg, W., Cooper, L. A., DeGrandpre, M., Tans, P. P., Miller, J. B., Alden, C., & White, J. W. C. (2015). Audit of the global carbon budget: Estimate errors and their impact on uptake uncertainty. *Biogeosciences*, *12*, 2565–2584. DOI: <https://doi.org/10.5194/bg-12-2565-2015>.
- Barbier, E. B., Delacote, P., & Wolfersberger, J. (2017). The economic analysis of the forest transition: A review. *Journal of Forest Economics*, *27*, 10–17. DOI: <https://doi.org/10.1016/j.jfe.2017.02.003>.
- Barona, E., Ramankutty, N., Hyman, G., & Coomes, O. T. (2010). The role of pasture and soybean in deforestation of the Brazilian Amazon. *Environmental Research Letters*, *5*, 024002. DOI: <https://doi.org/10.1088/1748-9326/5/2/024002>.
- Bastos, A. et al. (2022). On the use of Earth Observation to support estimates of national greenhouse gas emissions and sinks for the Global stocktake process: Lessons learned from ESA-CCI RECCAP2. *Carbon Balance and Management*, *17*, 15. DOI: <https://doi.org/10.1186/s13021-022-00214-w>.
- Bastos, A., Gouveia, C. M., Trigo, R. M., & Running, S. W. (2014). Analysing the spatio-temporal impacts of the 2003 and 2010 extreme heatwaves on plant productivity in Europe. *Biogeosciences*, *11*, 3421–3435. DOI: <https://doi.org/10.5194/bg-11-3421-2014>.
- Bastos, A., Hartung, K., Nützel, T. B., Nabel, J. E. M. S., Houghton, R. A., & Pongratz, J. (2021). Comparison of uncertainties in land-use change fluxes from bookkeeping model parameterisation. *Earth System Dynamics*, *12*, 745–762. DOI: <https://doi.org/10.5194/esd-12-745-2021>.

- g/10.5194/esd-12-745-2021.
- Bastos, A. et al. (2020). Sources of Uncertainty in Regional and Global Terrestrial CO<sub>2</sub> Exchange Estimates. *Global Biogeochemical Cycles*, *34*, e2019GB006393. DOI: <https://doi.org/10.1029/2019GB006393>.
- Bayer, A. D., Fuchs, R., Mey, R., Krause, A., Verburg, P. H., Anthoni, P., & Arneth, A. (2021). Diverging land-use projections cause large variability in their impacts on ecosystems and related indicators for ecosystem services. *Earth System Dynamics*, *12*, 327–351. DOI: <https://doi.org/10.5194/esd-12-327-2021>.
- Bayer, A. D., Lindeskog, M., Pugh, T. A. M., Anthoni, P. M., Fuchs, R., & Arneth, A. (2017). Uncertainties in the land-use flux resulting from land-use change reconstructions and gross land transitions. *Earth System Dynamics*, *8*, 91–111. DOI: <https://doi.org/10.5194/esd-8-91-2017>.
- Bell, L. W., & Moore, A. D. (2012). Integrated crop–livestock systems in Australian agriculture: Trends, drivers and implications. *Agricultural Systems*, *111*, 1–12. DOI: <https://doi.org/10.1016/j.agsy.2012.04.003>.
- Bellassen, V., & Luysaert, S. (2014). Carbon sequestration: Managing forests in uncertain times. *Nature*, *506*, 153–155. DOI: <https://doi.org/10.1038/506153a>.
- Bellassen, V., Viovy, N., Luysaert, S., Maire, G. L., Schelhaas, M.-J., & Ciais, P. (2011). Reconstruction and attribution of the carbon sink of European forests between 1950 and 2000. *Global Change Biology*, *17*, 3274–3292. DOI: <https://doi.org/10.1111/j.1365-2486.2011.02476.x>.
- Bellemare, M. F. (2015). Rising Food Prices, Food Price Volatility, and Social Unrest. *American Journal of Agricultural Economics*, *97*, 1–21. DOI: <https://doi.org/10.1093/ajae/aau038>.
- Belward, A. S., & Skøien, J. O. (2015). Who launched what, when and why; trends in global land-cover observation capacity from civilian earth observation satellites. *ISPRS Journal of Photogrammetry and Remote Sensing*, *103*, 115–128. DOI: <https://doi.org/10.1016/j.isprsjprs.2014.03.009>.
- de Beule, H., Jassogne, L. T. P., & van Asten, P. J. A. (2014). *Cocoa: Driver of Deforestation in the Democratic Republic of the Congo?*. Working Paper, .
- Biazin, B., & Sterk, G. (2013). Drought vulnerability drives land-use and land cover changes in the Rift Valley dry lands of Ethiopia. *Agriculture, Ecosystems & Environment*, *164*, 100–113. DOI: <https://doi.org/10.1016/j.agee.2012.09.012>.
- Blaustein-Rejto, D., Blomqvist, L., McNamara, J., & De Kirby, K. (2019). Achieving Peak Pasture: Shrinking Pasture’s Footprint by Spreading the Livestock Revolution, .
- Bloom, A. A., Exbrayat, J.-F., van der Velde, I. R., Feng, L., & Williams, M. (2016). The decadal state of the terrestrial carbon cycle: Global retrievals of terrestrial carbon

- allocation, pools, and residence times. *Proceedings of the National Academy of Sciences*, *113*, 1285–1290. DOI: <https://doi.org/10.1073/pnas.1515160113>.
- Bodart, C., Brink, A. B., Donnay, F., Lupi, A., Mayaux, P., & Achard, F. (2013). Continental estimates of forest cover and forest cover changes in the dry ecosystems of Africa between 1990 and 2000. *Journal of Biogeography*, *40*, 1036–1047. DOI: <https://doi.org/10.1111/jbi.12084>.
- Booth, R. (2021). Farming the future: Transforming the ownership of food systems research & data. <https://www.common-wealth.co.uk/reports/farming-the-future>.
- Bórawski, P., Pawlewicz, A., Parzonko, A., Harper, J., & Holden, L. (2020). Factors Shaping Cow's Milk Production in the EU. *Sustainability*, *12*, 420. DOI: <https://doi.org/10.3390/su12010420>.
- Briske, D. D., Zhao, M., Han, G., Xiu, C., Kemp, D. R., Willms, W., Havstad, K., Kang, L., Wang, Z., Wu, J., Han, X., & Bai, Y. (2015). Strategies to alleviate poverty and grassland degradation in Inner Mongolia: Intensification vs production efficiency of livestock systems. *Journal of Environmental Management*, *152*, 177–182. DOI: <https://doi.org/10.1016/j.jenvman.2014.07.036>.
- Brown, C., Seo, B., Alexander, P., Burton, V., Chacón-Montalván, E. A., Dunford, R., Merkle, M., Harrison, P. A., Prestele, R., Robinson, E. L., & Rounsevell, M. (2022a). Agent-Based Modeling of Alternative Futures in the British Land Use System. *Earth's Future*, *10*, e2022EF002905. DOI: <https://doi.org/10.1029/2022EF002905>.
- Brown, C. F. et al. (2022b). Dynamic World, Near real-time global 10 m land use land cover mapping. *Scientific Data*, *9*, 251. DOI: <https://doi.org/10.1038/s41597-022-01307-4>.
- Bruun, T. B., de Neergaard, A., Lawrence, D., & Ziegler, A. D. (2009). Environmental Consequences of the Demise in Swidden Cultivation in Southeast Asia: Carbon Storage and Soil Quality. *Human Ecology*, *37*, 375–388. DOI: <https://doi.org/10.1007/s10745-009-9257-y>.
- Bruun, T. B., Ryan, C. M., de Neergaard, A., & Berry, N. J. (2021). Soil organic carbon stocks maintained despite intensification of shifting cultivation. *Geoderma*, *388*, 114804. DOI: <https://doi.org/10.1016/j.geoderma.2020.114804>.
- Bryan, B. A. et al. (2018). China's response to a national land-system sustainability emergency. *Nature*, *559*, 193–204. DOI: <https://doi.org/10.1038/s41586-018-0280-2>.
- Buchhorn, M., Smets, B., Bertels, L., Lesiv, M., Tsendbazar, N. E., Herold, M., & Fritz, S. (2020). Copernicus Global Land Service: Land Cover 100m: Collection 3: Epoch 2015-2019: Globe. *Version V3. 0.1*. DOI: <https://doi.org/10.5281/zenodo.3939038>; <https://doi.org/10.5281/zenodo.3518026>; <https://doi.org/10.5281/zenodo.3518026>.

- .5281/zenodo.3518036;https://doi.org/10.5281/zenodo.3518038,https://doi.org/10.5281/zenodo.3939050;.
- Burchfield, E. K., Nelson, K. S., & Spangler, K. (2019). The impact of agricultural landscape diversification on U.S. crop production. *Agriculture, Ecosystems & Environment*, *285*, 106615. DOI: <https://doi.org/10.1016/j.agee.2019.106615>.
- Bürgi, M., Celio, E., Diogo, V., Hersperger, A. M., Kizos, T., Lieskovsky, J., Pazur, R., Plieninger, T., Prishchepov, A. V., & Verburg, P. H. (2022). Advancing the study of driving forces of landscape change. *Journal of Land Use Science*, *0*, 1–16. DOI: <https://doi.org/10.1080/1747423X.2022.2029599>.
- Bürgi, M., Hersperger, A. M., & Schneeberger, N. (2004). Driving forces of landscape change — current and new directions. *Landscape Ecology*, *19*, 857–868. DOI: <https://doi.org/10.1007/s10980-004-0245-8>.
- Busso, C. A., & Fernández, O. A. (2018). Arid and Semiarid Rangelands of Argentina. In M. K. Gaur, & V. R. Squires (Eds.), *Climate Variability Impacts on Land Use and Livelihoods in Drylands* (pp. 261–291). Cham: Springer International Publishing. DOI: [https://doi.org/10.1007/978-3-319-56681-8\\_13](https://doi.org/10.1007/978-3-319-56681-8_13).
- Byerlee, D., Stevenson, J., & Villoria, N. (2014). Does intensification slow crop land expansion or encourage deforestation? *Global Food Security*, *3*, 92–98. DOI: <https://doi.org/10.1016/j.gfs.2014.04.001>.
- Calvin, K., & Bond-Lamberty, B. (2018). Integrated human-earth system modeling—state of the science and future directions. *Environmental Research Letters*, *13*, 063006. DOI: <https://doi.org/10.1088/1748-9326/aac642>.
- CAMS (2020). CAMS global inversion-optimised greenhouse gas fluxes and concentrations. <https://ads.atmosphere.copernicus.eu/cdsapp#!/dataset/cams-global-greenhouse-gas-inversion?tab=overview>.
- CAMS (2021). CAMS global greenhouse gas reanalysis (EGG4) monthly averaged fields. <https://ads.atmosphere.copernicus.eu/cdsapp#!/dataset/cams-global-ghg-reanalysis-egg4-monthly?tab=overview>.
- Cannon, J. (2022). Study tracks global forest decline and expansion over six decades. <https://news.mongabay.com/2022/08/study-tracks-global-forest-decline-and-expansion-over-six-decades/>.
- CDRterra (2022). CDRterra – BMBF research program on land-based CO2 removal (CDR) methods. <https://cdrterra.de/en>.
- Ceccherini, G., Duveiller, G., Grassi, G., Lemoine, G., Avitabile, V., Pilli, R., & Cescatti, A. (2020). Abrupt increase in harvested forest area over Europe after 2015. *Nature*, *583*, 72–77. DOI: <https://doi.org/10.1038/s41586-020-2438-y>.
- Chatham House (2018). Resourcetrade.earth. <http://resourcetrade.earth/>.

- Chen, C. et al. (2019). China and India lead in greening of the world through land-use management. *Nature Sustainability*, 2, 122–129. DOI: <https://doi.org/10.1038/s41893-019-0220-7>.
- Chen, X., & Khanna, M. (2018). Effect of corn ethanol production on Conservation Reserve Program acres in the US. *Applied Energy*, 225, 124–134. DOI: <https://doi.org/10.1016/j.apenergy.2018.04.104>.
- Chen, Y., Li, X., Wang, L., & Wang, S. (2017). Is China different from other investors in global land acquisition? Some observations from existing deals in China's Going Global Strategy. *Land Use Policy*, 60, 362–372. DOI: <https://doi.org/10.1016/j.landuspol.2016.10.045>.
- Chini, L., Hurtt, G., Sahajpal, R., Frohling, S., Klein Goldewijk, K., Sitch, S., Ganzenmüller, R., Ma, L., Ott, L., Pongratz, J., & Poulter, B. (2021). Land-use harmonization datasets for annual global carbon budgets. *Earth System Science Data*, 13, 4175–4189. DOI: <https://doi.org/10.5194/essd-13-4175-2021>.
- Chini, L. P., Hurtt, G. C., & Frohling, S. (2014). LUH1: Harmonized Global Land Use for Years 1500-2100, V1. *ORNL DAAC*, . DOI: <https://doi.org/10.3334/ORNLDAAC/1248>.
- Chuvieco, E., Pettinari, M. L., Lizundia-Loiola, J., Storm, T., & Padilla Parellada, M. (2018). ESA Fire Climate Change Initiative (Fire\_cci): MODIS Fire\_cci Burned Area Pixel product, version 5.1. DOI: <https://doi.org/10.5285/58F00D8814064B79A0C49662AD3AF537>.
- Chuvieco, E., Pettinari, M. L., & Otón, G. (2020). ESA Fire Climate Change Initiative (Fire\_cci): AVHRR-LTDR Burned Area Grid product, version 1.1. DOI: <https://doi.org/10.5285/62866635AB074E07B93F17FBF87A2C1A>.
- Ciais, P. et al. (2019). Five decades of northern land carbon uptake revealed by the interhemispheric CO<sub>2</sub> gradient. *Nature*, 568, 221–225. DOI: <https://doi.org/10.1038/s41586-019-1078-6>.
- Clay, N., Garnett, T., & Lorimer, J. (2020). Dairy intensification: Drivers, impacts and alternatives. *Ambio*, 49, 35–48. DOI: <https://doi.org/10.1007/s13280-019-01177-y>.
- Copernicus Climate Change Service (2021). Soil moisture gridded data from 1978 to present, Land Service: Soil Moisture ECV. <https://cds.climate.copernicus.eu/cdsapp#!/dataset/eu.copernicus.climate.satellite-soil-moisture?tab=overview>.
- Crippa, M., Solazzo, E., Guizzardi, D., Monforti-Ferrario, F., Tubiello, F. N., & Leip, A. (2021). Food systems are responsible for a third of global anthropogenic GHG emissions. *Nature Food*, 2, 198–209. DOI: <https://doi.org/10.1038/s43016-021-00225-9>.

- Curtis, P. G., Slay, C. M., Harris, N. L., Tyukavina, A., & Hansen, M. C. (2018). Classifying drivers of global forest loss. *Science*, *361*, 1108–1111. DOI: <https://doi.org/10.1126/science.aau3445>.
- d'Amour, C. B., Wenz, L., Kalkuhl, M., Steckel, J. C., & Creutzig, F. (2016). Tele-connected food supply shocks. *Environmental Research Letters*, *11*, 035007. DOI: <https://doi.org/10.1088/1748-9326/11/3/035007>.
- Davison, C. W., Rahbek, C., & Morueta-Holme, N. (2021). Land-use change and biodiversity: Challenges for assembling evidence on the greatest threat to nature. *Global Change Biology*, *27*, 5414–5429. DOI: <https://doi.org/10.1111/gcb.15846>.
- Debonne, N., Bürgi, M., Diogo, V., Helfenstein, J., Herzog, F., Levers, C., Mohr, F., Swart, R., & Verburg, P. (2022). The geography of megatrends affecting European agriculture. *Global Environmental Change*, *75*, 102551. DOI: <https://doi.org/10.1016/j.gloenvcha.2022.102551>.
- Deng, Z. et al. (2022). Comparing national greenhouse gas budgets reported in UNFCCC inventories against atmospheric inversions. *Earth System Science Data*, *14*, 1639–1675. DOI: <https://doi.org/10.5194/essd-14-1639-2022>.
- Descals, A., Wich, S., Meijaard, E., Gaveau, D. L. A., Peedell, S., & Szantoi, Z. (2021). High-resolution global map of smallholder and industrial closed-canopy oil palm plantations. *Earth System Science Data*, *13*, 1211–1231. DOI: <https://doi.org/10.5194/essd-13-1211-2021>.
- Di Vittorio, A., Shi, X., Bond-Lamberty, B., Calvin, K., & Jones, A. (2020). Initial Land Use/Cover Distribution Substantially Affects Global Carbon and Local Temperature Projections in the Integrated Earth System Model. *Global Biogeochemical Cycles*, *34*, e2019GB006383. DOI: <https://doi.org/10.1029/2019GB006383>.
- Dias, L. C. P., Pimenta, F. M., Santos, A. B., Costa, M. H., & Ladle, R. J. (2016). Patterns of land use, extensification, and intensification of Brazilian agriculture. *Global Change Biology*, *22*, 2887–2903. DOI: <https://doi.org/10.1111/gcb.13314>.
- Díaz, S. et al. (2015). The IPBES Conceptual Framework — connecting nature and people. *Current Opinion in Environmental Sustainability*, *14*, 1–16. DOI: <https://doi.org/10.1016/j.cosust.2014.11.002>.
- Dolman, A. J., Shvidenko, A., Schepaschenko, D., Ciais, P., Tchepakova, N., Chen, T., van der Molen, M. K., Beletti Marchesini, L., Maximov, T. C., Maksyutov, S., & Schulze, E.-D. (2012). An estimate of the terrestrial carbon budget of Russia using inventory-based, eddy covariance and inversion methods. *Biogeosciences*, *9*, 5323–5340. DOI: <https://doi.org/10.5194/bg-9-5323-2012>.
- Dong, S. (2016). Overview: Pastoralism in the World. In S. Dong, K.-A. S. Kassam, J. F. Tourrand, & R. B. Boone (Eds.), *Building Resilience of Human-Natural Systems of Pastoralism in the Developing World: Interdisciplinary Perspectives* (pp. 1–37). Cham:

- Springer International Publishing. DOI: [https://doi.org/10.1007/978-3-319-30732-9\\_1](https://doi.org/10.1007/978-3-319-30732-9_1).
- Dorigo, W., Preimesberger, W., Moesinger, L., Pasik, A., Scanlon, T., Hahn, S., Van der Schalie, R., Van der Vliet, M., De Jeu, R., Kidd, R., Rodriguez-Fernandez, N., & Hirschi, M. (2020). ESA Soil Moisture Climate Change Initiative (Soil\_Moisture\_cci): Version 05.2 data collection. DOI: <https://doi.org/10.5285/B11F3FA3303E46E6B0D44B058947A3F5>.
- Dornelles, A. Z. et al. (2022). Transformation archetypes in global food systems. *Sustainability Science*, . DOI: <https://doi.org/10.1007/s11625-022-01102-5>.
- Du, Y. et al. (2018). A global strategy to mitigate the environmental impact of China's ruminant consumption boom. *Nature Communications*, 9, 4133. DOI: <https://doi.org/10.1038/s41467-018-06381-0>.
- DuBois, T., & Gao, A. (2017). Big Meat: The Rise and Impact of Mega-Farming in China's Beef, Sheep and Dairy Industries. *Asia-Pacific Journal, Japan Focus*, 15.
- Durant, J. L. (2022). Bees face many challenges – and climate change is ratcheting up the pressure. <http://theconversation.com/bees-face-many-challenges-and-climate-change-is-ratcheting-up-the-pressure-190296>.
- Duveiller, G., Filippini, F., Ceglar, A., Bojanowski, J., Alkama, R., & Cescatti, A. (2021). Revealing the widespread potential of forests to increase low level cloud cover. *Nature Communications*, 12, 4337. DOI: <https://doi.org/10.1038/s41467-021-24551-5>.
- Duveiller, G., Hooker, J., & Cescatti, A. (2018). The mark of vegetation change on Earth's surface energy balance. *Nature Communications*, 9, 679. DOI: <https://doi.org/10.1038/s41467-017-02810-8>.
- Earth, B. (2020). Monthly Land Average Temperature (TAVG; 1753 – Recent) [Dataset] <http://berkeleyearth.org/data/>. <http://berkeleyearth.org/data/>.
- Ebanyat, P., de Ridder, N., de Jager, A., Delve, R. J., Bekunda, M. A., & Giller, K. E. (2010). Drivers of land use change and household determinants of sustainability in smallholder farming systems of Eastern Uganda. *Population and Environment*, 31, 474–506. DOI: <https://doi.org/10.1007/s11111-010-0104-2>.
- Eco-Business (2021). Land-use change has affected 'almost a third' of world's terrain since 1960. <https://www.eco-business.com/news/land-use-change-has-affected-almost-a-third-of-worlds-terrain-since-1960/>.
- EcoWatch (2021). Land-Use Change Has Affected 'Almost a Third' of World's Terrain Since 1960.
- Eggleston, H. S., Buendia, L., Miwa, K., Ngara, T., & Tanabe, K. (2006). *2006 IPCC Guidelines for National Greenhouse Gas Inventories*. Technical Report, .
- Egli, L., Meyer, C., Scherber, C., Kreft, H., & Tschardtke, T. (2018). Winners and losers

- of national and global efforts to reconcile agricultural intensification and biodiversity conservation. *Global Change Biology*, *24*, 2212–2228. DOI: <https://doi.org/10.1111/gcb.14076>.
- Elagib, N. A. (2014). Development and application of a drought risk index for food crop yield in Eastern Sahel. *Ecological Indicators*, *43*, 114–125. DOI: <https://doi.org/10.1016/j.ecolind.2014.02.033>.
- Eldridge, D., & Soliveres, S. (2015). Are shrubs really a sign of declining ecosystem function? Disentangling the myths and truths of woody encroachment in Australia. *Australian Journal of Botany*, *62*, 594–608. DOI: <https://doi.org/10.1071/BT14137>.
- EM-DAT (2021). The international disasters database version 2021-01-20 [Dataset] <https://www.emdat.be/>. <https://www.emdat.be/>.
- Erb, K.-H., Haberl, H., Jepsen, M. R., Kuemmerle, T., Lindner, M., Müller, D., Verburg, P. H., & Reenberg, A. (2013). A conceptual framework for analysing and measuring land-use intensity. *Current Opinion in Environmental Sustainability*, *5*, 464–470. DOI: <https://doi.org/10.1016/j.cosust.2013.07.010>.
- Erb, K.-H. et al. (2017). Land management: Data availability and process understanding for global change studies. *Global Change Biology*, *23*, 512–533. DOI: <https://doi.org/10.1111/gcb.13443>.
- ESA (2017). *Land Cover CCI Product User Guide Version 2*. Technical Report, ESA.
- ESA (2023). WorldCover | Worldwide land cover mapping. <https://esa-worldcover.org/en>.
- Esper, J., & Schweingruber, F. H. (2004). Large-scale treeline changes recorded in Siberia. *Geophysical Research Letters*, *31*. DOI: <https://doi.org/10.1029/2003GL019178>.
- Estel, S., Kuemmerle, T., Alcántara, C., Levers, C., Prishchepov, A., & Hostert, P. (2015). Mapping farmland abandonment and recultivation across Europe using MODIS NDVI time series. *Remote Sensing of Environment*, *163*, 312–325. DOI: <https://doi.org/10.1016/j.rse.2015.03.028>.
- European Commission (2021). *REPORT on the Proposal for a Regulation of the European Parliament and of the Council on Making Available on the Union Market as Well as Export from the Union of Certain Commodities and Products Associated with Deforestation and Forest Degradation and Repealing Regulation (EU) No 995/2010 / A9-0219/2022 | European Parliament*. Technical Report, .
- European Forest Institute (2020). *Russian Forests and Climate Change* volume 11 of *What Science Can Tell Us*. European Forest Institute. DOI: <https://doi.org/10.36333/wsctu11>.
- Evenson, R. E., & Gollin, D. (2003). Assessing the Impact of the Green Revolution, 1960 to 2000. *Science*, *300*, 758–762. DOI: <https://doi.org/10.1126/science.1078710>.

- FAO (2016). FAOSTAT: Machinery [Dataset], Food and Agriculture Organization of the United Nations (FAO), <http://www.fao.org/faostat/en/#data/RM>.
- FAO (2019a). FAOSTAT Land Use [Dataset], Food and Agriculture Organization of the United Nations (FAO), <http://www.fao.org/faostat/en/#data/RL>.
- FAO (2019b). FAOSTAT Population, Annual population [Dataset], Food and Agriculture Organization of the United Nations (FAO), <http://www.fao.org/faostat/en/#data/OA>.
- FAO (2020a). FAOSTAT: Exchange rates - Annual [Dataset], Food and Agriculture Organization of the United Nations (FAO), <http://www.fao.org/faostat/en/#data/PE>.
- FAO (2020b). FAOSTAT: Investment, Foreign Direct Investment (FDI) [Dataset], Food and Agriculture Organization of the United Nations (FAO), <http://www.fao.org/faostat/en/#data/FDI>.
- FAO (2020c). FAOSTAT: Producer price [Dataset], Food and Agriculture Organization of the United Nations (FAO), <http://www.fao.org/faostat/en/#data/PP>.
- FAO (2020d). FAOSTAT Production, crops and livestock products [Dataset], Food and Agriculture Organization of the United Nations (FAO), <http://www.fao.org/faostat/en/#data/QC>.
- FAO (2020e). FAOSTAT Trade, Crops and livestock products [Dataset], Food and Agriculture Organization of the United Nations (FAO), <http://www.fao.org/faostat/en/#data/TP>.
- FAO (2020f). *Global Forest Resources Assessment 2020: Key Findings*, Food and Agriculture Organization of the United Nations (FAO). Rome, Italy: FAO. DOI: <https://doi.org/10.4060/ca8753en>.
- FAO (2021a). FAOSTAT: Food Balances (2014-) and Food Balances (-2013, old methodology and population), 2021/2017 [Dataset], Food and Agriculture Organization of the United Nations (FAO), <http://www.fao.org/faostat/en/#data/FBS>.
- FAO (2021b). FAOSTAT: Forestry, Forestry Production and Trade [Dataset], Food and Agriculture Organization of the United Nations (FAO), <http://www.fao.org/faostat/en/#data/FO/>.
- FAO (2021c). FAOSTAT: Macro Indicators [Dataset], Food and Agriculture Organization of the United Nations (FAO), <http://www.fao.org/faostat/en/#data/MK>.
- FAO (2021d). FAOSTAT: Temperature change [Dataset], Food and Agriculture Organization of the United Nations (FAO), <http://www.fao.org/faostat/en/#data/ET>.
- FAO (2022a). FAOSTAT Forestry Production and Trade [Dataset], last update: December 16, 2021, Food and Agriculture Organization of the United Nations (FAO), <https://www.fao.org/faostat/en/#data/FO>. <https://www.fao.org/faostat/en/#data/QCL>.

- FAO (2022b). FAOSTAT Production, crops and livestock products [Dataset], Food and Agriculture Organization of the United Nations (FAO), <http://www.fao.org/faostat/en/#data/QC>.
- FAO (2022c). FAOSTAT Production, crops and livestock products [Dataset], last update: February 17, 2022, Food and Agriculture Organization of the United Nations (FAO), <http://www.fao.org/faostat/en/#data/QC>. <https://www.fao.org/faostat/en/#data/QCL>.
- FAO (2023). AQUASTAT Core Database. Food and Agriculture Organization of the United Nations. Database accessed on 05/01/2023. [https://tableau.apps.fao.org/views/ReviewDashboard-v1/result\\_country?%3Aembed=y%3AisGuestRedirectFromVizportal=y](https://tableau.apps.fao.org/views/ReviewDashboard-v1/result_country?%3Aembed=y%3AisGuestRedirectFromVizportal=y).
- Feng, M., Sexton, J., Wang, P., Montesano, P., Calle, L., Carvalhais, N., Poulter, B., Wooten, M., Wagner, W., Elders, A., Channan, S., & Neigh, C. (2021). *Northward Migration of the Boreal Forest Confirmed by Satellite Record*. DOI: <https://doi.org/10.21203/rs.3.rs-327560/v1>.
- Feng, X., Fu, B., Piao, S., Wang, S., Ciais, P., Zeng, Z., Lü, Y., Zeng, Y., Li, Y., Jiang, X., & Wu, B. (2016). Revegetation in China's Loess Plateau is approaching sustainable water resource limits. *Nature Climate Change*, 6, 1019–1022. DOI: <https://doi.org/10.1038/nclimate3092>.
- Fischer, G. (2021). *Global Agro-Ecological Zones v4 – Model Documentation*. Rome, Italy: FAO. DOI: <https://doi.org/10.4060/cb4744en>.
- Foley, J. A. et al. (2011). Solutions for a cultivated planet. *Nature*, 478, 337–342. DOI: <https://doi.org/10.1038/nature10452>.
- Foote, R. L., & Grogan, P. (2010). Soil Carbon Accumulation During Temperate Forest Succession on Abandoned Low Productivity Agricultural Lands. *Ecosystems*, 13, 795–812. DOI: <https://doi.org/10.1007/s10021-010-9355-0>.
- Franzke, C. L. E., Ciullo, A., Gilmore, E. A., Matias, D. M., Nagabhatla, N., Orlov, A., Paterson, S. K., Scheffran, J., & Sillmann, J. (2022). Perspectives on tipping points in integrated models of the natural and human Earth system: Cascading effects and telecoupling. *Environmental Research Letters*, 17, 015004. DOI: <https://doi.org/10.1088/1748-9326/ac42fd>.
- Friedl, M. A., & Sulla-Menashe, D. (2019). MCD12Q1 MODIS/Terra+Aqua Land Cover Type Yearly L3 Global 500m SIN Grid V006.
- Friedlingstein, P. et al. (2021). Global Carbon Budget 2021. *Earth System Science Data Discussions*, (pp. 1–191). DOI: <https://doi.org/10.5194/essd-2021-386>.
- Friedlingstein, P. et al. (2022). Global Carbon Budget 2021. *Earth System Science Data*, 14, 1917–2005. DOI: <https://doi.org/10.5194/essd-14-1917-2022>.

- Friedlingstein, P. et al. (2019). Global Carbon Budget 2019. *Earth System Science Data*, 11, 1783–1838. DOI: <https://doi.org/10.5194/essd-11-1783-2019>.
- Friedlingstein, P. et al. (2020). Global Carbon Budget 2020. *Earth System Science Data*, 12, 3269–3340. DOI: <https://doi.org/10.5194/essd-12-3269-2020>.
- Fuchs, R. (2015). *A Data-Driven Reconstruction of Historic Land Cover/Use Change of Europe for the Period 1900 to 2010*. Ph.D. thesis Wageningen University Wageningen.
- Fuchs, R., Alexander, P., Brown, C., Cossar, F., Henry, R. C., & Rounsevell, M. (2019). Why the US–China trade war spells disaster for the Amazon. *Nature*, 567, 451–454. DOI: <https://doi.org/10.1038/d41586-019-00896-2>.
- Fuchs, R., Brown, C., & Rounsevell, M. (2020). Europe’s Green Deal offshores environmental damage to other nations. *Nature*, 586, 671–673. DOI: <https://doi.org/10.1038/d41586-020-02991-1>.
- Fuchs, R., Herold, M., & Verburg, P. H. (2013). A high-resolution and harmonized model approach for reconstructing and analysing historic land changes in Europe. *Biogeosciences*, 10, 1543–1559.
- Fuchs, R., Herold, M., Verburg, P. H., Clevers, J. G., & Eberle, J. (2015a). Gross changes in reconstructions of historic land cover/use for Europe between 1900 and 2010. *Global Change Biology*, 21, 299–313. DOI: <https://doi.org/10.1111/gcb.12714>.
- Fuchs, R., Schulp, C. J. E., Hengeveld, G. M., Verburg, P. H., Clevers, J. G. P. W., Schelhaas, M.-J., & Herold, M. (2016). Assessing the influence of historic net and gross land changes on the carbon fluxes of Europe. *Global Change Biology*, 22, 2526–2539. DOI: <https://doi.org/10.1111/gcb.13191>.
- Fuchs, R., Verburg, P. H., Clevers, J. G., & Herold, M. (2015b). The potential of old maps and encyclopaedias for reconstructing historic European land cover/use change. *Applied Geography*, 59, 43–55. DOI: <https://doi.org/10.1016/j.apgeog.2015.02.013>.
- Ganzenmüller, R., Bultan, S., Winkler, K., Fuchs, R., Zabel, F., & Pongratz, J. (2022). Land-use change emissions based on high-resolution activity data substantially lower than previously estimated. *Environmental Research Letters*, 17, 064050. DOI: <https://doi.org/10.1088/1748-9326/ac70d8>.
- García, V. R., Gaspart, F., Kastner, T., & Meyfroidt, P. (2020). Agricultural intensification and land use change: Assessing country-level induced intensification, land sparing and rebound effect. *Environmental Research Letters*, 15, 085007. DOI: <https://doi.org/10.1088/1748-9326/ab8b14>.
- Garrett, R. D., Grabs, J., Cammelli, F., Gollnow, F., & Levy, S. A. (2022). Should payments for environmental services be used to implement zero-deforestation supply chain policies? The case of soy in the Brazilian Cerrado. *World Development*, 152, 105814. DOI: <https://doi.org/10.1016/j.worlddev.2022.105814>.

- Garrett, R. D., Lambin, E. F., & Naylor, R. L. (2013). Land institutions and supply chain configurations as determinants of soybean planted area and yields in Brazil. *Land Use Policy*, *31*, 385–396. DOI: <https://doi.org/10.1016/j.landusepol.2012.08.002>.
- Gasser, T., Crepin, L., Quilcaille, Y., Houghton, R. A., Ciais, P., & Obersteiner, M. (2020). Historical CO<sub>2</sub> emissions from land use and land cover change and their uncertainty. *Biogeosciences*, *17*, 4075–4101. DOI: <https://doi.org/10.5194/bg-17-4075-2020>.
- Gatti, L. V. et al. (2021). Amazonia as a carbon source linked to deforestation and climate change. *Nature*, *595*, 388–393. DOI: <https://doi.org/10.1038/s41586-021-03629-6>.
- Gaveau, D. L. A., Linkie, M., Suyadi, Levang, P., & Leader-Williams, N. (2009). Three decades of deforestation in southwest Sumatra: Effects of coffee prices, law enforcement and rural poverty. *Biological Conservation*, *142*, 597–605. DOI: <https://doi.org/10.1016/j.biocon.2008.11.024>.
- Gaveau, D. L. A., Sheil, D., Husnayaen, Salim, M. A., Arjasakusuma, S., Ancrenaz, M., Pacheco, P., & Meijaard, E. (2016). Rapid conversions and avoided deforestation: Examining four decades of industrial plantation expansion in Borneo. *Scientific Reports*, *6*, 1–13. DOI: <https://doi.org/10.1038/srep32017>.
- Ghahramani, A., Kingwell, R. S., & Maraseni, T. N. (2020). Land use change in Australian mixed crop-livestock systems as a transformative climate change adaptation. *Agricultural Systems*, *180*, 102791. DOI: <https://doi.org/10.1016/j.agsy.2020.102791>.
- Gibbs, H. K., Brown, S., Niles, J. O., & Foley, J. A. (2007). Monitoring and estimating tropical forest carbon stocks: Making REDD a reality. *Environmental Research Letters*, *2*, 045023. DOI: <https://doi.org/10.1088/1748-9326/2/4/045023>.
- Gibbs, H. K., Ruesch, A. S., Achard, F., Clayton, M. K., Holmgren, P., Ramankutty, N., & Foley, J. A. (2010). Tropical forests were the primary sources of new agricultural land in the 1980s and 1990s. *Proceedings of the National Academy of Sciences*, *107*, 16732–16737. DOI: <https://doi.org/10.1073/pnas.0910275107>.
- Gibon, F., Pellarin, T., Román-Cascón, C., Alhassane, A., Traoré, S., Kerr, Y., Lo Seen, D., & Baron, C. (2018). Millet yield estimates in the Sahel using satellite derived soil moisture time series. *Agricultural and Forest Meteorology*, *262*, 100–109. DOI: <https://doi.org/10.1016/j.agrformet.2018.07.001>.
- Gilbert, M., Nicolas, G., Cinardi, G., Van Boeckel, T. P., Vanwambeke, S. O., Wint, G. R. W., & Robinson, T. P. (2018). Global distribution data for cattle, buffaloes, horses, sheep, goats, pigs, chickens and ducks in 2010. *Scientific Data*, *5*, 180227. DOI: <https://doi.org/10.1038/sdata.2018.227>.
- Gillespie, J., Nehring, R., Sandretto, C., & Hallahan, C. (2010). Forage Outsourcing in the Dairy Sector: The Extent of Use and Impact on Farm Profitability. *Agricultural*

- and Resource Economics Review*, 39, 399–414. DOI: <https://doi.org/10.1017/S1068280500007401>.
- Godde, C. M., Boone, R. B., Ash, A. J., Waha, K., Sloat, L. L., Thornton, P. K., & Herrero, M. (2020). Global rangeland production systems and livelihoods at threat under climate change and variability. *Environmental Research Letters*, 15, 044021. DOI: <https://doi.org/10.1088/1748-9326/ab7395>.
- Godde, C. M., Garnett, T., Thornton, P. K., Ash, A. J., & Herrero, M. (2018). Grazing systems expansion and intensification: Drivers, dynamics, and trade-offs. *Global Food Security*, 16, 93–105. DOI: <https://doi.org/10.1016/j.gfs.2017.11.003>.
- Godfray, H. C. J., Beddington, J. R., Crute, I. R., Haddad, L., Lawrence, D., Muir, J. F., Pretty, J., Robinson, S., Thomas, S. M., & Toulmin, C. (2010). Food Security: The Challenge of Feeding 9 Billion People. *Science*, 327, 812–818. DOI: <https://doi.org/10.1126/science.1185383>.
- Gold, S., Korotkov, A., & Sasse, V. (2006). The development of European forest resources, 1950 to 2000. *Forest Policy and Economics*, 8, 183–192. DOI: <https://doi.org/10.1016/j.forpol.2004.07.002>.
- Goldstein, A. et al. (2020). Protecting irrecoverable carbon in Earth’s ecosystems. *Nature Climate Change*, 10, 287–295. DOI: <https://doi.org/10.1038/s41558-020-0738-8>.
- Google, & World Resources Institute (2023). Dynamic World - 10m global land cover dataset in Google Earth Engine. <https://dynamicworld.app/>.
- Gormley-Gallagher, A. M., Sterl, S., Hirsch, A. L., Seneviratne, S. I., Davin, E. L., & Thiery, W. (2022). Agricultural management effects on mean and extreme temperature trends. *Earth System Dynamics*, 13, 419–438. DOI: <https://doi.org/10.5194/esd-13-419-2022>.
- Grassi, G., Conchedda, G., Federici, S., Abad Viñas, R., Korosuo, A., Melo, J., Rossi, S., Sandker, M., Somogyi, Z., & Tubiello, F. N. (2022). Carbon fluxes from land 2000-2020: Bringing clarity on countries’ reporting. *Earth System Science Data Discussions*, (pp. 1–49). DOI: <https://doi.org/10.5194/essd-2022-104>.
- Grassi, G., House, J., Dentener, F., Federici, S., den Elzen, M., & Penman, J. (2017). The key role of forests in meeting climate targets requires science for credible mitigation. *Nature Climate Change*, 7, 220–226. DOI: <https://doi.org/10.1038/nclimate3227>.
- Grassi, G. et al. (2018). Reconciling global-model estimates and country reporting of anthropogenic forest CO<sub>2</sub> sinks. *Nature Climate Change*, 8, 914–920. DOI: <https://doi.org/10.1038/s41558-018-0283-x>.
- Grassi, G. et al. (2021). Critical adjustment of land mitigation pathways for assessing countries’ climate progress. *Nature Climate Change*, 11, 425–434. DOI: <https://doi.org/10.1038/s41558-021-01033-6>.

- Green, J. K., Seneviratne, S. I., Berg, A. M., Findell, K. L., Hagemann, S., Lawrence, D. M., & Gentile, P. (2019). Large influence of soil moisture on long-term terrestrial carbon uptake. *Nature*, *565*, 476–479. DOI: <https://doi.org/10.1038/s41586-018-0848-x>.
- Griffin, P. (2021). Global snapshot of land use reveals humanity's massive impact. <https://www.stuff.co.nz/science/300307107/global-snapshot-of-land-use-reveals-humanity-s-massive-impact>.
- Griscom, B. W. et al. (2017). Natural climate solutions. *Proceedings of the National Academy of Sciences*, *114*, 11645–11650. DOI: <https://doi.org/10.1073/pnas.1710465114>.
- Grogan, D., Frohling, S., Wisser, D., Prusevich, A., & Glidden, S. (2022). Global gridded crop harvested area, production, yield, and monthly physical area data circa 2015. *Scientific Data*, *9*, 15. DOI: <https://doi.org/10.1038/s41597-021-01115-2>.
- Haddad, N. M. et al. (2015). Habitat fragmentation and its lasting impact on Earth's ecosystems. *Science Advances*, .
- Hanan, N. P., & Anchang, J. Y. (2020). Satellites could soon map every tree on Earth. *Nature*, *587*, 42–43. DOI: <https://doi.org/10.1038/d41586-020-02830-3>.
- Hansen, M. C. et al. (2013). High-Resolution Global Maps of 21st-Century Forest Cover Change. *Science*, *342*, 850–853. DOI: <https://doi.org/10.1126/science.1244693>.
- Hansis, E., Davis, S. J., & Pongratz, J. (2015). Relevance of methodological choices for accounting of land use change carbon fluxes. *Global Biogeochemical Cycles*, *29*, 1230–1246. DOI: <https://doi.org/10.1002/2014GB004997>.
- Harper, A. B. et al. (2018). Land-use emissions play a critical role in land-based mitigation for Paris climate targets. *Nature Communications*, *9*, 2938. DOI: <https://doi.org/10.1038/s41467-018-05340-z>.
- Harris, N., Goldman, E. D., & Gibbes, S. (2019). "Spatial Database of Planted Trees Version 1.0." Technical Note. Washington, DC: World Resources Institute. Available online at: <https://www.wri.org/research/spatial-database-planted-trees-sdpt-version-10>.
- Harris, N. L. et al. (2021). Global maps of twenty-first century forest carbon fluxes. *Nature Climate Change*, (pp. 1–7). DOI: <https://doi.org/10.1038/s41558-020-00976-6>.
- Hartung, K., Bastos, A., Chini, L., Ganzenmüller, R., Havermann, F., Hurtt, G. C., Loughran, T., Nabel, J. E. M. S., Nützel, T., Obermeier, W. A., & Pongratz, J. (2021). Bookkeeping estimates of the net land-use change flux – a sensitivity study with the CMIP6 land-use dataset. *Earth System Dynamics*, *12*, 763–782. DOI: <https://doi.org/10.5194/esd-12-763-2021>.
- Heinimann, A., Mertz, O., Frohling, S., Christensen, A. E., Hurni, K., Sedano, F., Chini, L. P., Sahajpal, R., Hansen, M., & Hurtt, G. (2017). A global view of shift-

- ing cultivation: Recent, current, and future extent. *PLOS ONE*, *12*, e0184479. DOI: <https://doi.org/10.1371/journal.pone.0184479>.
- Heistermann, M., Müller, C., & Ronneberger, K. (2006). Land in sight? Achievements, deficits and potentials of continental to global scale land-use modeling. *Agriculture, Ecosystems & Environment*, *114*, 141–158. DOI: <https://doi.org/10.1016/j.agee.2005.11.015>.
- Henchiri, M., Liu, Q., Essifi, B., Javed, T., Zhang, S., Bai, Y., & Zhang, J. (2020). Spatio-Temporal Patterns of Drought and Impact on Vegetation in North and West Africa Based on Multi-Satellite Data. *Remote Sensing*, *12*, 3869. DOI: <https://doi.org/10.3390/rs12233869>.
- Hendricks, N. P., & Er, E. (2018). Changes in cropland area in the United States and the role of CRP. *Food Policy*, *75*, 15–23. DOI: <https://doi.org/10.1016/j.foodpol.2018.02.001>.
- Hoegh-Guldberg, O. et al. (2019). The human imperative of stabilizing global climate change at 1.5°C. *Science*, *365*, eaaw6974. DOI: <https://doi.org/10.1126/science.aaw6974>.
- Holechek, J. L., Cibils, A. F., Bengaly, K., & Kinyamario, J. I. (2017). Human Population Growth, African Pastoralism, and Rangelands: A Perspective. *Rangeland Ecology & Management*, *70*, 273–280. DOI: <https://doi.org/10.1016/j.rama.2016.09.004>.
- Holmes, J. (2002). Diversity and change in Australia's rangelands: A post-productivist transition with a difference? *Transactions of the Institute of British Geographers*, *27*, 362–384. DOI: <https://doi.org/10.1111/1475-5661.00059>.
- Hong, C., Burney, J. A., Pongratz, J., Nabel, J. E. M. S., Mueller, N. D., Jackson, R. B., & Davis, S. J. (2021). Global and regional drivers of land-use emissions in 1961–2017. *Nature*, *589*, 554–561. DOI: <https://doi.org/10.1038/s41586-020-03138-y>.
- Hood, M. (2021). Nearly a fifth of Earth's surface transformed since 1960. <https://www.ctvnews.ca/climate-and-environment/nearly-a-fifth-of-earth-s-surface-transformed-since-1960-1.5423631>.
- Houghton, R. A., & Nassikas, A. A. (2017). Global and regional fluxes of carbon from land use and land cover change 1850–2015. *Global Biogeochemical Cycles*, *31*, 456–472. DOI: <https://doi.org/10.1002/2016GB005546>.
- Hruska, T., Huntsinger, L., Brunson, M., Li, W., Marshall, N., Oviedo, J. L., & Whitcomb, H. (2017). Rangelands as Social–Ecological Systems. In D. D. Briske (Ed.), *Rangeland Systems: Processes, Management and Challenges* Springer Series on Environmental Management (pp. 263–302). Cham: Springer International Publishing. DOI: [https://doi.org/10.1007/978-3-319-46709-2\\_8](https://doi.org/10.1007/978-3-319-46709-2_8).
- Hu, Q., Xiang, M., Chen, D., Zhou, J., Wu, W., & Song, Q. (2020). Global cropland

- intensification surpassed expansion between 2000 and 2010: A spatio-temporal analysis based on GlobeLand30. *Science of The Total Environment*, 746, 141035. DOI: <https://doi.org/10.1016/j.scitotenv.2020.141035>.
- Hua, L., & Squires, V. R. (2015). Managing China's pastoral lands: Current problems and future prospects. *Land Use Policy*, 43, 129–137. DOI: <https://doi.org/10.1016/j.landusepol.2014.11.004>.
- Humphrey, V., Berg, A., Ciais, P., Gentine, P., Jung, M., Reichstein, M., Seneviratne, S. I., & Frankenberg, C. (2021). Soil moisture–atmosphere feedback dominates land carbon uptake variability. *Nature*, 592, 65–69. DOI: <https://doi.org/10.1038/s41586-021-03325-5>.
- Hurt, G. C. et al. (2020). Harmonization of Global Land-Use Change and Management for the Period 850-2100 (LUH2) for CMIP6. *Geoscientific Model Development Discussions*, (pp. 1–65). DOI: <https://doi.org/10.5194/gmd-2019-360>.
- Hurt, G. C. et al. (2011). Harmonization of land-use scenarios for the period 1500–2100: 600 years of global gridded annual land-use transitions, wood harvest, and resulting secondary lands. *Climatic Change*, 109, 117–161. DOI: <https://doi.org/10.1007/s10584-011-0153-2>.
- Iizumi, T., & Sakai, T. (2020). The global dataset of historical yields for major crops 1981–2016. *Scientific Data*, 7, 97. DOI: <https://doi.org/10.1038/s41597-020-0433-7>.
- Ikuemonisan, E. S., Mafimisebi, T. E., Ajibefun, I., & Adenegan, K. (2020). Cassava production in Nigeria: Trends, instability and decomposition analysis (1970–2018). *Heliyon*, 6, e05089. DOI: <https://doi.org/10.1016/j.heliyon.2020.e05089>.
- International Labour Organization (ILO) (2020a). Indicator description: Earnings and labour cost. <https://ilostat.ilo.org/resources/concepts-and-definitions/description-earnings-and-labour-cost/>.
- International Labour Organization (ILO) (2020b). Indicator description: Labour force participation rate. <https://ilostat.ilo.org/resources/concepts-and-definitions/description-labour-force-participation-rate/>.
- IPBES (2019). *Global Assessment Report on Biodiversity and Ecosystem Services of the Intergovernmental Science-Policy Platform on Biodiversity and Ecosystem Services*. [E. S. Brondizio, J. Settele, S. Díaz, and H. T. Ngo (Eds.)]. Bonn, Germany: IPBES secretariat.
- IPCC (2019a). *2019 Refinement to the 2006 IPCC Guidelines for National Greenhouse Gas Inventories*. IPCC.
- IPCC (2019b). *Climate Change and Land: An IPCC Special Report on Climate Change, Desertification, Land Degradation, Sustainable Land Management, Food Security, and*

- Greenhouse Gas Fluxes in Terrestrial Ecosystems*. [P.R. Shukla, J. Skea, E. Calvo Buendia, V. Masson-Delmotte, H.-O. Pörtner, D. C. Roberts, P. Zhai, R. Slade, S. Connors, R. van Diemen, M. Ferrat, E. Haughey, S. Luz, S. Neogi, M. Pathak, J. Petzold, J. Portugal Pereira, P. Vyas, E. Huntley, K. Kissick, M. Belkacemi, J. Malley, (Eds.)]. IPCC.
- IPCC (2022). Climate Change 2022: Mitigation of Climate Change, Intergovernmental Panel on Climate Change Working Group III contribution to the Sixth Assessment Report. <https://www.ipcc.ch/report/ar6/wg3/>.
- Jew, E. K. K., Dougill, A. J., & Sallu, S. M. (2017). Tobacco cultivation as a driver of land use change and degradation in the miombo woodlands of south-west Tanzania. *Land Degradation & Development*, 28, 2636–2645. DOI: <https://doi.org/10.1002/ldr.2827>.
- Jia, G. et al. (2019). SPM2 Land–climate interactions. In *Climate Change and Land: An IPCC Special Report on Climate Change, Desertification, Land Degradation, Sustainable Land Management, Food Security, and Greenhouse Gas Fluxes in Terrestrial Ecosystems* In Press (p. 118). IPCC.
- Jiang, F., He, W., Ju, W., Wang, H., Wu, M., Wang, J., Feng, S., Zhang, L., & Chen, J. M. (2022). The status of carbon neutrality of the world’s top 5 CO<sub>2</sub> emitters as seen by carbon satellites. *Fundamental Research*, 2, 357–366. DOI: <https://doi.org/10.1016/j.fmre.2022.02.001>.
- Jiang, L., Deng, X., & Seto, K. C. (2013). The impact of urban expansion on agricultural land use intensity in China. *Land Use Policy*, 35, 33–39. DOI: <https://doi.org/10.1016/j.landusepol.2013.04.011>.
- Junquera, V., Meyfroidt, P., Sun, Z., Latthachack, P., & Grêt-Regamey, A. (2020). From global drivers to local land-use change: Understanding the northern Laos rubber boom. *Environmental Science & Policy*, 109, 103–115. DOI: <https://doi.org/10.1016/j.envsci.2020.04.013>.
- Kaimowitz, D., & Angelsen, A. (2008). Will Livestock Intensification Help Save Latin America’s Tropical Forests? *Journal of Sustainable Forestry*, 27, 6–24. DOI: <https://doi.org/10.1080/10549810802225168>.
- Kaplan, J. O., Krumhardt, K. M., Ellis, E. C., Ruddiman, W. F., Lemmen, C., & Goldewijk, K. K. (2010). Holocene carbon emissions as a result of anthropogenic land cover change. *The Holocene*, 21, 775–791. DOI: <https://doi.org/10.1177/0959683610386983>.
- Kaplan, J. O., Krumhardt, K. M., & Zimmermann, N. E. (2012). The effects of land use and climate change on the carbon cycle of Europe over the past 500 years. *Global Change Biology*, 18, 902–914. DOI: <https://doi.org/10.1111/j.1365-2486.2011.02580.x>.
- Kastner, T. et al. (2022). Land use intensification increasingly drives the spatiotemporal

- patterns of the global human appropriation of net primary production in the last century. *Global Change Biology*, *28*, 307–322. DOI: <https://doi.org/10.1111/gcb.15932>.
- Kaufmann, D., Kraay, A., & Mastruzzi, M. (2010). *The Worldwide Governance Indicators: Methodology and Analytical Issues*. SSRN Scholarly Paper ID 1682130, Social Science Research Network Rochester, NY.
- Kauppi, P. E., Ausubel, J. H., Fang, J., Mather, A. S., Sedjo, R. A., & Waggoner, P. E. (2006). Returning forests analyzed with the forest identity. *Proceedings of the National Academy of Sciences*, *103*, 17574–17579. DOI: <https://doi.org/10.1073/pnas.0608343103>.
- Keenan, R. J., Reams, G. A., Achard, F., de Freitas, J. V., Grainger, A., & Lindquist, E. (2015). Dynamics of global forest area: Results from the FAO Global Forest Resources Assessment 2015. *Forest Ecology and Management*, *352*, 9–20. DOI: <https://doi.org/10.1016/j.foreco.2015.06.014>.
- Kharuk, V. I., Ranson, K. J., Im, S. T., Oskorbin, P. A., Dvinskaya, M. L., & Ovchinnikov, D. V. (2013). Tree-Line Structure and Dynamics at the Northern Limit of the Larch Forest: Anabar Plateau, Siberia, Russia. *Arctic, Antarctic, and Alpine Research*, *45*, 526–537. DOI: <https://doi.org/10.1657/1938-4246-45.4.526>.
- Kleemann, J., Baysal, G., Bulley, H. N. N., & Fürst, C. (2017). Assessing driving forces of land use and land cover change by a mixed-method approach in north-eastern Ghana, West Africa. *Journal of Environmental Management*, *196*, 411–442. DOI: <https://doi.org/10.1016/j.jenvman.2017.01.053>.
- Klein, T., Nilsson, M., Persson, A., & Håkansson, B. (2017). From Open Data to Open Analyses—New Opportunities for Environmental Applications? *Environments*, *4*, 32. DOI: <https://doi.org/10.3390/environments4020032>.
- Klein Goldewijk, K. (2001). Estimating global land use change over the past 300 years: The HYDE Database. *Global Biogeochemical Cycles*, *15*, 417–433. DOI: <https://doi.org/10.1029/1999GB001232>.
- Klein Goldewijk, K., Beusen, A., Doelman, J., & Stehfest, E. (2017). Anthropogenic land use estimates for the Holocene – HYDE 3.2. *Earth System Science Data*, *9*, 927–953. DOI: <https://doi.org/10.5194/essd-9-927-2017>.
- Klein Goldewijk, K., Beusen, A., & Janssen, P. (2010). Long-term dynamic modeling of global population and built-up area in a spatially explicit way: HYDE 3.1. *The Holocene*, *20*, 565–573. DOI: <https://doi.org/10.1177/0959683609356587>.
- Klein Goldewijk, K., Beusen, A., Van Drecht, G., & De Vos, M. (2011). The HYDE 3.1 spatially explicit database of human-induced global land-use change over the past 12,000 years: HYDE 3.1 Holocene land use. *Global Ecology and Biogeography*, *20*, 73–86. DOI: <https://doi.org/10.1111/j.1466-8238.2010.00587.x>.

- Klein Goldewijk, K., & Ramankutty, N. (2004). Land cover change over the last three centuries due to human activities: The availability of new global data sets. *GeoJournal*, *61*, 335–344. DOI: <https://doi.org/10.1007/s10708-004-5050-z>.
- Koh, L. P., & Wilcove, D. S. (2008). Is oil palm agriculture really destroying tropical biodiversity? *Conservation Letters*, *1*, 60–64. DOI: <https://doi.org/10.1111/j.1755-263X.2008.00011.x>.
- Kondo, M. et al. (2022). Are Land-Use Change Emissions in Southeast Asia Decreasing or Increasing? *Global Biogeochemical Cycles*, *36*, e2020GB006909. DOI: <https://doi.org/10.1029/2020GB006909>.
- Krausmann, F., & Langthaler, E. (2019). Food regimes and their trade links: A socio-ecological perspective. *Ecological Economics*, *160*, 87–95. DOI: <https://doi.org/10.1016/j.ecolecon.2019.02.011>.
- Kroeger, A., Bakhtary, H., Haupt, F., & Streck, C. (2017). *Eliminating Deforestation from the Cocoa Supply Chain*. World Bank.
- Kuemmerle, T. et al. (2013). Challenges and opportunities in mapping land use intensity globally. *Current Opinion in Environmental Sustainability*, *5*, 484–493. DOI: <https://doi.org/10.1016/j.cosust.2013.06.002>.
- Kuemmerle, T., Kaplan, J. O., Prishchepov, A. V., Rylsky, I., Chaskovskyy, O., Tikunov, V. S., & Müller, D. (2015). Forest transitions in Eastern Europe and their effects on carbon budgets. *Global Change Biology*, *21*, 3049–3061. DOI: <https://doi.org/10.1111/gcb.12897>.
- Kühling, I., Broll, G., & Trautz, D. (2016). Spatio-temporal analysis of agricultural land-use intensity across the Western Siberian grain belt. *Science of The Total Environment*, *544*, 271–280. DOI: <https://doi.org/10.1016/j.scitotenv.2015.11.129>.
- Kurganova, I., Lopes de Gerenyu, V., & Kuzyakov, Y. (2015). Large-scale carbon sequestration in post-agrogenic ecosystems in Russia and Kazakhstan. *CATENA*, *133*, 461–466. DOI: <https://doi.org/10.1016/j.catena.2015.06.002>.
- Lambin, E. F., Geist, H. J., & Lepers, E. (2003). Dynamics of Land-Use and Land-Cover Change in Tropical Regions. *Annual Review of Environment and Resources*, *28*, 205–241. DOI: <https://doi.org/10.1146/annurev.energy.28.050302.105459>.
- Lambin, E. F. et al. (2018). The role of supply-chain initiatives in reducing deforestation. *Nature Climate Change*, *8*, 109–116. DOI: <https://doi.org/10.1038/s41558-017-0061-1>.
- Lambin, E. F., & Meyfroidt, P. (2011). Global land use change, economic globalization, and the looming land scarcity. *Proceedings of the National Academy of Sciences*, *108*, 3465–3472. DOI: <https://doi.org/10.1073/pnas.1100480108>.
- Landholm, D. M., Pradhan, P., & Kropp, J. P. (2019). Diverging forest land use dynamics

- induced by armed conflict across the tropics. *Global Environmental Change*, *56*, 86–94. DOI: <https://doi.org/10.1016/j.gloenvcha.2019.03.006>.
- Lapola, D. M., Schaldach, R., Alcamo, J., Bondeau, A., Koch, J., Koelking, C., & Priess, J. A. (2010). Indirect land-use changes can overcome carbon savings from biofuels in Brazil. *Proceedings of the National Academy of Sciences*, *107*, 3388–3393. DOI: <https://doi.org/10.1073/pnas.0907318107>.
- Lark, T. J., Hendricks, N. P., Smith, A., Pates, N., Spawn-Lee, S. A., Bougie, M., Booth, E. G., Kucharik, C. J., & Gibbs, H. K. (2022). Environmental outcomes of the US Renewable Fuel Standard. *Proceedings of the National Academy of Sciences*, *119*, e2101084119. DOI: <https://doi.org/10.1073/pnas.2101084119>.
- Lark, T. J., Salmon, J. M., & Gibbs, H. K. (2015). Cropland expansion outpaces agricultural and biofuel policies in the United States. *Environmental Research Letters*, *10*, 044003. DOI: <https://doi.org/10.1088/1748-9326/10/4/044003>.
- Le Provost, G., Badenhauer, I., Le Bagousse-Pinguet, Y., Clough, Y., Henckel, L., Violle, C., Bretagnolle, V., Roncoroni, M., Manning, P., & Gross, N. (2020). Land-use history impacts functional diversity across multiple trophic groups. *Proceedings of the National Academy of Sciences*, *117*, 1573–1579. DOI: <https://doi.org/10.1073/pnas.1910023117>.
- Le Quéré, C. et al. (2013). The global carbon budget 1959–2011. *Earth System Science Data*, *5*, 165–185. DOI: <https://doi.org/10.5194/essd-5-165-2013>.
- Le Quéré, C. et al. (2018a). Global Carbon Budget 2018. *Earth System Science Data*, *10*, 2141–2194. DOI: <https://doi.org/10.5194/essd-10-2141-2018>.
- Le Quéré, C. et al. (2018b). Global Carbon Budget 2017. *Earth System Science Data*, *10*, 405–448. DOI: <https://doi.org/10.5194/essd-10-405-2018>.
- Lerner, A. M., Zuluaga, A. F., Chará, J., Etter, A., & Searchinger, T. (2017). Sustainable Cattle Ranching in Practice: Moving from Theory to Planning in Colombia’s Livestock Sector. *Environmental Management*, *60*, 176–184. DOI: <https://doi.org/10.1007/s00267-017-0902-8>.
- Lesiv, M. et al. (2022). Global forest management data for 2015 at a 100 m resolution. *Scientific Data*, *9*, 199. DOI: <https://doi.org/10.1038/s41597-022-01332-3>.
- Lesiv, M. et al. (2018). Spatial distribution of arable and abandoned land across former Soviet Union countries. *Scientific Data*, *5*, 1–12. DOI: <https://doi.org/10.1038/sdata.2018.56>.
- Lewis, S. L., Wheeler, C. E., Mitchard, E. T. A., & Koch, A. (2019). Restoring natural forests is the best way to remove atmospheric carbon. *Nature*, *568*, 25–28. DOI: <https://doi.org/10.1038/d41586-019-01026-8>.
- Li, D., Hruska, T., Talinbayi, S., & Li, W. (2019). Changing Agro-Pastoral Livelihoods

- under Collective and Private Land Use in Xinjiang, China. *Sustainability*, *11*, 166. DOI: <https://doi.org/10.3390/su11010166>.
- Li, W., MacBean, N., Ciais, P., Defourny, P., Lamarche, C., Bontemps, S., Houghton, R. A., & Peng, S. (2018). Gross and net land cover changes in the main plant functional types derived from the annual ESA CCI land cover maps (1992–2015). *Earth System Science Data*, *10*, 219–234. DOI: <https://doi.org/10.5194/essd-10-219-2018>.
- Licker, R., Johnston, M., Foley, J. A., Barford, C., Kucharik, C. J., Monfreda, C., & Ramankutty, N. (2010). Mind the gap: How do climate and agricultural management explain the ‘yield gap’ of croplands around the world?: Investigating drivers of global crop yield patterns. *Global Ecology and Biogeography*, *19*, 769–782. DOI: <https://doi.org/10.1111/j.1466-8238.2010.00563.x>.
- Lindroth, A., Lagergren, F., Grelle, A., Klemedtsson, L., Langvall, O., Weslien, P., & Tuulik, J. (2009). Storms can cause Europe-wide reduction in forest carbon sink. *Global Change Biology*, *15*, 346–355. DOI: <https://doi.org/10.1111/j.1365-2486.2008.01719.x>.
- Liu, H., Gong, P., Wang, J., Clinton, N., Bai, Y., & Liang, S. (2020). Annual dynamics of global land cover and its long-term changes from 1982 to 2015. *Earth System Science Data*, *12*, 1217–1243. DOI: <https://doi.org/10.5194/essd-12-1217-2020>.
- Liu, T., & Yang, X. (2015). Land Change Modeling: Status and Challenges. In J. Li, & X. Yang (Eds.), *Monitoring and Modeling of Global Changes: A Geomatics Perspective* (pp. 3–16). Dordrecht: Springer Netherlands. DOI: [https://doi.org/10.1007/978-94-017-9813-6\\_1](https://doi.org/10.1007/978-94-017-9813-6_1).
- Liu, X., Zheng, J., Yu, L., Hao, P., Chen, B., Xin, Q., Fu, H., & Gong, P. (2021). Annual dynamic dataset of global cropping intensity from 2001 to 2019. *Scientific Data*, *8*, 283. DOI: <https://doi.org/10.1038/s41597-021-01065-9>.
- Liu, Y. Y., van Dijk, A. I. J. M., de Jeu, R. A. M., Canadell, J. G., McCabe, M. F., Evans, J. P., & Wang, G. (2015). Recent reversal in loss of global terrestrial biomass. *Nature Climate Change*, *5*, 470–474. DOI: <https://doi.org/10.1038/nclimate2581>.
- Llopis, J. C., Harimalala, P. C., Bär, R., Heinimann, A., Rabemananjara, Z. H., & Zaehring, J. G. (2019). Effects of protected area establishment and cash crop price dynamics on land use transitions 1990–2017 in north-eastern Madagascar. *Journal of Land Use Science*, *14*, 52–80. DOI: <https://doi.org/10.1080/1747423X.2019.1625979>.
- Luyssaert, S. et al. (2014). Land management and land-cover change have impacts of similar magnitude on surface temperature. *Nature Climate Change*, *4*, 389–393. DOI: <https://doi.org/10.1038/nclimate2196>.
- Macedo, M. N., DeFries, R. S., Morton, D. C., Stickler, C. M., Galford, G. L., & Shimabukuro, Y. E. (2012). Decoupling of deforestation and soy production in the

- southern Amazon during the late 2000s. *Proceedings of the National Academy of Sciences*, *109*, 1341–1346. DOI: <https://doi.org/10.1073/pnas.1111374109>.
- Macrotrends LLC (2010). Crude Oil Prices - 70 Year Historical Chart. <https://www.macrotrends.net/1369/crude-oil-price-history-chart>.
- Malins, C., Plevin, R., & Edwards, R. (2020). How robust are reductions in modeled estimates from GTAP-BIO of the indirect land use change induced by conventional biofuels? *Journal of Cleaner Production*, *258*, 120716. DOI: <https://doi.org/10.1016/j.jclepro.2020.120716>.
- Marques, A. et al. (2019). Increasing impacts of land use on biodiversity and carbon sequestration driven by population and economic growth. *Nature Ecology & Evolution*, *3*, 628–637. DOI: <https://doi.org/10.1038/s41559-019-0824-3>.
- Matson, P. A., & Vitousek, P. M. (2006). Agricultural Intensification: Will Land Spared from Farming be Land Spared for Nature? *Conservation Biology*, *20*, 709–710. DOI: <https://doi.org/10.1111/j.1523-1739.2006.00442.x>.
- Maxwell, S. L., Evans, T., Watson, J. E. M., Morel, A., Grantham, H., Duncan, A., Harris, N., Potapov, P., Runting, R. K., Venter, O., Wang, S., & Malhi, Y. (2019). Degradation and forgone removals increase the carbon impact of intact forest loss by 626%. *Science Advances*, *5*, eaax2546. DOI: <https://doi.org/10.1126/sciadv.aax2546>.
- McManus, C., Barcellos, J. O. J., Formenton, B. K., Hermuche, P. M., Jr, O. A. d. C., Guimarães, R., Gianezini, M., Dias, E. A., Lampert, V. d. N., Zago, D., & Neto, J. B. (2016). Dynamics of Cattle Production in Brazil. *PLOS ONE*, *11*, e0147138. DOI: <https://doi.org/10.1371/journal.pone.0147138>.
- McNicol, I. M., Berry, N. J., Bruun, T. B., Hergoualc'h, K., Mertz, O., de Neergaard, A., & Ryan, C. M. (2015). Development of allometric models for above and belowground biomass in swidden cultivation fallows of Northern Laos. *Forest Ecology and Management*, *357*, 104–116. DOI: <https://doi.org/10.1016/j.foreco.2015.07.029>.
- Mechiche-Alami, A., Piccardi, C., Nicholas, K. A., & Seaquist, J. W. (2019). Transnational land acquisitions beyond the food and financial crises. *Environmental Research Letters*, *14*, 084021. DOI: <https://doi.org/10.1088/1748-9326/ab2e4b>.
- Meiyappan, P., Dalton, M., O'Neill, B. C., & Jain, A. K. (2014). Spatial modeling of agricultural land use change at global scale. *Ecological Modelling*, *291*, 152–174. DOI: <https://doi.org/10.1016/j.ecolmodel.2014.07.027>.
- Mertz, O., Padoch, C., Fox, J., Cramb, R. A., Leisz, S. J., Lam, N. T., & Vien, T. D. (2009). Swidden Change in Southeast Asia: Understanding Causes and Consequences. *Human Ecology*, *37*, 259–264. DOI: <https://doi.org/10.1007/s10745-009-9245-2>.
- Meyfroidt, P., Börner, J., Garrett, R., Gardner, T., Godar, J., Kis-Katos, K., Soares-Filho, B. S., & Wunder, S. (2020). Focus on leakage and spillovers: Informing land-use

- governance in a tele-coupled world. *Environmental Research Letters*, 15, 090202. DOI: <https://doi.org/10.1088/1748-9326/ab7397>.
- Meyfroidt, P. et al. (2022). Ten facts about land systems for sustainability. *Proceedings of the National Academy of Sciences*, 119, e2109217118. DOI: <https://doi.org/10.1073/pnas.2109217118>.
- Meyfroidt, P., Lambin, E. F., Erb, K.-H., & Hertel, T. W. (2013). Globalization of land use: Distant drivers of land change and geographic displacement of land use. *Current Opinion in Environmental Sustainability*, 5, 438–444. DOI: <https://doi.org/10.1016/j.cosust.2013.04.003>.
- Meyfroidt, P. et al. (2018). Middle-range theories of land system change. *Global Environmental Change*, 53, 52–67. DOI: <https://doi.org/10.1016/j.gloenvcha.2018.08.006>.
- Meyfroidt, P., Rudel, T. K., & Lambin, E. F. (2010). Forest transitions, trade, and the global displacement of land use. *Proceedings of the National Academy of Sciences*, 107, 20917–20922. DOI: <https://doi.org/10.1073/pnas.1014773107>.
- Meyfroidt, P., Schierhorn, F., Prishchepov, A. V., Müller, D., & Kuemmerle, T. (2016). Drivers, constraints and trade-offs associated with recultivating abandoned cropland in Russia, Ukraine and Kazakhstan. *Global Environmental Change*, 37, 1–15. DOI: <https://doi.org/10.1016/j.gloenvcha.2016.01.003>.
- Mitchard, E. T. A., & Flintrop, C. M. (2013). Woody encroachment and forest degradation in sub-Saharan Africa's woodlands and savannas 1982–2006. *Philosophical Transactions of the Royal Society B: Biological Sciences*, 368, 20120406. DOI: <https://doi.org/10.1098/rstb.2012.0406>.
- Moesinger, L., Dorigo, W., de Jeu, R., van der Schalie, R., Scanlon, T., Teubner, I., & Forkel, M. (2020). The global long-term microwave Vegetation Optical Depth Climate Archive (VODCA). *Earth System Science Data*, 12, 177–196. DOI: <https://doi.org/10.5194/essd-12-177-2020>.
- Mon, M. S., Mizoue, N., Htun, N. Z., Kajisa, T., & Yoshida, S. (2012). Factors affecting deforestation and forest degradation in selectively logged production forest: A case study in Myanmar. *Forest Ecology and Management*, 267, 190–198. DOI: <https://doi.org/10.1016/j.foreco.2011.11.036>.
- Monfreda, C., Ramankutty, N., & Foley, J. A. (2008). Farming the planet: 2. Geographic distribution of crop areas, yields, physiological types, and net primary production in the year 2000: GLOBAL CROP AREAS AND YIELDS IN 2000. *Global Biogeochemical Cycles*, 22, n/a–n/a. DOI: <https://doi.org/10.1029/2007GB002947>.
- Monteil, G. et al. (2020). The regional European atmospheric transport inversion comparison, EUROCOM: First results on European-wide terrestrial carbon fluxes for the period 2006–2015. *Atmospheric Chemistry and Physics*, 20, 12063–12091. DOI:

- <https://doi.org/10.5194/acp-20-12063-2020>.
- Mueller, N. D., Gerber, J. S., Johnston, M., Ray, D. K., Ramankutty, N., & Foley, J. A. (2012). Closing yield gaps through nutrient and water management. *Nature*, *490*, 254–257. DOI: <https://doi.org/10.1038/nature11420>.
- Munteanu, C. et al. (2014). Forest and agricultural land change in the Carpathian region—A meta-analysis of long-term patterns and drivers of change. *Land Use Policy*, *38*, 685–697. DOI: <https://doi.org/10.1016/j.landusepol.2014.01.012>.
- Murray-Rust, D., Brown, C., van Vliet, J., Alam, S. J., Robinson, D. T., Verburg, P. H., & Rounsevell, M. (2014). Combining agent functional types, capitals and services to model land use dynamics. *Environmental Modelling & Software*, *59*, 187–201. DOI: <https://doi.org/10.1016/j.envsoft.2014.05.019>.
- Nabuurs, G.-J., Lindner, M., Verkerk, P. J., Gunia, K., Deda, P., Michalak, R., & Grassi, G. (2013). First signs of carbon sink saturation in European forest biomass. *Nature Climate Change*, *3*, 792–796. DOI: <https://doi.org/10.1038/nclimate1853>.
- Nackoney, J., Molinario, G., Potapov, P., Turubanova, S., Hansen, M. C., & Furuichi, T. (2014). Impacts of civil conflict on primary forest habitat in northern Democratic Republic of the Congo, 1990–2010. *Biological Conservation*, *170*, 321–328. DOI: <https://doi.org/10.1016/j.biocon.2013.12.033>.
- Naing Tun, Z., Dargusch, P., McMoran, D. J., McAlpine, C., & Hill, G. (2021). Patterns and Drivers of Deforestation and Forest Degradation in Myanmar. *Sustainability*, *13*, 7539. DOI: <https://doi.org/10.3390/su13147539>.
- Newbold, T. et al. (2016). Has land use pushed terrestrial biodiversity beyond the planetary boundary? A global assessment. *Science*, *353*, 288–291. DOI: <https://doi.org/10.1126/science.aaf2201>.
- Newbold, T. et al. (2015). Global effects of land use on local terrestrial biodiversity. *Nature*, *520*, 45–50. DOI: <https://doi.org/10.1038/nature14324>.
- Nomura, K., Mitchard, E. T. A., Patenaude, G., Bastide, J., Oswald, P., & Nwe, T. (2019). Oil palm concessions in southern Myanmar consist mostly of unconverted forest. *Scientific Reports*, *9*, 1–9. DOI: <https://doi.org/10.1038/s41598-019-48443-3>.
- Nzabarinda, V., Bao, A., Xu, W., Uwamahoro, S., Huang, X., Gao, Z., Umugwaneza, A., Kayumba, P. M., Maniraho, A. P., & Jiang, Z. (2021). Impact of cropland development intensity and expansion on natural vegetation in different African countries. *Ecological Informatics*, *64*, 101359. DOI: <https://doi.org/10.1016/j.ecoinf.2021.101359>.
- Obermeier, W. A. et al. (2021). Modelled land use and land cover change emissions - A spatio-temporal comparison of different approaches. *Earth System Dynamics Discussions*, (pp. 1–43). DOI: <https://doi.org/10.5194/esd-2020-93>.
- Ordway, E. M., Asner, G. P., & Lambin, E. F. (2017). Deforestation risk due to commodity

- crop expansion in sub-Saharan Africa. *Environmental Research Letters*, 12, 044015. DOI: <https://doi.org/10.1088/1748-9326/aa6509>.
- Oswalt, S. N., Smith, W. B., Miles, P. D., & Pugh, S. A. (2019). Forest Resources of the United States, 2017: A technical document supporting the Forest Service 2020 RPA Assessment. *Gen. Tech. Rep. WO-97*. Washington, DC: U.S. Department of Agriculture, Forest Service, Washington Office., 97. DOI: <https://doi.org/10.2737/WO-GTR-97>.
- Our World in Data (2021a). Biofuel energy production [Dataset] <https://ourworldindata.org/grapher/biofuel-production>. <https://ourworldindata.org/grapher/biofuel-production>.
- Our World in Data (2021b). Crude oil prices [Dataset] <https://ourworldindata.org/grapher/crude-oil-prices>. <https://ourworldindata.org/grapher/crude-oil-prices>.
- Palmero-Iniesta, M., Pino, J., Pesquer, L., & Espelta, J. M. (2021). Recent forest area increase in Europe: Expanding and regenerating forests differ in their regional patterns, drivers and productivity trends. *European Journal of Forest Research*, 140, 793–805. DOI: <https://doi.org/10.1007/s10342-021-01366-z>.
- Paul, B. K., & Rashid, H. (2017). Chapter Six - Land Use Change and Coastal Management. In B. K. Paul, & H. Rashid (Eds.), *Climatic Hazards in Coastal Bangladesh* (pp. 183–207). Boston: Butterworth-Heinemann. DOI: <https://doi.org/10.1016/B978-0-12-805276-1.00006-5>.
- Payn, T., Carnus, J.-M., Freer-Smith, P., Kimberley, M., Kollert, W., Liu, S., Orazio, C., Rodriguez, L., Silva, L. N., & Wingfield, M. J. (2015). Changes in planted forests and future global implications. *Forest Ecology and Management*, 352, 57–67. DOI: <https://doi.org/10.1016/j.foreco.2015.06.021>.
- Pendrill, F. et al. (2022). Disentangling the numbers behind agriculture-driven tropical deforestation. *Science*, 377, eabm9267. DOI: <https://doi.org/10.1126/science.abm9267>.
- Pendrill, F., Persson, U. M., Godar, J., & Kastner, T. (2019). Deforestation displaced: Trade in forest-risk commodities and the prospects for a global forest transition. *Environmental Research Letters*, 14, 055003. DOI: <https://doi.org/10.1088/1748-9326/ab0d41>.
- Peng, S., Ciais, P., Maignan, F., Li, W., Chang, J., Wang, T., & Yue, C. (2017). Sensitivity of land use change emission estimates to historical land use and land cover mapping: Land Use and Land Cover Mapping. *Global Biogeochemical Cycles*, 31, 626–643. DOI: <https://doi.org/10.1002/2015GB005360>.
- Petrescu, A. M. R. et al. (2021). The consolidated European synthesis of CO<sub>2</sub> emissions and removals for the European Union and United Kingdom: 1990–2018. *Earth System Science Data*, 13, 2363–2406. DOI: <https://doi.org/10.5194/essd-13-2363-2021>.

- Pettersson, T., Davies, S., Deniz, A., Engström, G., Hawach, N., Höglbladh, S., & Öberg, M. S. M. (2021). Organized violence 1989–2020, with a special emphasis on Syria. *Journal of Peace Research*, *58*, 809–825. DOI: <https://doi.org/10.1177/00223433211026126>.
- Peyraud, J.-L., Taboada, M., & Delaby, L. (2014). Integrated crop and livestock systems in Western Europe and South America: A review. *European Journal of Agronomy*, *57*, 31–42. DOI: <https://doi.org/10.1016/j.eja.2014.02.005>.
- Phiri, D., Simwanda, M., Salekin, S., Nyirenda, V. R., Murayama, Y., & Ranagalage, M. (2020). Sentinel-2 Data for Land Cover/Use Mapping: A Review. *Remote Sensing*, *12*, 2291. DOI: <https://doi.org/10.3390/rs12142291>.
- Piquer-Rodríguez, M., Butsic, V., Gärtner, P., Macchi, L., Baumann, M., Gavier Pizarro, G., Volante, J. N., Gasparri, I. N., & Kuemmerle, T. (2018). Drivers of agricultural land-use change in the Argentine Pampas and Chaco regions. *Applied Geography*, *91*, 111–122. DOI: <https://doi.org/10.1016/j.apgeog.2018.01.004>.
- Plieninger, T., Draux, H., Fagerholm, N., Bieling, C., Bürgi, M., Kizos, T., Kuemmerle, T., Primdahl, J., & Verburg, P. H. (2016). The driving forces of landscape change in Europe: A systematic review of the evidence. *Land Use Policy*, *57*, 204–214. DOI: <https://doi.org/10.1016/j.landusepol.2016.04.040>.
- Podbregar, N. (2021). Landnutzungsänderungen größer als gedacht. <https://www.wissenschaft.de/erde-umwelt/landnutzungsänderungen-groesser-als-gedacht/>.
- Pongratz, J., Dolman, H., Don, A., Erb, K.-H., Fuchs, R., Herold, M., Jones, C., Kuemmerle, T., Luysaert, S., Meyfroidt, P., & Naudts, K. (2017). Models meet data: Challenges and opportunities in implementing land management in Earth system models. *Global Change Biology*, *24*, 1470–1487. DOI: <https://doi.org/10.1111/gcb.13988>.
- Pongratz, J., Reick, C., Raddatz, T., & Claussen, M. (2008). A reconstruction of global agricultural areas and land cover for the last millennium. *Global Biogeochemical Cycles*, *22*, GB3018. DOI: <https://doi.org/10.1029/2007GB003153>.
- Pongratz, J., Reick, C. H., Houghton, R. A., & House, J. I. (2014). Terminology as a key uncertainty in net land use and land cover change carbon flux estimates. *Earth System Dynamics*, *5*, 177–195. DOI: <https://doi.org/10.5194/esd-5-177-2014>.
- Pongratz, J., Schwingshackl, C., Bultan, S., Obermeier, W., Havermann, F., & Guo, S. (2021). Land Use Effects on Climate: Current State, Recent Progress, and Emerging Topics. *Current Climate Change Reports*, *7*, 99–120. DOI: <https://doi.org/10.1007/s40641-021-00178-y>.
- Popp, A., Humpenöder, F., Weindl, I., Bodirsky, B. L., Bonsch, M., Lotze-Campen, H., Müller, C., Biewald, A., Rolinski, S., Stevanovic, M., & Dietrich, J. P. (2014). Land-use protection for climate change mitigation. *Nature Climate Change*, *4*, 1095–1098. DOI: <https://doi.org/10.1038/nclimate2444>.

- Potapov, P., Turubanova, S., Hansen, M. C., Tyukavina, A., Zalles, V., Khan, A., Song, X.-P., Pickens, A., Shen, Q., & Cortez, J. (2022). Global maps of cropland extent and change show accelerated cropland expansion in the twenty-first century. *Nature Food*, *3*, 19–28. DOI: <https://doi.org/10.1038/s43016-021-00429-z>.
- Potapov, P. V., Turubanova, S. A., Tyukavina, A., Krylov, A. M., McCarty, J. L., Radeloff, V. C., & Hansen, M. C. (2015). Eastern Europe's forest cover dynamics from 1985 to 2012 quantified from the full Landsat archive. *Remote Sensing of Environment*, *159*, 28–43. DOI: <https://doi.org/10.1016/j.rse.2014.11.027>.
- Power, A. G. (2010). Ecosystem services and agriculture: Tradeoffs and synergies. *Philosophical Transactions of the Royal Society B: Biological Sciences*, *365*, 2959–2971. DOI: <https://doi.org/10.1098/rstb.2010.0143>.
- Powers, R. P., & Jetz, W. (2019). Global habitat loss and extinction risk of terrestrial vertebrates under future land-use-change scenarios. *Nature Climate Change*, *9*, 323–329. DOI: <https://doi.org/10.1038/s41558-019-0406-z>.
- Prestele, R. et al. (2016). Hotspots of uncertainty in land-use and land-cover change projections: A global-scale model comparison. *Global Change Biology*, *22*, 3967–3983. DOI: <https://doi.org/10.1111/gcb.13337>.
- Prestele, R., Arneeth, A., Bondeau, A., de Noblet-Ducoudré, N., Pugh, T. A. M., Sitch, S., Stehfest, E., & Verburg, P. H. (2017). Current challenges of implementing anthropogenic land-use and land-cover change in models contributing to climate change assessments. *Earth System Dynamics*, *8*, 369–386. DOI: <https://doi.org/10.5194/esd-8-369-2017>.
- Prishchepov, A. V., Müller, D., Dubinin, M., Baumann, M., & Radeloff, V. C. (2013). Determinants of agricultural land abandonment in post-Soviet European Russia. *Land Use Policy*, *30*, 873–884. DOI: <https://doi.org/10.1016/j.landusepol.2012.06.011>.
- Qaim, M. (2020). Role of New Plant Breeding Technologies for Food Security and Sustainable Agricultural Development. *Applied Economic Perspectives and Policy*, *42*, 129–150. DOI: <https://doi.org/10.1002/aep.13044>.
- Rahimi, J., Haas, E., Grote, R., Kraus, D., Smerald, A., Laux, P., Goopy, J., & Butterbach-Bahl, K. (2021). Beyond livestock carrying capacity in the Sahelian and Sudanian zones of West Africa. *Scientific Reports*, *11*, 22094. DOI: <https://doi.org/10.1038/s41598-021-01706-4>.
- Rajcaniova, M., Kancs, d., & Ciaian, P. (2014). Bioenergy and global land-use change. *Applied Economics*, *46*, 3163–3179. DOI: <https://doi.org/10.1080/00036846.2014.925076>.
- Raleigh, C., Linke, A., Hegre, H., & Karlsen, J. (2010). Introducing ACLED: An Armed Conflict Location and Event Dataset: Special Data Feature. *Journal of Peace Research*,

- 47, 651–660. DOI: <https://doi.org/10.1177/0022343310378914>.
- Ramankutty, N., Evan, A. T., Monfreda, C., & Foley, J. A. (2008). Farming the planet: 1. Geographic distribution of global agricultural lands in the year 2000: GLOBAL AGRICULTURAL LANDS IN 2000. *Global Biogeochemical Cycles*, 22, n/a–n/a. DOI: <https://doi.org/10.1029/2007GB002952>.
- Ramankutty, N., & Foley, J. A. (1999). Estimating historical changes in land cover: North American croplands from 1850 to 1992. *Global Ecology and Biogeography*, 8, 381–396. DOI: <https://doi.org/10.1046/j.1365-2699.1999.00141.x>.
- Ramankutty, N., Heller, E., & Rhemtulla, J. (2010). Prevailing Myths About Agricultural Abandonment and Forest Regrowth in the United States. *Annals of the Association of American Geographers*, 100, 502–512. DOI: <https://doi.org/10.1080/00045601003788876>.
- Ramankutty, N., Mehrabi, Z., Waha, K., Jarvis, L., Kremen, C., Herrero, M., & Rieseberg, L. H. (2018). Trends in Global Agricultural Land Use: Implications for Environmental Health and Food Security. *Annual Review of Plant Biology*, 69, 789–815. DOI: <https://doi.org/10.1146/annurev-arplant-042817-040256>.
- Ray, D. K., & Foley, J. A. (2013). Increasing global crop harvest frequency: Recent trends and future directions. *Environmental Research Letters*, 8, 044041. DOI: <https://doi.org/10.1088/1748-9326/8/4/044041>.
- Ray, D. K., Ramankutty, N., Mueller, N. D., West, P. C., & Foley, J. A. (2012). Recent patterns of crop yield growth and stagnation. *Nature Communications*, 3, 1293. DOI: <https://doi.org/10.1038/ncomms2296>.
- Ray, D. K., Sloat, L. L., Garcia, A. S., Davis, K. F., Ali, T., & Xie, W. (2022). Crop harvests for direct food use insufficient to meet the UN's food security goal. *Nature Food*, 3, 367–374. DOI: <https://doi.org/10.1038/s43016-022-00504-z>.
- Reenberg, A., & Fenger, N. A. (2011). Globalizing land use transitions: The soybean acceleration. *Geografisk Tidsskrift-Danish Journal of Geography*, 111, 85–92. DOI: <https://doi.org/10.1080/00167223.2011.10669524>.
- Reuter, M. et al. (2017). How Much CO<sub>2</sub> Is Taken Up by the European Terrestrial Biosphere? *Bulletin of the American Meteorological Society*, 98, 665–671. DOI: <https://doi.org/10.1175/BAMS-D-15-00310.1>.
- Reuter, M. et al. (2014). Satellite-inferred European carbon sink larger than expected. *Atmospheric Chemistry and Physics*, 14, 13739–13753. DOI: <https://doi.org/10.5194/acp-14-13739-2014>.
- Richards, D. R., & Friess, D. A. (2016). Rates and drivers of mangrove deforestation in Southeast Asia, 2000–2012. *Proceedings of the National Academy of Sciences*, 113, 344–349. DOI: <https://doi.org/10.1073/pnas.1510272113>.

- Rinnovabili.it (2021). Uso del suolo: l'uomo ha modificato il 32% della superficie terrestre dal 1960. <https://www.rinnovabili.it/ambiente/politiche-ambientali/uso-del-suolo-uomo-modifica-32-per-cento-terra/>.
- Ritchie, H., & Roser, M. (2013). Land Use. <https://ourworldindata.org/land-use>.
- Ritchie, H., & Roser, M. (2021). Forests and Deforestation. <https://ourworldindata.org/forest-area>.
- Ritchie, H., Roser, M., & Rosado, P. (2022). Crop Yields. <https://ourworldindata.org/crop-yields>.
- Robinson, T. P., Wint, G. R. W., Conchedda, G., Boeckel, T. P. V., Ercoli, V., Palamara, E., Cinardi, G., D'Aiotti, L., Hay, S. I., & Gilbert, M. (2014). Mapping the Global Distribution of Livestock. *PLOS ONE*, *9*, e96084. DOI: <https://doi.org/10.1371/journal.pone.0096084>.
- Roe, S. et al. (2019). Contribution of the land sector to a 1.5 °C world. *Nature Climate Change*, *9*, 817–828. DOI: <https://doi.org/10.1038/s41558-019-0591-9>.
- Rohde, R. A., & Hausfather, Z. (2020). The Berkeley Earth Land/Ocean Temperature Record. *Earth System Science Data*, *12*, 3469–3479. DOI: <https://doi.org/10.5194/essd-12-3469-2020>.
- Rolo, V., & Moreno, G. (2019). Shrub encroachment and climate change increase the exposure to drought of Mediterranean wood-pastures. *Science of The Total Environment*, *660*, 550–558. DOI: <https://doi.org/10.1016/j.scitotenv.2019.01.029>.
- Rosan, T. M. et al. (2021). A multi-data assessment of land use and land cover emissions from Brazil during 2000-2019. *Environmental Research Letters*, . DOI: <https://doi.org/10.1088/1748-9326/ac08c3>.
- Rosenzweig, S. T., Stromberger, M. E., & Schipanski, M. E. (2018). Intensified dryland crop rotations support greater grain production with fewer inputs. *Agriculture, Ecosystems & Environment*, *264*, 63–72. DOI: <https://doi.org/10.1016/j.agee.2018.05.017>.
- Runge, J. (2022). Tigramite – Causal inference and causal discovery for time series datasets. <https://github.com/jakobrunge/tigramite>.
- Runge, J., Nowack, P., Kretschmer, M., Flaxman, S., & Sejdinovic, D. (2019). Detecting and quantifying causal associations in large nonlinear time series datasets. *Science Advances*, *5*, eaau4996. DOI: <https://doi.org/10.1126/sciadv.aau4996>.
- Santoro, M., & Cartus, O. (2021). ESA biomass climate change initiative (Biomass\_cci): Global datasets of forest above-ground biomass for the years 2010, 2017 and 2018, v2. Centre for Environmental Data Analysis, 17 March 2021. <https://doi.org/doi:10.5285/84403d09cef3485883158f4df2989b0c>.
- Santoro, M. et al. (2021). The global forest above-ground biomass pool for 2010 estimated

- from high-resolution satellite observations. *Earth System Science Data*, *13*, 3927–3950. DOI: <https://doi.org/10.5194/essd-13-3927-2021>.
- Savage, S. (2022). We are asking for more than food from our farms. A new cropping option may help meet the demand. <https://www.forbes.com/sites/stevensavage/2022/08/17/we-are-asking-for-more-than-food-from-our-farms-a-new-cropping-option-may-help-meet-the-demand/>.
- Schaphoff, S., Reyer, C. P. O., Schepaschenko, D., Gerten, D., & Shvidenko, A. (2016). Tamm Review: Observed and projected climate change impacts on Russia's forests and its carbon balance. *Forest Ecology and Management*, *361*, 432–444. DOI: <https://doi.org/10.1016/j.foreco.2015.11.043>.
- Schenuit, F., Böttcher, M., & Geden, O. (2022). *Carbon Dioxide Removal as an Integral Building Block of the European Green Deal* volume 40/2022 of *SWP Comment*. Berlin: Stiftung Wissenschaft und Politik -SWP- Deutsches Institut für Internationale Politik und Sicherheit. DOI: <https://doi.org/10.18449/2022C40>.
- Schenuit, F., Colvin, R., Fridahl, M., McMullin, B., Reisinger, A., Sanchez, D. L., Smith, S. M., Torvanger, A., Wreford, A., & Geden, O. (2021). Carbon Dioxide Removal Policy in the Making: Assessing Developments in 9 OECD Cases. *Frontiers in Climate*, *3*.
- Schepaschenko, D. et al. (2021). Russian forest sequesters substantially more carbon than previously reported. *Scientific Reports*, *11*, 12825. DOI: <https://doi.org/10.1038/s41598-021-92152-9>.
- Schierhorn, F., Faramarzi, M., Prishchepov, A. V., Koch, F. J., & Müller, D. (2014). Quantifying yield gaps in wheat production in Russia. *Environmental Research Letters*, *9*, 084017. DOI: <https://doi.org/10.1088/1748-9326/9/8/084017>.
- Schierhorn, F., Kastner, T., Kuemmerle, T., Meyfroidt, P., Kurganova, I., Prishchepov, A. V., Erb, K.-H., Houghton, R. A., & Müller, D. (2019). Large greenhouse gas savings due to changes in the post-Soviet food systems. *Environmental Research Letters*, *14*, 065009. DOI: <https://doi.org/10.1088/1748-9326/ab1cf1>.
- Schierhorn, F., Müller, D., Beringer, T., Prishchepov, A. V., Kuemmerle, T., & Balmann, A. (2013). Post-Soviet cropland abandonment and carbon sequestration in European Russia, Ukraine, and Belarus. *Global Biogeochemical Cycles*, *27*, 1175–1185. DOI: <https://doi.org/10.1002/2013GB004654>.
- Schimel, D., Stephens, B. B., & Fisher, J. B. (2015). Effect of increasing CO<sub>2</sub> on the terrestrial carbon cycle. *Proceedings of the National Academy of Sciences*, *112*, 436–441. DOI: <https://doi.org/10.1073/pnas.1407302112>.
- Scholze, M. et al. (2019). Mean European Carbon Sink Over 2010–2015 Estimated by Simultaneous Assimilation of Atmospheric CO<sub>2</sub>, Soil Moisture, and Vegetation Optical Depth. *Geophysical Research Letters*, *46*, 13796–13803. DOI: <https://doi.org/10.1029/2019GL085725>.

- Scott, C. E. (2020). The role of agricultural expansion, land cover and land-use change in contributing to climate change. In *Climate Change and Agriculture* (pp. 167–194). Burleigh Dodds Science Publishing.
- Searchinger, T., Heimlich, R., Houghton, R. A., Dong, F., Elobeid, A., Fabiosa, J., Tokgoz, S., Hayes, D., & Yu, T.-H. (2008). Use of U.S. Croplands for Biofuels Increases Greenhouse Gases through Emissions from Land-Use Change. *Science, New Series*, *319*, 1238–1240.
- Searchinger, T., Waite, R., Hanson, C., Ranganathan, J., Dumas, P., Matthews, E., & Klirs, C. (2019). *Creating a Sustainable Food Future: A Menu of Solutions to Feed Nearly 10 Billion People by 2050. Final Report*. Technical Report, WRI.
- Shvidenko, A. Z., & Schepaschenko, D. G. (2013). Climate change and wildfires in Russia. *Contemporary Problems of Ecology*, *6*, 683–692. DOI: <https://doi.org/10.1134/S199542551307010X>.
- Sikuzani, Y. U., Muteya, H. K., & Bogaert, J. (2020). Miombo woodland, an ecosystem at risk of disappearance in the Lufira Biosphere Reserve (Upper Katanga, DR Congo)? A 39-years analysis based on Landsat images. *Global Ecology and Conservation*, *24*, e01333. DOI: <https://doi.org/10.1016/j.gecco.2020.e01333>.
- Sitch, S. (2022). TRENDY: Trends in the land carbon cycle - Information and data on the TRENDY project <https://blogs.exeter.ac.uk/trendy/>.
- Sitch, S. et al. (2015). Recent trends and drivers of regional sources and sinks of carbon dioxide. *Biogeosciences*, *12*, 653–679. DOI: <https://doi.org/10.5194/bg-12-653-2015>.
- Sitch, S., Smith, B., Prentice, I. C., Arneth, A., Bondeau, A., Cramer, W., Kaplan, J. O., Levis, S., Lucht, W., Sykes, M. T., Thonicke, K., & Venevsky, S. (2003). Evaluation of ecosystem dynamics, plant geography and terrestrial carbon cycling in the LPJ dynamic global vegetation model. *Global Change Biology*, *9*, 161–185. DOI: <https://doi.org/10.1046/j.1365-2486.2003.00569.x>.
- Song, X.-P. et al. (2021). Massive soybean expansion in South America since 2000 and implications for conservation. *Nature Sustainability*, *4*, 784–792. DOI: <https://doi.org/10.1038/s41893-021-00729-z>.
- Song, X.-P., Hansen, M. C., Stehman, S. V., Potapov, P. V., Tyukavina, A., Vermote, E. F., & Townshend, J. R. (2018). Global land change from 1982 to 2016. *Nature*, *560*, 639–643. DOI: <https://doi.org/10.1038/s41586-018-0411-9>.
- Spawn, S. A., Sullivan, C. C., Lark, T. J., & Gibbs, H. K. (2020). Harmonized global maps of above and belowground biomass carbon density in the year 2010. *Scientific Data*, *7*, 112. DOI: <https://doi.org/10.1038/s41597-020-0444-4>.
- SPEI Global Drought Monitor (2021). [Dataset]

- <https://spei.csic.es/map/maps.html#months=1#month=7#year=2021>.
- Spera, S. A., Winter, J. M., & Partridge, T. F. (2020). Brazilian maize yields negatively affected by climate after land clearing. *Nature Sustainability*, *3*, 845–852. DOI: <https://doi.org/10.1038/s41893-020-0560-3>.
- Stocker, B. D., Feissli, F., Strassmann, K. M., Spahni, R., & Joos, F. (2014). Past and future carbon fluxes from land use change, shifting cultivation and wood harvest. *Tellus B: Chemical and Physical Meteorology*, *66*, 23188. DOI: <https://doi.org/10.3402/tellusb.v66.23188>.
- Stockholm International Peace Research Institute (SIPRI) (2020). SIPRI Military Expenditure Database [Dataset]. <https://www.sipri.org/databases/milex>.
- Stürck, J., Levers, C., van der Zanden, E. H., Schulp, C. J. E., Verkerk, P. J., Kuemmerle, T., Helming, J., Lotze-Campen, H., Tabeau, A., Popp, A., Schrammeijer, E., & Verburg, P. (2018). Simulating and delineating future land change trajectories across Europe. *Regional Environmental Change*, *18*, 733–749. DOI: <https://doi.org/10.1007/s10113-015-0876-0>.
- Sudmanns, M., Tiede, D., Lang, S., Bergstedt, H., Trost, G., Augustin, H., Baraldi, A., & Blaschke, T. (2020). Big Earth data: Disruptive changes in Earth observation data management and analysis? *International Journal of Digital Earth*, *13*, 832–850. DOI: <https://doi.org/10.1080/17538947.2019.1585976>.
- Sy, V. D., Herold, M., Achard, F., Avitabile, V., Baccini, A., Carter, S., Clevers, J. G. P. W., Lindquist, E., Pereira, M., & Verchot, L. (2019). Tropical deforestation drivers and associated carbon emission factors derived from remote sensing data. *Environmental Research Letters*, *14*, 094022. DOI: <https://doi.org/10.1088/1748-9326/ab3dc6>.
- Sy, V. D., Herold, M., Achard, F., Beuchle, R., Clevers, J. G. P. W., Lindquist, E., & Verchot, L. (2015). Land use patterns and related carbon losses following deforestation in South America. *Environmental Research Letters*, *10*, 124004. DOI: <https://doi.org/10.1088/1748-9326/10/12/124004>.
- Syampungani, S., Chirwa, P. W., Akinnifesi, F. K., Sileshi, G., & Ajayi, O. C. (2009). The miombo woodlands at the cross roads: Potential threats, sustainable livelihoods, policy gaps and challenges. *Natural Resources Forum*, *33*, 150–159. DOI: <https://doi.org/10.1111/j.1477-8947.2009.01218.x>.
- Tagesson, T. et al. (2020). Recent divergence in the contributions of tropical and boreal forests to the terrestrial carbon sink. *Nature Ecology & Evolution*, *4*, 202–209. DOI: <https://doi.org/10.1038/s41559-019-1090-0>.
- Tahmasebi, T., Karami, E., & Keshavarz, M. (2020). Agricultural land use change under climate variability and change: Drivers and impacts. *Journal of Arid Environments*, *180*, 104202. DOI: <https://doi.org/10.1016/j.jaridenv.2020.104202>.

- Tanrivermis, H. (2003). Agricultural land use change and sustainable use of land resources in the mediterranean region of Turkey. *Journal of Arid Environments*, *54*, 553–564. DOI: <https://doi.org/10.1006/jare.2002.1078>.
- Taylor, C. A., & Rising, J. (2021). Tipping point dynamics in global land use. *Environmental Research Letters*, *16*, 125012. DOI: <https://doi.org/10.1088/1748-9326/ac3c6d>.
- Tchebakova, N. M., Parfenova, E., & Soja, A. J. (2009). The effects of climate, permafrost and fire on vegetation change in Siberia in a changing climate. *Environmental Research Letters*, *4*, 045013. DOI: <https://doi.org/10.1088/1748-9326/4/4/045013>.
- Terefe, B., & Kim, D.-G. (2020). Shifting cultivation maintains but its conversion to mono-cropping decreases soil carbon and nitrogen stocks compared to natural forest in Western Ethiopia. *Plant and Soil*, *453*, 105–117. DOI: <https://doi.org/10.1007/s11104-019-03942-0>.
- Tharammal, T., Bala, G., Devaraju, N., & Nemani, R. (2019). A review of the major drivers of the terrestrial carbon uptake: Model-based assessments, consensus, and uncertainties. *Environmental Research Letters*, *14*, 093005. DOI: <https://doi.org/10.1088/1748-9326/ab3012>.
- The Hindu (2021). Nearly a fifth of Earth's surface transformed since 1960. <https://www.thehindu.com/sci-tech/energy-and-environment/nearly-a-fifth-of-earths-surface-transformed-since-1960/article34541134.ece>.
- The Taipei Times (2021). Study shows vast extent of the repurposing of land - Taipei Times. <https://www.taipeitimes.com/News/front/archives/2021/05/13/2003757321>.
- Thomas, P. W., & Vazquez, L.-B. (2022). A novel approach to combine food production with carbon sequestration, biodiversity and conservation goals. *Science of The Total Environment*, *806*, 151301. DOI: <https://doi.org/10.1016/j.scitotenv.2021.151301>.
- Thoning, K. W., Tans, P. P., & Komhyr, W. D. (1989). Atmospheric carbon dioxide at Mauna Loa Observatory: 2. Analysis of the NOAA GMCC data, 1974–1985. *Journal of Geophysical Research: Atmospheres*, *94*, 8549–8565. DOI: <https://doi.org/10.1029/JD094iD06p08549>.
- Tilman, D., & Clark, M. (2014). Global diets link environmental sustainability and human health. *Nature*, *515*, 518–522. DOI: <https://doi.org/10.1038/nature13959>.
- Tilman, D., Clark, M., Williams, D. R., Kimmel, K., Polasky, S., & Packer, C. (2017). Future threats to biodiversity and pathways to their prevention. *Nature*, *546*, 73–81. DOI: <https://doi.org/10.1038/nature22900>.
- Titeux, N., Henle, K., Mihoub, J.-B., & Brotons, L. (2016). Climate change distracts

- us from other threats to biodiversity. *Frontiers in Ecology and the Environment*, *14*, 291–291. DOI: <https://doi.org/10.1002/fee.1303>.
- Trainor, A. M., McDonald, R. I., & Fargione, J. (2016). Energy Sprawl Is the Largest Driver of Land Use Change in United States. *PLOS ONE*, *11*, e0162269. DOI: <https://doi.org/10.1371/journal.pone.0162269>.
- Trueblood, M. A., & Arnade, C. (2001). Crop Yield Convergence: How Russia's Yield Performance Has Compared to Global Yield Leaders. *Comparative Economic Studies*, *43*, 59–81. DOI: <https://doi.org/10.1057/ces.2001.8>.
- Turner, M. D., Hiernaux, P., & Schlecht, E. (2005). The Distribution of Grazing Pressure in Relation to Vegetation Resources in Semi-arid West Africa: The Role of Herding. *Ecosystems*, *8*, 668–681. DOI: <https://doi.org/10.1007/s10021-003-0099-y>.
- Turubanova, S., Potapov, P. V., Tyukavina, A., & Hansen, M. C. (2018). Ongoing primary forest loss in Brazil, Democratic Republic of the Congo, and Indonesia. *Environmental Research Letters*, *13*, 074028. DOI: <https://doi.org/10.1088/1748-9326/aacd1c>.
- Uereyen, S., Bachofer, F., Klein, I., & Kuenzer, C. (2022). Multi-faceted analyses of seasonal trends and drivers of land surface variables in Indo-Gangetic river basins. *Science of The Total Environment*, *847*, 157515. DOI: <https://doi.org/10.1016/j.scitotenv.2022.157515>.
- UNFCCC (a). Greenhouse Gas Inventory Data - Time Series - Annex I. [https://data.unfccc.int/time\\_series](https://data.unfccc.int/time_series).
- UNFCCC (b). National Inventory Submissions 2022 | UNFCCC. <https://unfccc.int/ghg-inventories-annex-i-parties/2022>.
- United Nations (UN) (2019). World Population Prospects 2019, Online Edition. Rev. 1, Department of Economic and Social Affairs United Nations, .
- Valbuena, R., & Lovejoy, T. (2021). Deforestation is driven by global markets. <http://theconversation.com/deforestation-is-driven-by-global-markets-161049>.
- Vali, A., Comai, S., & Matteucci, M. (2020). Deep Learning for Land Use and Land Cover Classification Based on Hyperspectral and Multispectral Earth Observation Data: A Review. *Remote Sensing*, *12*, 2495. DOI: <https://doi.org/10.3390/rs12152495>.
- Van Auken, O. W. (2000). Shrub Invasions of North American Semiarid Grasslands. *Annual Review of Ecology and Systematics*, *31*, 197–215. DOI: <https://doi.org/10.1146/annurev.ecolsys.31.1.197>.
- van der Sluis, T., Pedroli, B., Kristensen, S. B. P., Lavinia Cosor, G., & Pavlis, E. (2016). Changing land use intensity in Europe – Recent processes in selected case studies. *Land Use Policy*, *57*, 777–785. DOI: <https://doi.org/10.1016/j.landusepol.2014.12.005>.
- van Meijl, H., van Rheenen, T., Tabeau, A., & Eickhout, B. (2006). The impact of different

- policy environments on agricultural land use in Europe. *Agriculture, Ecosystems & Environment*, 114, 21–38. DOI: <https://doi.org/10.1016/j.agee.2005.11.006>.
- van Soest, H. L., den Elzen, M. G. J., & van Vuuren, D. P. (2021). Net-zero emission targets for major emitting countries consistent with the Paris Agreement. *Nature Communications*, 12, 2140. DOI: <https://doi.org/10.1038/s41467-021-22294-x>.
- van Vliet, J., de Groot, H. L. F., Rietveld, P., & Verburg, P. H. (2015). Manifestations and underlying drivers of agricultural land use change in Europe. *Landscape and Urban Planning*, 133, 24–36. DOI: <https://doi.org/10.1016/j.landurbplan.2014.09.001>.
- van Vliet, N. et al. (2012). Trends, drivers and impacts of changes in swidden cultivation in tropical forest-agriculture frontiers: A global assessment. *Global Environmental Change*, 22, 418–429. DOI: <https://doi.org/10.1016/j.gloenvcha.2011.10.009>.
- Varkkey, H., Tyson, A., & Choiruzzad, S. A. B. (2018). Palm oil intensification and expansion in Indonesia and Malaysia: Environmental and socio-political factors influencing policy. *Forest Policy and Economics*, 92, 148–159. DOI: <https://doi.org/10.1016/j.forpol.2018.05.002>.
- Verburg, P. H., Alexander, P., Evans, T., Magliocca, N. R., Malek, Z., Rounsevell, M. D., & van Vliet, J. (2019). Beyond land cover change: Towards a new generation of land use models. *Current Opinion in Environmental Sustainability*, 38, 77–85. DOI: <https://doi.org/10.1016/j.cosust.2019.05.002>.
- VERIFY (2018). VERIFY project: VERIFYing greenhouse gas emissions. <https://verify.lsce.ipsl.fr/>.
- Viglione, G. (2021). Land-use change has affected ‘almost a third’ of world’s terrain since 1960. <https://www.carbonbrief.org/land-use-change-has-affected-almost-a-third-of-worlds-terrain-since-1960/>.
- Villa, P. M., Martins, S. V., de Oliveira Neto, S. N., Rodrigues, A. C., Hernández, E. P., & Kim, D.-G. (2020). Policy forum: Shifting cultivation and agroforestry in the Amazon: Premises for REDD+. *Forest Policy and Economics*, 118, 102217. DOI: <https://doi.org/10.1016/j.forpol.2020.102217>.
- Villoria, N., Garrett, R., Gollnow, F., & Carlson, K. (2022). Leakage does not fully offset soy supply-chain efforts to reduce deforestation in Brazil. *Nature Communications*, 13, 5476. DOI: <https://doi.org/10.1038/s41467-022-33213-z>.
- Vuichard, N., Ciais, P., Belelli, L., Smith, P., & Valentini, R. (2008). Carbon sequestration due to the abandonment of agriculture in the former USSR since 1990. *Global Biogeochemical Cycles*, 22. DOI: <https://doi.org/10.1029/2008GB003212>.
- Walker, N. F., Patel, S. A., & Kalif, K. A. B. (2013). From Amazon Pasture to the High Street: Deforestation and the Brazilian Cattle Product Supply Chain. *Tropical*

- Conservation Science*, 6, 446–467. DOI: <https://doi.org/10.1177/194008291300600309>.
- Wang, Q., Wu, J., Lei, T., He, B., Wu, Z., Liu, M., Mo, X., Geng, G., Li, X., Zhou, H., & Liu, D. (2014). Temporal-spatial characteristics of severe drought events and their impact on agriculture on a global scale. *Quaternary International*, 349, 10–21. DOI: <https://doi.org/10.1016/j.quaint.2014.06.021>.
- Wang, S. et al. (2020). Recent global decline of CO<sub>2</sub> fertilization effects on vegetation photosynthesis. *Science*, 370, 1295–1300. DOI: <https://doi.org/10.1126/science.abb7772>.
- Wegren, S. K. (2022). Sanctions Likely to Derail the Trajectory of Russia’s Agricultural Sector. *Political Regime Stability/Universities/Agriculture*, 29, 22.
- Weinzettel, J., Hertwich, E. G., Peters, G. P., Steen-Olsen, K., & Galli, A. (2013). Affluence drives the global displacement of land use. *Global Environmental Change*, 23, 433–438. DOI: <https://doi.org/10.1016/j.gloenvcha.2012.12.010>.
- Wertebach, T.-M., Hölzel, N., Kämpf, I., Yurtaev, A., Tupitsin, S., Kiehl, K., Kamp, J., & Kleinebecker, T. (2017). Soil carbon sequestration due to post-Soviet cropland abandonment: Estimates from a large-scale soil organic carbon field inventory. *Global Change Biology*, 23, 3729–3741. DOI: <https://doi.org/10.1111/gcb.13650>.
- Westram, H. (2021). Weltweite Landnutzung ändert sich viel stärker als gedacht. <https://www.br.de/nachrichten/wissen/weltweite-landnutzung-aendert-sich-viel-staerker-als-gedacht,SX6CCBe>.
- Wicke, B., Sikkema, R., Dornburg, V., & Faaij, A. (2011). Exploring land use changes and the role of palm oil production in Indonesia and Malaysia. *Land Use Policy*, 28, 193–206. DOI: <https://doi.org/10.1016/j.landusepol.2010.06.001>.
- Wigley, B. J., Bond, W. J., & Hoffman, M. T. (2010). Thicket expansion in a South African savanna under divergent land use: Local vs. global drivers? *Global Change Biology*, 16, 964–976. DOI: <https://doi.org/10.1111/j.1365-2486.2009.02030.x>.
- Wigneron, J.-P., Fan, L., Ciais, P., Bastos, A., Brandt, M., Chave, J., Saatchi, S., Baccini, A., & Fensholt, R. (2020). Tropical forests did not recover from the strong 2015–2016 El Niño event. *Science Advances*, . DOI: <https://doi.org/10.1126/sciadv.aay4603>.
- Wigneron, J.-P., Li, X., Frappart, F., Fan, L., Al-Yaari, A., De Lannoy, G., Liu, X., Wang, M., Le Masson, E., & Moisy, C. (2021). SMOS-IC data record of soil moisture and L-VOD: Historical development, applications and perspectives. *Remote Sensing of Environment*, 254, 112238. DOI: <https://doi.org/10.1016/j.rse.2020.112238>.
- Wilenskijeld, S., Kloster, S., Pongratz, J., Raddatz, T., & Reick, C. H. (2014). Comparing the influence of net and gross anthropogenic land-use and land-cover changes on the carbon cycle in the MPI-ESM. *Biogeosciences*, 11, 4817–4828. DOI: <https://doi.org/10.5194/bg-11-4817-2014>.

- g/10.5194/bg-11-4817-2014.
- Winkler, K., Fuchs, R., Rounsevell, M., & Herold, M. (2020). HILDA+ (HIstoric Land Dynamics Assessment+) Global Land Use Change between 1960 and 2019. PANGAEA, <https://doi.org/10.1594/PANGAEA.921846>.
- Winkler, K., Fuchs, R., Rounsevell, M., & Herold, M. (2021). Global land use changes are four times greater than previously estimated. *Nature Communications*, *12*, 2501. DOI: <https://doi.org/10.1038/s41467-021-22702-2>.
- Winkler, K., Gessner, U., & Hochschild, V. (2017). Identifying Droughts Affecting Agriculture in Africa Based on Remote Sensing Time Series between 2000–2016: Rainfall Anomalies and Vegetation Condition in the Context of ENSO. *Remote Sensing*, *9*, 831. DOI: <https://doi.org/10.3390/rs9080831>.
- World Bank (2019a). Birth rate, crude (per 1,000 people) [Dataset]. <https://data.worldbank.org/indicator/SP.DYN.CBRT.IN>.
- World Bank (2019b). Net migration [Dataset]. <https://data.worldbank.org/indicator/SM.POP.NETM>.
- World Bank (2021a). GDP per capita (current US\$) [Dataset]. <https://data.worldbank.org/indicator/NY.GDP.PCAP.CD>.
- World Bank (2021b). Gini index (World Bank estimate) [Dataset]. <https://data.worldbank.org/indicator/SI.POV.GINI>.
- World Bank (2021c). Life expectancy at birth, total (years) [Dataset]. <https://data.worldbank.org/indicator/SP.DYN.LE00.IN>.
- World Bank (2021d). Population density (people per sq. km of land area) [Dataset]. <https://data.worldbank.org/indicator/EN.POP.DNST>.
- World Bank (2021e). Subsidies and other transfers (current LCU) [Dataset]. <https://data.worldbank.org/indicator/GC.XPN.TRFT.CN>.
- Xu, L. et al. (2021). Changes in global terrestrial live biomass over the 21st century. *Science Advances*, *7*, eabe9829. DOI: <https://doi.org/10.1126/sciadv.abe9829>.
- Yale University (2020). Environmental Performance Index [Dataset]. <https://epi.yale.edu/downloads>.
- Yan, H., Lai, C., Akshalov, K., Qin, Y., Hu, Y., & Zhen, L. (2020). Social institution changes and their ecological impacts in Kazakhstan over the past hundred years. *Environmental Development*, *34*, 100531. DOI: <https://doi.org/10.1016/j.envdev.2020.100531>.
- Yang, M., Wang, G., Ahmed, K. F., Adugna, B., Eggen, M., Atsbeha, E., You, L., Koo, J., & Anagnostou, E. (2020). The role of climate in the trend and variability of Ethiopia's cereal crop yields. *Science of The Total Environment*, *723*, 137893. DOI:

- <https://doi.org/10.1016/j.scitotenv.2020.137893>.
- Yang, Y., Zhang, S., Yang, J., Chang, L., Bu, K., & Xing, X. (2014). A review of historical reconstruction methods of land use/land cover. *Journal of Geographical Sciences*, *24*, 746–766. DOI: <https://doi.org/10.1007/s11442-014-1117-z>.
- Yin, H., Butsic, V., Buchner, J., Kuemmerle, T., Prishchepov, A. V., Baumann, M., Bragina, E. V., Sayadyan, H., & Radeloff, V. C. (2019). Agricultural abandonment and re-cultivation during and after the Chechen Wars in the northern Caucasus. *Global Environmental Change*, *55*, 149–159. DOI: <https://doi.org/10.1016/j.gloenvcha.2019.01.005>.
- Yu, Q., You, L., Wood-Sichra, U., Ru, Y., Joglekar, A. K. B., Fritz, S., Xiong, W., Lu, M., Wu, W., & Yang, P. (2020). A cultivated planet in 2010 – Part 2: The global gridded agricultural-production maps. *Earth System Science Data*, *12*, 3545–3572. DOI: <https://doi.org/10.5194/essd-12-3545-2020>.
- Yu, Y., Feng, K., & Hubacek, K. (2013). Tele-connecting local consumption to global land use. *Global Environmental Change*, *23*, 1178–1186. DOI: <https://doi.org/10.1016/j.gloenvcha.2013.04.006>.
- Yu, Z., & Lu, C. (2018). Historical cropland expansion and abandonment in the continental U.S. during 1850 to 2016. *Global Ecology and Biogeography*, *27*, 322–333. DOI: <https://doi.org/10.1111/geb.12697>.
- Yu, Z., Lu, C., Tian, H., & Canadell, J. G. (2019). Largely underestimated carbon emission from land use and land cover change in the conterminous United States. *Global Change Biology*, *25*, 3741–3752. DOI: <https://doi.org/10.1111/gcb.14768>.
- Yue, C., Ciais, P., & Li, W. (2018). Smaller global and regional carbon emissions from gross land use change when considering sub-grid secondary land cohorts in a global dynamic vegetation model. *Biogeosciences*, *15*, 1185–1201. DOI: <https://doi.org/10.5194/bg-15-1185-2018>.
- Zamolodchikov, D. G., Grabovskii, V. I., Shulyak, P. P., & Chestnykh, O. V. (2017). Recent decrease in carbon sink to Russian forests. *Doklady Biological Sciences*, *476*, 200–202. DOI: <https://doi.org/10.1134/S0012496617050064>.
- Zamolodchikov, D. G., Grabowsky, V. I., & Chestnykh, O. V. (2018). Dynamic pattern of carbon balance in the forests of federal districts of the Russian Federation. *Forest Science Issues*, *2*, 1–19.
- Zeimetz, K. A., United States, Department of Agriculture, Economic Research Service, & Agriculture and Trade Analysis Division (1987). *Effects on the USSR of the 1980 U.S. Embargo on Agricultural Exports*. Washington, DC] (1301 New York Ave., NW, Washington 20005-4788): U.S. Dept. of Agriculture, Economic Research Service, Agriculture and Trade Analysis Division.

- 
- Zhang, X., Lark, T. J., Clark, C. M., Yuan, Y., & LeDuc, S. D. (2021). Grassland-to-cropland conversion increased soil, nutrient, and carbon losses in the US Midwest between 2008 and 2016. *Environmental Research Letters*, *16*, 054018. DOI: <https://doi.org/10.1088/1748-9326/abecbe>.
- Zhou, G., Zhang, W., & Xu, X. (2012). China's meat industry revolution: Challenges and opportunities for the future. *Meat Science*, *92*, 188–196. DOI: <https://doi.org/10.1016/j.meatsci.2012.04.016>.
- Zomer, R. J., Neufeldt, H., Xu, J., Ahrends, A., Bossio, D., Trabucco, A., van Noordwijk, M., & Wang, M. (2016). Global Tree Cover and Biomass Carbon on Agricultural Land: The contribution of agroforestry to global and national carbon budgets. *Scientific Reports*, *6*, 29987. DOI: <https://doi.org/10.1038/srep29987>.
- Zuo, L. et al. (2018). Progress towards sustainable intensification in China challenged by land-use change. *Nature Sustainability*, *1*, 304–313. DOI: <https://doi.org/10.1038/s41893-018-0076-2>.
- Zvoleff, A., Wandersee, S., An, L., & López-Carr, D. (2014). Land Use and Cover Change. In B. Warf (Ed.), *Geography Oxford Bibliographies*. Oxford, UK: Oxford University Press.



# Acknowledgements

This PhD thesis is the result of a long journey full of ups and downs, laughs and tales, exciting encounters, new experiences, hard work, despair and, above all, lots of fun. Many people have contributed to making the PhD expedition a success for me.

First and foremost, I would like to thank my supervisors, who not only formally fulfilled their role, but have been a complementary dream support team for me. Thank you all for giving me the opportunity to start a PhD with you. I still remember the day of my interview for the PhD position. It just matched! I was so impressed by you as a team. You were a crucial reason that made me decide to go from a full scientific position to a 4-year PhD adventure with an underpaid stipend. And my impression was not wrong: you gave me a creative space for ideas, an appreciative working atmosphere and my ideal image of research that is more fun with friends. You have enriched my PhD time with much inspiration, research freedom and supportive guidance. This enabled me to grow as a scientist. A huge thank you for that! Although we could not often meet in person (but every now and then at ESA conferences) and COVID prevented further visits, Martin was always a good connection to Wageningen for me. He supported me very much in all phases of the PhD. I was particularly impressed by his many good scientific ideas, his pragmatic manner and his talent for management. Thank you so much Martin for the helpful advices, the good, solution-oriented discussions and that you were always available for questions and online meetings. Mark is the best group leader I know and a role model for me. His humorous, inspiring personality, his talent to encourage and his abundance of creative ideas have enriched my PhD work. Thank you Mark for your positive support, your magical linguistic polishing of each manuscript, many a philosophical debate over wine, and for always keeping the big picture in mind. You always managed to give me a motivational boost through our meetings. Richard has been my closest and nearly daily advisor during the ups and down of the PhD time. He set up the whole project in the first place and played an overwhelming part in its success. Where should I start? His incredible analytical ability to recognize patterns from even the most chaotic pixel cluster; his enthusiasm, which often raises the most exciting research questions; his ambition, which led me to venture into the world of high-ranking journals; or his strategic career tips, which met my non-strategic lack of planning - all this helped me on my way to my PhD. Thank you Richard for all your support, good advice, many heated but fruitful

---

debates, hoppy "progress" meetings, lunchtime walks, your equally rebellious spirit, and most of all for always being there for me throughout my PhD. You are the best supervisor I could imagine. And as you know, it's all a question of mindset!

I had the opportunity to learn from and be inspired by several co-authors, particularly during the collaboration in the VERIFY project. Thank you all for sharing data, for giving valuable suggestions and useful feedback on my manuscripts, and for providing me insights into the world of carbon modelling. Thank you Raphael and Julia for being early adopters and integrating my data into your modelling so quickly. Thank you, Philippe for giving me the opportunity to lead the paper on the Eastern European carbon sink and for allowing me to benefit from your network.

Next, I would like to thank my colleagues and friends at IFU, particularly the Land Use Change and Climate research group, a top team with great cohesion that has accompanied me since the start of my PhD in 2018. Although some of you have moved or are in the process of moving, I associate many great moments during the PhD with you: Mark, Calum, Penelope, Richard, Sylvia, Heera, Bumsuk, Verena – thanks for the many social events, some long mountain adventures and the overall incomparably brilliant team spirit in which I was able to design my PhD work. I miss those times. Thanks also goes to Reinhard, Kathi and to all our newer team members. Many people from the IFU sphere contributed directly but mostly indirectly to this PhD thesis. Thanks to my (former) colleagues and friends, Kathi, Elli, Kevin, Nico, Luca, Julius, Baldur, Krischan, Johannes, Hannes, David, François, Benni, Tanja, Luise, Ricky, Elizabeth, Anne, Stefanie, Romy, Verena, and many more for the fun during and outside of work. Thanks to my staff council colleagues, Carsten, Anja, Christoph, Sylvia, for allowing me to look beyond my own work through a meaningful side activity. Thanks to Elija, for her commitment running the PhD seminar and organising lots of useful courses for young scientists. I also acknowledge all people keeping the scientific activities at IFU running: IT, security and cleaning staff.

A special thanks goes to my former flatmates and colleagues François, David and Julius. You guys shaped my PhD journey and provided the best needed distraction from work. Cheers to the legendary parties in the best shared house in sleepy Partenkirchen, to the never completed construction of an enormous snow igloo in the garden and to countless beautiful flat share evenings and fun activities! Thanks also to the Hasental-WG, Johannes, Hannah, Andi, Sören and Julian for the fun evening events.

Because I cannot be scientifically productive without political side activities, I would like to thank my friends from the underground cycling activists Radlinitiative in Garmisch-Partenkirchen. Thank you for the night-and-fog campaigns, the Ausbremsst is! demonstrations and the many conspiratorial meetings. Thanks also to my Green Party colleagues for the opportunity to look into the conservative abyss of local politics and transform it for the better.

---

I would also like to thank my friends from former times: from geography studies in Giessen and Tübingen – Roland, Flo, Sina, the elks team Ika, Julia and Caro – from working at DLR – Soner, Daniela, Ayim, Christian, Kersten, Anna, Sarah, Ursula, Juliane, Julian, Felix – and from my time abroad in Bolivia and Colombia – Nora, Annika, Michi, Steffen, Eric, Rodrigo, the Torrico family, Fabi, Amalia, Davor, Isra, the Aywiña family, Camilo, and Andrés. Even though I haven't seen many of you for a while, you have accompanied and shaped my path in different ways. Thanks goes also to my longstanding friends at home in Franconia – Vroni, Andi, Basti, Sonja, Sasi, Tessa, Lisa, FFW Wolkersdorf and Kärwaboum & Madli folks – for the beautiful times and for the good company on my path.

A special heartfelt thanks goes to my family in Wolkersdorf. Thanks to my parents Gerda and Helmut for always believing in me, for your unconditional support and for being so proud of me. Thanks to my sister Leni and my brother-in-law Hannes for always being there for me, for the outstanding celebrations, evenings full of funny stories and for the visits to Garmisch. It is always nice to come home. You keep me grounded and make me aware that the world is not just made up of theory.

From the bottom of the heart, I would like to thank Johannes. Thank you for your unconditional support, your honest and constructive criticism, the many wonderful mountain/ski tours and for bringing me back down to earth when I sometimes fly high. You make me happy. Thank you for being with me.

Finally, I would also like to thank the great mountain landscape around Garmisch-Partenkirchen, without which I would never have lasted so long on this PhD journey.



# About the author

Karina Winkler was born on 5 March 1990 in Schwabach, Germany. She grew up on a farm and attended an artistic secondary school. Along the way, her world revolved around voluntary fire brigades, Kärwa (tradition of beery Franconian village festivals) and making music in her band. She could never have imagined becoming a scientist one day. However, she was driven by great curiosity to discover the world and eagerness to learn. After graduating from secondary school, her voluntary social year in Bolivia in 2009-2010 turned Karina's world view upside down. This experience gave her the confidence to follow up on her new-found interest in human-environment relations and global interconnections.

Karina studied a Bachelor's degree in Geography at the Justus Liebig University of Gießen in 2011-2014 with a minor in Environmental and Political Sciences. She enjoyed being out in the field and had the opportunity to participate in exciting excursions. After a semester abroad in Colombia and the back-and-forth between human and physical geography courses, Karina focused her studies on soil science and geomorphology. Her bachelor thesis was about the analysis of soil erosion forms by means of Geographic Information Systems and remote sensing.

With the aim to learn more about remote sensing methods, Karina studied her Master in Physical Geography in Tübingen in 2014-2017. In addition to a strong focus on remote sensing and landscape systems, she took computer science and ecology courses. An internship opened the door to Karina writing her Master's thesis in the Land Surface Dynamics team at the German Aerospace Center (DLR) in Oberpfaffenhofen in 2016-2017. Her thesis on the satellite-based analysis of large-scale agricultural droughts in Africa in the context of climate variability resulted in her first paper publication due to the good collaboration with her supervisor Ursula and other great colleagues.

After finishing her Master's degree, Karina was able to work as a research assistant in the SAR group at DLR in 2017-2018. Her tasks were more operational - the post-processing and verification of radar remote sensing data. Karina realised that she wanted to do independent research.

Since funding for a PhD at DLR was unclear, Karina applied for a PhD position with stipend in the Land Use Change and Climate research group at KIT IMK-IFU in

---

Garmisch-Partenkirchen. Thereupon, she started her PhD on a data-driven reconstruction of global land use change as a cooperation between KIT and Wageningen University in May 2018. Karina was affiliated with both KIT IMK-IFU and Wageningen University. During 2018-2022, she spent a lot of time developing and programming her land use reconstruction model, HILDA+, and studying the dynamics of global land use change. In the course of her PhD, Karina was able to win a few awards and grants – the Wikimedia Open Science Fellowship, the ESA ESDL early adopter’s grant, and the FVFF-IFU-Förderpreis 2021.

In May 2022, Karina started a PostDoc position at KIT IMK-IFU by joining the STEPSEC project on land-based Carbon Dioxide Removal (CDR) and modelling the future of the German land system. While finishing her PhD project, she started learning about agent-based land use modelling in the new project. Karina looks forward to coming years of exciting research by building on the results of her PhD, developing new skills and gaining insights into land use modelling in her PostDoc time.

## Peer-reviewed journal publications

Bastos, A., Ciais, P., Sitch, S., Aragão, L.E.O.C., Chevallier, F., Fawcett, D., Rosan, T.M., Saunois, M., Günther, D., Perugini, L., Robert, C., Deng, Z., Pongratz, J., Ganzenmüller, R., Fuchs, R., **Winkler, K.**, Zaehle, S. & Albergel, C. (2022). On the use of Earth Observation to support estimates of national greenhouse gas emissions and sinks for the Global stocktake process: lessons learned from ESA-CCI RECCAP2. *Carbon Balance and Management*, 17, 15. DOI: <https://doi.org/10.1186/s13021-022-00214-w>.

Estoque, R.C., Dasgupta, R., **Winkler, K.**, Avitabile, V., Johnson, B.A., Myint, S.W., Gao, Y., Ooba, M., Murayama, Y. & Lasco, R.D. (2022). Spatiotemporal pattern of global forest change over the past 60 years and the forest transition theory. *Environmental Research Letters*, 17, 084022. DOI: <https://doi.org/10.1088/1748-9326/ac7df5>.

Ganzenmüller, R., Bultan, S., **Winkler, K.**, Fuchs, R., Zabel, F. & Pongratz, J. (2022). Land-use change emissions based on high-resolution activity data substantially lower than previously estimated. *Environmental Research Letters*, 17, 064050. DOI: <https://doi.org/10.1088/1748-9326/ac70d8>.

**Winkler, K.**, Fuchs, R., Rounsevell, M. & Herold, M. (2021). Global land use changes are four times greater than previously estimated. *Nature Communications*, 12, 2501. DOI: <https://doi.org/10.1038/s41467-021-22702-2>.

---

Roth, A., Marschalk, U., **Winkler, K.**, Schättler, B., Huber, M., Georg, I., Künzer, C., & Dech, S. (2018). Ten Years of Experience with Scientific TerraSAR-X Data Utilization. *Remote Sensing*, *10*, 1170. DOI: <https://doi.org/10.3390/rs10081170>.

Wohlfart, C., **Winkler, K.**, Wendleder, A. & Roth, A. (2018). TerraSAR-X and Wetlands: A Review. *Remote Sensing*, *10*, 916. DOI: <https://doi.org/10.3390/rs10060916>.

Müller, I., Hipondoka, M., **Winkler, K.**, Geßner, U., Martinis, S. & Taubenböck, H. (2018). Monitoring flood and drought events - earth observation for multiscale assessment of water-related hazards and exposed elements. *Biodiversity & Ecology*, *6*, 136–143. DOI: <https://doi.org/10.7809/b-e.00315>.

**Winkler, K.**, Gessner, U. & Hochschild, V. (2017). Identifying Droughts Affecting Agriculture in Africa Based on Remote Sensing Time Series between 2000–2016: Rainfall Anomalies and Vegetation Condition in the Context of ENSO. *Remote Sensing*, *9*, 831. DOI: <https://doi.org/10.3390/rs9080831>.

## Other scientific publications

### Data publications

**Winkler, K.**, Fuchs, R., Rounsevell, M., Herold, M. (2020). HILDA+ (Historic Land Dynamics Assessment+) Global Land Use Change between 1960 and 2019. PANGAEA, DOI: <https://doi.org/10.1594/PANGAEA.921846>.

### Conference publications

**Winkler, K.**, Yang, H., Ganzenmüller, R., Fuchs, R., Ceccherini, G., Duveiller, G., Grassi, G., Pongratz, J., Bastos, A. Shvidenko, A. Araza, A., Herold, M. & Ciais, P. (2022). The Eastern European land carbon sink, ESA Living Planet Symposium, 23–27 May 2022, Bonn, Germany.

**Winkler, K.**, Fuchs, R., Rounsevell, M., Herold, M. (2022). Global land use transitions and their drivers during 1960-2019, EGU General Assembly 2022, 23–27 May 2022, Vienna, Austria. DOI: <https://doi.org/10.5194/egusphere-egu22-9145>.

**Winkler, K.**, Fuchs, R., Rounsevell, M., Herold, M. (2021). Spatiotemporal patterns of global land use change: Understanding processes and drivers, EGU General Assembly 2021, 19–30 Apr 2021, DOI: <https://doi.org/10.5194/egusphere-egu21-14471>.

**Winkler, K.**, Fuchs, R., Rounsevell, M., Herold, M. (2020). What open data tells us - Reconstructing 55 years of global land use/cover change (video contribution), EGU General Assembly 2020, 4–8 May 2020, DOI: <https://doi.org/10.5194/egusphere-egu2020-18199>.

---

**Winkler, K.**, Fuchs, R., Rounsevell, M., Herold, M. (2019). A data-driven reconstruction of global land use change from 1960 to 2015 at 1 km spatial resolution (poster presentation), ESA Living Planet Symposium, May 13-17 2019, Milan, Italy.

**Winkler, K.** (2019). Exploring the "Earth System Data Lab": Co-Designing the Data Cube Idea (side event), Phi-week, September 9-13 2019, ESRIN, Frascati, Italy.

**Winkler, K.**, Fuchs, R., Rounsevell, M., Herold, M. (2019) Towards a data-driven reconstruction of land use change and its linkage with land management at the global scale, Global Land Programme Open Science Meeting, April 23-36 2019, Bern, Switzerland.

# PE&RC Training and Education Statement

With the training and education activities listed below the PhD candidate has complied with the requirements set by the C.T. de Wit Graduate School for Production Ecology and Resource Conservation (PE&RC) which comprises of a minimum total of 32 ECTS (= 22 weeks of activities)



## **Review / project proposal (9 ECTS)**

- State of the art in land change reconstruction
- A data-driven reconstruction of global land change: land use change and land management in a globalised world

## **Post-graduate courses (7 ECTS)**

- Summer school on ecosystems and land use change; KIT/ IMK-IFU (2018)
- Advanced programming in Python; NextGen at Helmholtz, GFZ Potsdam (2018)
- Spatial ecology: international summer school; Spatial Ecology, Matera (2019)

## **Competence strengthening / skills courses (4.8 ECTS)**

- Improving your rhetorical and communication skills; KIT/ IMK-IFU (2018)
- How to publish in peer-reviewed journals; KIT/ IMK-IFU (2019)
- How to become an independent researcher; KIT/ IMK-IFU (2022)

## **PE&RC Annual meetings, seminars and the PE&RC weekend (0.9 ECTS)**

- PE&RC First years weekend (2018)

---

**Discussion groups / local seminars or scientific meetings (8.9 ECTS)**

- MICMOR PhD seminars; IMK-IFU (2018-2022)
- VERIFY Project meetings; Reading, UK; Paris, France (2018-2022)
- IFU Institute seminars; IMK-IFU (2018-2022)
- GRS Lab meeting; WUR (2018-2022)
- Paper/collaboration meetings; WUR (2021)

**International symposia, workshops and conferences (11.2 ECTS)**

- Global land programme 4th open science meeting (2019)
- ESA Living planet symposium (2019, 2022)
- ESA Phi week (2019)
- EGU general assembly (2020, 2021, 2022)

**Lecturing / supervision of practical's / tutorials (1.2 ECTS)**

- Lecture in summer school on ecosystems and land use change (2019, 2021, 2022)

**BSc/MSc thesis supervision**

- Crop type mapping



This research received funding from the European Commission through Horizon 2020 Framework Programme (VERIFY, Grant No. 776810).

Cover design by Karina Winkler